NOAA Technical Report ERL 450–AOML 36

Upper Ocean Thermal Structure of the Eastern Tropical Pacific

Maria C. Donoso
Rosenstiel School of Marine and Atmospheric Science
University of Miami

Jessie E. Harris
Atlantic Oceanographic and Meteorological Laboratory

David B. Enfield
Atlantic Oceanographic and Meteorological Laboratory

Atlantic Oceanographic and Meteorological Laboratory
Miami, Florida

November 1994

U.S. Department of Commerce
Ronald H. Brown, Secretary

National Oceanic and Atmospheric Administration
D. James Baker, Under Secretary for Oceans and Atmosphere/Administrator

Environmental Research Laboratories
Silver Spring, Maryland
James L. Rasmussen, Director

NOTICE

Mention of a commercial company or product does not constitute an endorsement by NOAA Environmental Research Laboratories. Use for publicity or advertising purposes of information from this publication concerning proprietary products is not authorized.

CONTENTS

Upper Ocean Thermal Structure of the Eastern Tropical Pacific

Maria C. Donoso[1], **Jessie E. Harris**[2], **and David B. Enfield**[3]

Abstract. A rigorous quality control (QC) procedure developed to assure the research quality of upper ocean thermal data, mainly from expendable bathythermographs, is described in detail. The QC scheme takes into account recommendations from different data centers and is carried out completely by oceanographers. The region of interest corresponds to the tropical Pacific from 30°N to 30°S and from the dateline to the west coast of the Americas. For a 15 year period (1979-93) 212,891 stations from five data sources (National Oceanographic Data Center, Joint Environmental Data Analysis Center, southeast Pacific, Navy declassified, and Tropical Ocean and Global Atmosphere Subsurface Data Center) were originally processed, of which 113,589 profiles were kept after rejecting duplicates and submitting the data to the scientific QC process. The accepted temperature-depth profiles were binned into boxes of 2° latitude by 5° longitude. The climatology and bimonthly thermal fields (sea surface temperature, temperature at 50 m, temperature at 100 m, temperature of the 0-400 m layer, 20°C isotherm depth, and 15°C isotherm depth) are mapped.

1. INTRODUCTION

With the increasing interest in climate change, scientists are seeking to understand the role of oceans in influencing short- and long-term climate variability. Numerous theoretical investigations and more recently numerical modeling simulations have focused on studying how the world oceans vary in time and space (White *et al.*, 1982; Levitus, 1984; Donguy and Meyers, 1987, Hayes *et al.*, 1989; Ji *et al.*, 1994). Because the oceans play a key role in the global climate system, a more precise knowledge of the upper ocean, especially in the El Niño-Southern Oscillation (ENSO) region, is a crucial factor in the endeavor to comprehend seasonal to interannual climate variability (Clancy *et al.*, 1992). Because sea surface temperature (SST) patterns and their variability are thought to influence short-term climate (Enfield, 1989), an improved knowledge of the upper ocean processes that control SST is essential. Moreover, ocean general circulation models (OGCMs) that assimilate upper ocean data provide useful SST

---

[1] University of Miami, RSMAS, Department of Meteorology and Physical Oceanography, 4600 Rickenbacker Causeway, Miami, FL 33149 (e-mail: donoso@aoml.erl.gov).
[2] NOAA, Atlantic Oceanographic and Meteorological Laboratory, Physical Oceanography Division, 4301 Rickenbacker Causeway, Miami, FL 33149-1097 (e-mail: jharris@aoml.erl.gov).
[3] NOAA, Atlantic Oceanographic and Meteorological Laboratory, Physical Oceanography Division, 4301 Rickenbacker Causeway, Miami, FL 33149-1097 (e-mail: enfield@aoml.erl.gov).

analyses as well as initial conditions for predictive model runs. Carefully processed thermal profiles are clearly useful in many other ways, e.g., to verify and calibrate satellite altimeter data.

To understand how the ocean-atmosphere system works and ultimately make predictions, we need to analyze upper ocean processes using the existing data. The insufficient availability of high-quality data over adequate temporal and spatial scales frequently hampers this task, which in turn precludes the assessment of theoretical formulations or model simulations. As concluded by Chao and Philander (1993), the outcome of individual modeling approaches is directly dependent on observations over the entire region of interest. Multiple process studies under the National Oceanic and Atmospheric Administration (NOAA) Climate and Global Change Program, e.g., Pan-American Climate Studies (PACS), require upper ocean thermal data of scientific quality.

Networks of volunteer observing ships (VOSs) have been developed to monitor the variability of the near-surface thermal structure of the ocean (Phillips *et al.,* 1990; Sprintall and Meyers, 1991; Meyers *et al.,* 1991). The primary method is the deployment of expendable bathythermograph (XBT) probes from vessels of opportunity (commercial, military, fisheries) by nonspecialized personnel. These are supplemented by XBT and conductivity-temperature-depth (CTD) measurements by research cruises. The temperature profiles so obtained are subject to errors of many kinds and must be properly processed to assure research quality and subsequently be made available to the scientific community. Today, data processing and storage are being carried out by individual researchers, national institutions, e.g., National Oceanographic Data Center (NODC), National Climatic Data Center (NCDC), and Fleet Numerical Meteorology and Oceanography Center (FNMOC), and international data centers, under the auspices of large-scale international programs, e.g., Tropical Ocean and Global Atmosphere (TOGA), World Ocean Circulation Experiment (WOCE), International Geosphere-Biosphere Programme (IGBP), and World Climate Research Programme (WCRP). The formats and quality control procedures vary from one data management unit to another, although universal norms are increasingly being adhered to.

The specific goal of the present work was to process and screen subsurface data from different sources, but primarily from XBTs, and to integrate them into a single data base. This data set will provide ready-to-use upper ocean thermal data to interested researchers and organizations. The final objective of the project is to understand the seasonal to interannual variability of the tropical Pacific.

This effort forms part of the contribution of the NOAA Atlantic Oceanographic and Meteorological Laboratory (AOML) to the Equatorial Pacific Ocean Climate Studies (EPOCS) Program.

The structure of the document is as follows: Section 2 gives a summary of the different data sources; Section 3 describes the data base processing and quality control procedures; Section 4 presents a brief discussion of the methods used to map the thermal structure of the eastern tropical Pacific; and Section 5 summarizes the outcome of the present work. Appendix A describes the mapping interpolation scheme, and Appendix B defines the acronyms used in this report. Following the appendices, maps are presented, showing the following fields: SST, temperature at 50 m, temperature at 100 m, mean temperature of the 0-400 m layer, depth of the 20°C isotherm, and depth of the 15°C isotherm. The first set of maps shows the bimonthly climatological fields for the entire 1979-93 study period. The second set shows the bimonthly fields for each year of the study period.

2. DATA SOURCES

Subsurface thermal data archived at different management units consists of XBT profiles, mechanical bathythermograph (MBT) cast data, digital bathythermograph (digital BT) profiles, CTD profiles, and bottle cast data. Contributing vessels collect and transmit data in real, near-real, and delayed time. More recently, data collected from buoys, both moored Tropical Atmosphere Ocean (TAO) buoys (Hayes *et al.*, 1991) and drifters (Reynolds and Smith, 1994), have augmented considerably the number of available subsurface observations in the tropical Pacific.

In the present effort to integrate various data sets (see Table 1) into a single, primarily XBT, data base, we integrated, checked, and flagged 212,891 temperatures profiles from different sources for the period January 1979 to December 1993. NODC and the Joint Environmental Data Analysis (JEDA) Center were the major data contributors. Much redundancy existed among these two data bases. However, the number of profiles unique to JEDA was still significant. This is because we used the NODC delayed-mode data obtained from the XBT data archive files of the Global Ocean and Salinity Profiles CD-ROMs (NODC, 1991), and JEDA provided us with real-time data, radio messages, and other bathythermograph profiles (i.e., MBT, digital BT, etc.) along with delayed-mode data. The high rejection totals for JEDA reflect our decision to retain the NODC profiles in cases of exact duplicates.

Table 1. Number and percentage of rejected and accepted temperature profiles from each data source

Years	Source	Original	Rejected		Accepted	
		No.	No.	%	No.	%
1979-90	NODC	45,645	1,536	3	44,109	97
1979-93	JEDA	129,109	87,241	68	41,868	32
1979-87	SE Pac.	3,098	659	21	2,439	79
1986-88	Navy	5,281	1,100	21	4,181	79
1989-93	TSDC	29,758	8,766	29	20,992	71
1979-93	Total	212,891	99,302	47	113,589	53

The TOGA Subsurface Data Center (TSDC) in Brest, France, provided a substantial number of profiles for the last 4 years of the study period, where data from NODC and JEDA were lacking. French research vessels and the French-American cooperative VOS program provided most of the profiles exclusive to this data set. Data for the southeast tropical Pacific was augmented by reprocessing the 1979-87 portion of the data compiled by Lagos *et al.* (1991). JEDA provided declassified data from the U.S. Navy (1986-88) as a separate group of unprocessed data, which we also processed and integrated into the data base. We also intended to merge the AOML data base with the carefully edited data of Kessler (1989). However, problems with the Kessler header formats would have prevented proper checking for duplicates, and it was estimated that few (if any) profiles would have been unique additions. Figure 1 summarizes the contributions of each data source to the fully processed data.

Although most of the data sets integrated in the present work went through a certain amount of quality control processing, the inhomogeneity of the procedures and flagging systems used in each case forced us to reprocess all acquired observations. Eliminating duplicate profiles and submitting the data to the rigorous scientific quality control procedures described in the following section reduced the total number of profiles from 212,891 to 113,589.

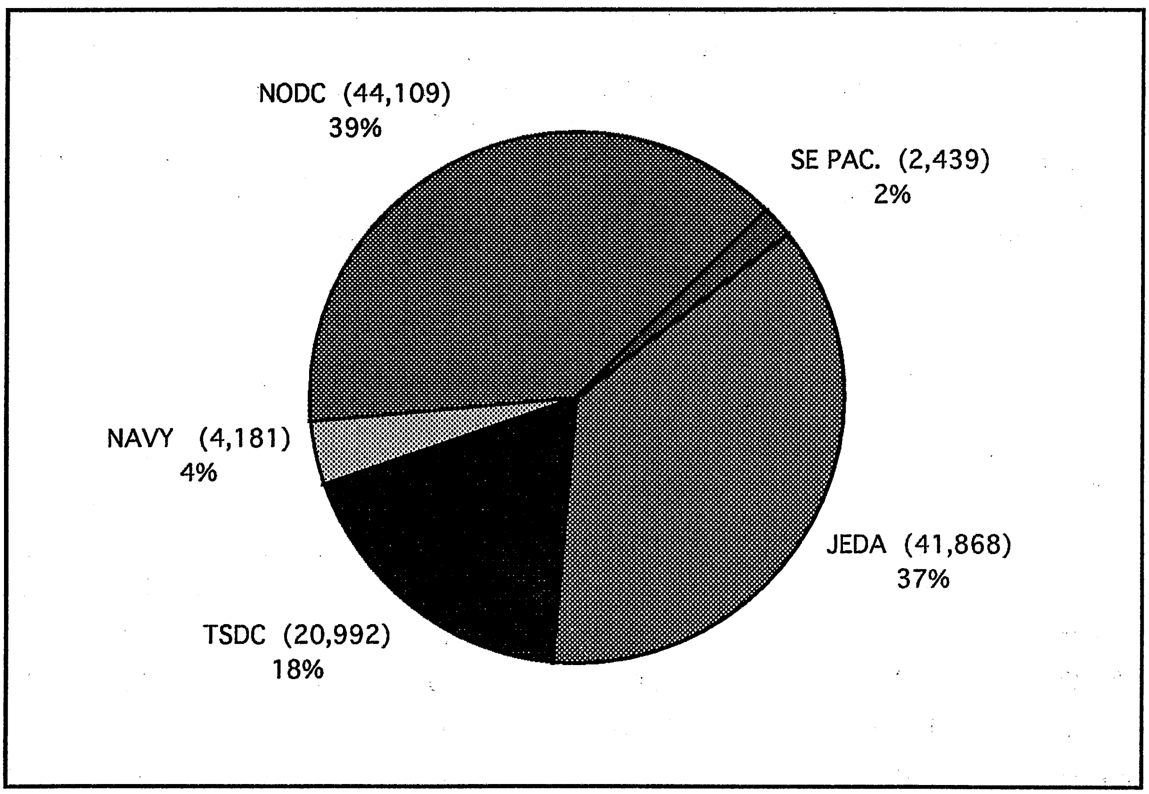

Figure 1. Number of processed observations and percentage of the total, by source.

Figure 2a maps the positions of all the stations for the period 1979-93 and Figs. 2b-2f show the contributions of individual data sources. Figures 3a-3f give the spatial distribution of the observations for each bimonth of the calendar year. The dots on the plots presented in this report display the positions of the stations used to derive the corresponding thermal fields.

Figure 4 shows the distribution of profiles in time, by source and in total. Although some additional delayed-mode data will undoubtedly become available subsequent to this compilation, the total monthly profile numbers shown here are fairly homogeneous in time. The average number of profiles per individual bimonthly period per 2° x 5° bin is 2.

3. PROCEDURES

Quality control (QC) has ranged, over the years, from none to complex comparison techniques (Smith *et al.*, 1991; Pazan and White, 1993; CSIRO, 1993; Bailey *et al.*, 1994). The effort needed to process a particular data set is highly dependent on the QC procedures applied to it. The formation of a readily accessible data base of research quality requires a hierarchy of processing levels. The procedure used in preparing this data base included data acquisition, testing for regionality and prohibited locations (polygon test), exclusion of duplicate data, preliminary detection of questionable profiles, and fine, mostly subjective, scientific quality control (SQC).

3.1. Initial Screening

After acquiring the data from the sources described in the previous sections, and prior to any level of processing, we applied the polygon test for regionality (i.e., is the profile in the area of interest?) and prohibited locations (e.g., is the profile located over land?).

Significant redundancy exists within individual data sets and among the profiles from different sources. The most common case of duplication consists of profiles that were included in the data sets initially in real or near-real time in the form of radio messages and later on as delayed-mode submissions. The first level of data processing therefore consisted of detecting duplicate profiles inside a data set (intrasource). Once a data set was determined to be free of duplicates and ready to be included into the data base, we used a similar procedure to detect duplicate profiles between separate data sources (intersource).

Each profile was checked against its neighbors in both space and time. Any two profiles within a distance of 0.5° and 25 h of each other were identified as possible duplicates. We defined three types of duplicate data: exact , quasi-exact, and non-exact duplicates.

Exact duplicates are profiles with exactly identical temperature values at all depths as well as identical headers (date-time group, location, vessel, etc.). Exact duplicates were trivial to detect and were dealt with objectively (without human intervention) by the software developed at AOML.

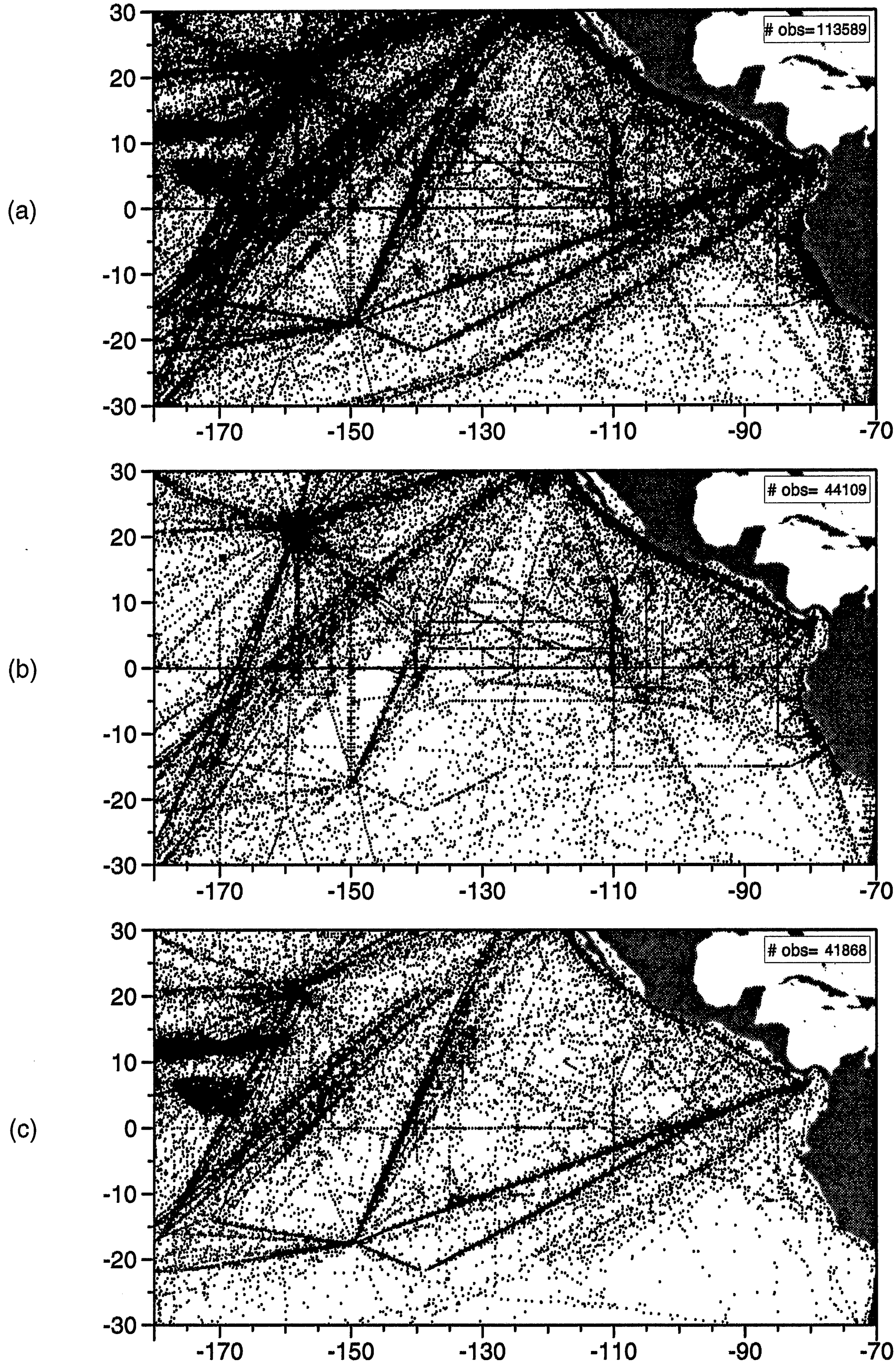

Figure 2. Observations during the period 1979-93 for (a) all sources, (b) NODC, and (c) JEDA.

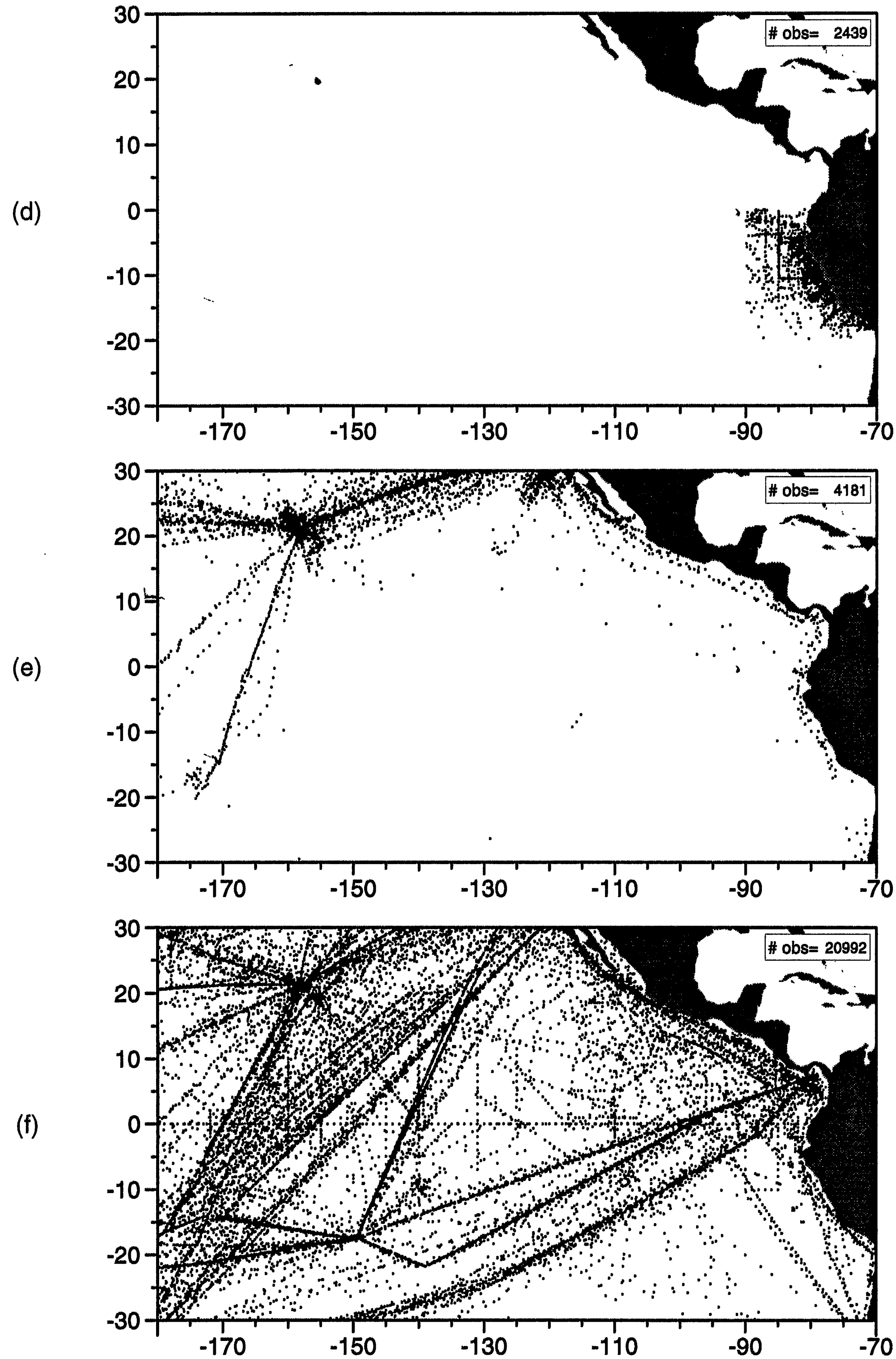

Figure 2 – *continued*. Observations during the period 1979-93 for (d) southeast Pacific, (e) Navy declassified, and (f) TSDC.

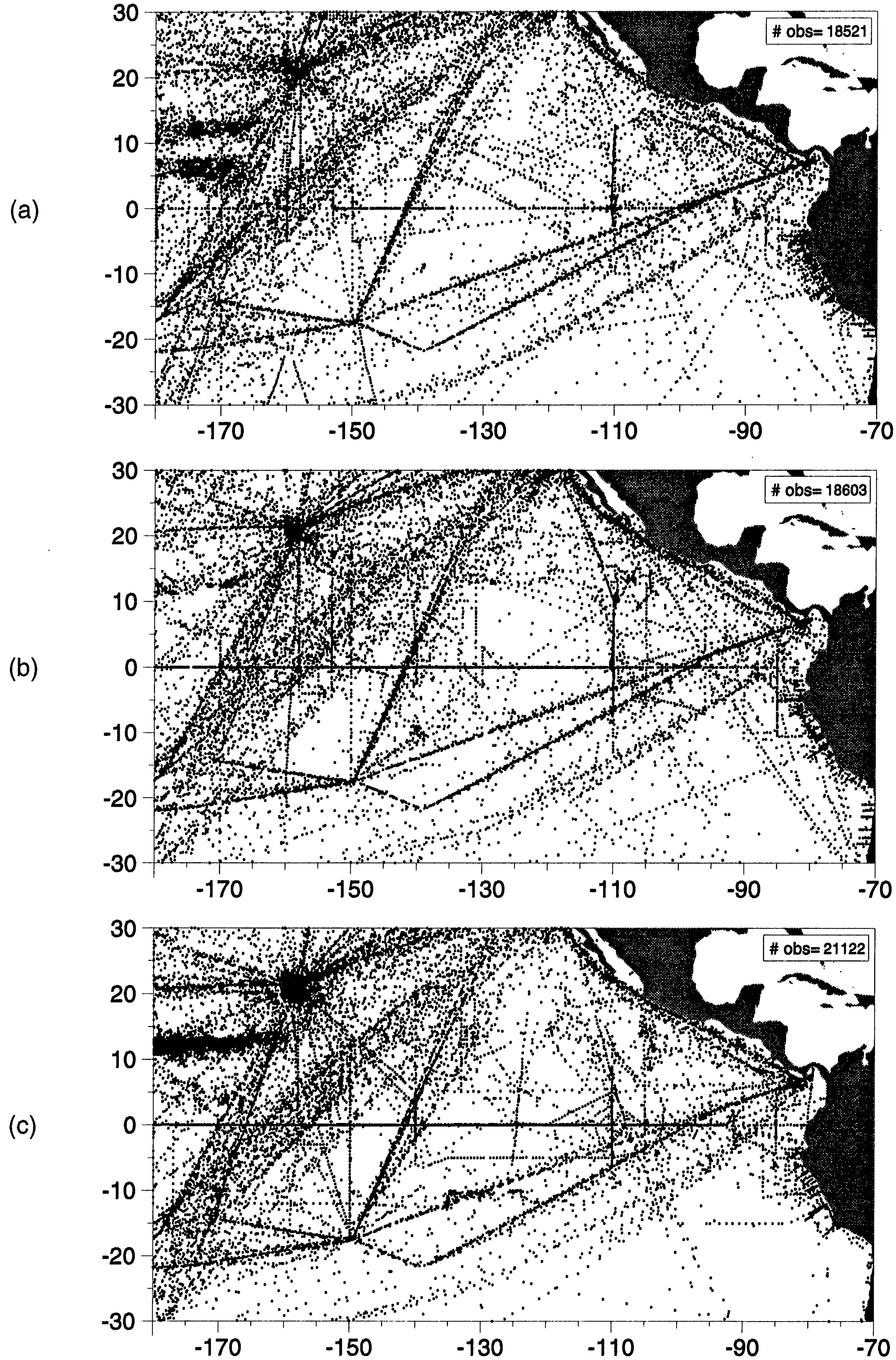

Figure 3. Observations during the period 1979-93 for (a) January-February, (b) March-April, and (c) May-June.

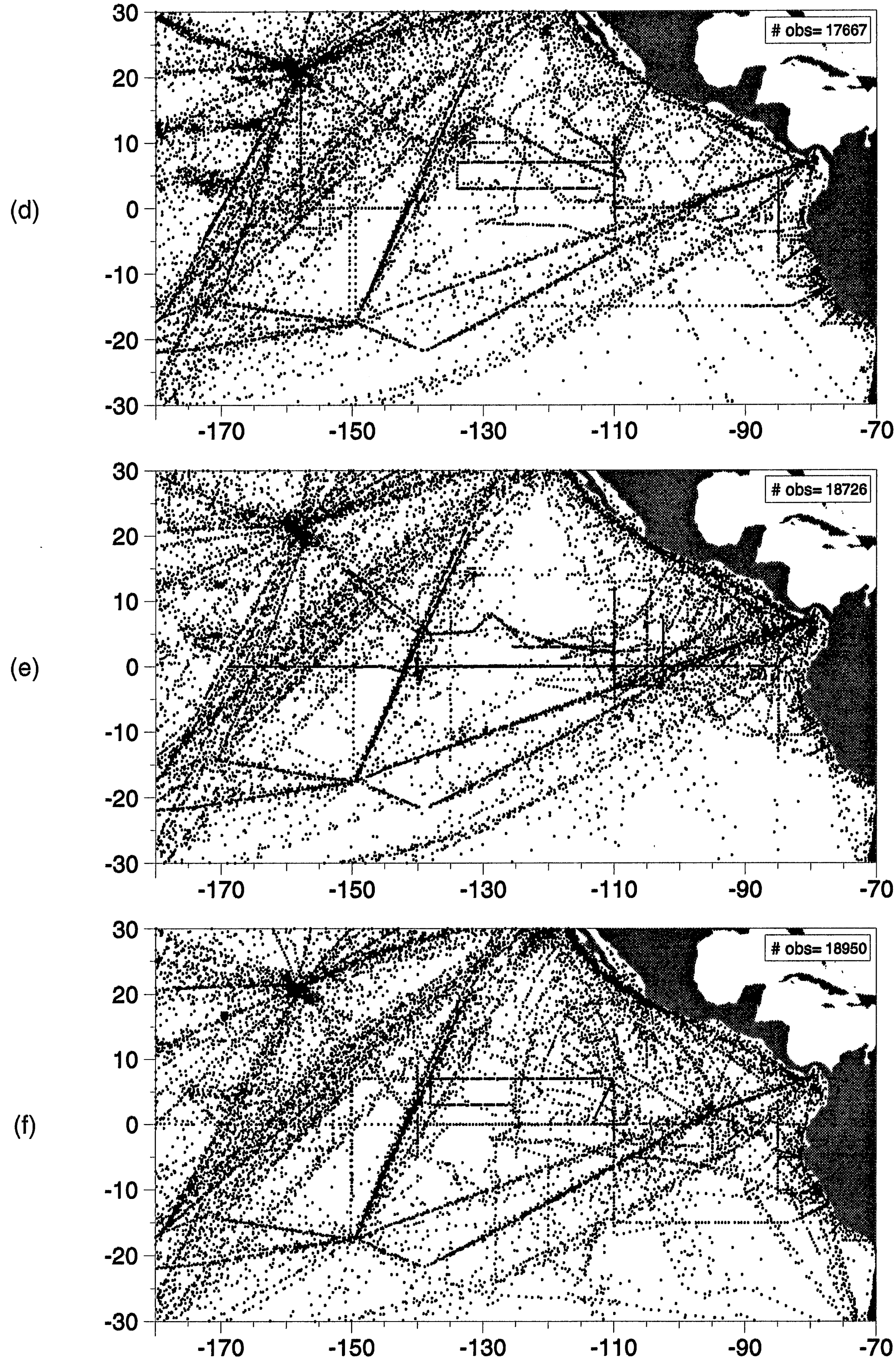

Figure 3 – *continued*. Observations during the period 1979-93 for (d) July-August, (e) September-October, and (f) November-December.

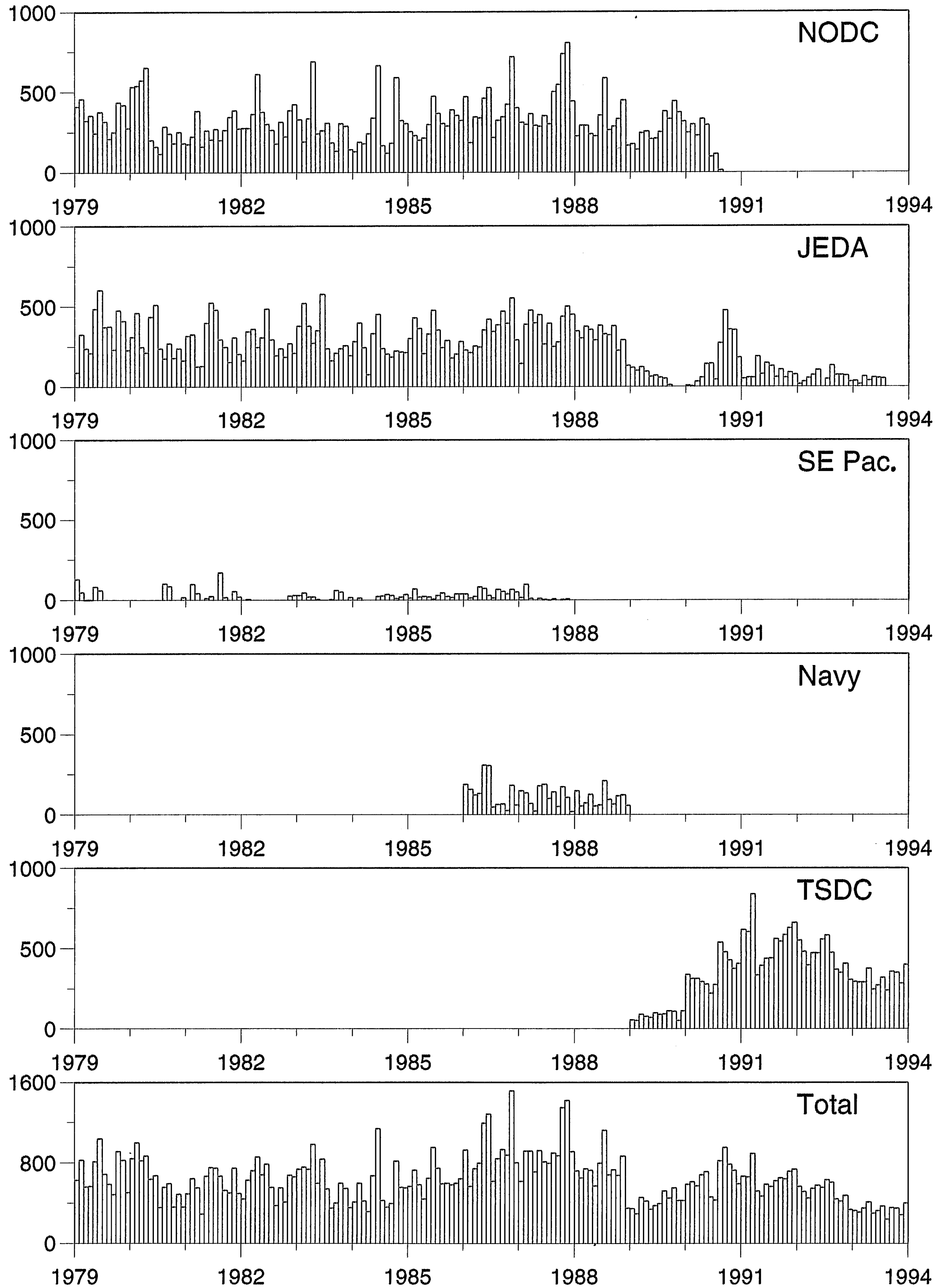

Figure 4. Distribution of number of observations per month by source.

Quasi-exact duplicates have very similar, though not necessarily the same, depth-temperature profiles and header information. Quasi-exact duplicates are required to have temperature values within a tolerance of 0.3°C at any depth and be within a distance of 0.1°. The header of these stations must exhibit the same hour and day. Examples of these types of duplicates are those found when comparing real-time radio messages and delayed-mode data, or inflection point cast data and selected depth profiles. In the first case, we kept the delayed-mode data, and in the second case, we retained the inflection point profiles. To avoid the possibility of rejecting time series stations (research cruises), we labeled quasi-exact duplicates as such only in cases where the original data sources were different. Software was developed to detect quasi-exact duplicates after we worked with the data for a period of time and gained insight that allowed us to define selection criteria with confidence.

All groups of profiles within 25 h and 0.5° distance that were not identified as exact or quasi-exact duplicates were examined by an oceanographer. When a pair was identified as duplicates at this stage, they were referred to as non-exact duplicates. In all cases we attempted to retain as much information as possible in the data base. The case with the most header information or higher density profile was kept. Those profiles considered to be duplicates (rejected) were ignored in later processing and are not part of the final data base.

After we tested all profiles within a set for redundancy, we used a similar procedure to detect duplicate profiles between separate data sources. The first data incorporated in our data base were acquired from JEDA, followed by those from NODC. If duplicates were detected among these two sources, we retained the NODC profile, with few exceptions (e.g., when the NODC profile truncated at a lesser depth). This joint NODC-JEDA set of unique profiles constituted our initial core data base against which data from other sources (Navy declassified, southeast Pacific, TSDS) were checked for duplicates during the intersource phase of the processing.

3.2. Quality Control

The quality of the data from different sources is not the same. We developed a SQC procedure to set flags on the temperature-depth profiles without changing or deleting a data value from any profile. The flagging system took into account recommendations from different data centers (Pazan and Noe, 1987; CSIRO, 1993; Daneshzadeh *et al.,* 1994). Flags were set for individual temperature-depth pairs as well as for entire profiles.

The QC process consists of two stages, a preliminary detection of questionable profiles and a SQC. In both stages the data are submitted to objective (no human intervention) and subjective (human-machine interaction) tests. The following subsections present a description of each of the two QC stages.

3.2.1. Detection of questionable profiles

The detection of questionable profiles is an objective-subjective process. As a first step, we estimated the statistics (mean and standard deviation) for 5° latitude/longitude boxes with sufficient data to carry out these computations. Initially, we calculated the raw mean directly from the data base for the period 1979-93. Subsequently, after discarding all profiles that were more than 2 standard deviations from the raw mean, we recalculated a second mean, the "bootstrap" mean. When new data were added to the core data base, the raw and bootstrap mean were recalculated. The tendency of the bootstrap climatology is to improve from one calculation to another as the number of profiles increases.

Individual profiles were then objectively compared with statistics derived from the data base. Profiles were also checked against the mean climatology derived by Levitus (1982) for 1° longitude/latitude boxes. In regions with not enough data to calculate the raw and bootstrap means and standard deviations, the data were compared only with the Levitus 1° x 1° climatological mean profiles. The objective screening software allows a user to specify the acceptable tolerance (in standard deviation multiples) within which the data can fall. For the present work, we set the tolerance to 3-sigma about the clean bootstrap mean and 5°C about the Levitus 1° x 1° climatology. If the temperature at any depth in a profile exceeded either tolerance, we identified the profile for subsequent subjective evaluation.

We also subjected the data to an objective QC procedure that made a series of gross-error checks on every temperature-depth profile. The tolerances we used were based upon the current scientific knowledge of the upper ocean temperature variability in the tropical ocean. The data were tested and selected for further scrutiny according to the following criteria:

- Depth of the first temperature value greater than or equal to 5.0 m.
- Depth of the second temperature value greater than or equal to 200.0 m.
- Temperature-depth pairs separated by more than 350.0 m.
- Temperature less than 2.0°C or greater than 35.0°C.
- Temperature-depth pairs associated with spikes defined by a vertical gradient of temperature exceeding 1.0°C m^{-1}.
- Temperature-depth pairs with temperature greater than or equal to 20.0°C at depths of 350.0 m or more.
- Temperature-depth pairs associated with a vertical gradient of temperature exceeding 5.0°C m^{-1}.
- Number of inversions of more than 0.2°C greater than or equal to one-third of the total number of temperature-depth pairs in the profile.

As a final test, an iterative software package developed for this purpose allowed an oceanographer to examine "waterfall" plots of profiles along ship tracks to detect irregularities in their time-space continuity. The expert identified inconsistent profiles for future examination.

3.2.2. Scientific quality control

The SQC procedure is a subjective process in which an oceanographer scrutinizes previously selected profiles both individually and within the oceanographic context set by a subsample of stations within a prespecified time/space neighborhood. Graphics windows are opened in two programs that run simultaneously for solo-mode and context-mode screening. In solo-mode screening the suspicious profile is displayed in detail and the oceanographer can ask for other profiles occurring historically at the same time of year to be superimposed, color-coded to a displayed list of time and location information. The average and sigma-level profiles from both the bootstrap and Levitus climatologies are also displayed. If a flagging decision is not obvious at this stage, a waterfall plot of the station and its space-time neighbors is requested and displayed by the context-mode program, together with a geographics plot of the station positions. The oceanographer then makes a final decision regarding the profile and assigns flags accordingly. The structure of the flagging system is summarized in Table 2.

Table 2. Description of the flagging system used in the quality control process

Flag	Quality	Description
1	Good data	Temperature-depth pair accepted as good without reservation
2	"Probably" good data	Temperature-depth pair corresponding to an anomalous but probably real feature
3	Bad data	Temperature-depth pair representing a doubtful or obviously erroneous feature at an intermediate depth; used in cases where there is enough confidence in the validity of the observed data deeper than the feature
4	Bad data	Temperature-depth pair representing a doubtful or obviously erroneous feature; used in cases where the data below the depth of such feature is also erroneous (truncation)
5	Undefined	Not used
6	Bad data	Temperature-depth pair representing an erroneous feature; used when the entire profile is rejected

For this study, if the profile was accepted as good without reservation, the profile was reassigned a flag value of 1, identical to profiles not selected for scrutiny at earlier stages. If a profile was to be rejected in its entirety, all temperature-depth pairs in the profile were flagged with a value of 6.

Frequently, profiles previously singled out as questionable contained good data in which one or more unusual but realistic features were observed. In such cases, we considered the data as "probably good" and assigned a flag value of 2 to the temperature-depth pairs representing features (probably real) that triggered selection at an earlier stage.

Profiles identified as inconsistent or questionable during the previous stage were still sometimes partially accepted provided the station registered apparently good data in which some unusual, doubtful, or obviously erroneous features were embedded. We rejected the temperature-depth pairs at or below the depth of such an anomalous feature by assigning them a flag value of 4 (profile truncation). However, if the profile presented a single spike (inversion > 0.2°C) at an intermediate depth and there was enough confidence in the observed data deeper than this feature, then we rejected the feature (assigned a flag value of 3), while accepting the rest of the profile. Unlike other data management units (Pazan and Noe, 1987; CSIRO, 1993; Daneshzadeh *et al*, 1994) we accepted the possibility for a profile to recover after an anomalous reading. The software allowed individual scientists to override this decision by truncating the profile from the depth of the shallowest temperature-depth pair with a flag value of 3.

We exercised caution when flagging temperature-depth pairs as good (1), probably good (2), or bad (3, 4, 6), because our experience confirmed that the thermal structure in many regions presents singular but real variations such as salinity-compensated inversions offshore of upwelling zones and steplike behavior along the equator. We could frequently validate or reject singular or anomalous features by viewing them in the context of neighboring stations and/or by otherwise using our knowledge of oceanographic features in particular regions.

Erroneous features due to instrument malfunction, mainly wire stretch and leakage, were also observed. The distinction between probably real features and instrument errors was sometimes a difficult and subjective process that required experience and knowledge of the region under consideration, because there can be a variety of errors and oceanographic features recorded within the profile. When such cases could not be resolved, they were identified with a special flag for later scrutiny by another (usually more experienced) oceanographer. In cases of persistent doubt, a decision was usually made in favor of rejection.

In the final step of the SQC we displayed and printed contoured monthly thermal fields to further identify suspicious data (i.e., profiles that produced "bull's-eyes") within the large-scale geographic context of all data from the tropical Pacific domain. At that stage we used only the temperature-depth pairs with flag values of 2 or less. We generated contoured fields at several depth levels: surface (SST), 50 m, 100 m, 200 m, 300 m, 400 m and the average temperature of the upper 400 m layer. Here too, "oceanographic sense" played a role. What appears as a bull's-eye may be an artifact of how a legitimate oceanographic feature was sampled. For example, a single XBT section crossing the North Equatorial Countercurrent (NECC) may cause the northern edge of the NECC to appear as a low-valued bull's-eye near the top of the thermocline (as opposed to a zonal trough) if little or no data are available to the east or west of the section. In such a case, the anomaly would be smaller at the surface and decrease or disappear at deeper levels. Suspicious profiles causing unexplainable bull's-eyes were flagged for scrutiny and subjected to a second pass through the SQC procedure.

It must be emphasized that we did not modify or delete from the archives the rejected or partially rejected profiles (temperature-depth pairs with flag values of 3 or higher); thus the original profiles may always be retrieved. When the data base is prepared for a particular research application, the flagging scheme allows the researcher the flexibility to use or ignore the flagged data in accordance with his/her own criteria.

The QC procedure described herein was developed to assure the research quality of the temperature data. During the process, caution was exercised at any instance of uncertainty, while ensuring that good data were not rejected. Table 1 gives the number of profiles from each data source that were accepted after being submitted to the QC procedure.

4. GENERATION OF OBSERVED FIELDS

Profiles having temperature-depth pairs with flag values of 2 or less constituted the "clean" data base that was used as input for the thermal fields shown in this report. We binned the selected data into boxes of 2° latitude by 5° longitude for bimonthly periods, for 1979 through 1993 (15 years). Bimonthly averaging is the minimum required to clearly resolve the seasonal variations at the 2° x 5° spatial resolution.

White *et al.* (1982) and Hansen and Herman (1989) estimated zonal decorrelation scales of 1500 km and 2000 km, respectively, for the tropical Pacific and meridional scales of 100 km and 900 km. These estimated scales are influenced by interannual variability, which in turn is dominated by ENSO cycles (Meyers, 1993). Using a data set that did not include ENSO events, Meyers *et al.* (1991) estimated a zonal scale of 1500 km and a meridional scale of 300 km, and a time scale of 2 months. White (1993) analyzed temperature-depth observations from 1979 to 1991 and proposed a 2° latitude by 5° longitude grid for mapping variability in the upper 400 m of the global ocean. He argued that his grid size resolves the spatial features of the annual cycle, the Quasi-Biennial Oscillation (QBO), and the ENSO variability. Also, according to Kessler and Taft (1987), the meridional scale of 2° latitude is the largest bin size that can resolve the major zonal currents in the tropical Pacific. The 5° longitude scale is at least twice the size of the internal (first baroclinic mode) Rossby radius everywhere in the region of interest (Kessler, 1989). In summary, binning the data in 2° latitude by 5° longitude boxes provided an adequate scale to achieve our analysis within the limitations of the data available.

Figure 5 presents the total number of observations per bin for the study period, 1979-93. As can be seen from this figure, most of the tropical north Pacific is adequately sampled, but the southern hemisphere presents regions of very sparse data. To fill in grid points where no data are available, we used in the mapping stage an interpolation scheme based on cost function minimization (Thacker, 1988). Appendix A gives a brief description of the method. This interpolation routine has been applied in previous studies at NOAA/AOML (Roa *et al.*, 1989; Mayer and Weisberg, 1993). Dot plots of the XBT stations used superimposed on the bimonthly thermal fields show where the data are sparse in each bimonthly period.

5. DISCUSSION AND CONCLUSIONS

An improved knowledge of the upper ocean thermal structure is required to better understand the present climate and ultimately make predictions of its seasonal to interannual

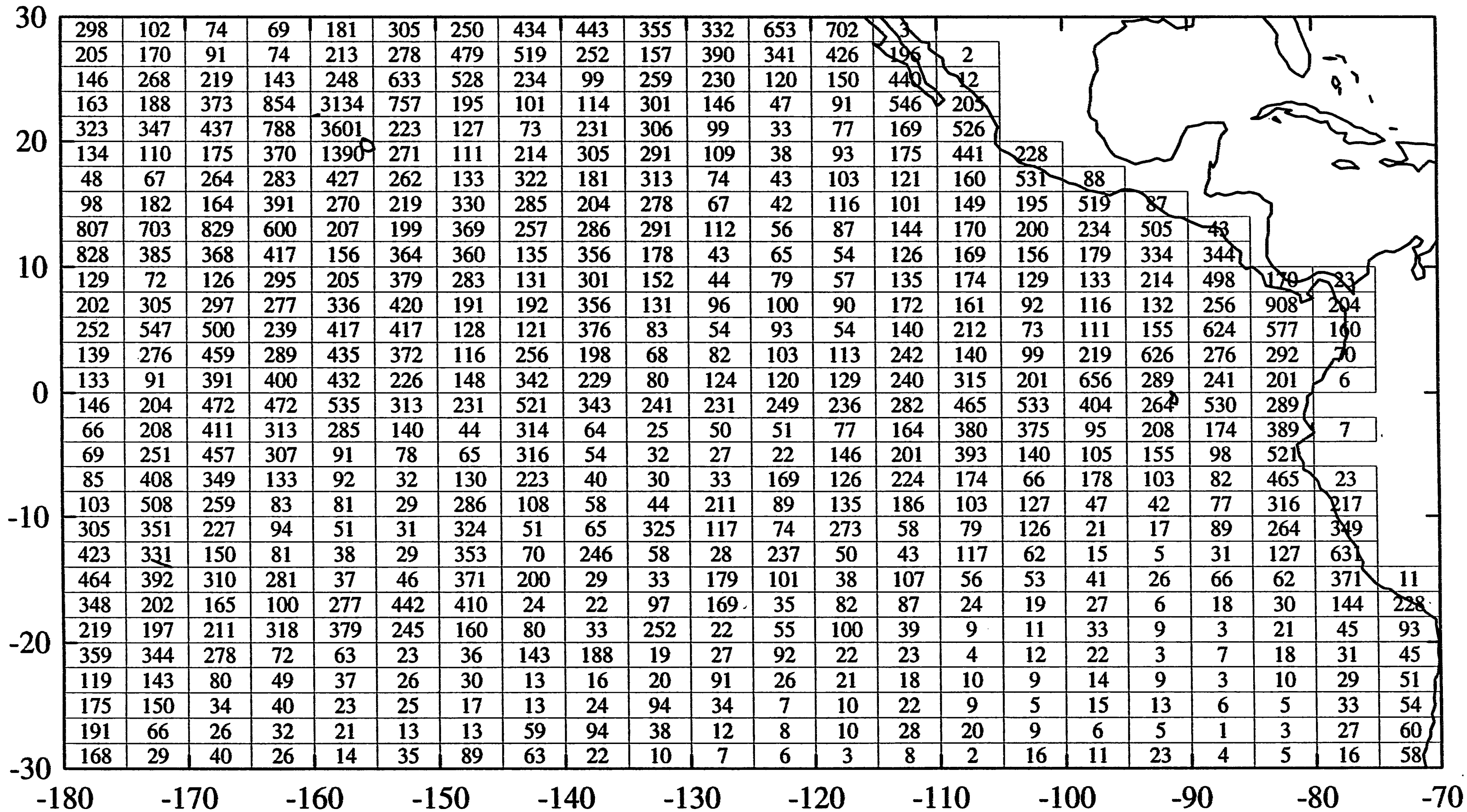

Figure 5. Total number of observations per 2° latitude by 5° longitude box for the period 1979-93.

variability. This requires the analysis of complete and carefully processed ocean thermal data. For this purpose, we have methodically combined tropical Pacific XBT profiles from five different data sources and reprocessed more than 200,000 temperature profiles for the period 1979-93 (Table 1). The effort far exceeded our original estimates. We attribute this to a number of discrepancies between the actual and previously imagined quality of the available data sources, including critical errors and deficiencies in the header information from years preceding currently adopted norms. This required reformulation of the data base formats and flagging system, and the creation of interactive software for reprocessing virtually all the data from scratch. After rejecting duplicates and submitting the data to our rigorous scientific quality control process, 113,589 profiles were accepted. We now feel we have a subsurface thermal archive of research quality that can be successfully applied to problems of ocean climate variability.

The distribution of XBT observations in the eastern tropical Pacific is not homogeneous (Figs. 4 and 5). XBT coverage is dense in the vicinity of Hawaii, off the west coast of North America, and along the major Pacific VOS lines. Sampling is adequate for deriving climatological fields in the northern part of the study area (north of 10°S). The concentration of observations is considerably reduced in the southeastern corner of the region (especially within the triangle with vertices at 130°W, 70°W, and 10°N). In this area, some features are climatologically representative, some are not, depending on the data availability for each bimonthly period. The spatial and temporal distribution of the data should be taken into account when interpreting the upper ocean thermal fields. The fields shown in this report (SST, T50, T100, T0-400, D20, and D10) were chosen because their signal clearly represents the thermal variability observed in the region.

The SST average variability is 2°C. The highest temperature changes are observed at the equatorial band and along the two major boundary currents, the California current and the Peru current. Off the coast, especially in the vicinity of Central America (i.e., near the Gulf of Tehuantepec), SST variability can be greater than 5°C. This is due to local air-sea interaction processes, more specifically, vortex genesis related to the effect of strong locally intense winter wind outbreaks that occur intermittently in this region (Donoso and Chassignet, 1992). The coldest waters are found off the coast of Baja California and along the coast of South America. West of Galápagos, centered slightly south of the equator, lies a seasonally modulated band of cooler water, the equatorial cold tongue, that is always apparent to some degree except during strong ENSO events. Two zonal bands of warm water, with mean average temperature greater than 27°C, extend from the west, centered at 5°N and 10°S, respectively. The northern band reaches the coast of Central America and expands from near the equator to as far north as 15°N. The southern band rarely extends east of 120°W, but in the northern winter it can reach as far as 23°S. The extension and intensity of these bands increase during the corresponding hemispheric summer-autumn period.

The average temperature at 50 m is 24°C. This field is highly variable, especially over the easternmost sector where the upper thermocline penetrates this depth in places. At certain times and locations, the variability is dominated by seasonal features such as the Costa Rica Dome and wind-forced eddies from the Gulfs of Tehuantepec and Papagayo.

The T100 field is characterized by the presence of a pronounced ridge usually centered along 10°N, and a less distinct ridge at the equator. The first ridge delimits the northern border of the NECC (countercurrent ridge) and it corresponds to the zone of surface divergence and upwelling between the NECC and the NEC. The fact that the countercurrent ridge is only faintly seen at T50 suggests that the 50 m level is penetrated only weakly and less permanently by the thermocline. The presence and extent of the NECC is depicted by the strong gradient between the countercurrent ridge (10°N) and the countercurrent trough (4°N). Despite the unevenness of the XBT sampling, the north-south displacement of the countercurrent ridge (associated with a seasonal migration of the meridional position of the ITCZ) can be well observed along specific longitudinal sections that coincide with VOS lines (not shown in this document).

In the eastern Pacific, the 20°C isotherm is usually near the middle of the thermocline (Donguy and Meyers, 1987), and the distribution of the 20°C isotherm depth (D20) is frequently used in oceanographic studies to represent thermocline variability (Hansen and Herman, 1989; Lagos *et al.*, 1991; Fiedler, 1992). The D20 variability is not homogeneous throughout the study area. Changes of more than ±20 m are observed at higher latitudes (poleward of 20°N and 20°S). Considerable interannual variability of the thermocline depth (D20) is observed in the equatorial band, which reflects the effect of anomalous events associated with ENSO cycles.

In some coastal areas, the 20°C isotherm surfaces during part of the year, which is evidence of upwelling in these regions. The most prominent signal is detected in the southeast, off the coast of South America. There the 20°C isotherm surfaces for about 4-5 months (August-December). Away from the coast, between 12° and 22° (north and south), relatively little annual variation (≤10 m) is found in the D20 field. The 15°C isotherm depth (D15) gives a useful indication of the location of the lower boundary of the thermocline, especially in the eastern Pacific where the 20°C isotherm frequently surfaces. Although variability is observed on interannual and seasonal scales, it is less pronounced than that of the D20 field.

Vertically averaged temperatures over the upper 400 m (T0-400) are proportional to the heat content. The anomalies observed in this field reflect the variability of the upper layer thickness and consequently provide input as to how the heat is distributed in the region. T0-400 is also distributed in a manner very similar to dynamic topography. The mean vertically averaged temperature in the study area is 15°C. The highest variability occurs along the equator and over nearshore areas where we also notice larger fluctuations in the depth-dependent distributions. The average spatial and temporal variability of the T0-400 field is 1.2°C.

To optimally use our unevenly distributed profiles, we recommend the application of a data-adaptive analysis strategy. The analysis of the thermal fields derived with this new XBT data set should be consistent with the observation density in time and space. Thus, for deriving long-term mean fields and seasonal climatologies, a monthly time resolution may be feasible for 2° latitude by 5° longitude bins or even smaller, depending on the application, over most of the region north of 10°S. The time-variable departures from long-term means places more severe constraints on resolution, with a grid no thinner than 2° x 5°, and time averages of at least 2 months or a season. In both instances, the poor data coverage in the southern portion of the tropical Pacific, especially in the southeast region off the coast of South America, may dictate even less resolution.

6. ACKNOWLEDGMENTS

The authors thank Stephan Pazan and Steve Diggs at JEDA, Jean Paul Rebert at TOGA Subsurface Data Center, William S. Kessler at PMEL, and Pablo Lagos, for providing the original data sets. We are grateful to the NOAA/AOML Atlantic XBT Group, Robert L. Molinari (P.I.), John Festa, Sidney M. Minton, and Yuen-Ho Daneshzadeh, for sharing their expertise.

We also acknowledge Warren Krug (NOAA/AOML) and Chris Noe (NOS) who furnished us with the ship identification codes. We express our appreciation to W. Carlisle Thacker for providing advice on the mapping interpolation scheme.

Our special acknowledgment to Maria del Pilar Cornejo for processing the southeast Pacific data and participating in some stages of the quality control.

This work was supported in part by the Equatorial Pacific Ocean Climate Studies (EPOCS) Program.

7. REFERENCES

Bailey, R., A. Gronell, H. Phillips, G. Meyers, and E. Tanner, 1994: CSIRO cookbook for quality control of expendable bathythermograph (XBT) data. Rep. No. 220, CSIRO Marine Laboratories, Hobart, Australia, 75 pp. (in press).

Chao, Y., and S.G.H. Philander, 1993: On the structure of the Southern Oscillation. *J. Clim.*, *6*, 450-469.

Clancy, R.M., J.M. Harding, K.D. Pollak, and P. May, 1992: Quantification of improvements in an operational global-scale ocean thermal analysis system. *J. Atmos. Oceanic Tech.*, *9*, 55-66.

CSIRO (Commonwealth Scientific and Industrial Research Organization), 1993: CSIRO cookbook for quality control of expendable bathythermograph (XBT) data: Version 1. CSIRO Marine Laboratories, Hobart, Australia, 74 pp.

Daneshzadeh, Y-H. C., J.F. Festa, and S.M. Minton, 1994: Procedures used at NOAA-AOML to quality control real time XBT data collected in the Atlantic ocean. NOAA Tech. Memo. ERL AOML-78, NOAA Atlantic Oceanographic and Meteorological Laboratory, Miami, FL, 44 pp.

Derber, J.C., 1985: The variational four-dimensional assimilation of analyses using filtered models as constrains. Ph.D. Dissertation, University of Wisconsin, Madison, 142 pp.

Donguy, J.R., and G. Meyers, 1987: Observed and modeled topography of the 20°C isotherm in tropical Pacific. *Oceanol. Acta*, *10*, 41-48.

Donoso, M.C., and E.P. Chassignet, 1992: Genesis and evolution of vortices off the Coast of Central America. Presented at the Central American and Caribbean Congress in Marine Sciences, Oct. 26-30, Santa Marta, Colombia, 14 pp.

Enfield, D.B., 1989: El Niño, past and present. *Rev. Geophys., 27,* 159-187.

Fiedler, P.C., 1992: Seasonal climatologies and variability of eastern tropical Pacific surface waters. NOAA Tech. Rep. NMFS-109, NOAA National Marine Fisheries Service, La Jolla, CA, 65 pp.

Hansen, D., and A. Herman, 1989: Evolution of isotherm depth anomalies in the eastern tropical Pacific Ocean during El Niño event of 1982-1983. *J. Geophys. Res., 94,* 14,461-14,473.

Hasdorff, L., 1976: *Gradient Optimization and Nonlinear Control.* John Wiley & Sons, New York, 264 pp.

Hayes, S.P., M.J. McPhaden, and A. Leetmaa, 1989: Observational verification of quasi real time simulation of the tropical Pacific ocean. *J. Geophys. Res., 94,* 2147-2157.

Hayes, S.P., L.J. Magnun, J. Picaut, A. Sumi, and K. Takenchi, 1991: TOGA-TAO: A moored array for real-time measurements in the tropical Pacific Ocean. *Bull. Am. Meteor. Soc., 72,* 339-347.

Ji, M., A. Leetmaa, and J. Derber, 1994: An ocean analysis system for seasonal and interannual climate studies. *Mon. Wea. Rev.* (in press).

Kessler, W.S., 1989: Observation of long Rossby waves in the northern tropical Pacific. NOAA Tech. Memo. ERL PMEL-86, NOAA Pacific Marine Environmental Laboratory, Seattle, 120 pp.

Kessler, W.S., and B.A. Taft, 1987: Dynamic height and zonal geostrophic transports in the central tropical Pacific during 1979-84. *J. Phys. Oceanogr., 17,* 97-122.

Lagos, P., D. Hansen, and A. Herman, 1991: Climatological atlas of the subsurface thermal structure of the eastern tropical south Pacific Ocean. NOAA Tech. Rep. ERL 444-AOML 34, NOAA Atlantic Oceanographic and Meteorological Laboratory, Miami, FL, 303 pp.

Levitus, S., 1982: Climatological atlas of the world ocean. NOAA Professional Paper 13, U.S. Gov. Printing Off., Washington, D.C., 173 pp.

Levitus, S., 1984: Annual cycle of temperature and heat storage in the world ocean. *J. Phys. Oceanogr., 14,* 727-746.

Long, R.B., 1989: Notes on assimilating observations into numerical models. Delft Hydraulics, The Netherlands, 41 pp.

Mayer, D.A., and R.H. Weisberg, 1993: A description of COADS surface meteorological fields and the implied Sverdrup transports for the Atlantic Ocean from 30°S to 30°N. *J. Phys. Oceanogr., 23,* 2202-2221.

Meyers, G., 1993: Past studies of space and time-scales for network design. *In* The use of sub-surface thermal data for climate studies, ITPO Rep. No. 9, WOCE Rep. No. 110/93, International TOGA Project Office, Geneva, Switzerland, 42.

Meyers, G., H. Phillips, N. Smith, and J. Sprintall, 1991: Space-time scales for optimal interpolation of temperature - tropical Pacific Ocean. *Prog. Oceanogr., 28,* 189-218.

NODC (National Oceanographic Data Center), 1991: Global ocean temperature and salinity profiles. CD-ROMs NODC-02 and NODC-03, Inf. Rep. No. 11, Washington, DC, 14 pp.

Pazan, S.E., and C. Noe, 1987: User's introduction guide to the Joint Environmental Data Analysis (JEDA) Center. SIO Ref. No. 88-1, Joint Environmental Data Analysis Center, La Jolla, CA, 13 pp.

Pazan, S.E., and W.B. White, 1993: JEDA Center annual report on global subsurface thermal structure - 1989. SIO Ref. No. 93-38, Joint Environmental Data Analysis Center, La Jolla, CA, 55 pp.

Phillips, H., R. Baley, and G. Meyers, 1990: Design of an ocean temperature observing network in the seas north of Australia: Part II, Tropical Indian Ocean: Statistics. Rep. 211, CSIRO Marine Laboratories, Hobart, Australia. 58 pp.

Reynolds, R.W., and T.M. Smith, 1994: Improved global sea surface temperature analysis using optimal interpolation. *J. Clim., 7,* 929-948.

Roa, R.R., R.L. Molinari, and J.F. Festa, 1989: Evolution of the climatological near-surface thermal structure of the tropical Indian Ocean: Description of the mean monthly mixed layer depth, and sea surface temperature, surface current, and surface meteorological fields. *J. Geophys. Res., 94,* 10801-10815.

Smith, N.R., J.E. Bloomley, and G. Meyers, 1991: A univariate statistical interpolation scheme for subsurface thermal analysis in the tropical oceans. *Prog. Oceanogr., 28,* 219-256.

Sprintall, J., and G. Meyers, 1991: An optimum XBT sampling network of the eastern Pacific Ocean. *J. Geophys. Res., 96,* 10539-10552.

Thacker, W.C., 1988: Three lectures on fitting numerical models to observations. GKSS 87/E/65, GKSS-Forschungszentrum Geesthacht GmbH, Geesthacht, Germany, 64 pp.

White, W., 1993: Global analysis of upper ocean temperature scales. *In* The use of sub-surface thermal data for climate studies, ITPO Rep. No. 9, WOCE Rep. No. 110/93, International TOGA Project Office, Geneva, Switzerland, 43-44.

White, W.B., G. Meyers, and K. Hasunuma, 1982: Space/time statistics of short-term climatic variability in the western north Pacific. *J. Geophys. Res., 87*, 1979-1989.

APPENDIX A: MAPPING INTERPOLATION SCHEME

The interpolation scheme estimates values of the thermal variables (SST, T50, T100, D20, D15, T0-400) on a regular computational grid, considering that the data are distributed over a two-dimensional space. The method consists of fitting the data with a piecewise-bilinear model surface using adjustable penalty terms to filter out unresolved features.

The technique assumes that all measurements (data) are equally accurate and that errors in the various measurements are uncorrelated. Two conditions may occur: (1) more than one observation in each grid box or (2) no data.

First the routine examines the case when there are several observations in each grid box. The model variables are the estimates $E_{i,j}$ at the grid points (x_i, y_j). The initial guess of $E_{i,j}$ is set to the average of all data values. All model variables are considered to be independent. The model counterparts M_n of the observations Z_n at the location given by (x_n, y_n) are defined by the bilinear equation

$$M_n = \alpha_n E_{i,j} + \beta_n E_{i+1,j} + \gamma_n E_{i,j+1} + \delta_n E_{i+1,j+1} \ .$$

Here, α_n, β_n, γ_n, and δ_n are distance functions calculated for each data point:

$$\alpha_n = \frac{(x_{i+1} - x_n)(y_{j+1} - y_n)}{dx\,dy}$$

$$\beta_n = \frac{(x_n - x_i)(y_{j+1} - y_n)}{dx\,dy}$$

$$\gamma_n = \frac{(x_{i+1} - x_n)(y_n - y_j)}{dx\,dy}$$

$$\delta_n = \frac{(x_n - x_i)(y_n - y_j)}{dx\,dy} \ ,$$

where $x_i \leq x_n \leq x_{i+1}$ and $y_j \leq y_n \leq y_{j+1}$. Also dx and dy are the distances between two consecutive grid points in the west-east direction and south-north direction, respectively:

$$dx = x_{i+1} - x_i = \text{const}$$

$$dy = y_{i+1} - y_i = \text{const} \ .$$

The grid variables are found by minimizing a cost function:

$$J = \frac{1}{2\sigma^2} \sum_n (M_n - Z_n)^2 \ ,$$

where σ is a measure of the confidence of the data point. In the present analysis, all data are considered equally confident. Consequently $\sigma = 1$.

We now consider the case where none of the four grid squares surrounding one of the grid points contains any data; that is, there will be no information about what data value to use at this point. The approach used to solve this problem consists of supplementing the inadequate data with prior knowledge. This criterion is incorporated by penalizing curvature in each direction, x and y, while minimizing the cost function. The penalized cost function is represented as

$$J_p = J + J_x + J_y \ ,$$

where J_x introduces a penalty in the x direction, excluding corners,

$$J_x = \frac{S_x}{2} \sum_{j=2,i=2}^{\Upsilon-1,\mathcal{X}-1} (E_{i+1,j} + E_{i-1,j} - 2E_{i,j})^2 \ ,$$

and J_y introduces a penalty in the y direction, excluding corners,

$$J_y = \frac{S_y}{2} \sum_{i=2,j=2}^{\mathcal{X}-1,\Upsilon-1} (E_{i,j+1} + E_{i,j-1} - 2E_{i,j})^2 \ .$$

Here $\mathcal{X}$ and Υ are the total number of points in the east-west and south-north direction, respectively.

The terms in parentheses in the previous two equations are the penalty terms. Their effect is similar to introducing "new data." These terms correspond to the model counterparts of the new data. S_x and S_y are smoothing terms.

The penalty terms act like a low-pass filter. The values of S_x and S_y set the half-power point of the filter in the x and y direction, respectively. This technique is discussed in more detail by Thacker (1988).

The values of the variable at the grid coordinates are given by the minimum of the penalized cost function. A conjugate gradient descent algorithm (Long, 1989) is used to compute the minimum of the cost function.

The method establishes that at the r-th iteration of the descent algorithm, the value of the variable $E_{i,j}$ (model) is given by

$$E_{r+1} = E_r + \zeta_r d_r$$

where,

$$d_r = -g_r + B_{r\text{-}1} d_{r\text{-}1} \ .$$

Here d_r denotes the direction of the increment to be added to the initial value (E_r) to drive the value of the variable toward the minimum of the cost function. The algorithm is that discussed by Hasdorff (1976); g_r is the gradient of the cost function with respect to the variable $E_{i,j}$ at the r-th iteration; and $B_{r\text{-}1}$ is a scalar coefficient that measures the relation between g_r and g_{r+1}.

ζ_r is the scalar "stepsize" to be taken in the direction of d_r. A trial stepsize is used to increment the variable's initial value (first-guess estimate). Then the optimal stepsize is computed following the procedure of Derber (1985). This optimal stepsize is computed from previous cost, gradient, and trial cost. The cost is assumed to vary approximately quadratically in the descent. The variable $E_{i,j}$, the initial value, is then incremented using this optimal stepsize.

APPENDIX B: LIST OF ACRONYMS

AOML	Atlantic Oceanographic and Meteorological Laboratory
CSIRO	Commonwealth Scientific and Industrial Research Organization
CTD	conductivity-temperature-depth [profilers]
ENSO	El Niño-Southern Oscillation
EPOCS	Equatorial Pacific Ocean Climate Studies
FNMOC	Fleet Numerical Meteorology and Oceanography Center
IGBP	International Geosphere-Biosphere Programme
JEDA	Joint Environmental Data Analysis
MBT	mechanical bathythermograph
NCDC	National Climatic Data Center
NEC	North Equatorial Current
NECC	North Equatorial Countercurrent
NOAA	National Oceanic and Atmospheric Administration
NODC	National Oceanographic Data Center
NOS	National Ocean Service
OGCM	ocean general circulation model
PACS	Pan-American Climate Studies
PMEL	Pacific Marine Environmental Laboratory
QBO	Quasi-Biennial Oscillation
QC	quality control
RV	Research Vessel
SQC	scientific quality control
SST	sea surface temperature
TAO	Tropical Atmosphere Ocean
TOGA	Tropical Ocean and Global Atmosphere
TSDC	TOGA Subsurface Data Center
VOS	volunteer observing ship
WCRP	World Climate Research Programme
WOCE	World Ocean Circulation Experiment
XBT	expendable bathythermograph

CLIMATOLOGY

The maps in this section show the bimonthly climatological fields for the entire study period, 1979-93. An average of 32 profiles per 2° latitude by 5° longitude grid box was used to generate these fields. For each bimonthly period the following fields are presented: sea surface temperature (SST), temperature at 50 m depth (T50), temperature at 100 m depth (T100), temperature of the upper 400 m layer (T0-400), depth of the 20°C isotherm (D20), and depth of the 15°C isotherm (D15).

Temperatures are given in degrees Celsius (°C) with a contour interval of 1°C. Depths are given in meters (m) with a contour interval of 20 m.

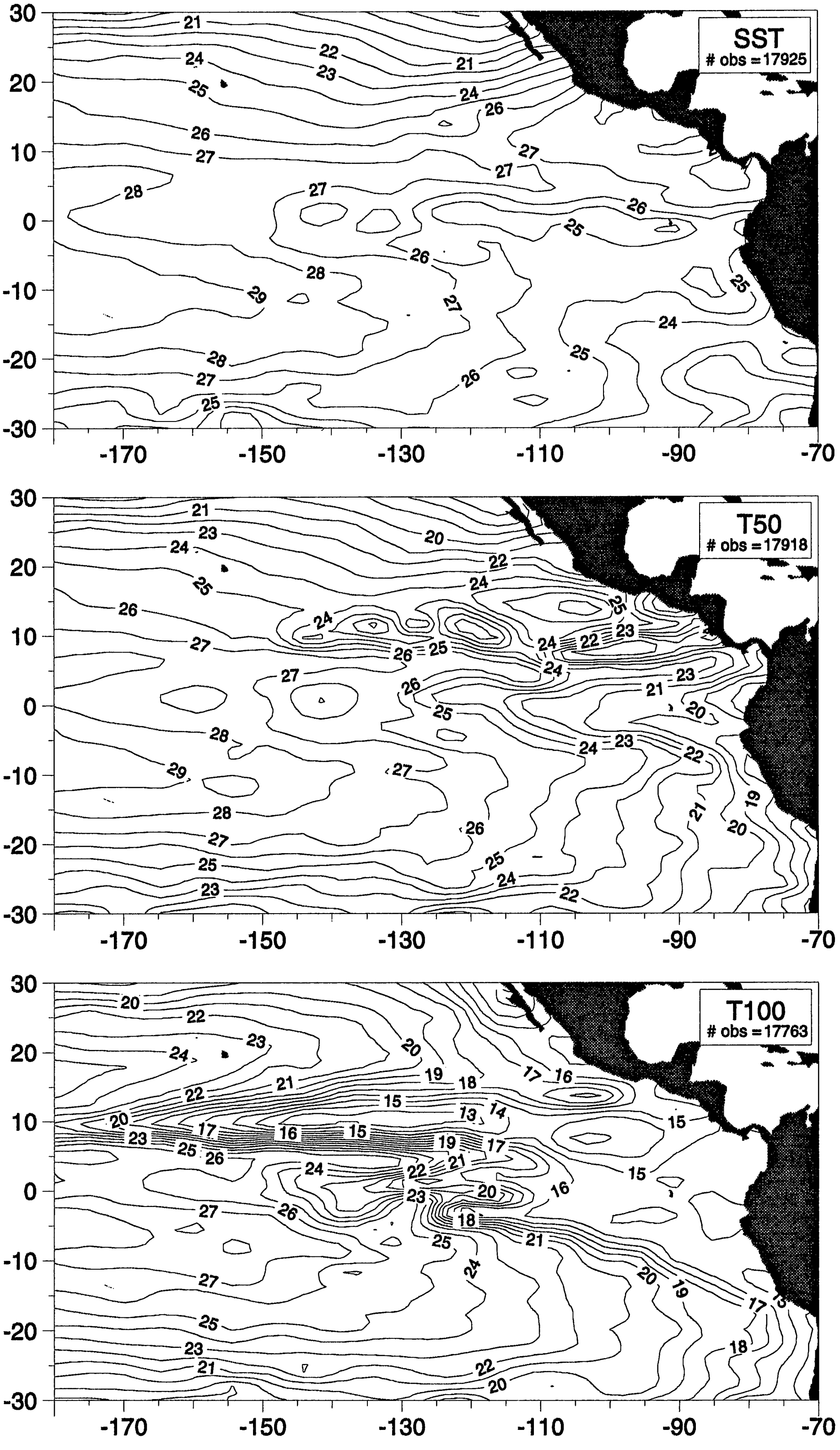

Plate 1. Climatologies for January-February, 1979-93.

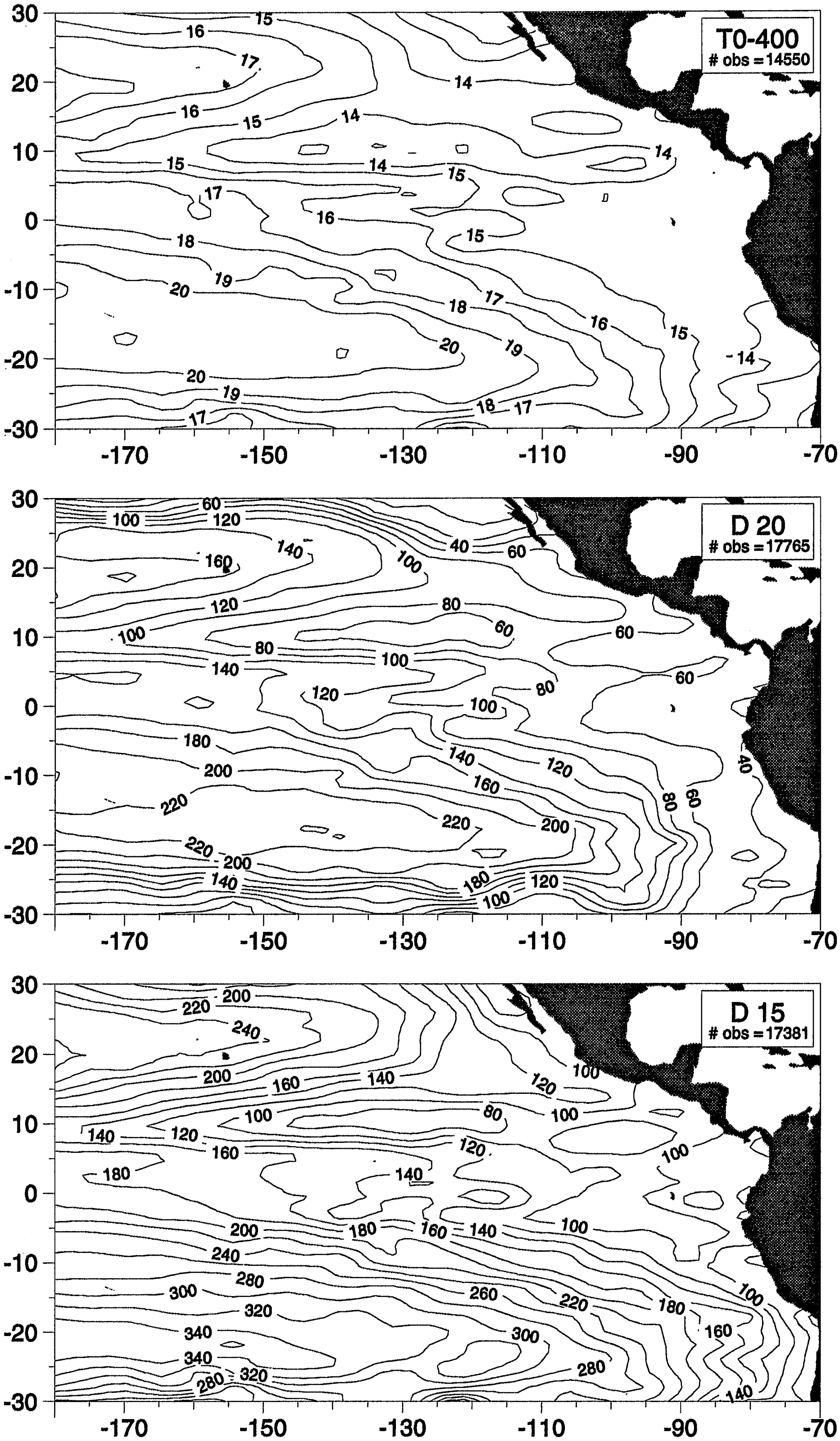

Plate 1 – *continued*. Climatologies for January-February, 1979-93.

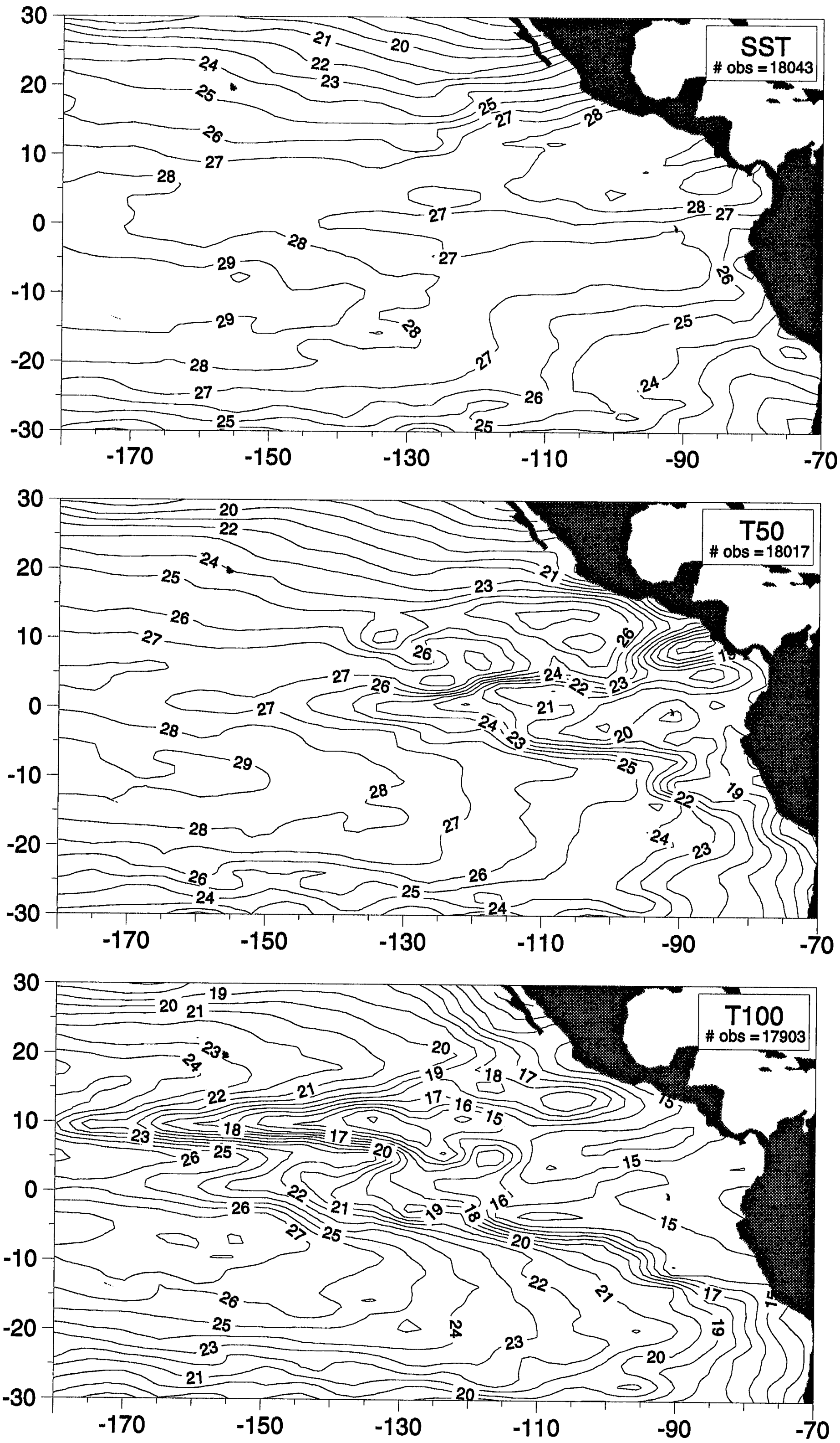

Plate 2. Climatologies for March-April, 1979-93.

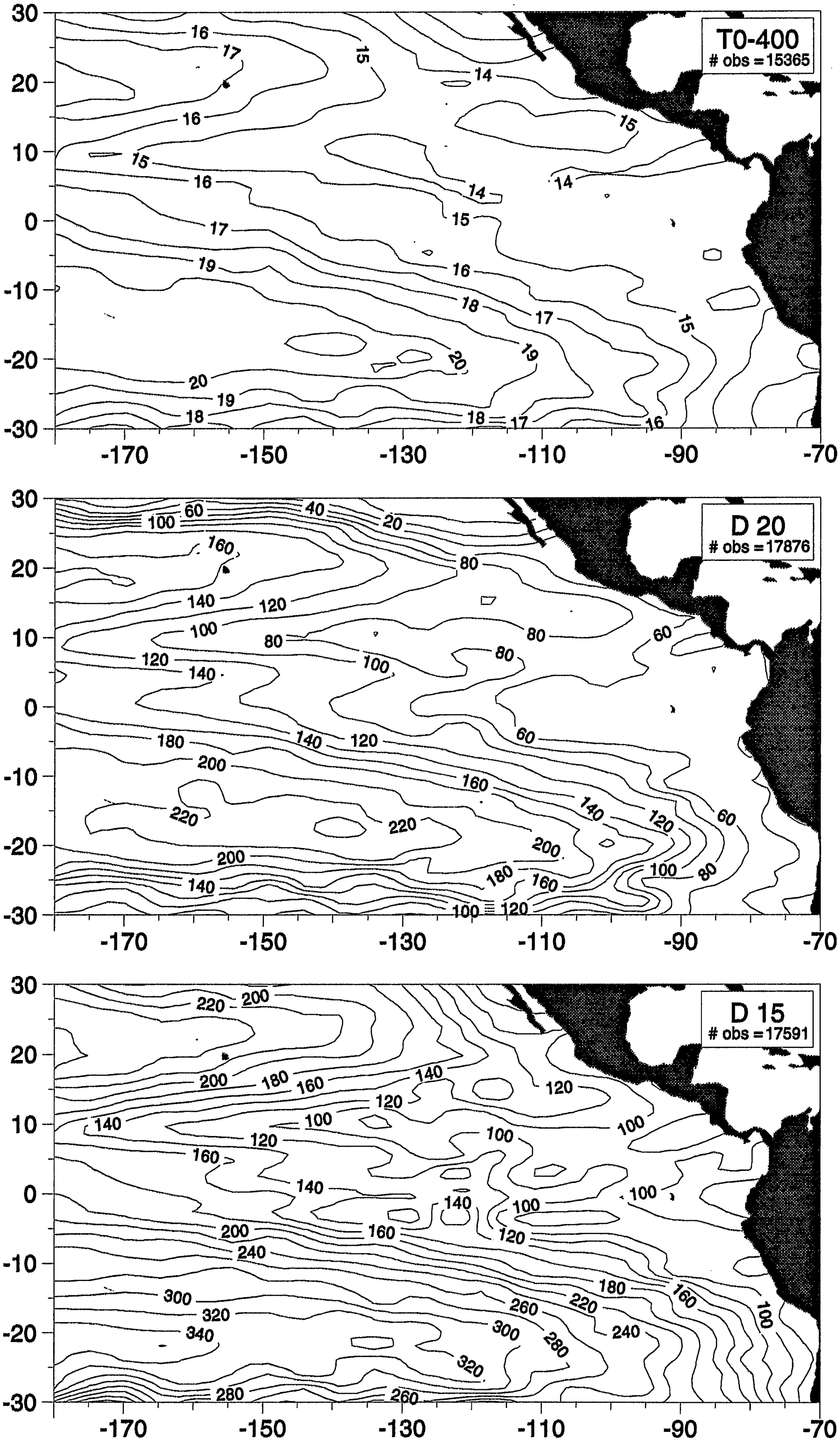

Plate 2 – *continued*. Climatologies for March-April, 1979-93.

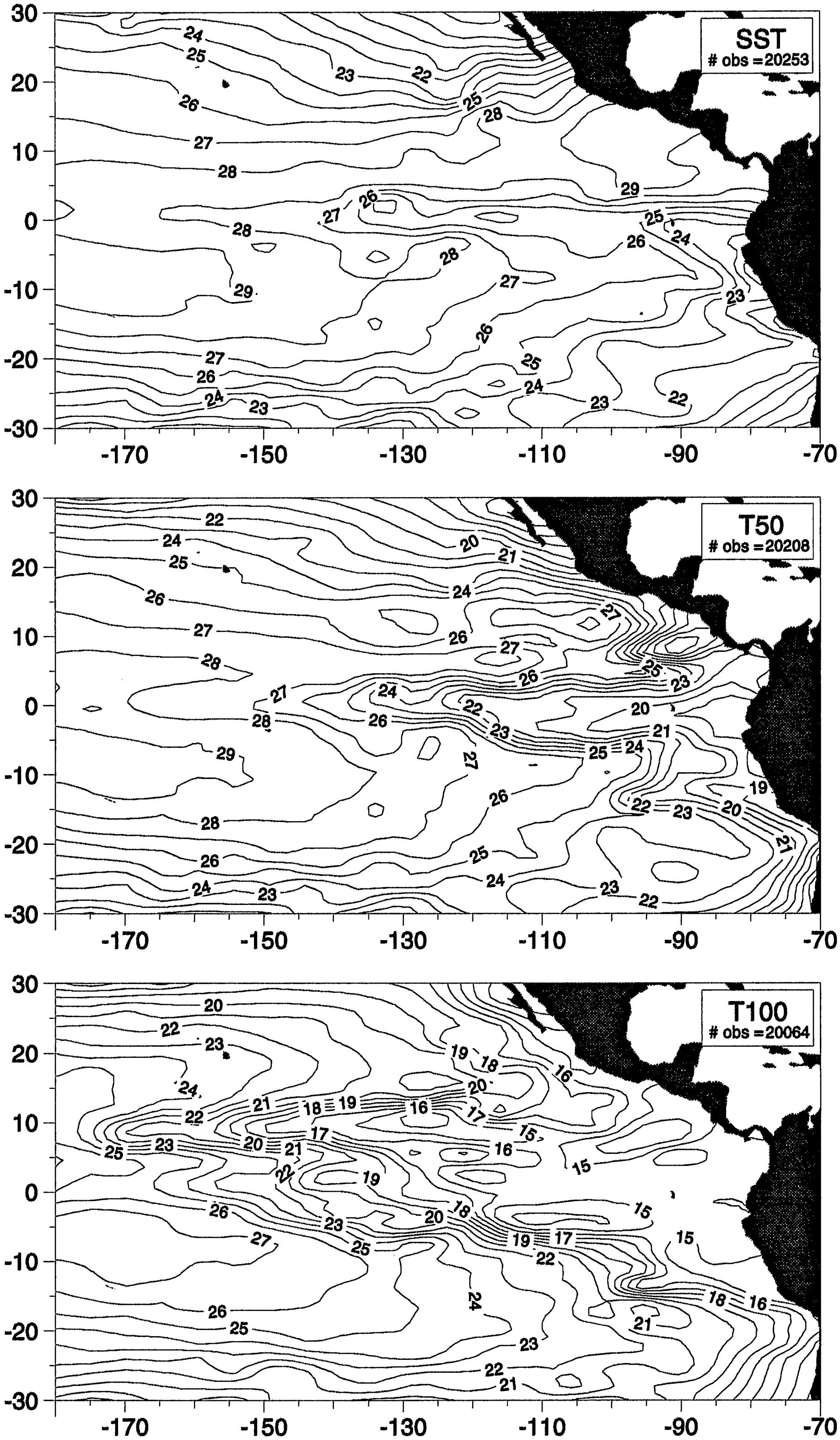

Plate 3. Climatologies for May-June, 1979-93.

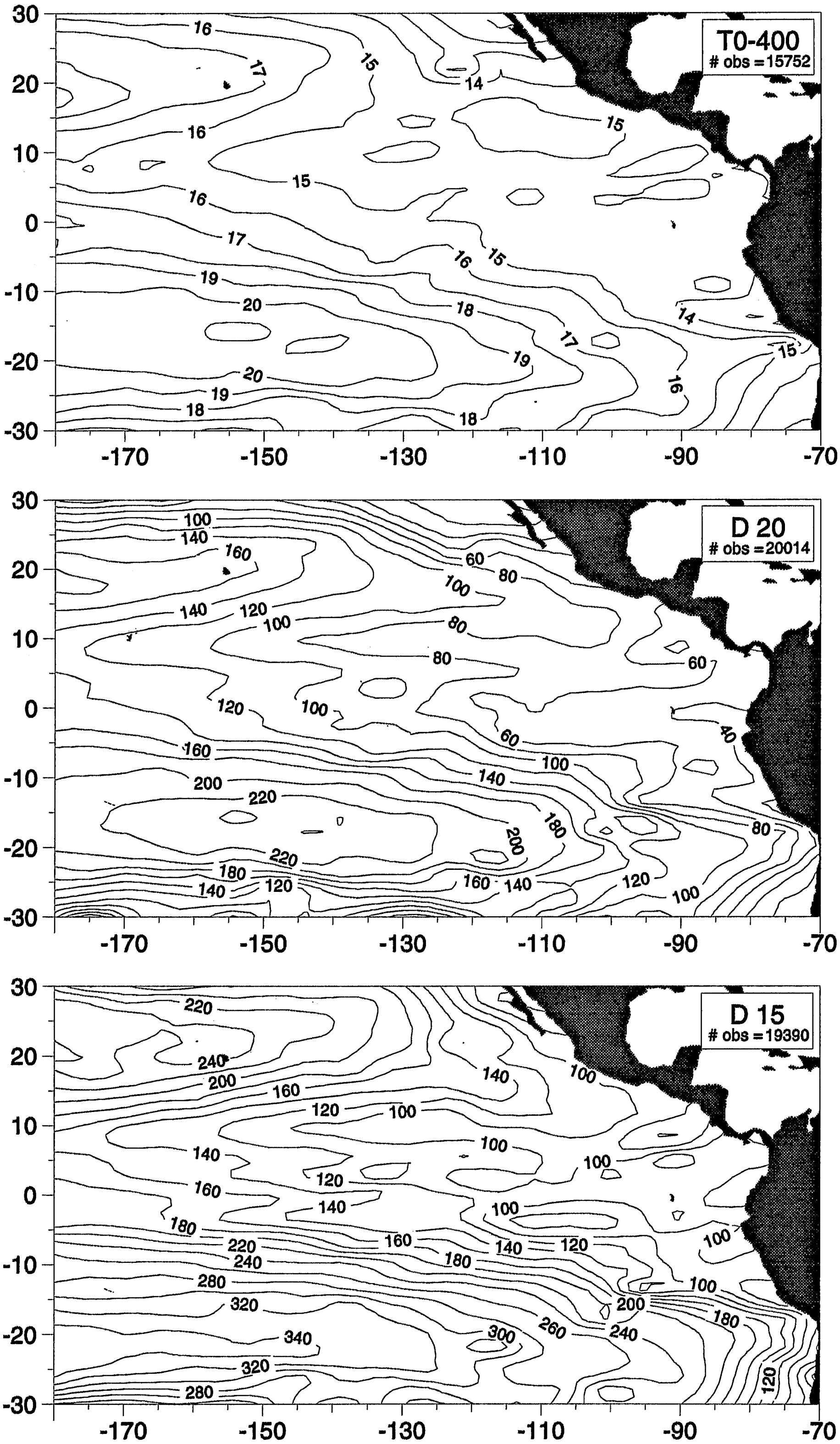

Plate 3 – *continued*. Climatologies for May-June, 1979-93.

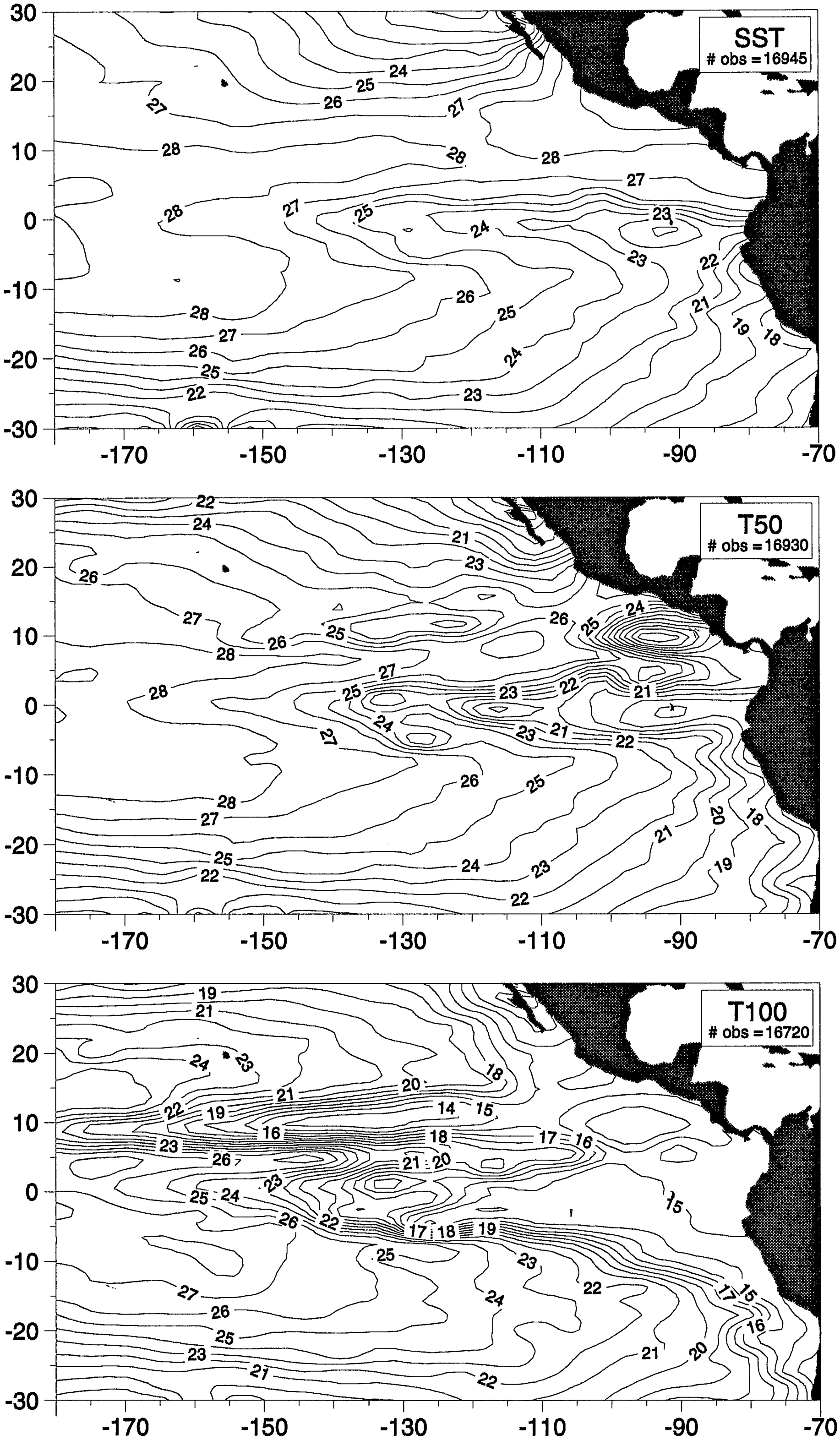

Plate 4. Climatologies for July-August, 1979-93.

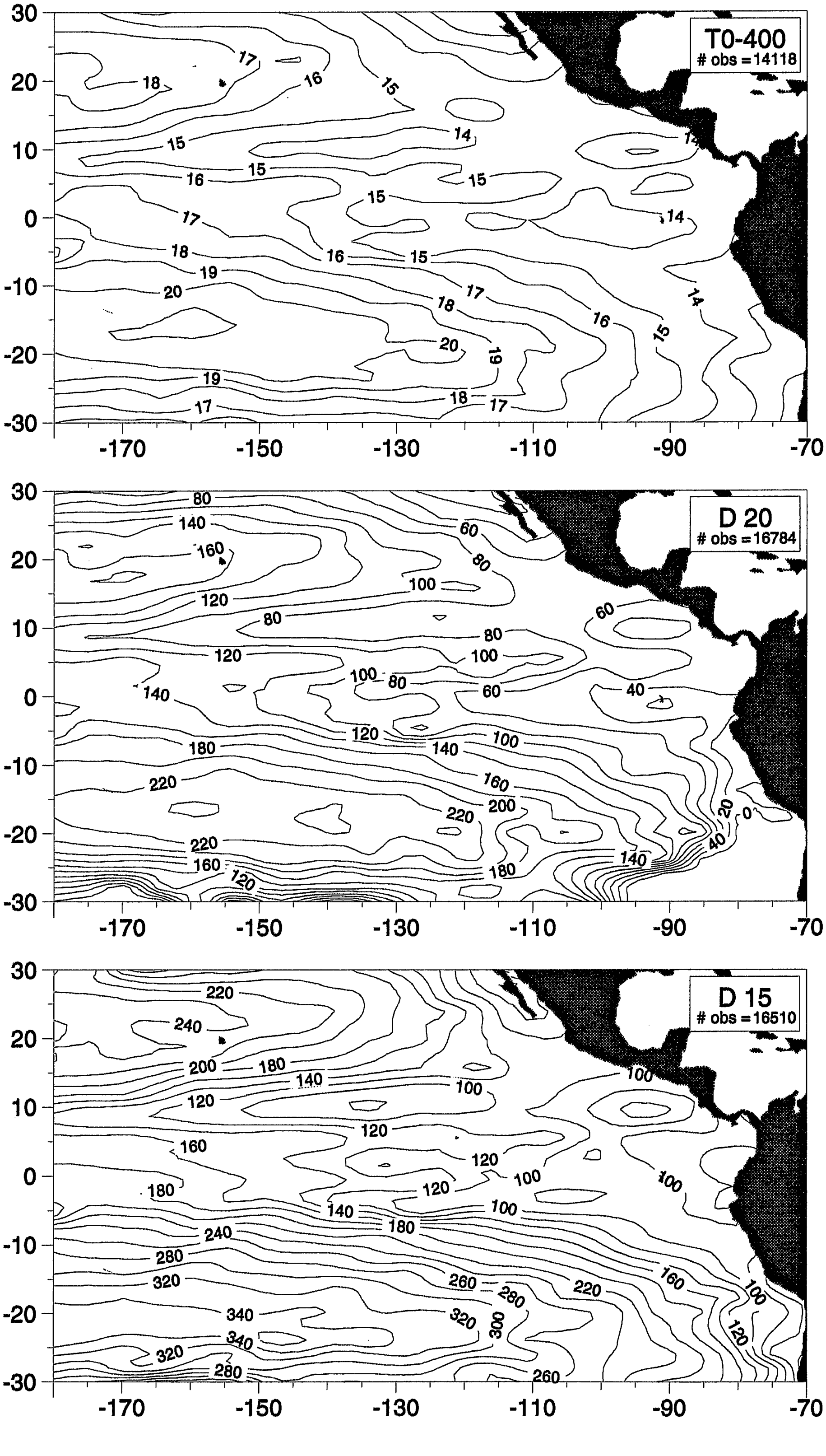

Plate 4 – *continued*. Climatologies for July-August, 1979-93.

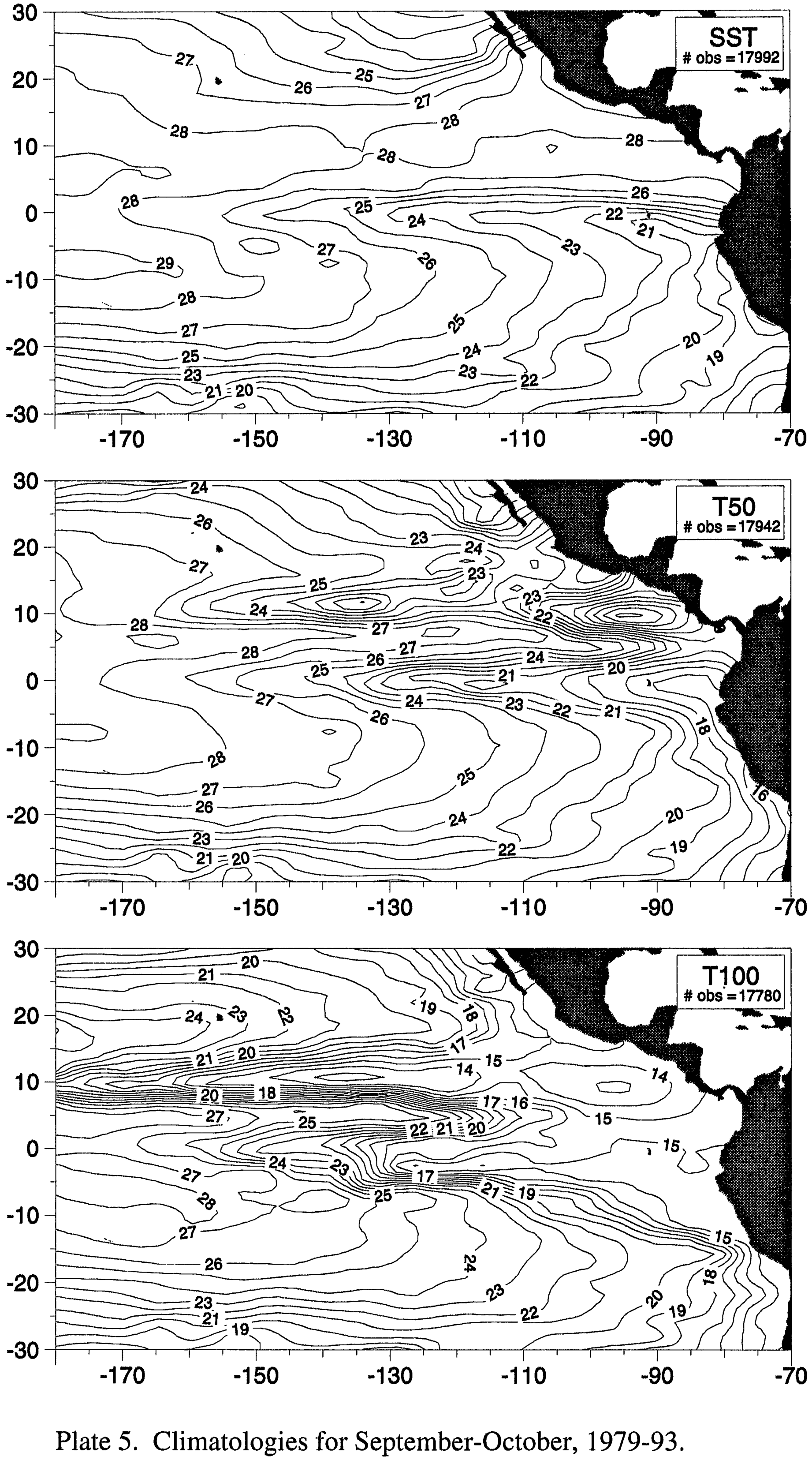

Plate 5. Climatologies for September-October, 1979-93.

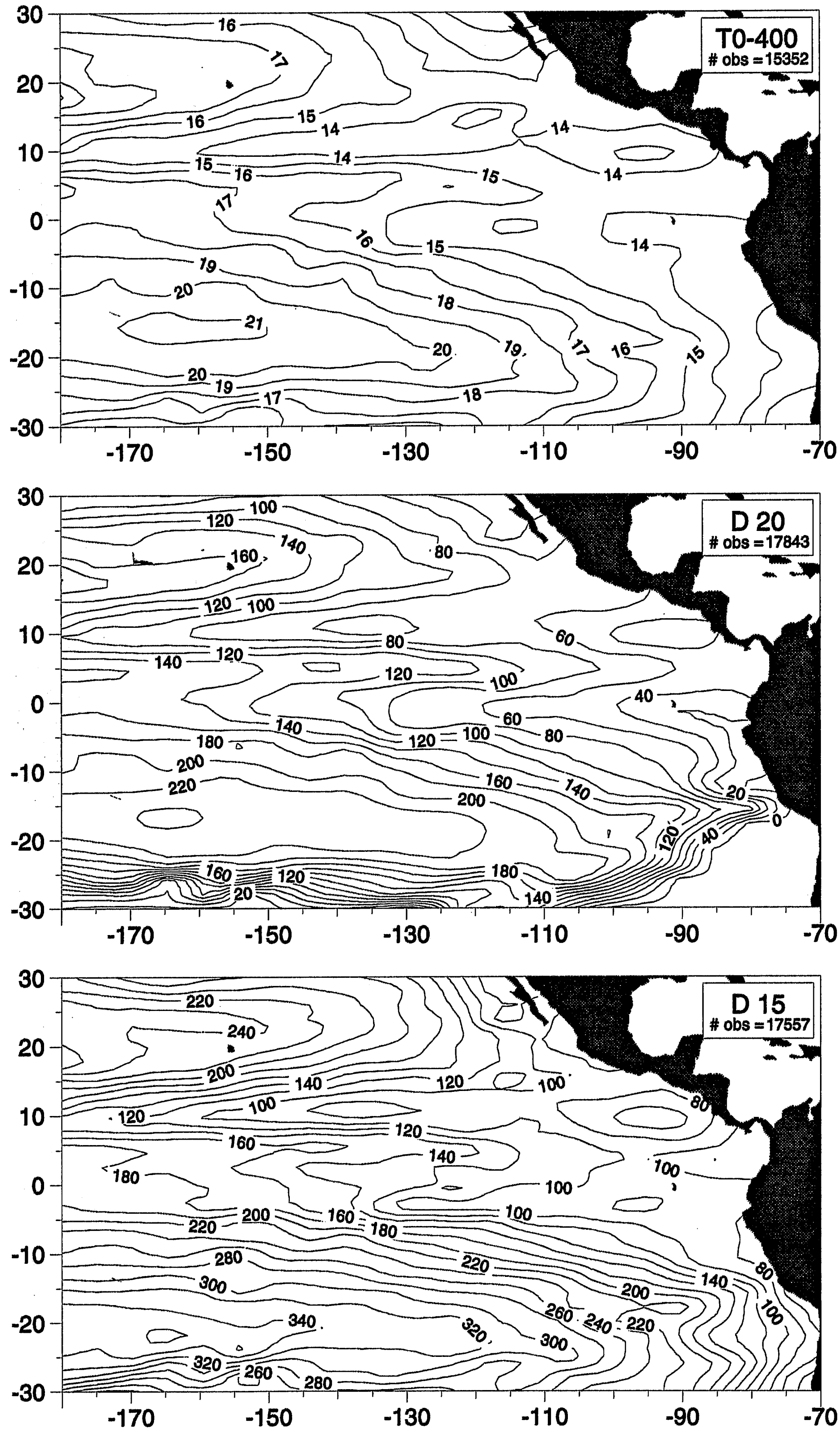

Plate 5 – *continued*. Climatologies for September-October, 1979-93.

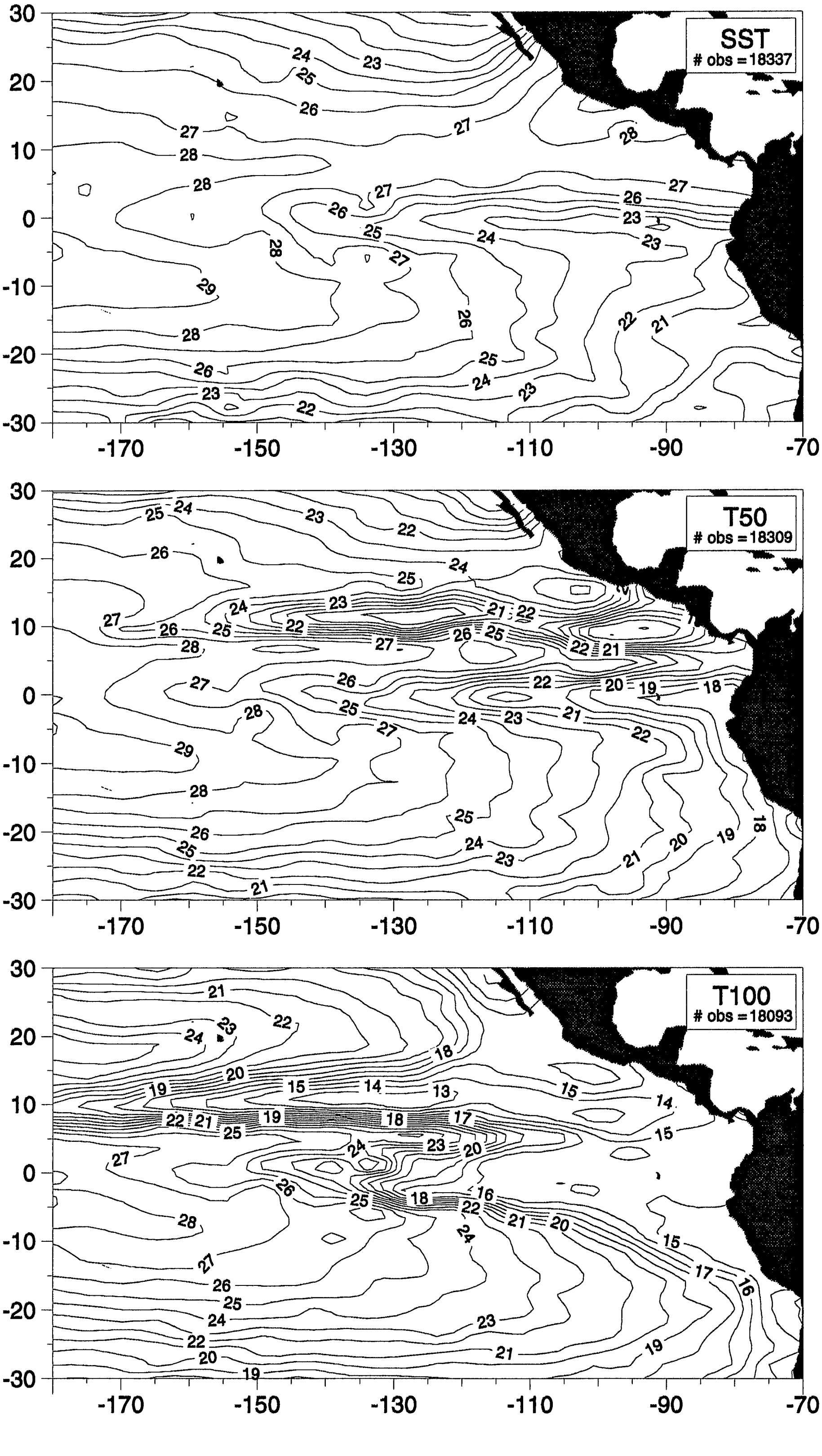

Plate 6. Climatologies for November-December, 1979-93.

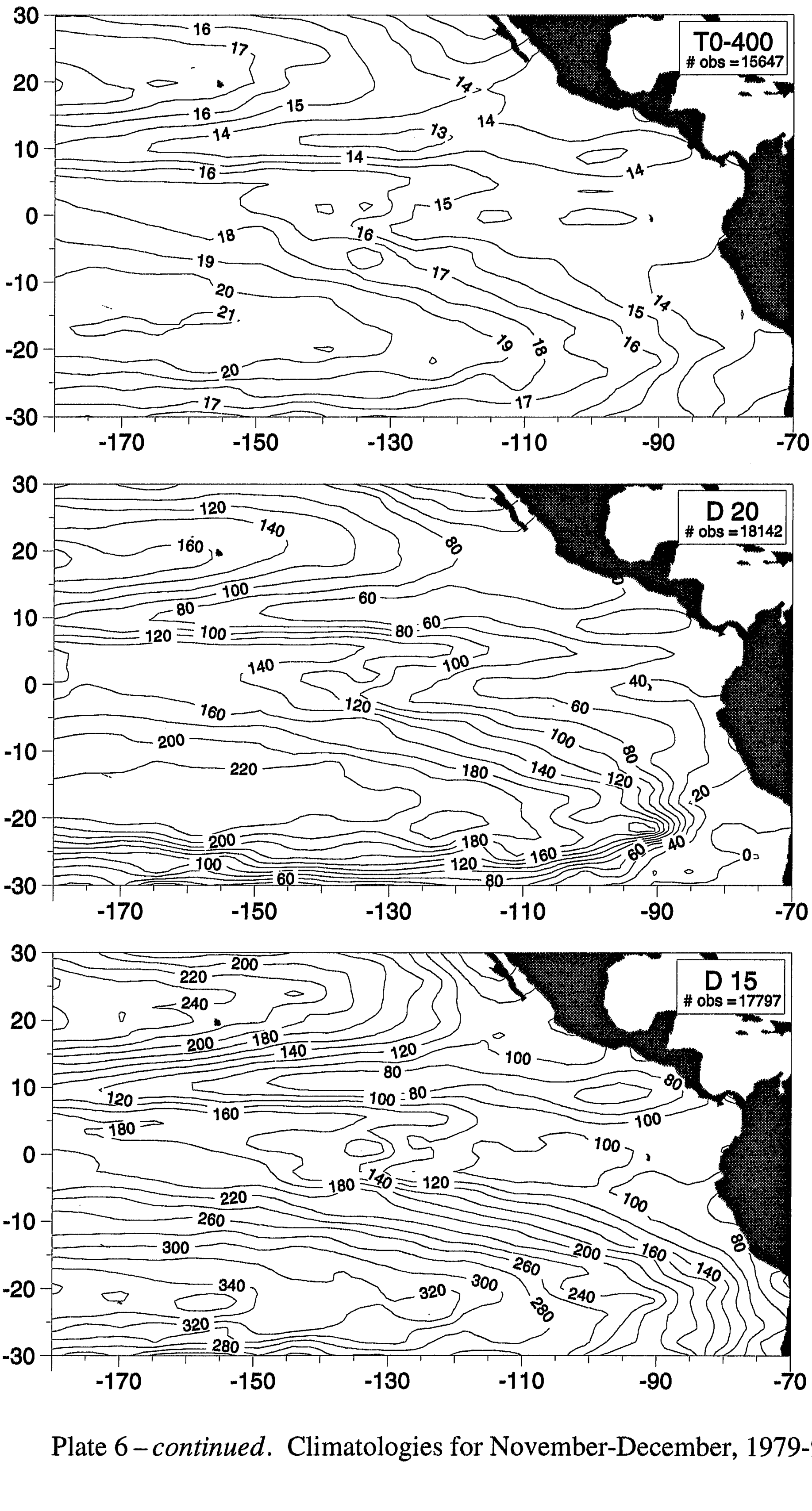

Plate 6 – *continued*. Climatologies for November-December, 1979-93.

BIMONTHLY THERMAL FIELDS

The maps in this section show the bimonthly fields for each year of the study period of 1979 to 1993. For each bimonthly period the following fields are presented: sea surface temperature (SST), temperature at 50 m depth (T50), temperature at 100 m depth (T100), temperature of the upper 400 m layer (T0-400), depth of the 20°C isotherm (D20), and depth of the 15°C isotherm (D15).

Temperatures are given in degrees Celsius (°C) with a contour interval of 1°C. Depths are given in meters (m) with a contour interval of 20 m.

Superimposed dot plots show the locations of the stations used to derive the corresponding thermal fields.

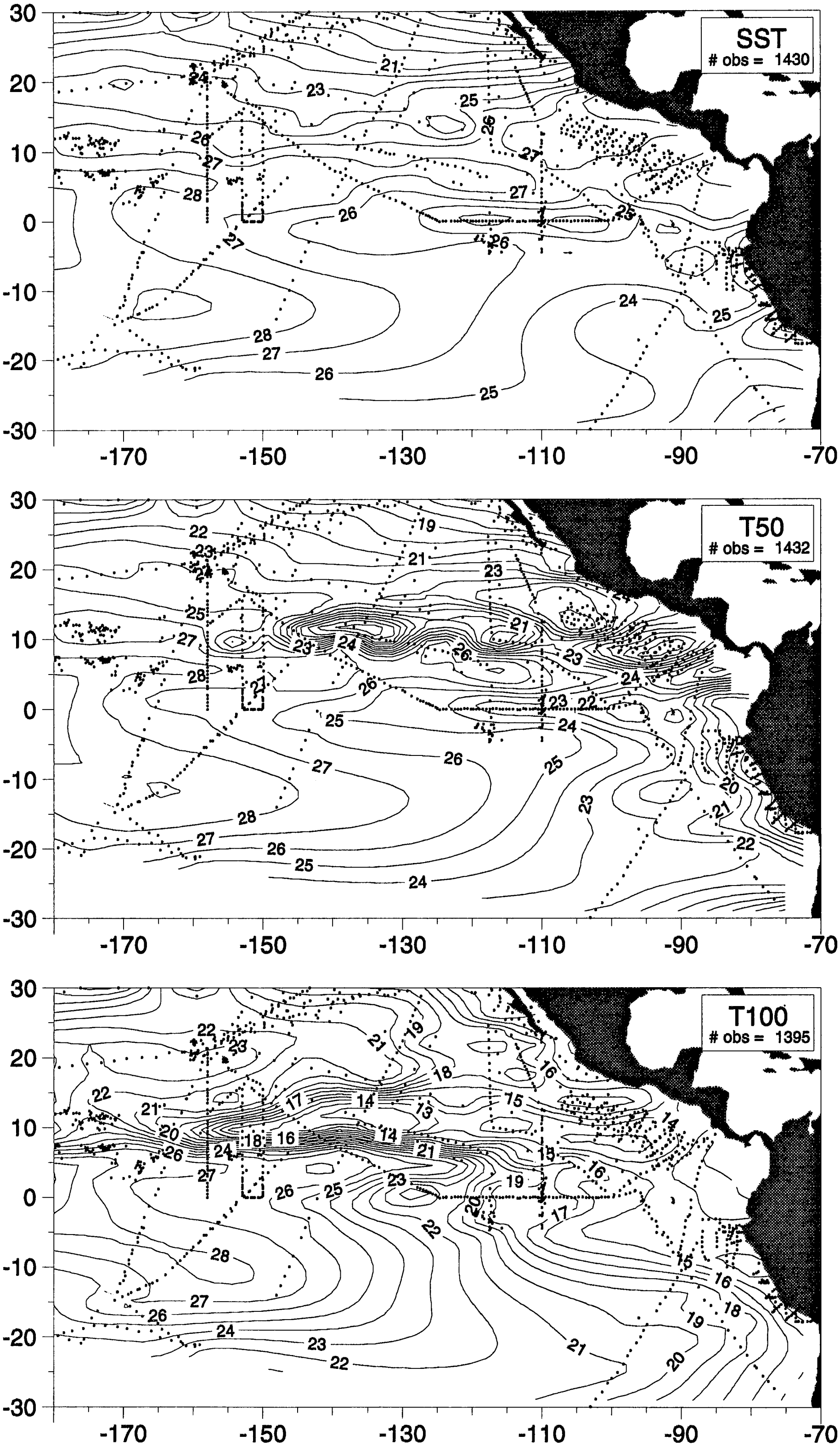

Plate 7. Bimonthly fields for January-February 1979.

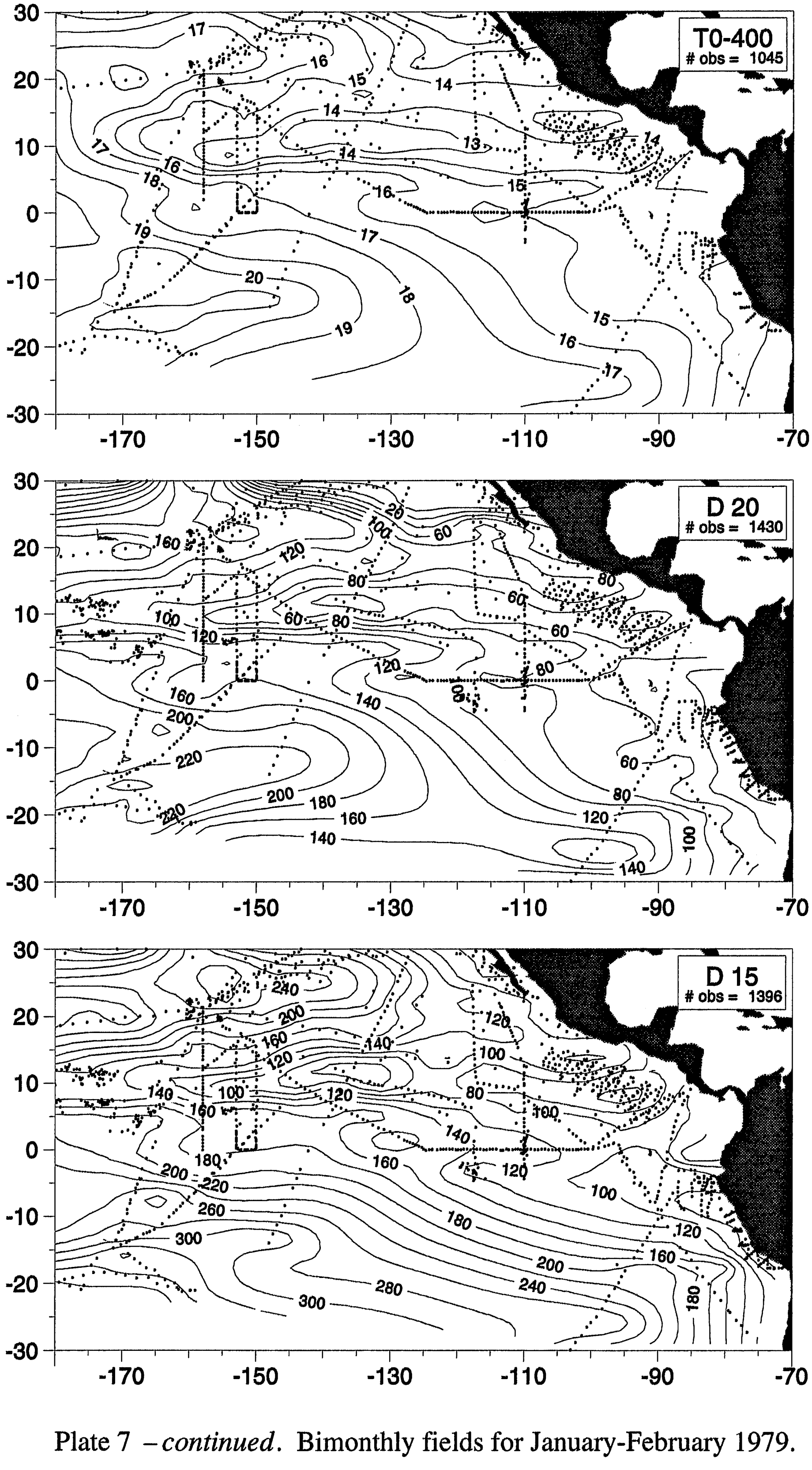

Plate 7 *– continued.* Bimonthly fields for January-February 1979.

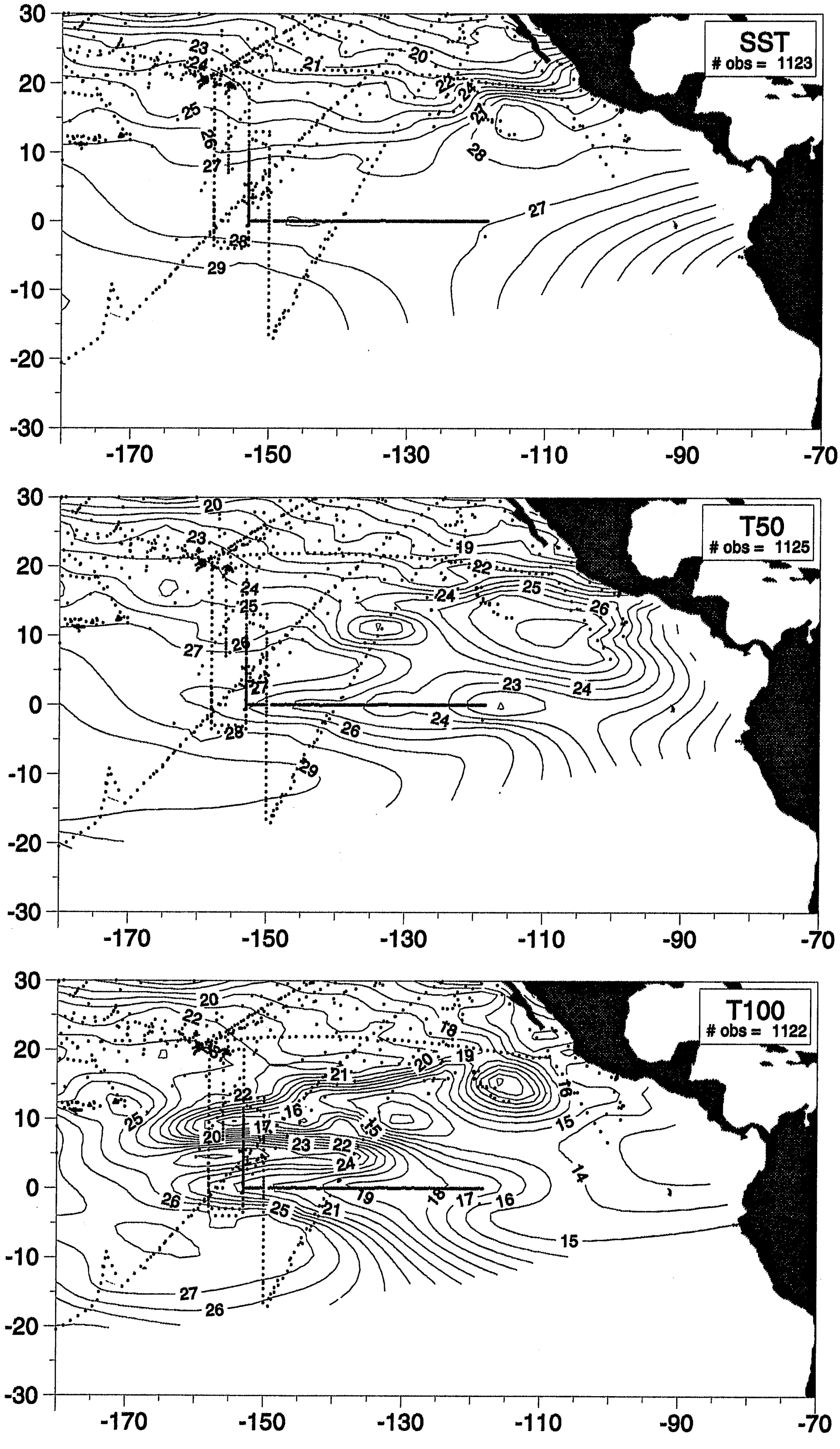

Plate 8. Bimonthly fields for March-April 1979.

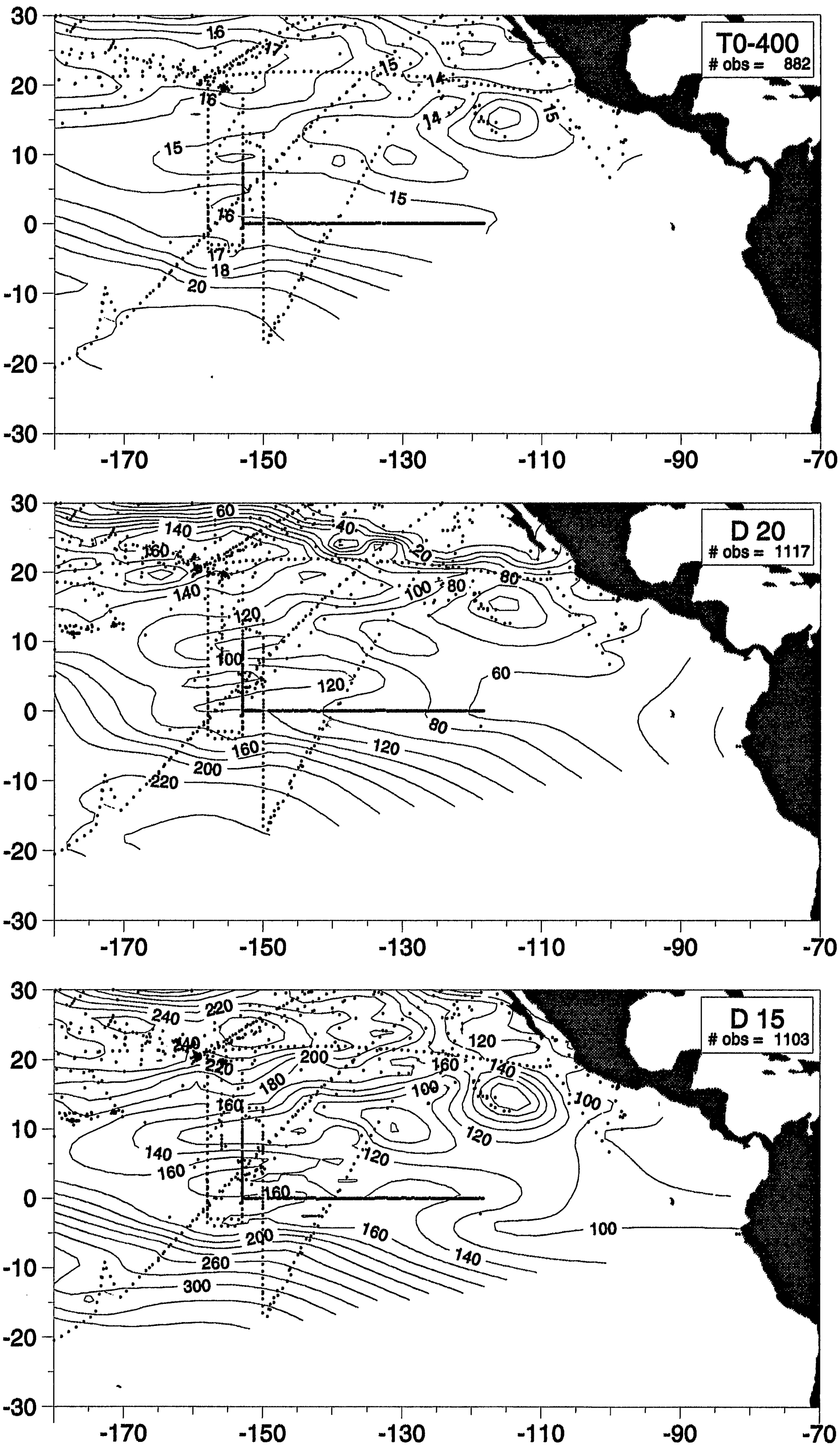

Plate 8 – *continued*. Bimonthly fields for March-April 1979.

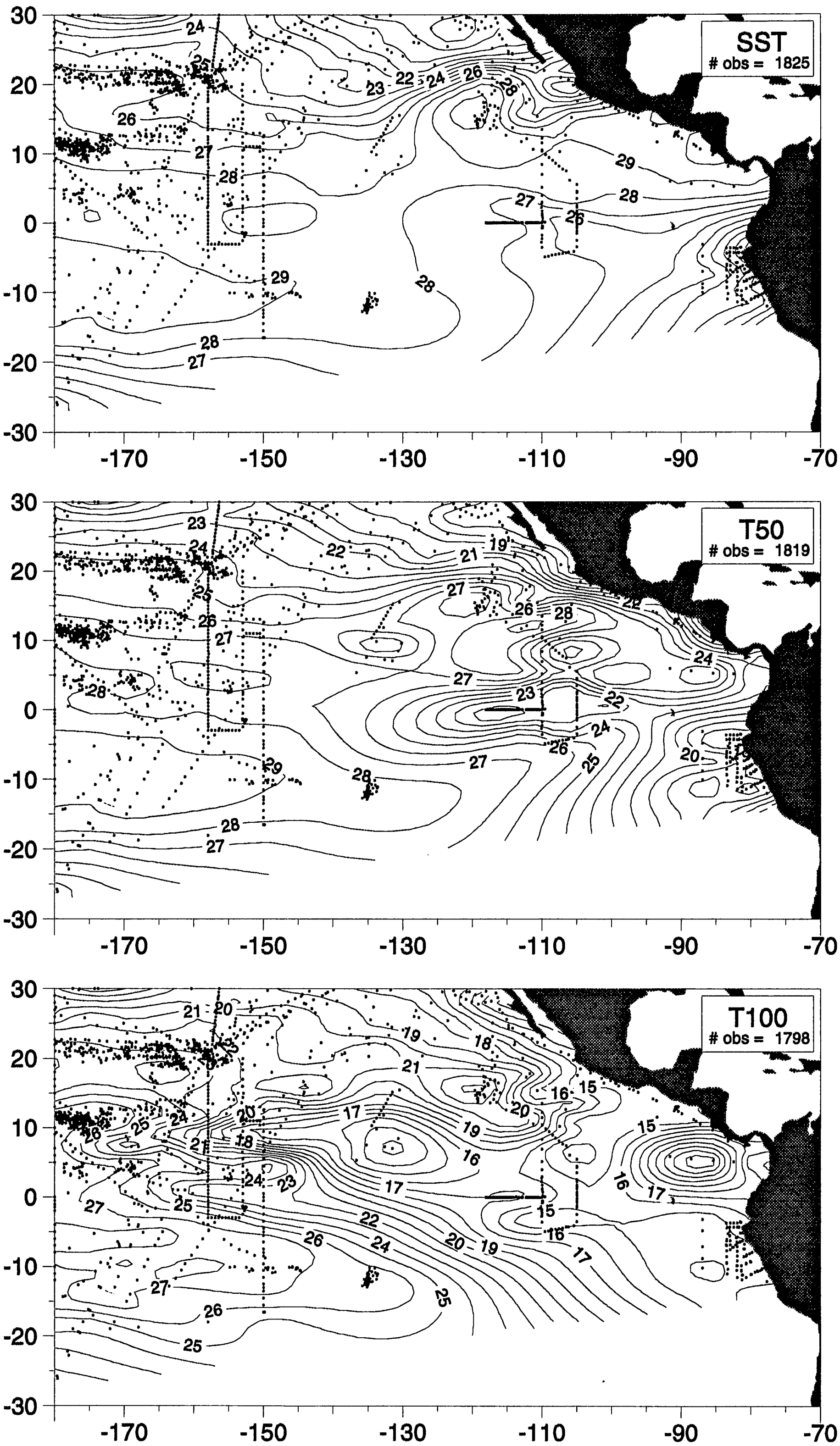

Plate 9. Bimonthly fields for May-June 1979.

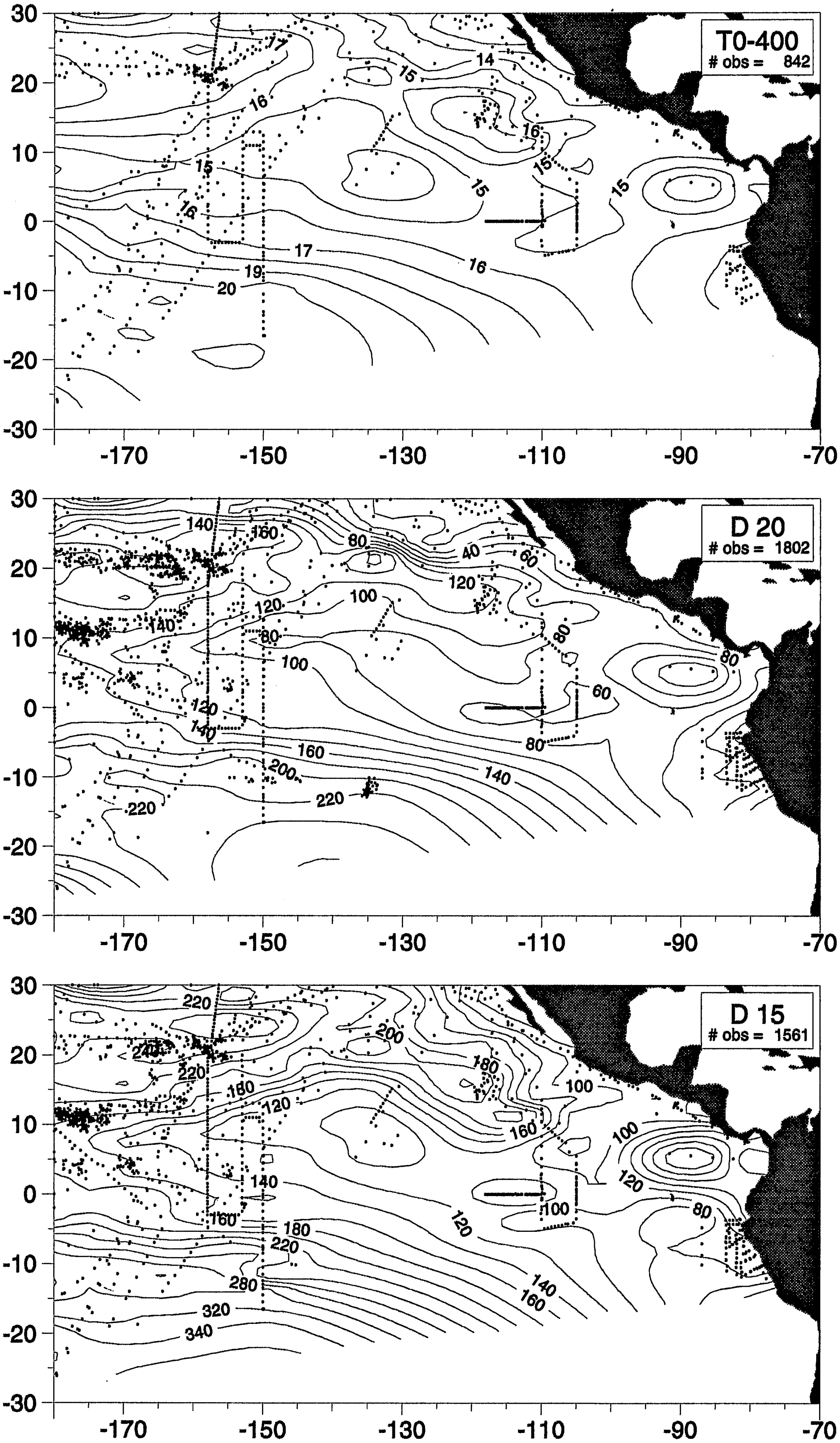

Plate 9 – *continued*. Bimonthly fields for May-June 1979.

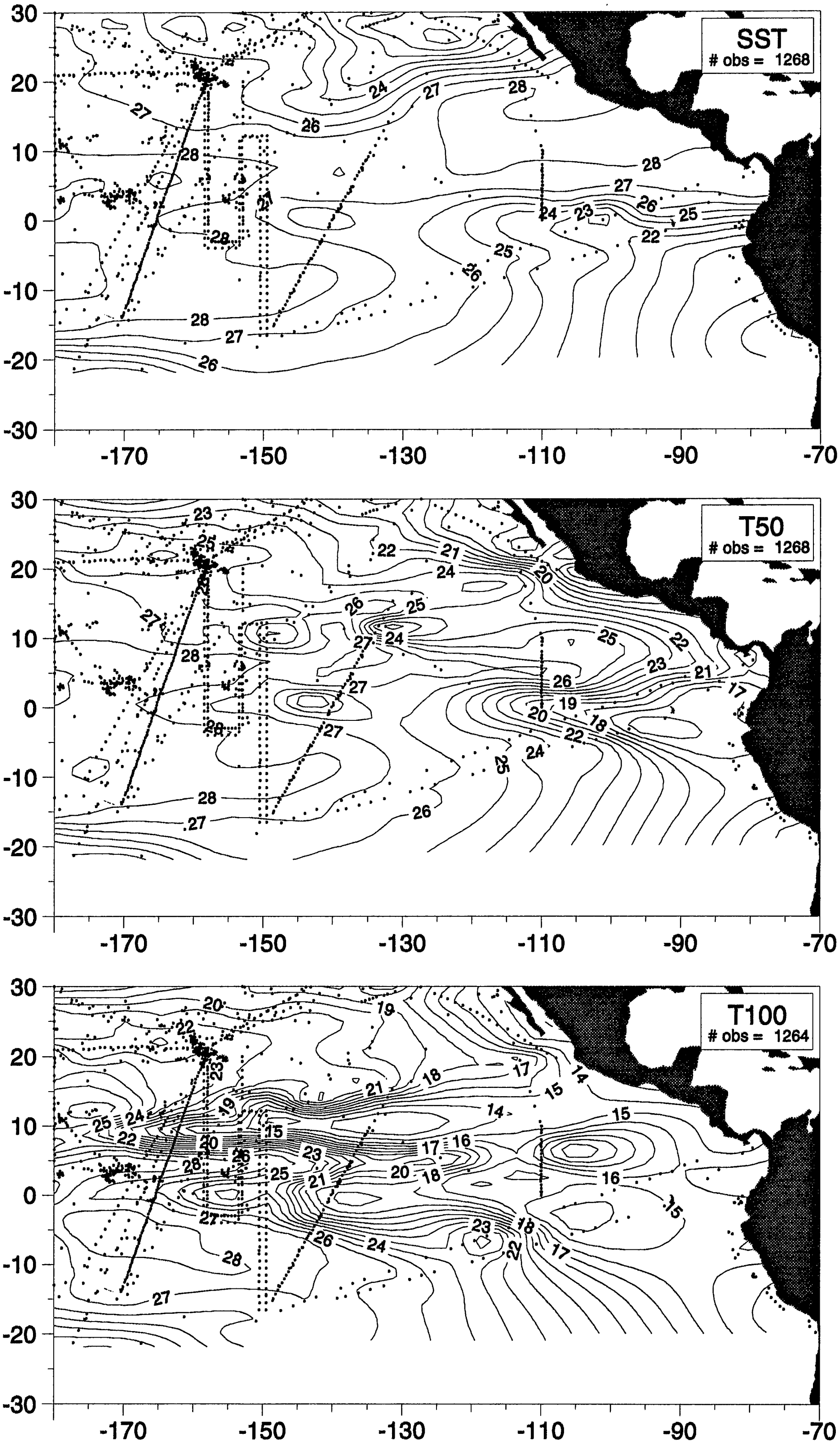

Plate 10. Bimonthly fields for July-August 1979.

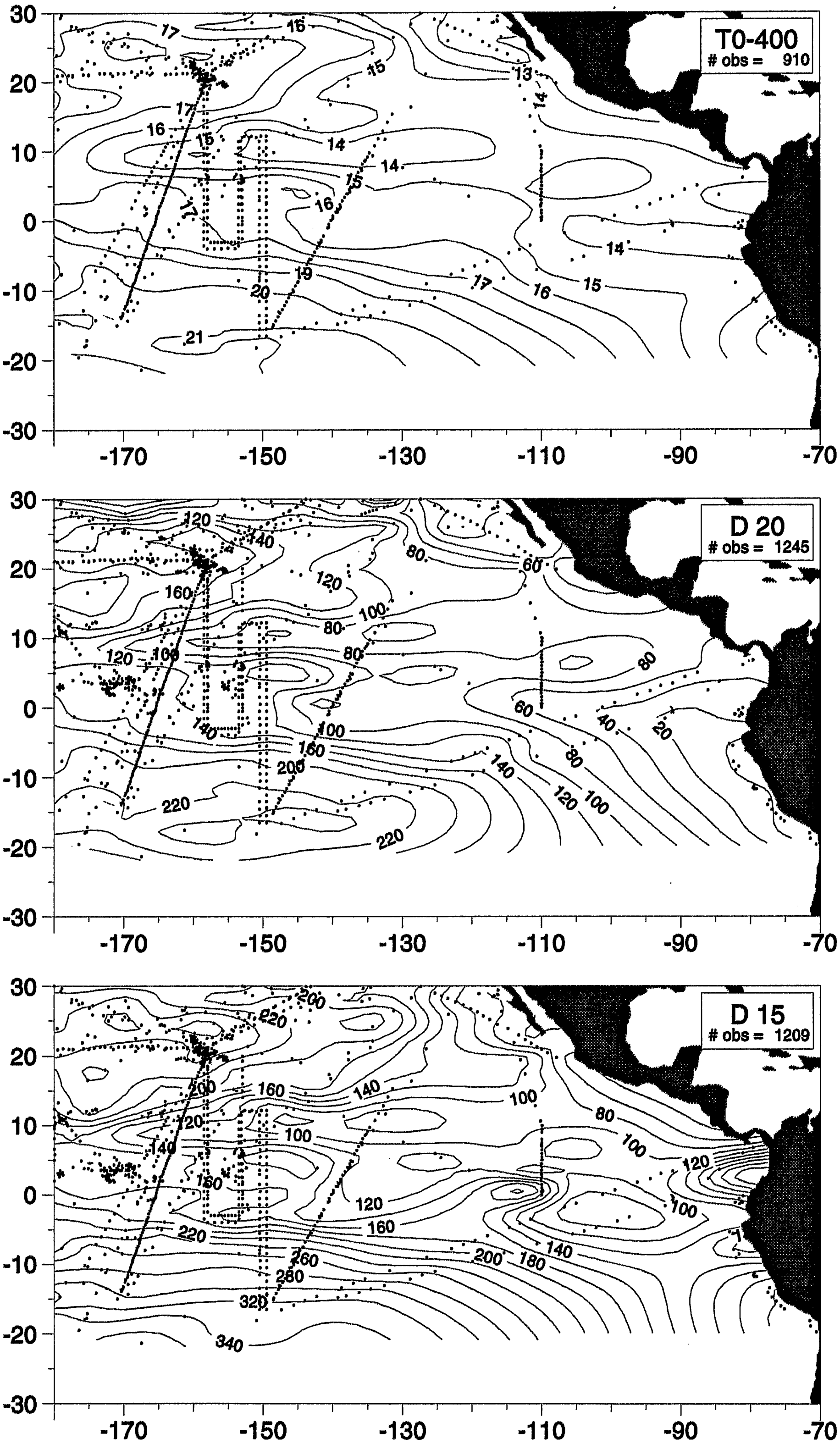

Plate 10 – *continued*. Bimonthly fields for July-August 1979.

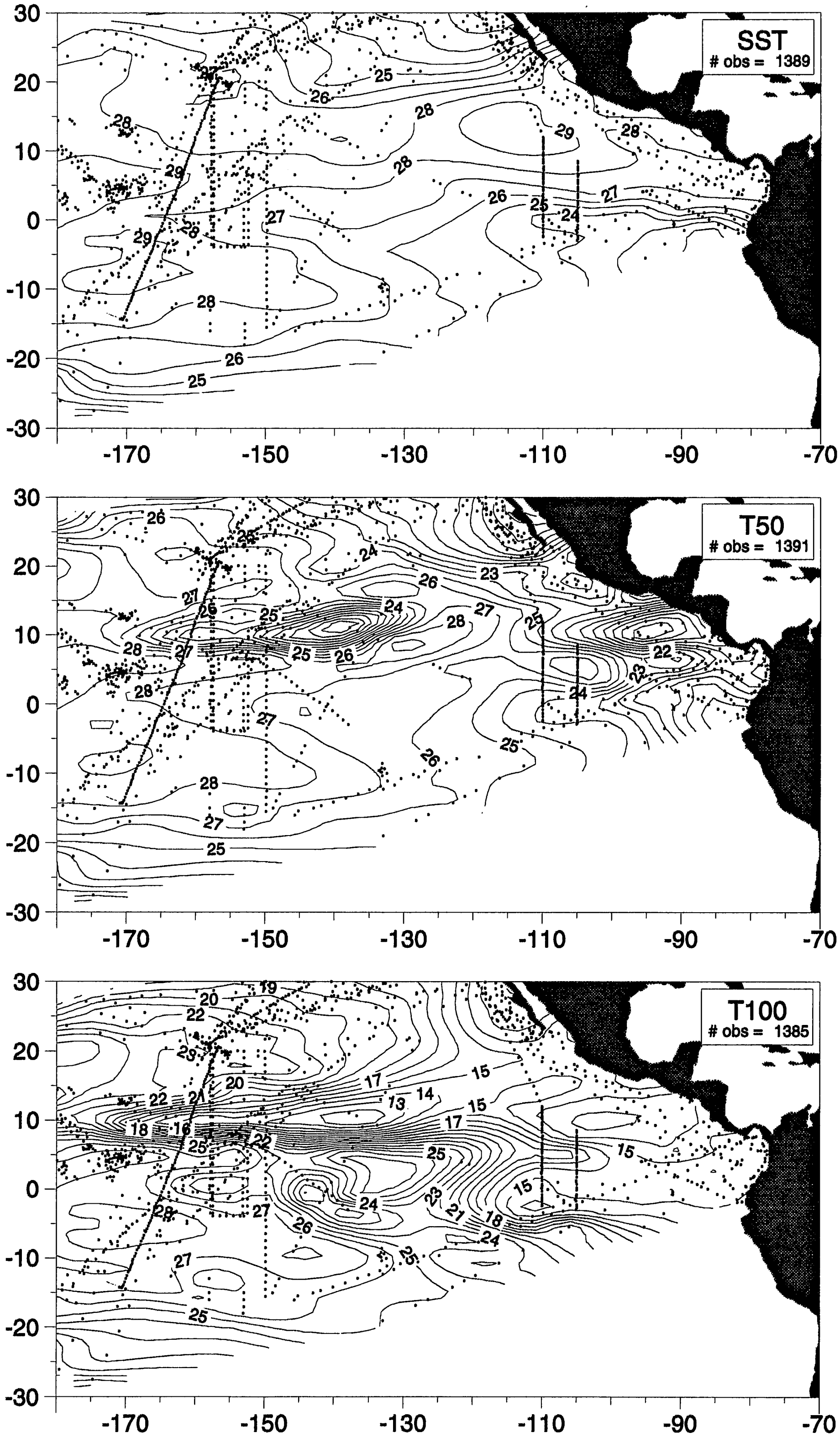

Plate 11. Bimonthly fields for September-October 1979.

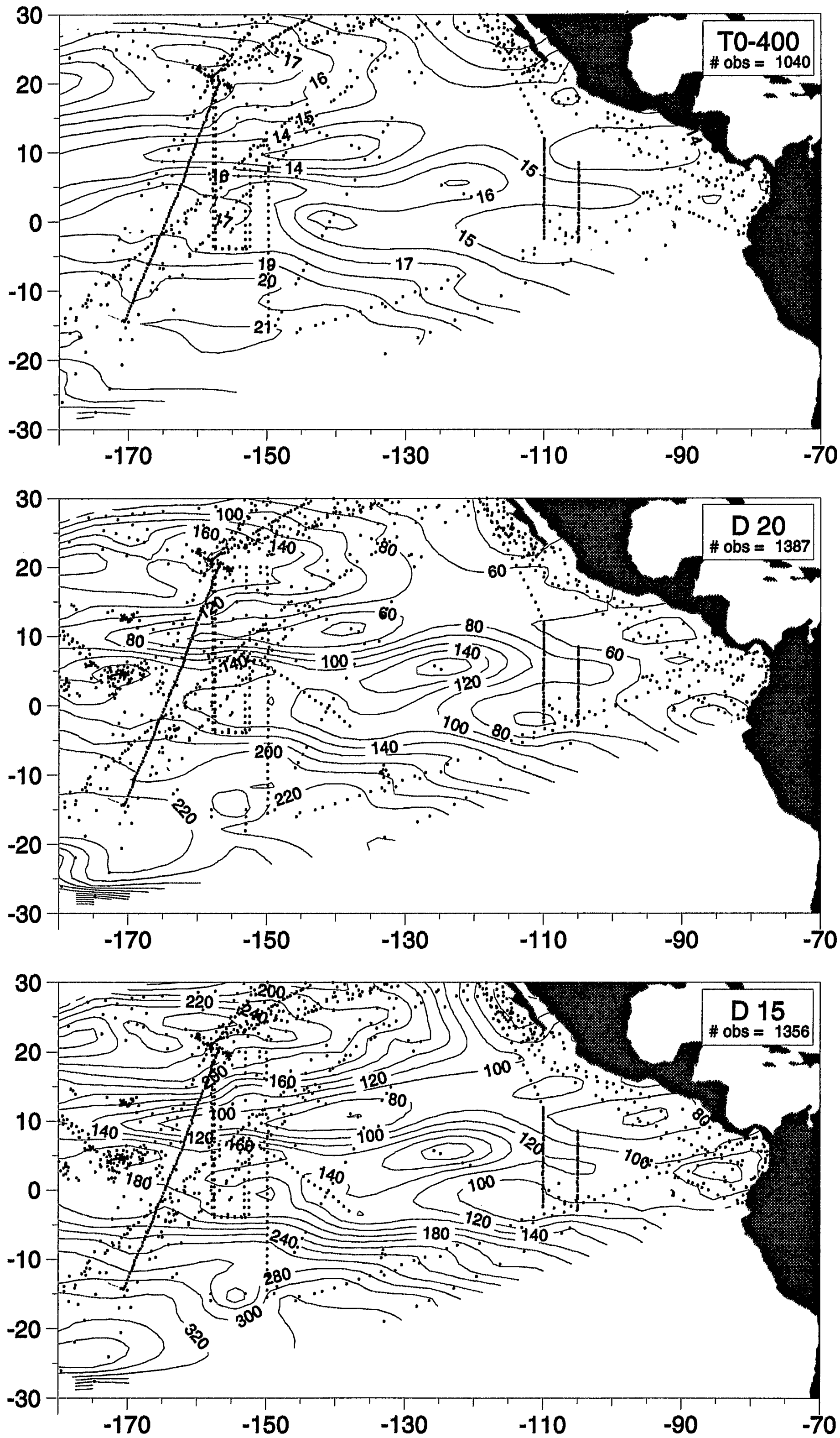

Plate 11 – *continued.* Bimonthly fields for September-October 1979.

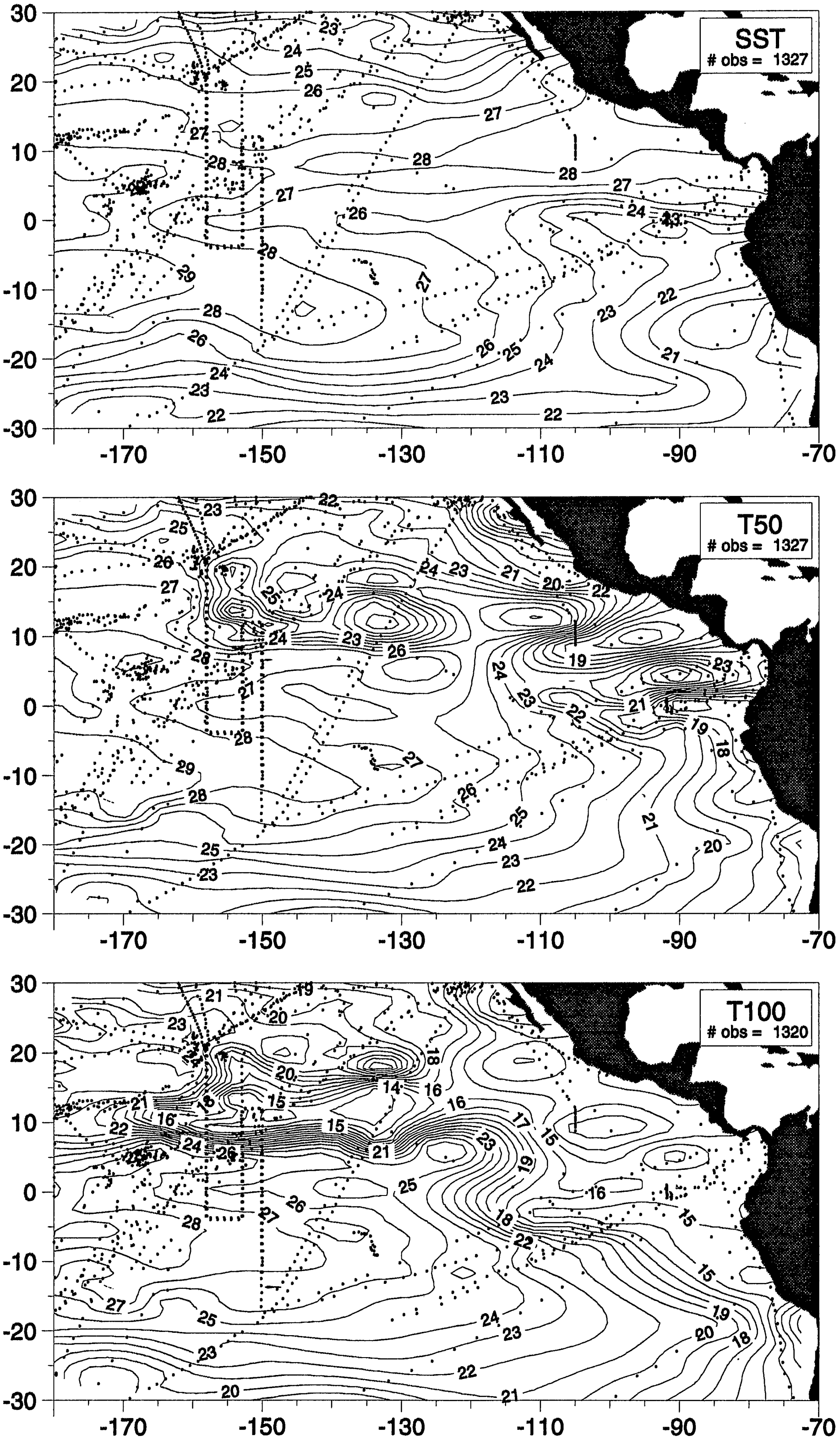

Plate 12. Bimonthly fields for November-December 1979.

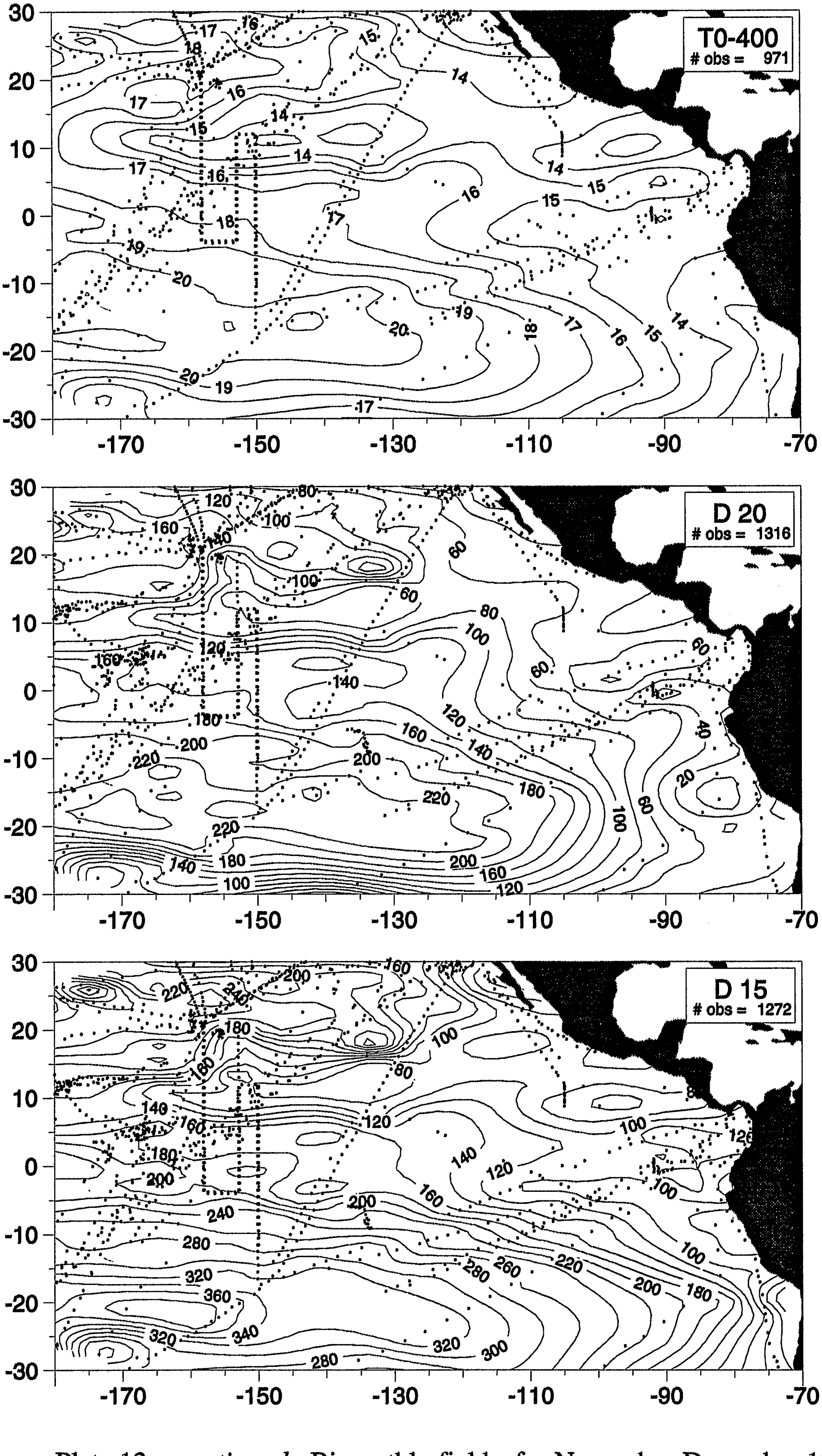

Plate 12 – *continued*. Bimonthly fields for November-December 1979.

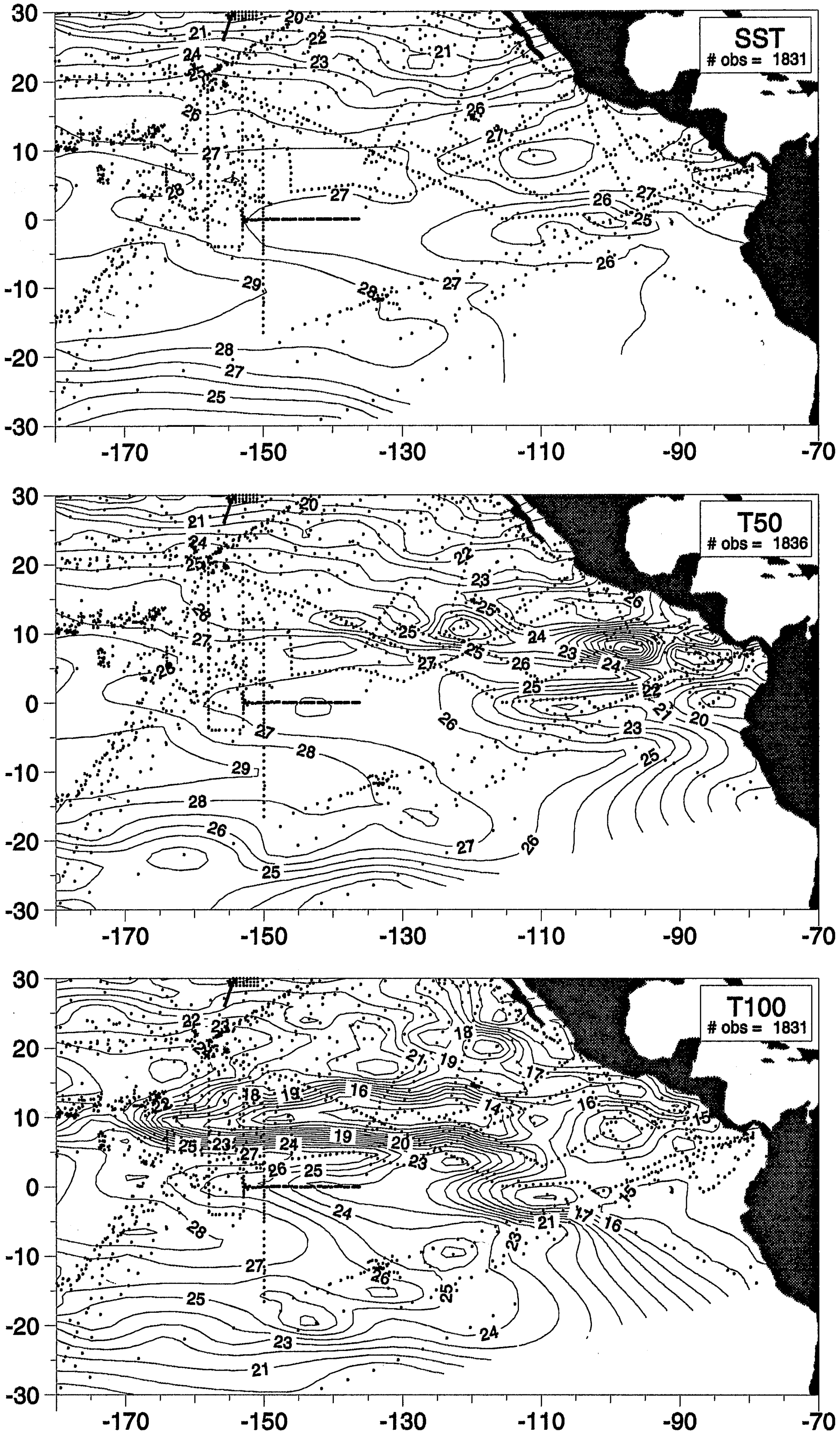

Plate 13. Bimonthly fields for January-February 1980.

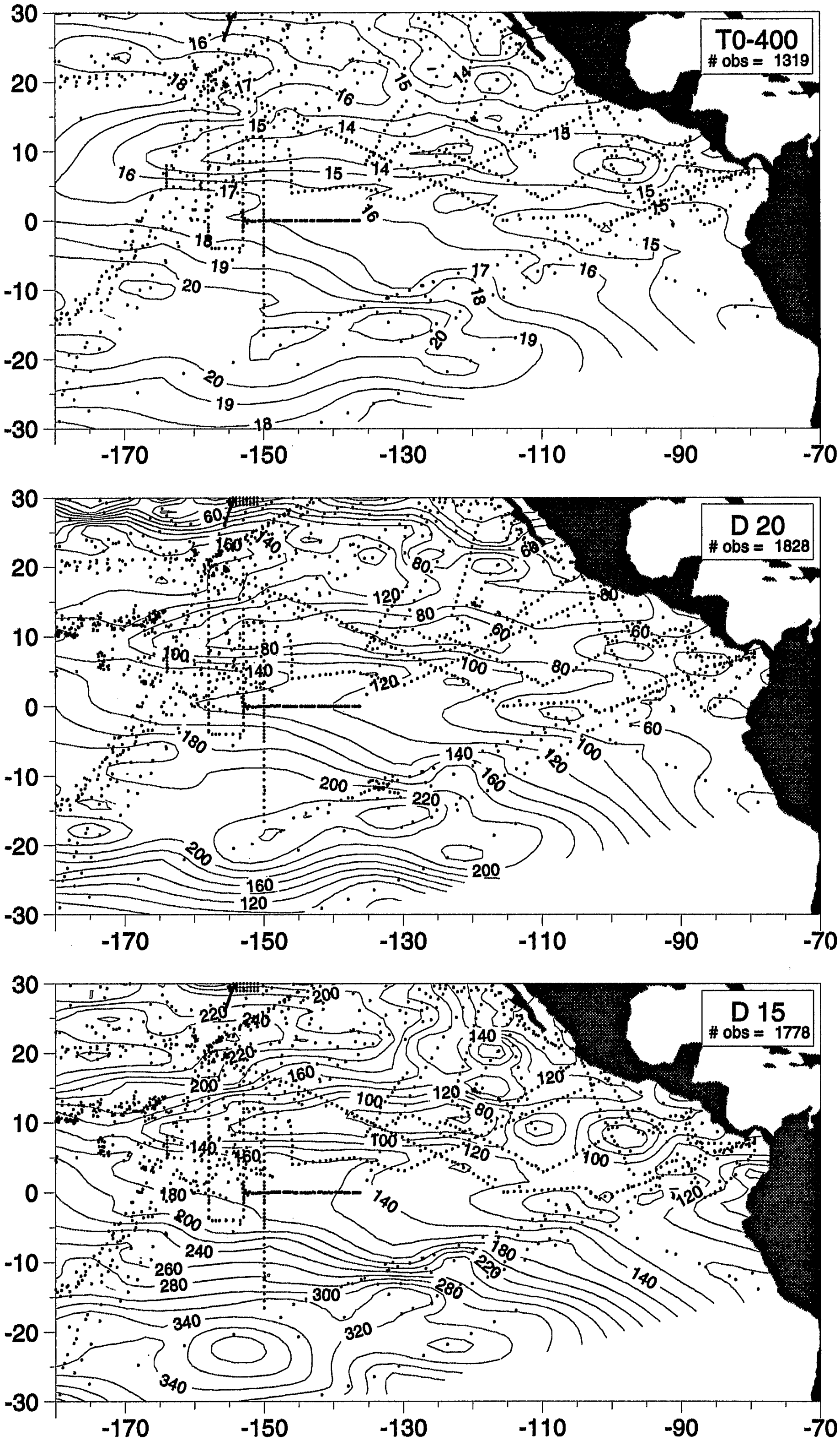

Plate 13 – *continued*. Bimonthly fields for January-February 1980.

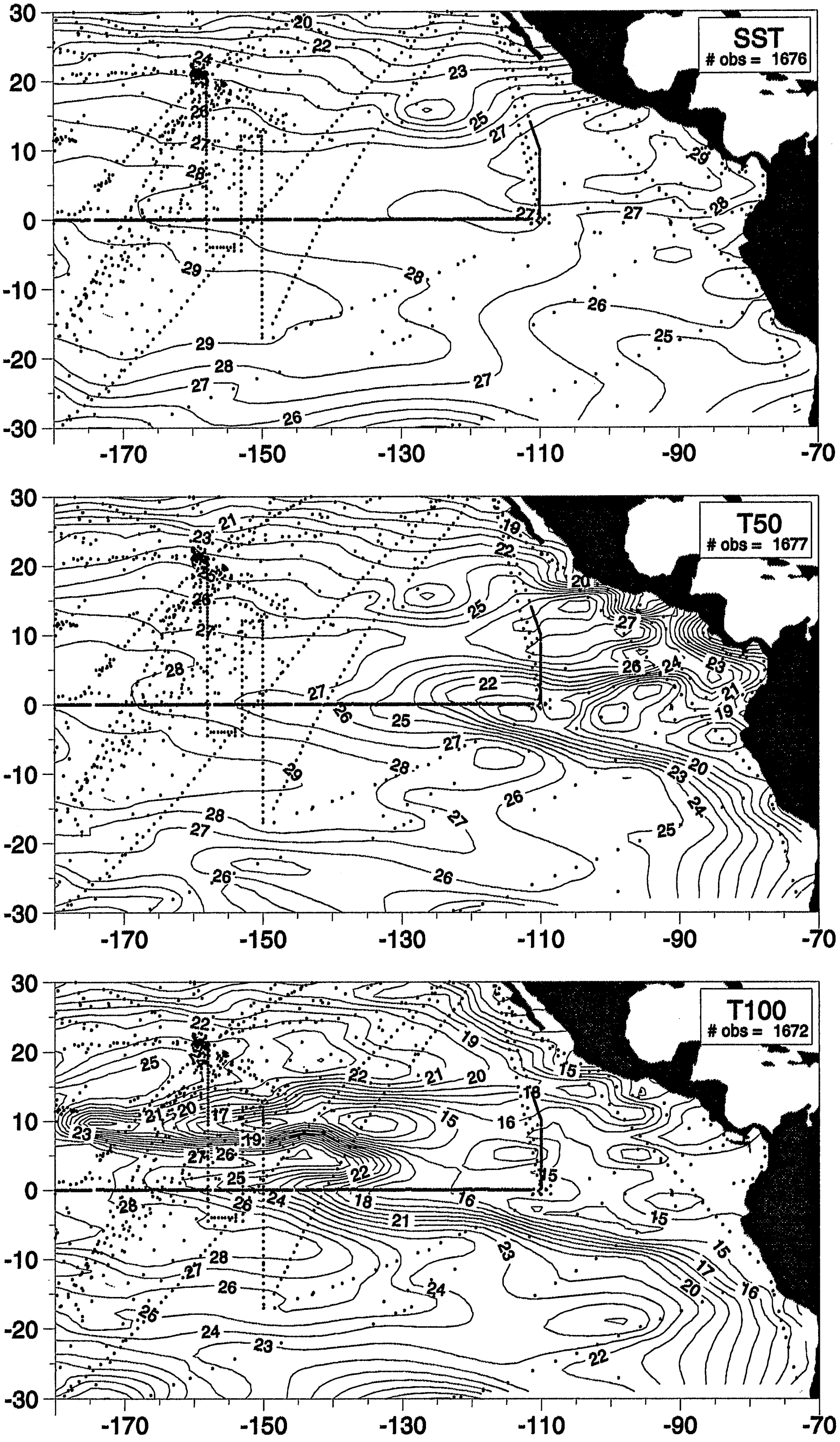

Plate 14. Bimonthly fields for March-April 1980.

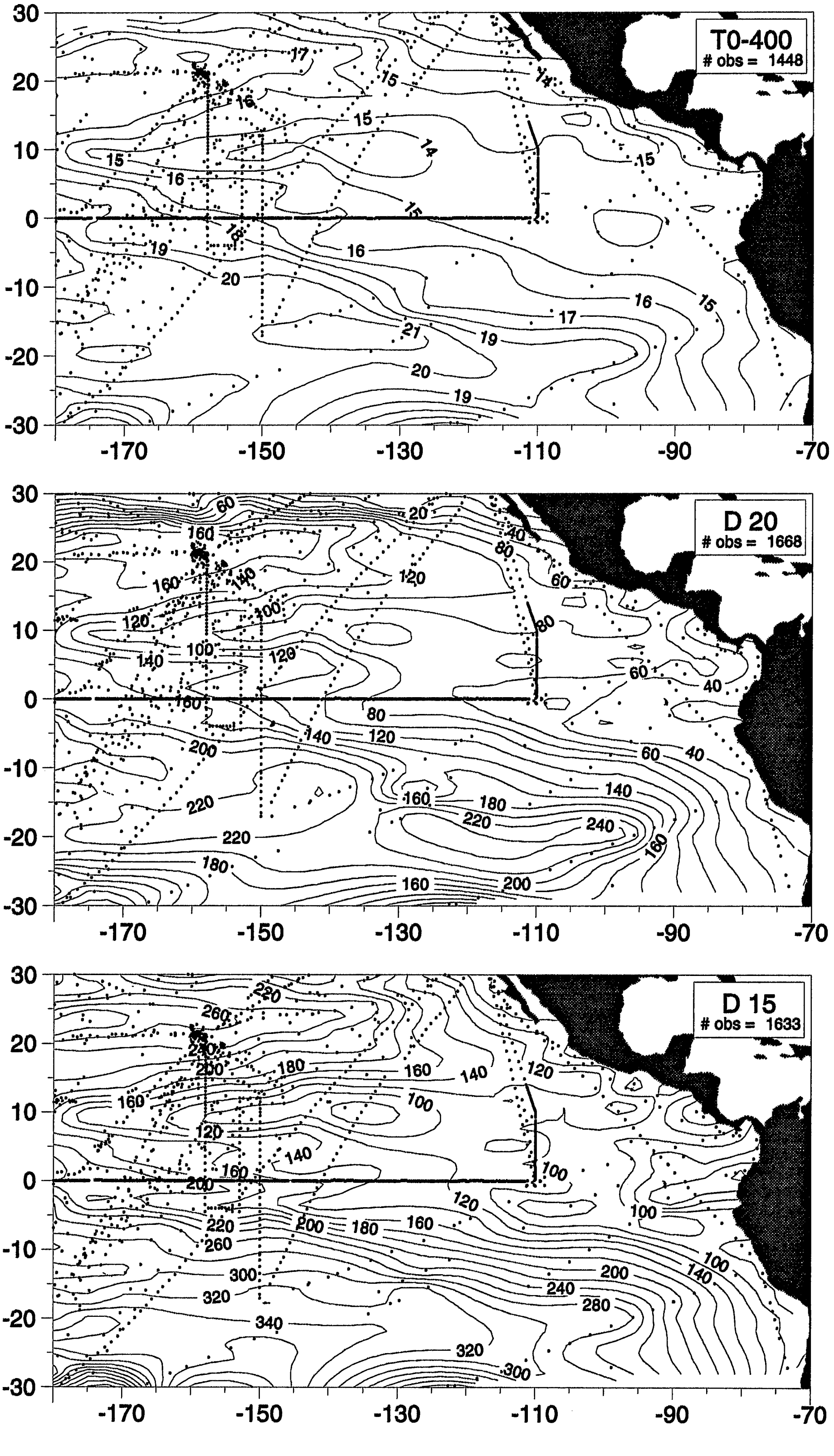

Plate 14 – *continued*. Bimonthly fields for March-April 1980.

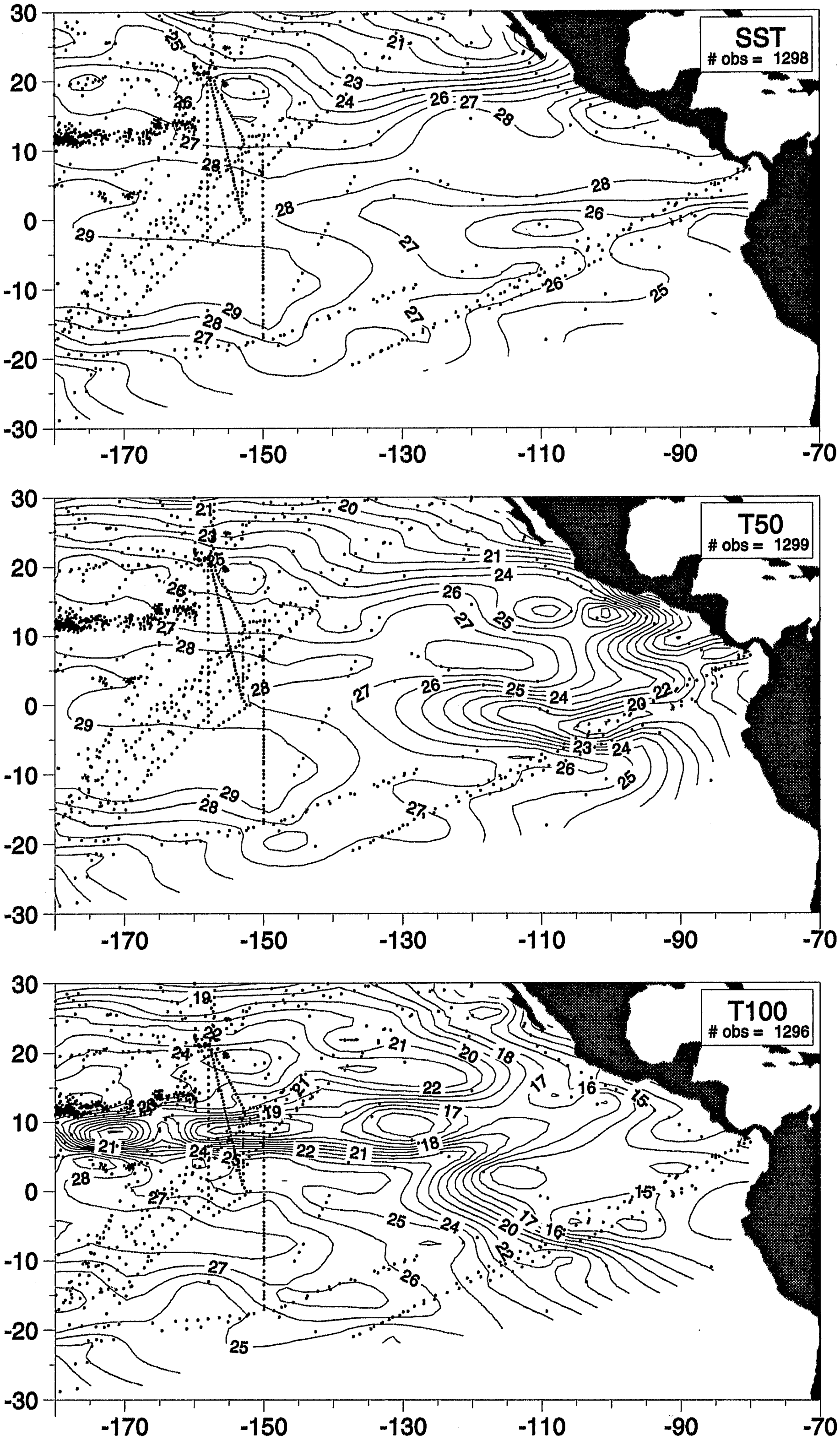

Plate 15. Bimonthly fields for May-June 1980.

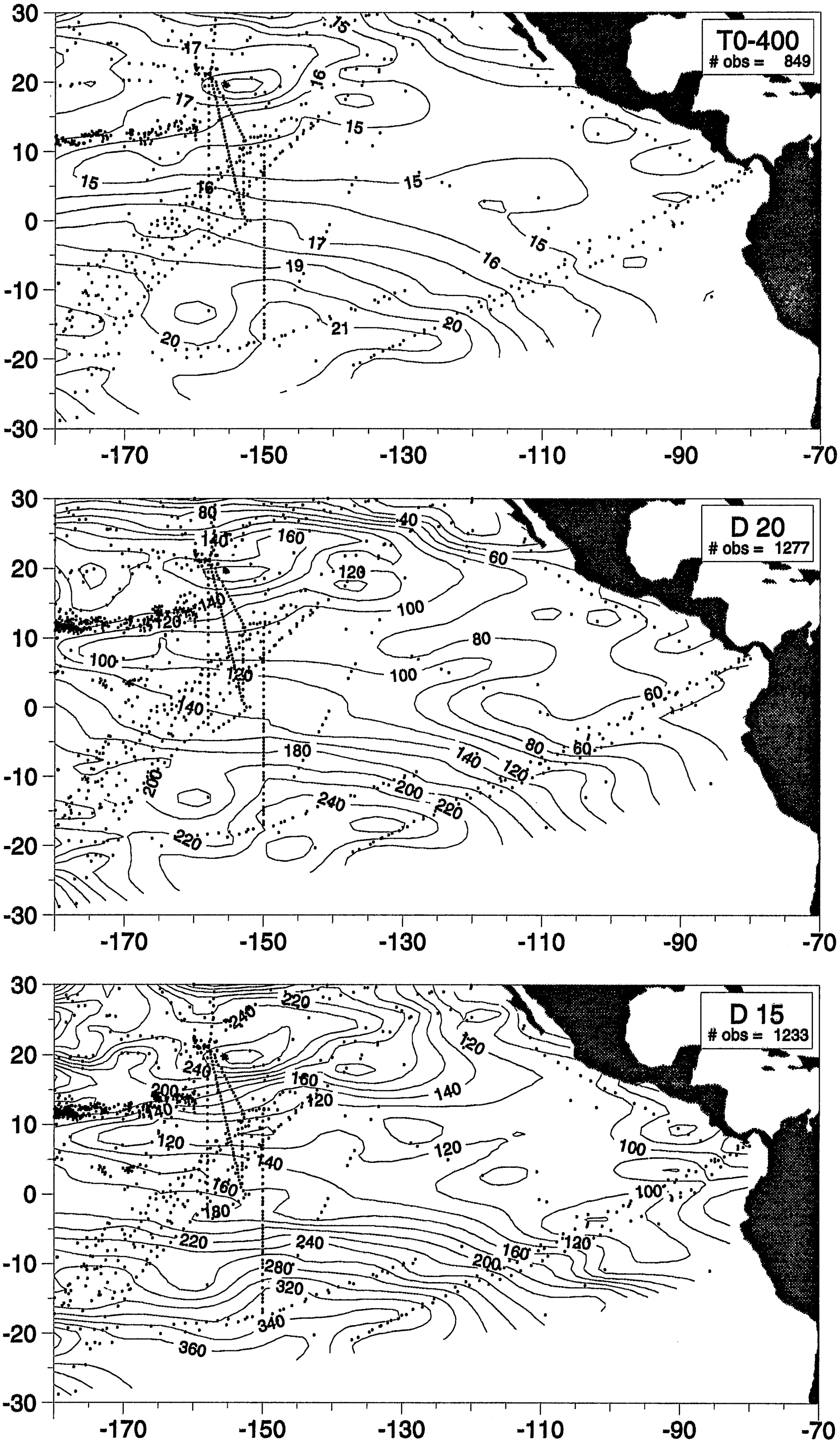

Plate 15 – *continued*. Bimonthly fields for May-June 1980.

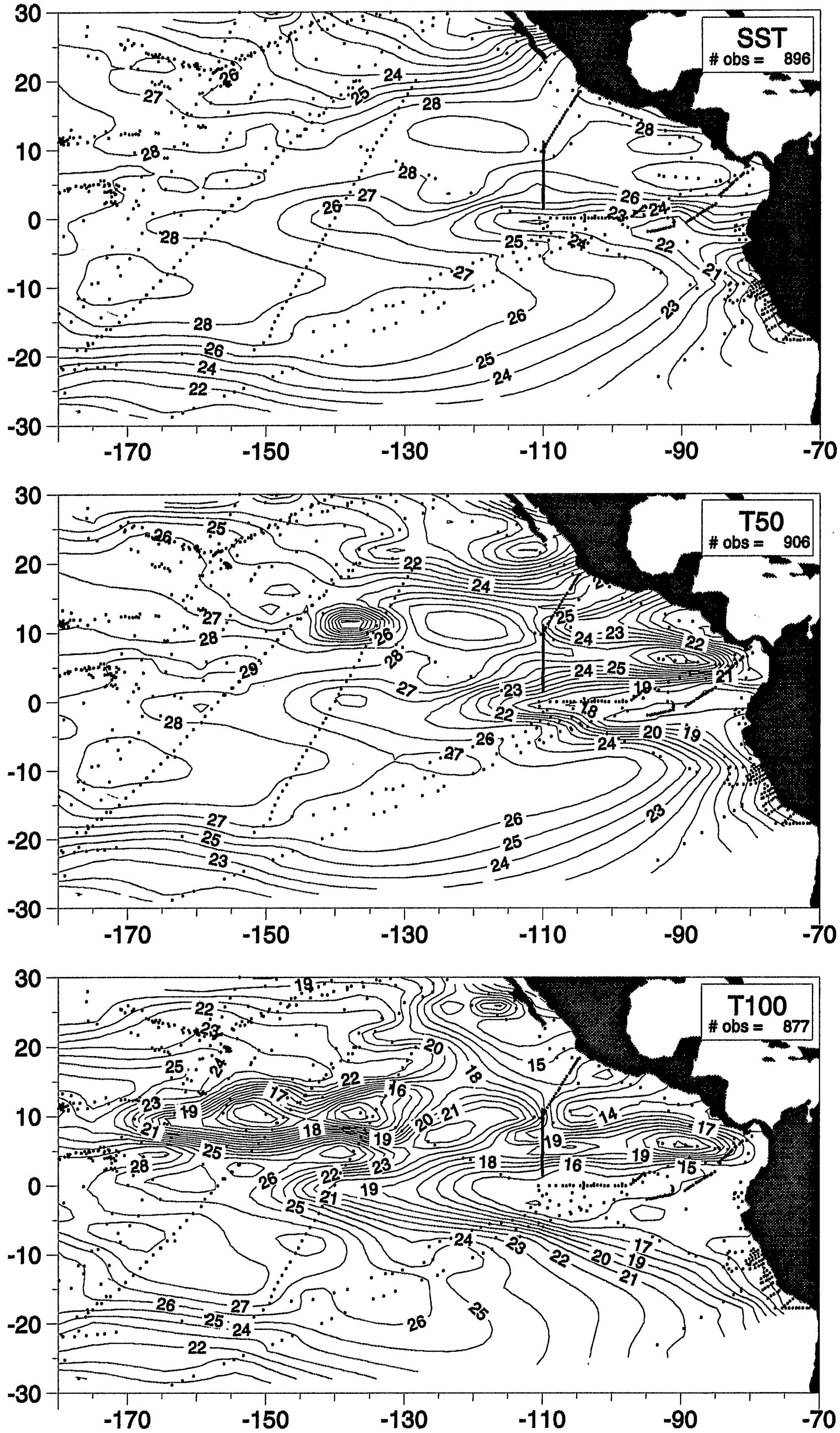

Plate 16. Bimonthly fields for July-August 1980.

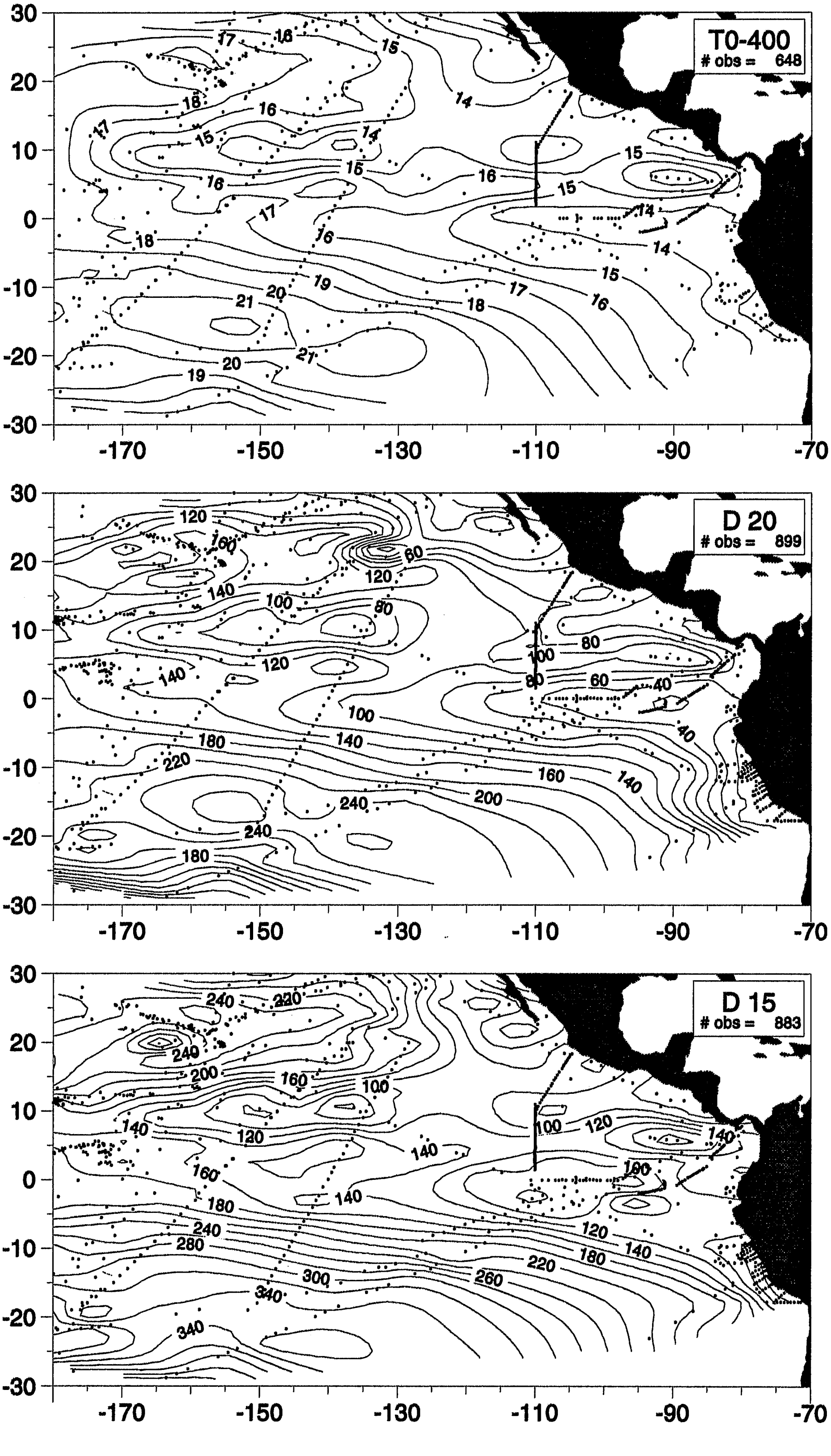

Plate 16 – *continued*. Bimonthly fields for July-August 1980.

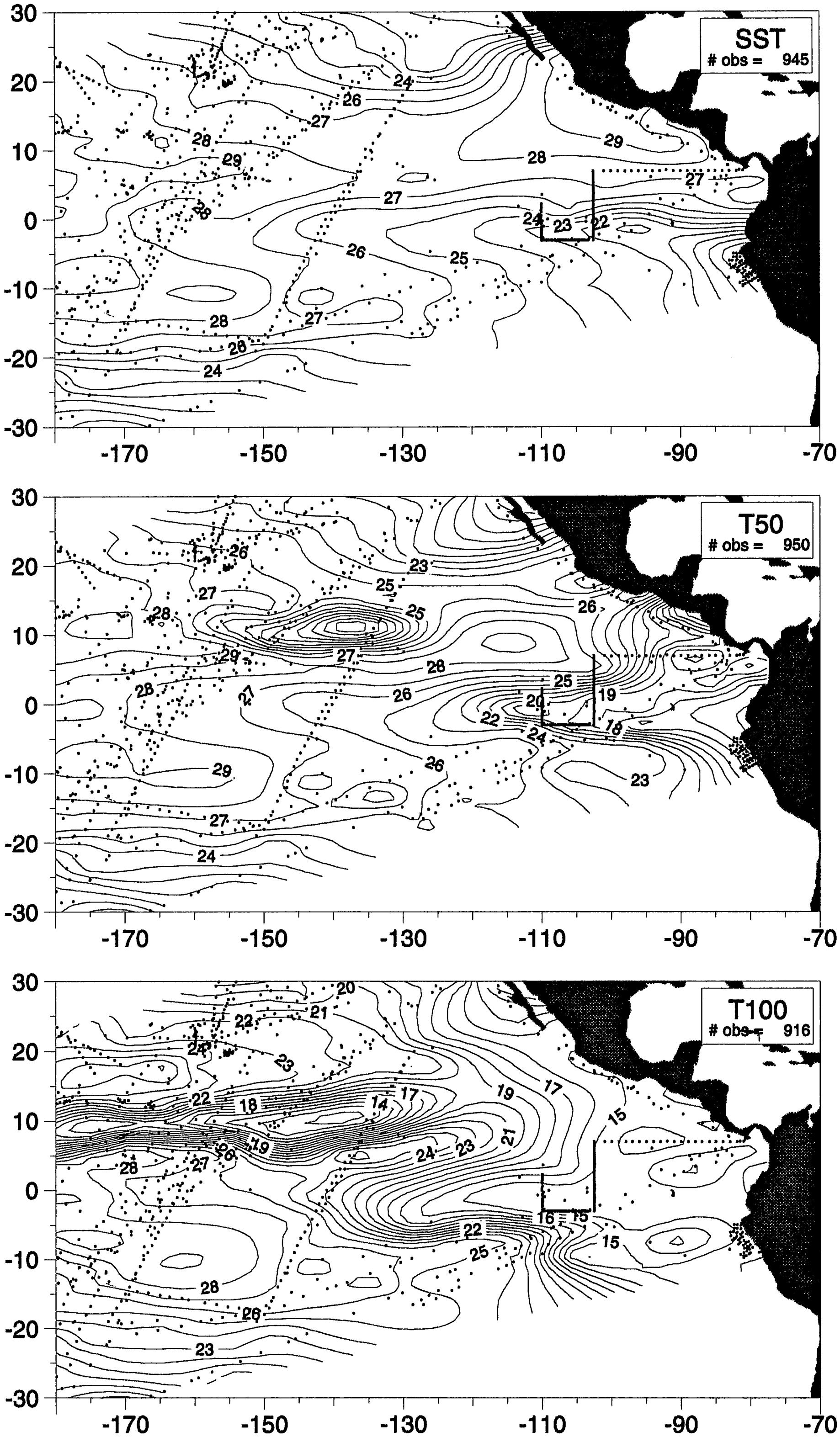

Plate 17. Bimonthly fields for September-October 1980.

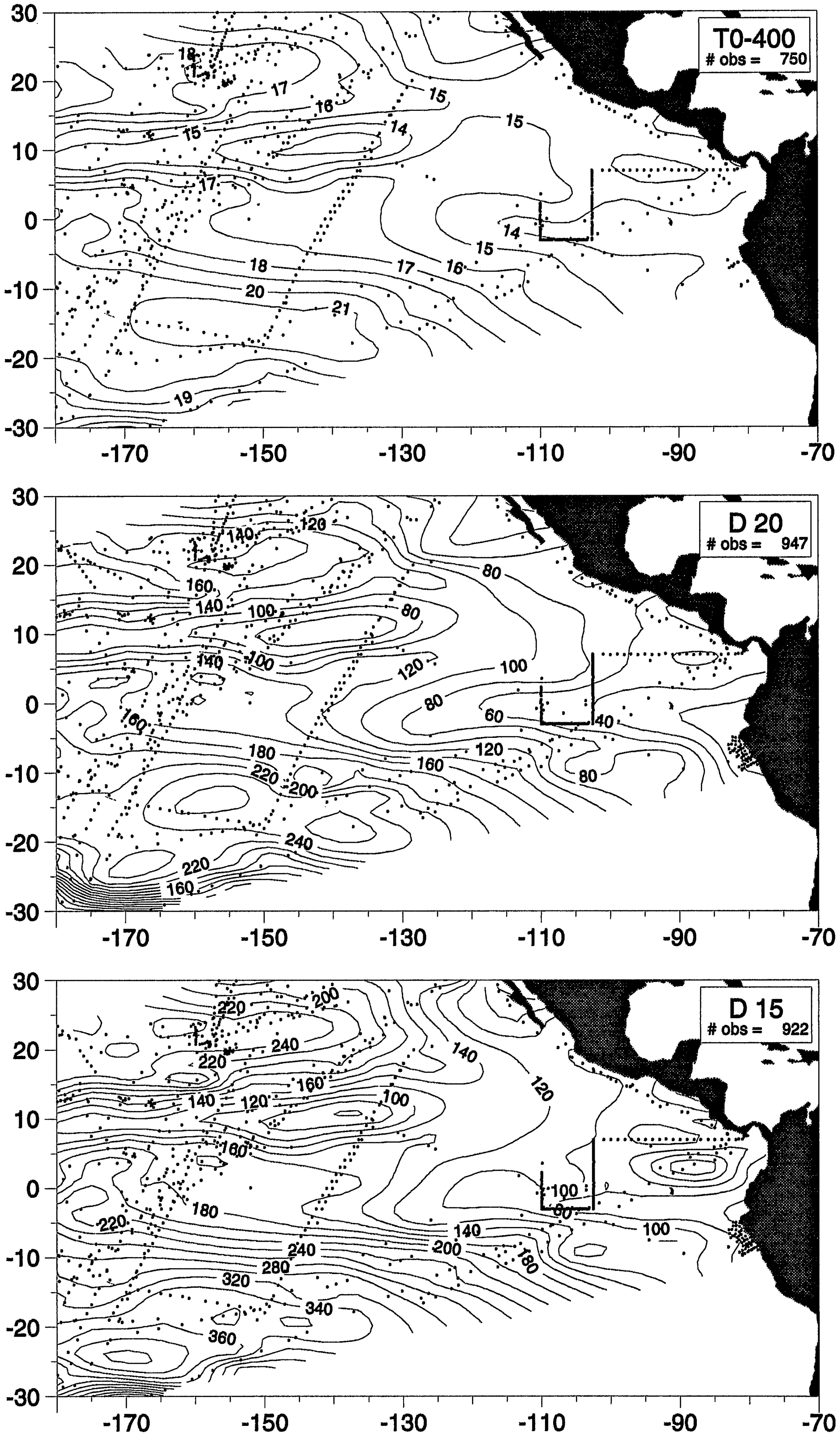

Plate 17 – *continued*. Bimonthly fields for September-October 1980.

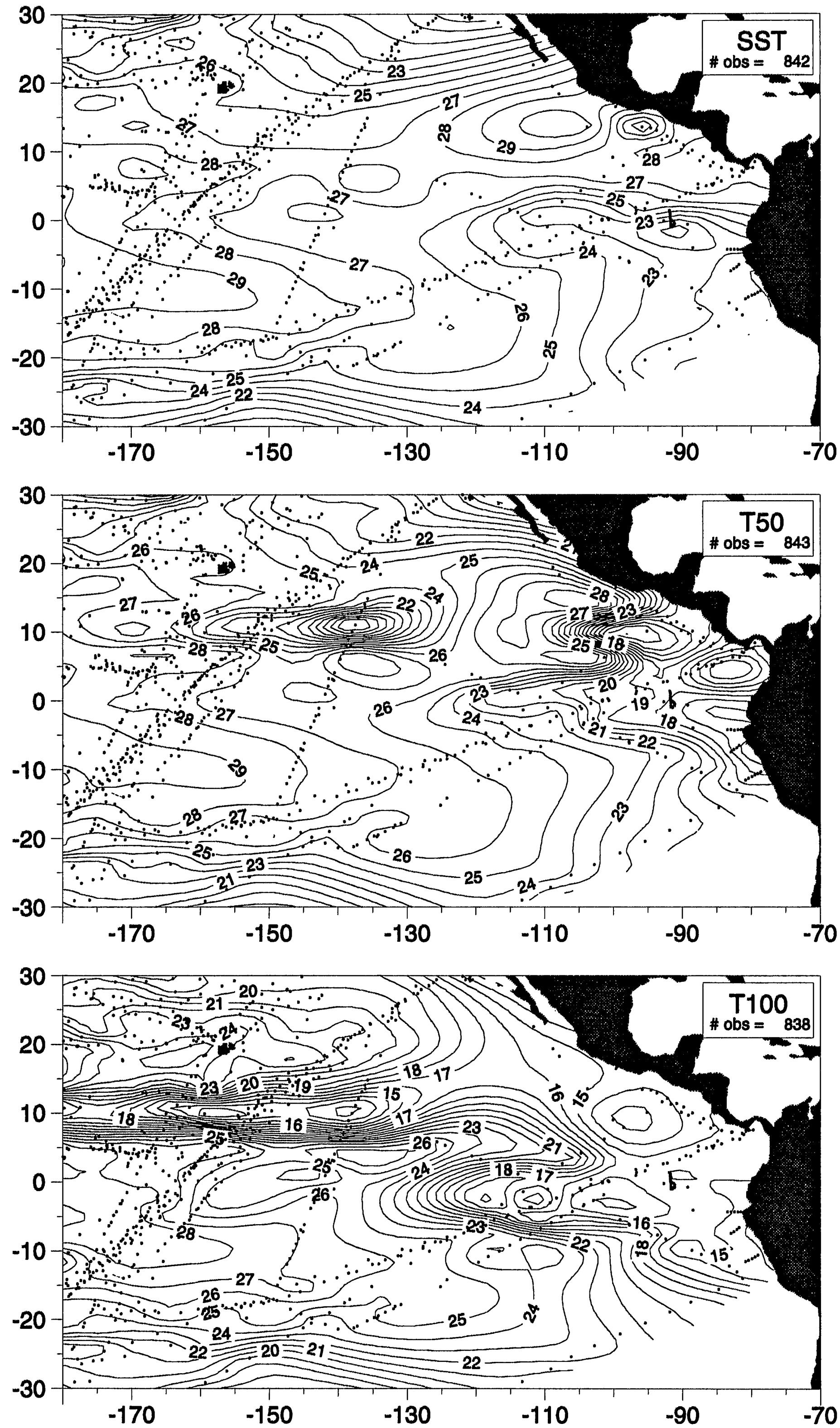

Plate 18. Bimonthly fields for November-December 1980.

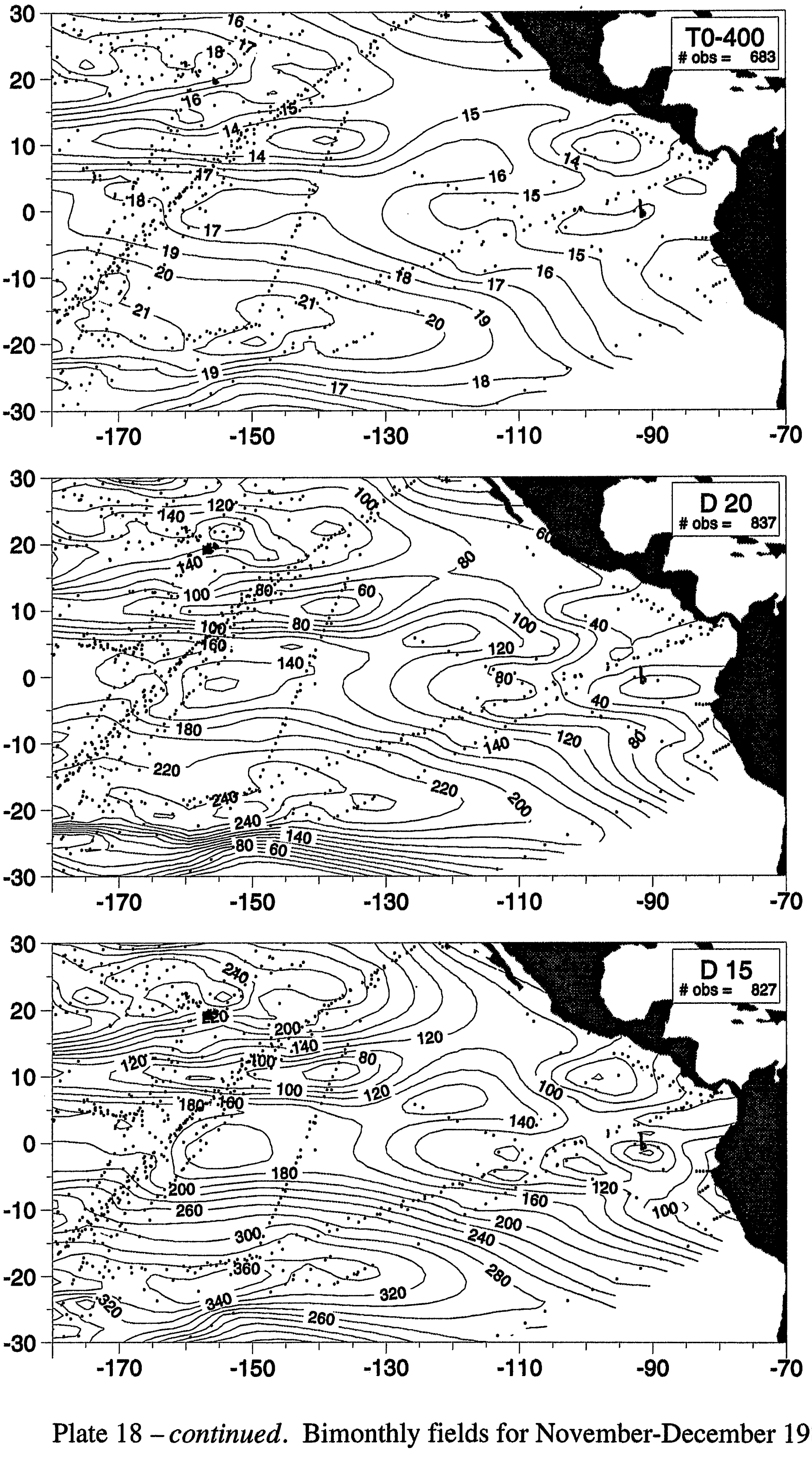

Plate 18 – *continued.* Bimonthly fields for November-December 1980.

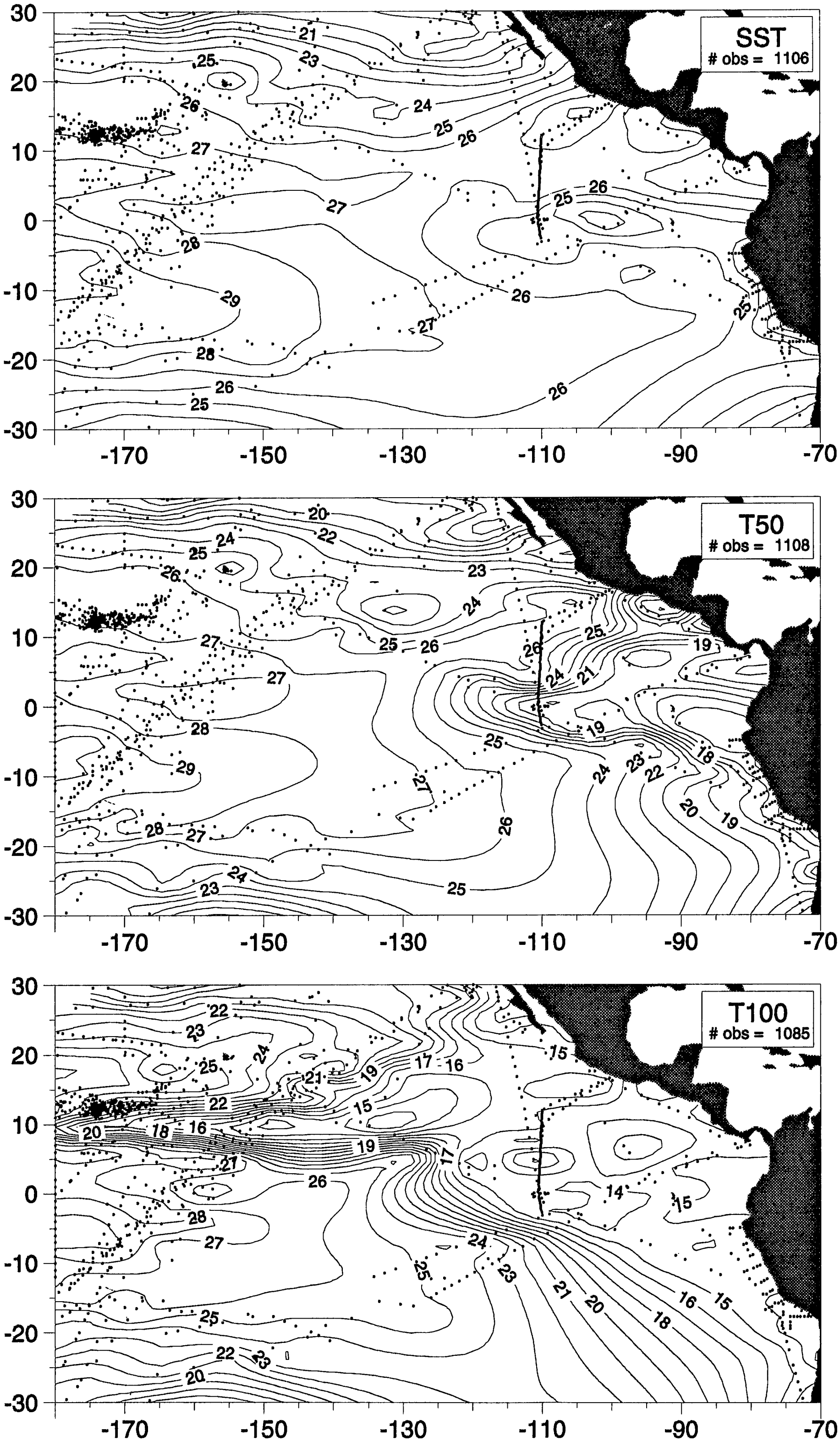

Plate 19. Bimonthly fields for January-February 1981.

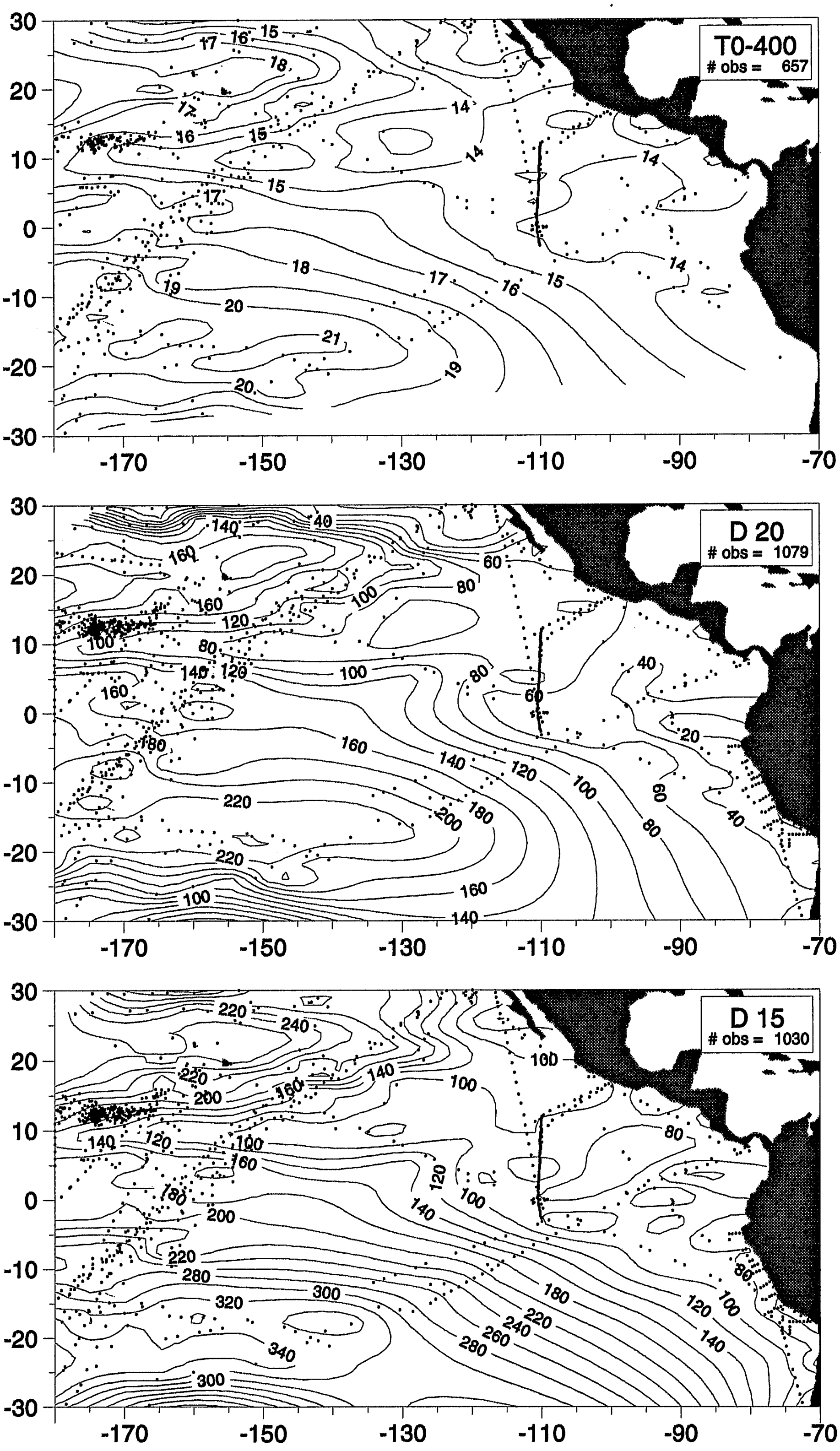

Plate 19 – *continued.* Bimonthly fields for January-February 1981.

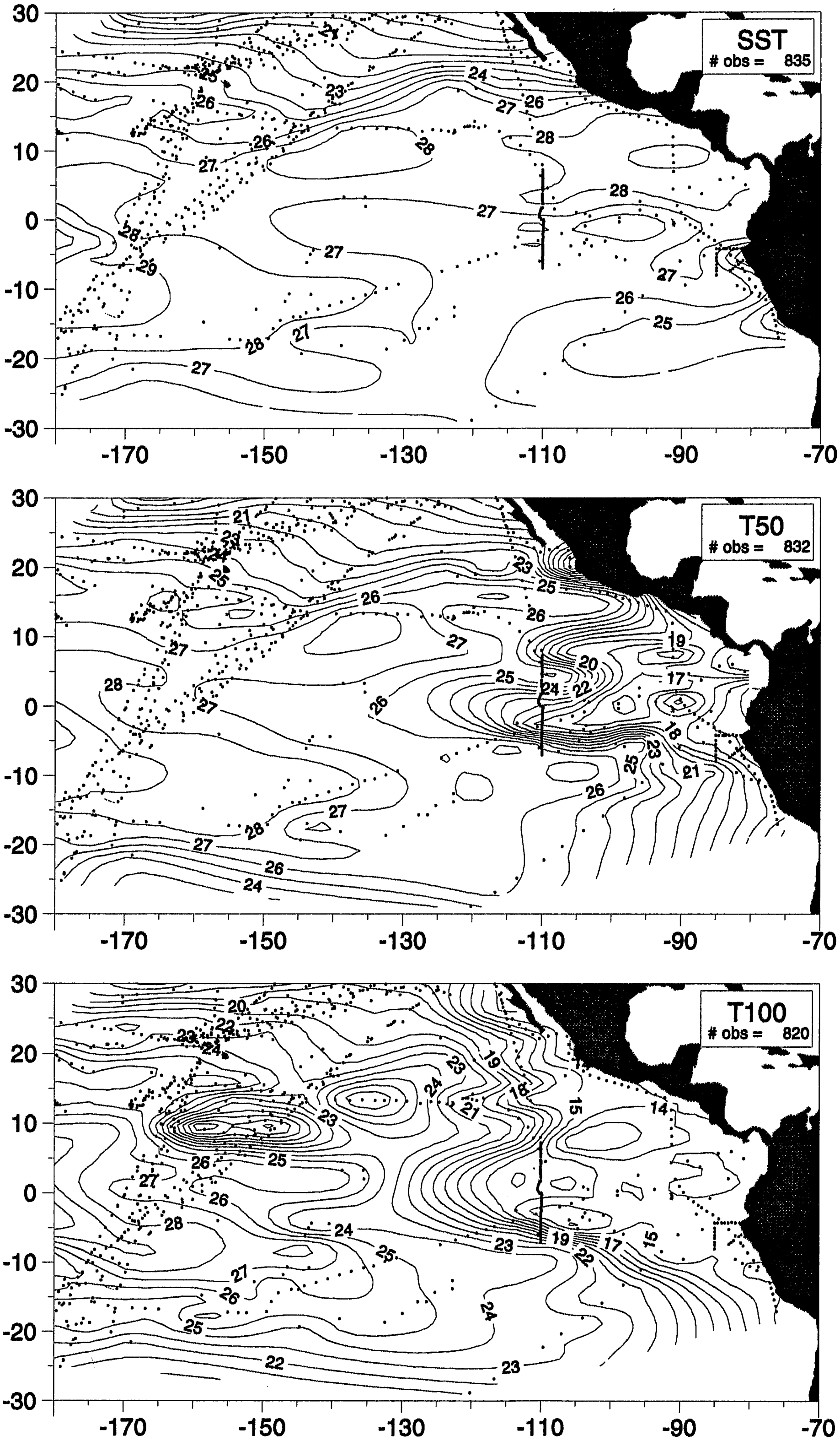

Plate 20. Bimonthly fields for March-April 1981.

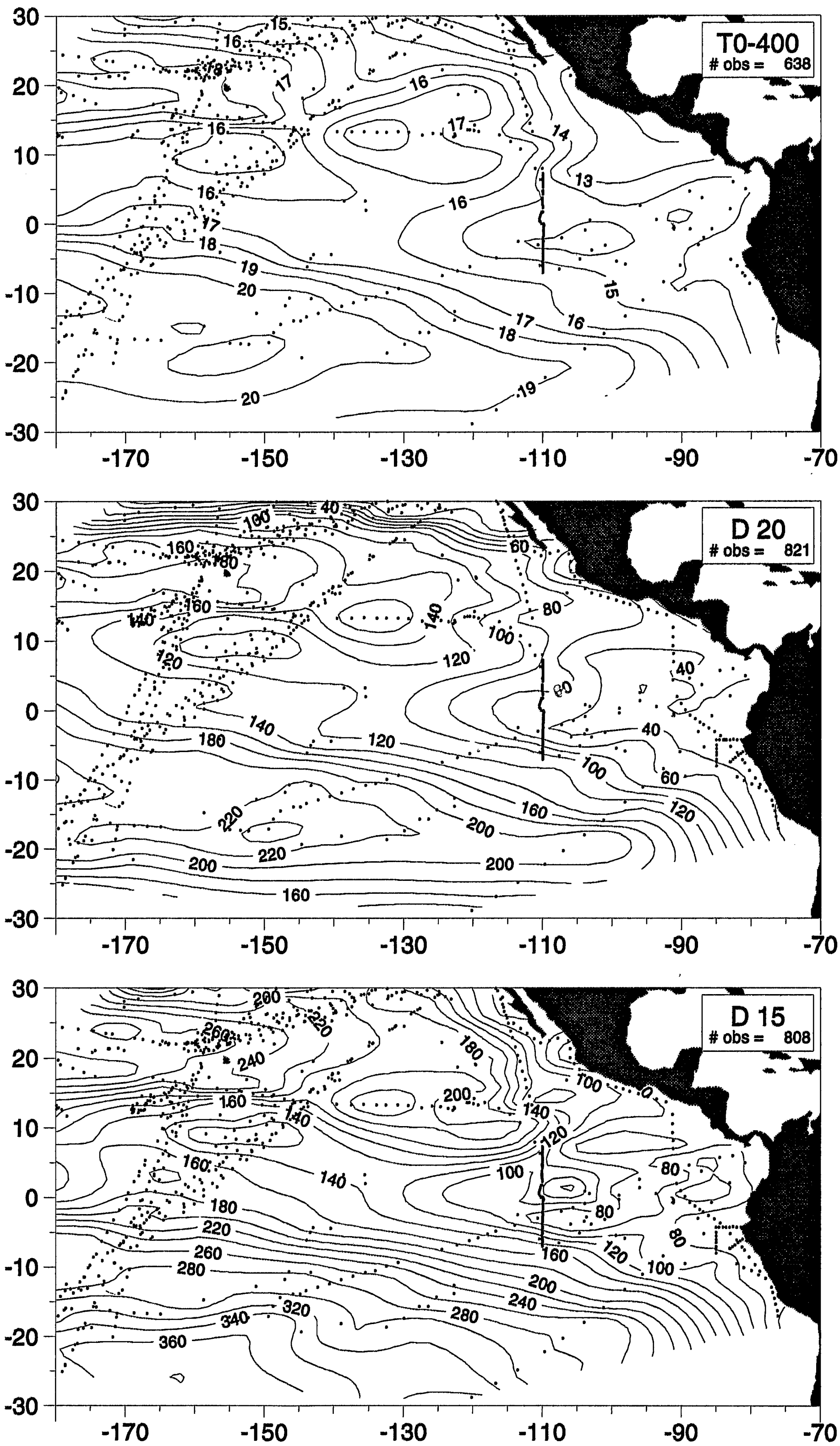

Plate 20 – *continued*. Bimonthly fields for March-April 1981.

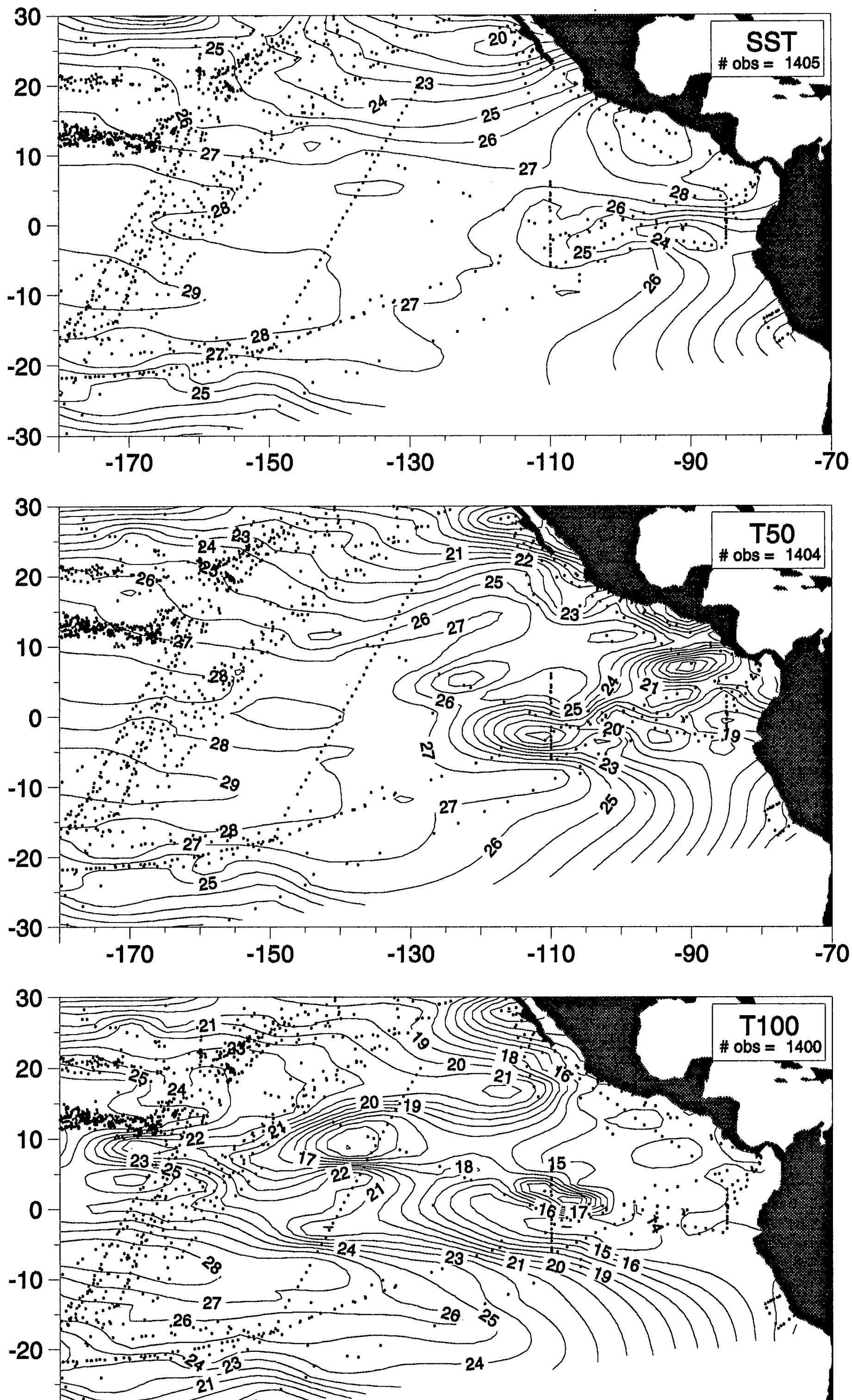

Plate 21. Bimonthly fields for May-June 1981.

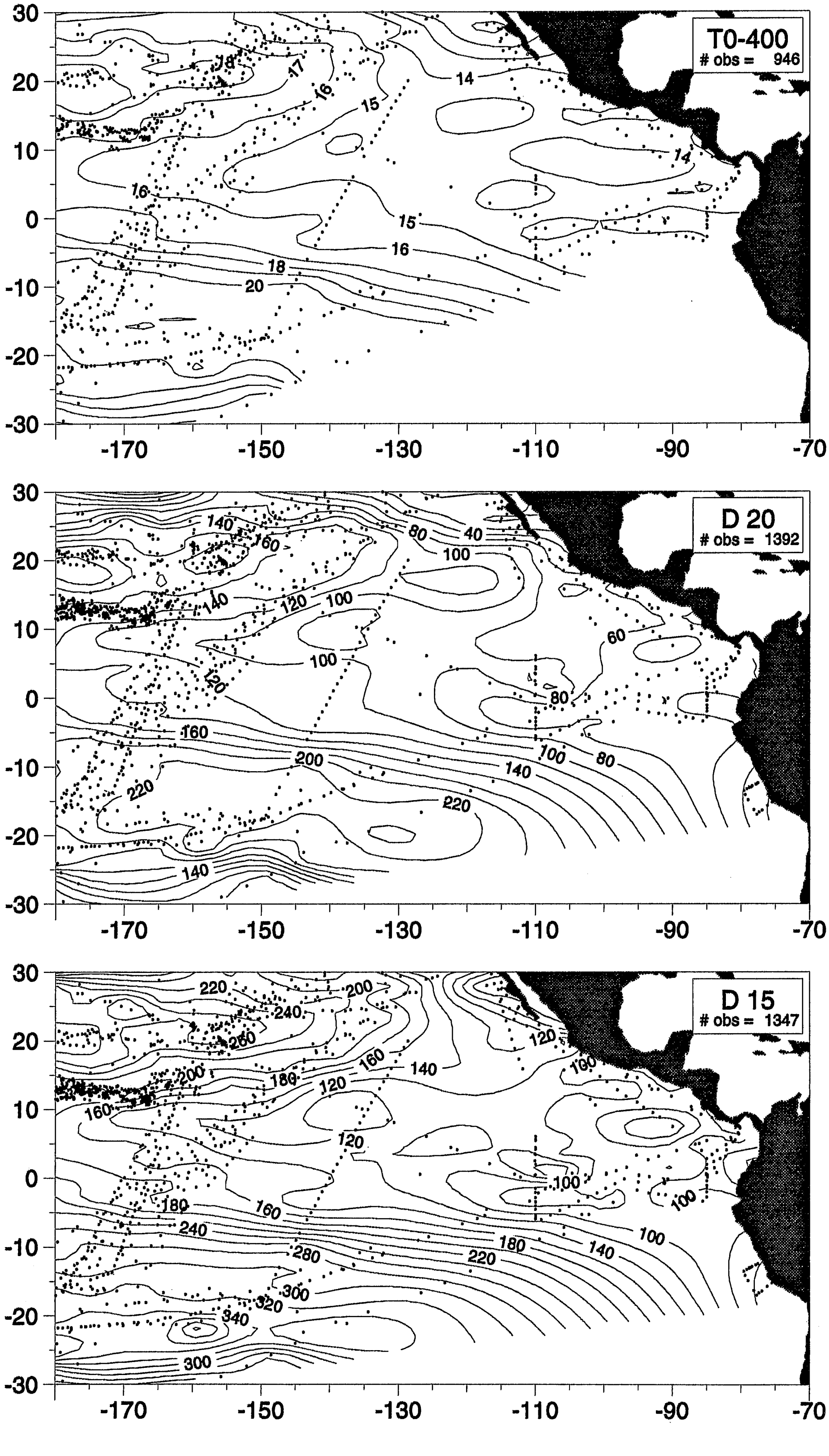

Plate 21 – *continued*. Bimonthly fields for May-June 1981.

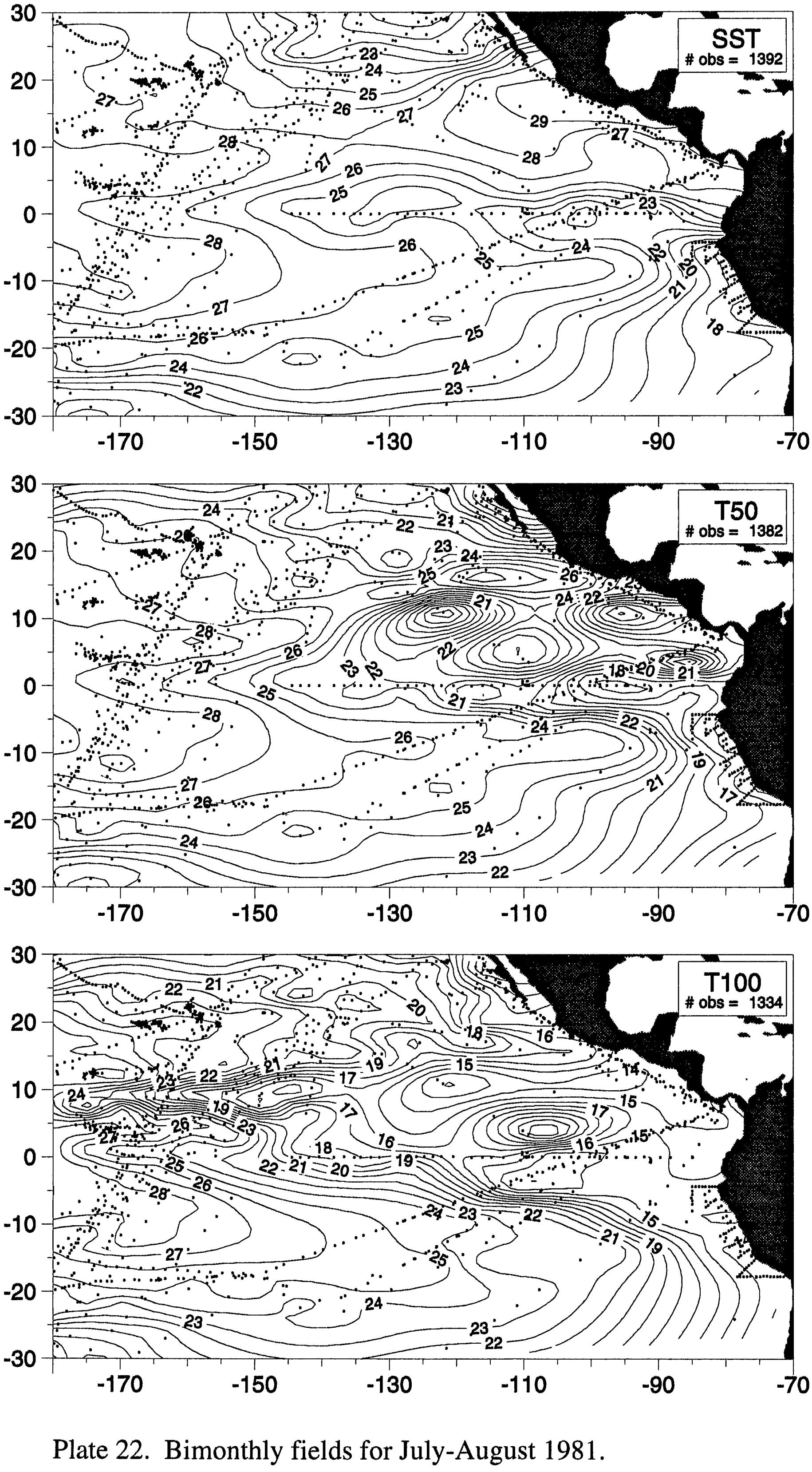

Plate 22. Bimonthly fields for July-August 1981.

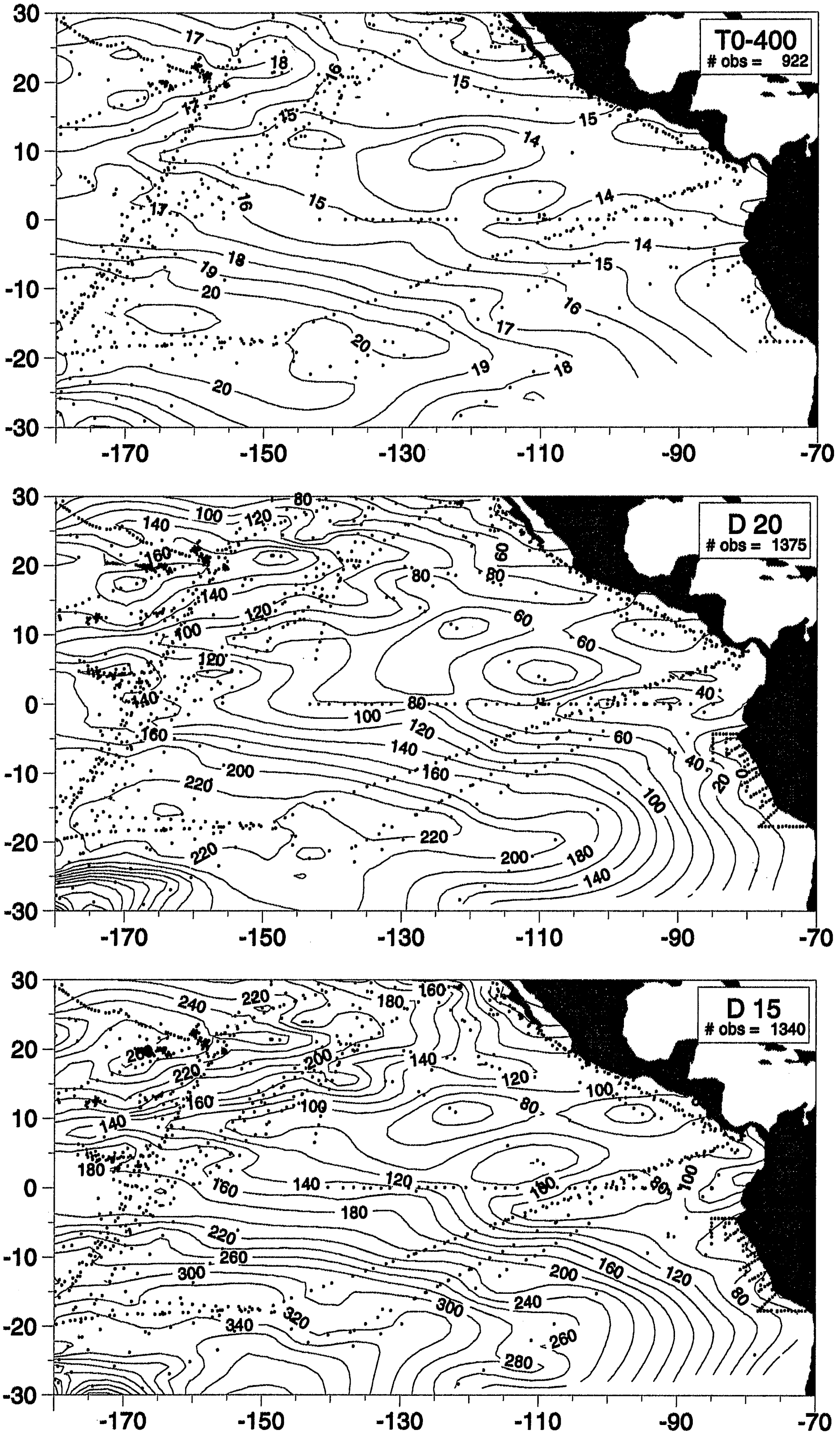

Plate 22 – *continued*. Bimonthly fields for July-August 1981.

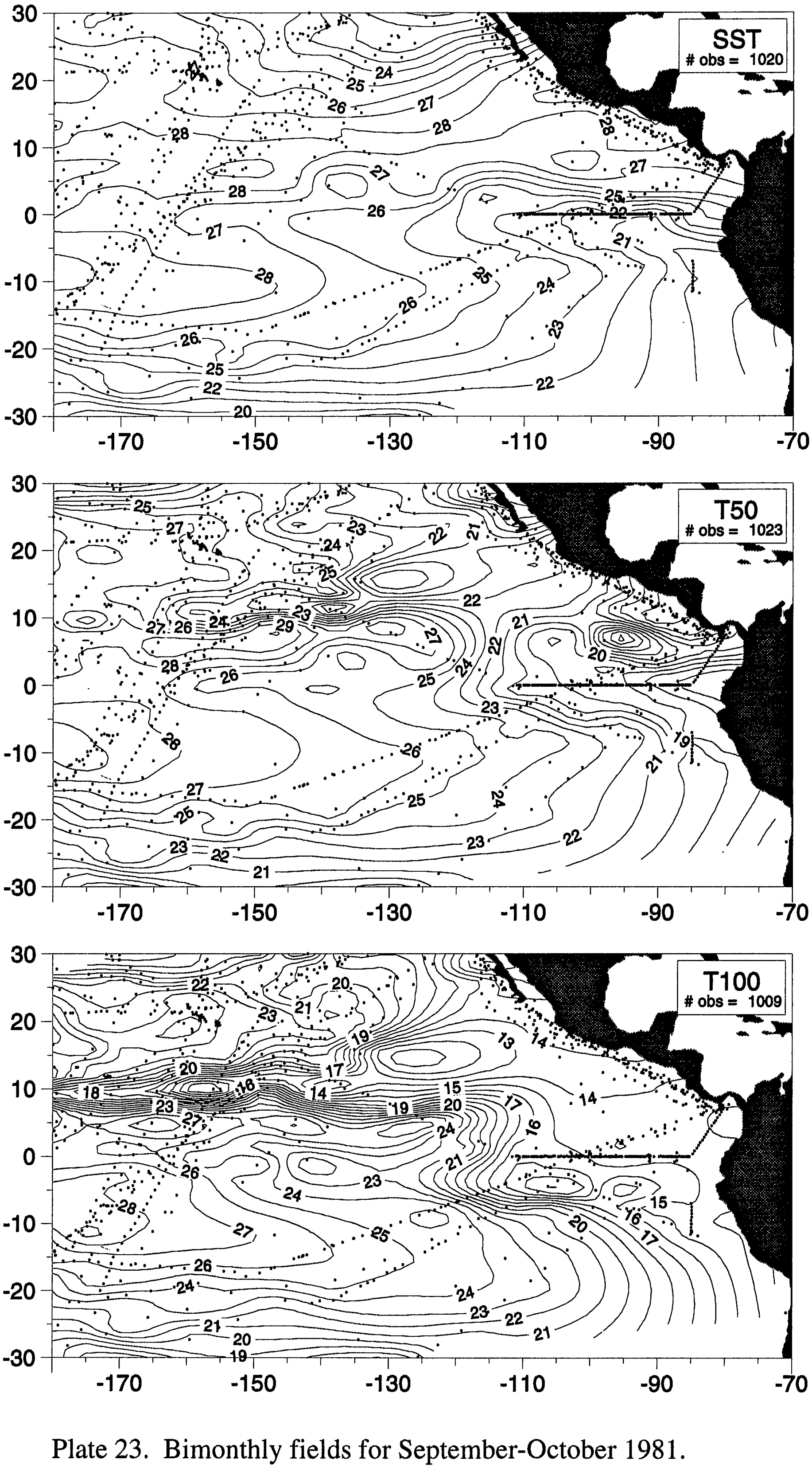

Plate 23. Bimonthly fields for September-October 1981.

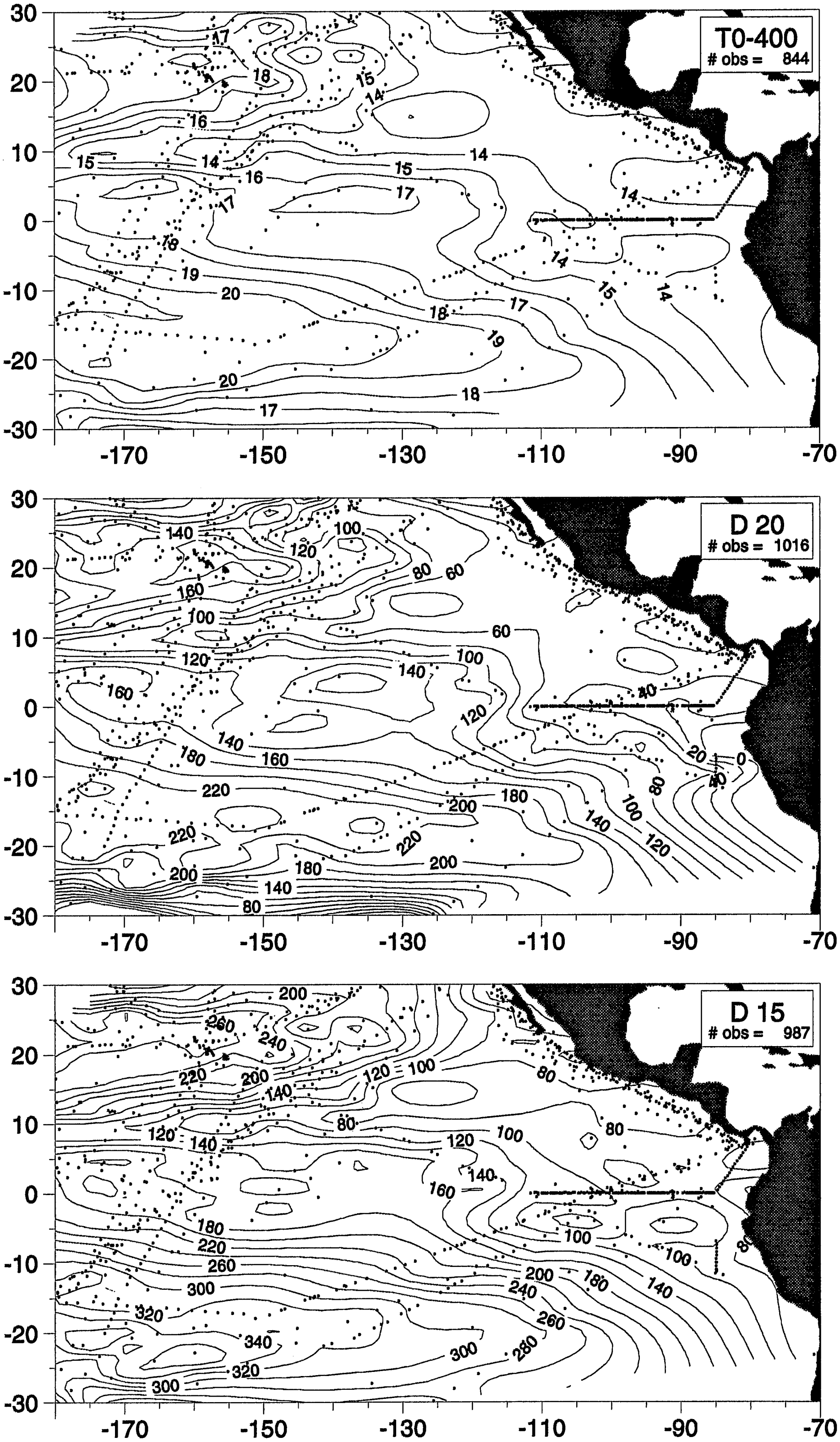

Plate 23 – *continued*. Bimonthly fields for September-October 1981.

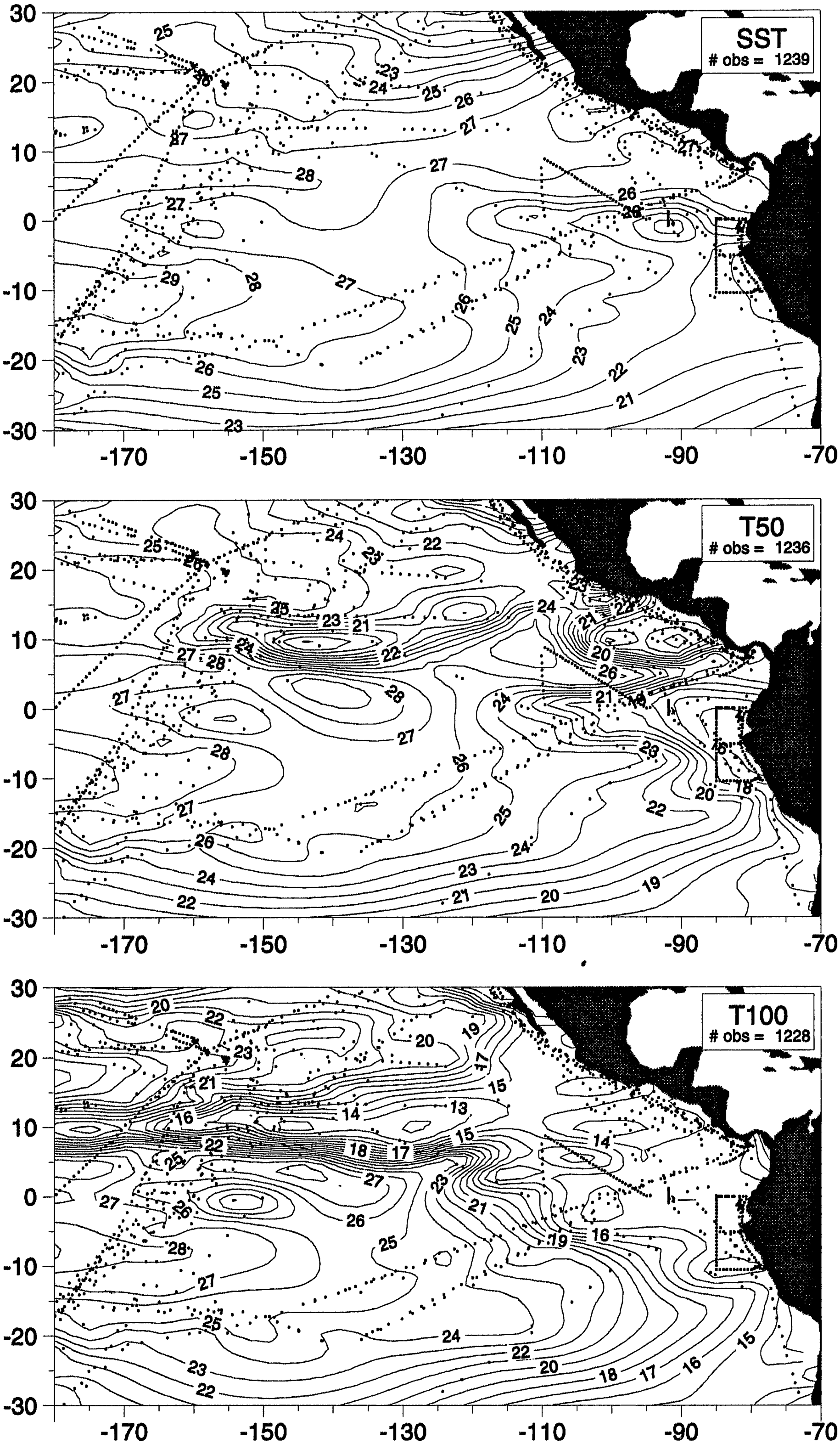

Plate 24. Bimonthly fields for November-December 1981.

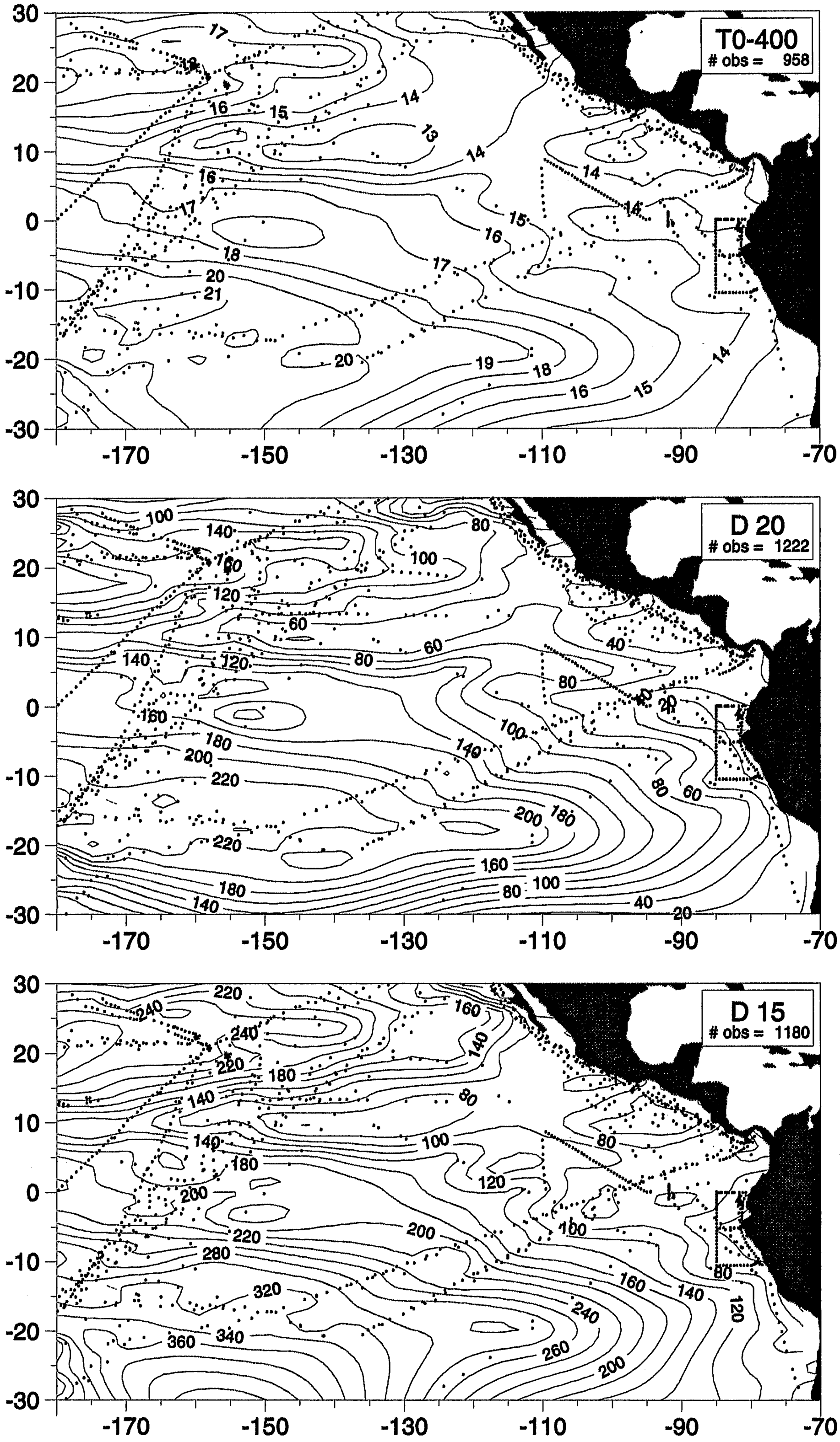

Plate 24 – *continued*. Bimonthly fields for November-December 1981.

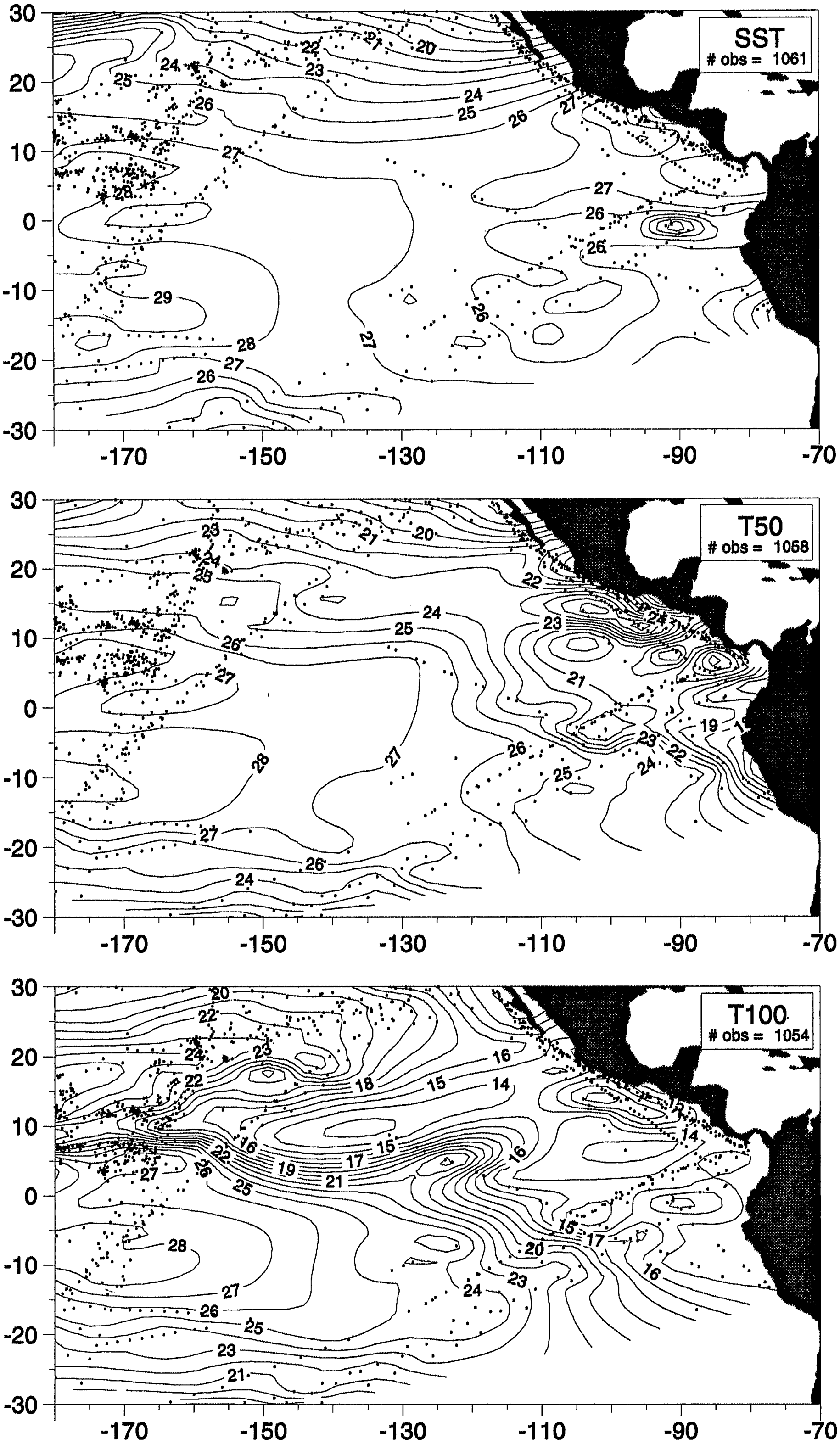

Plate 25. Bimonthly fields for January-February 1982.

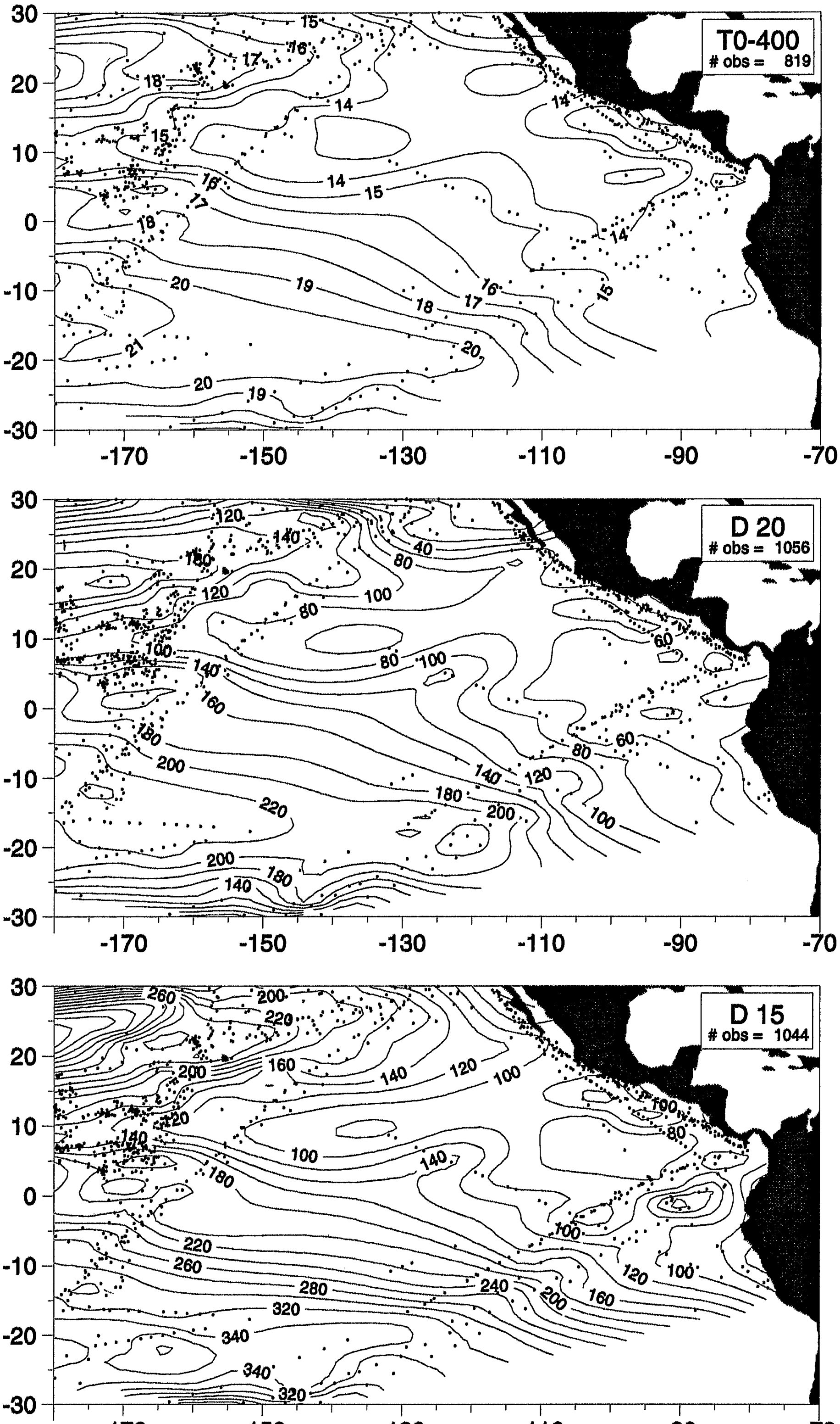

Plate 25 – *continued.* Bimonthly fields for January-February 1982.

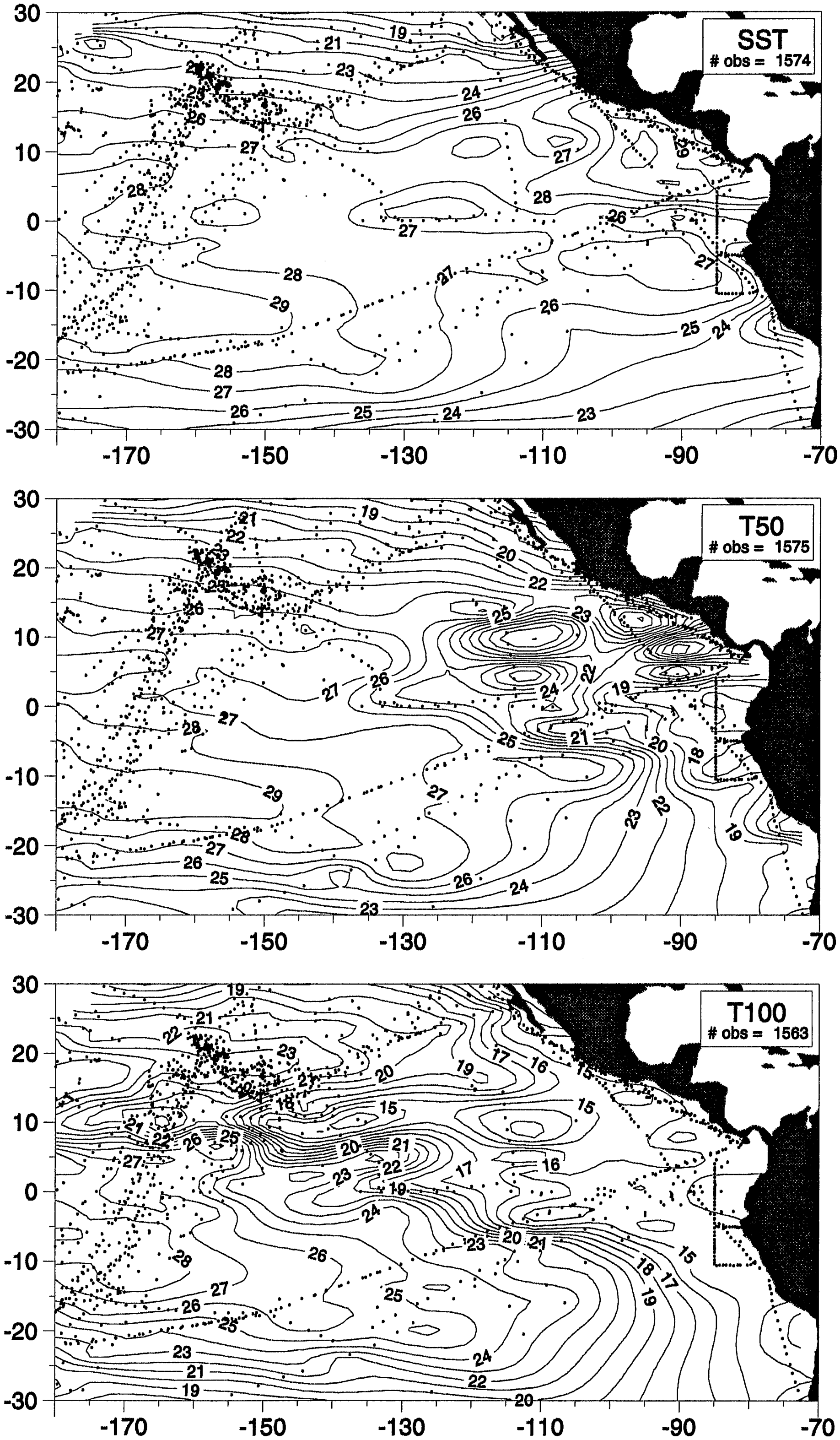

Plate 26. Bimonthly fields for March-April 1982.

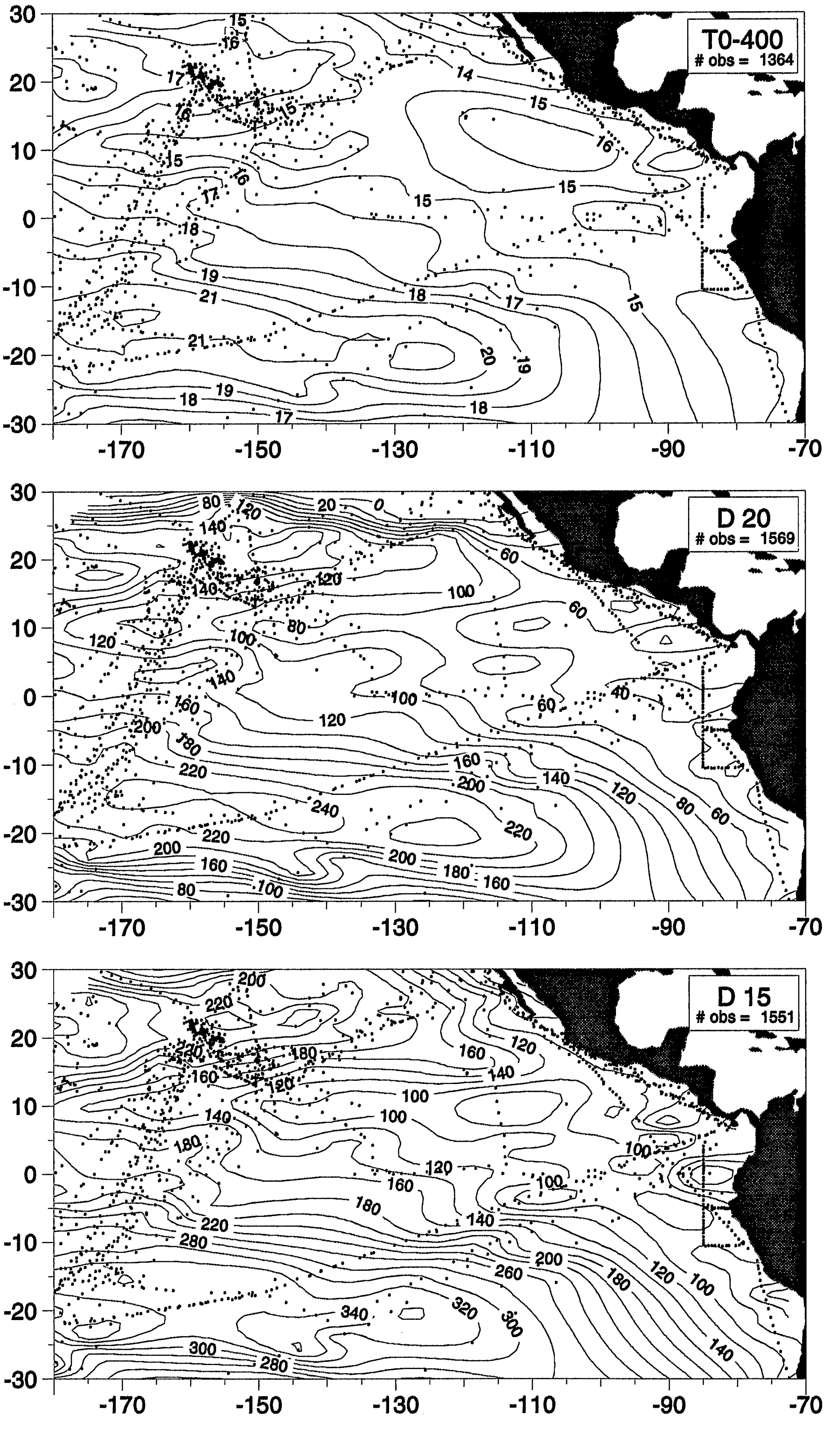

Plate 26 – *continued*. Bimonthly fields for March-April 1982.

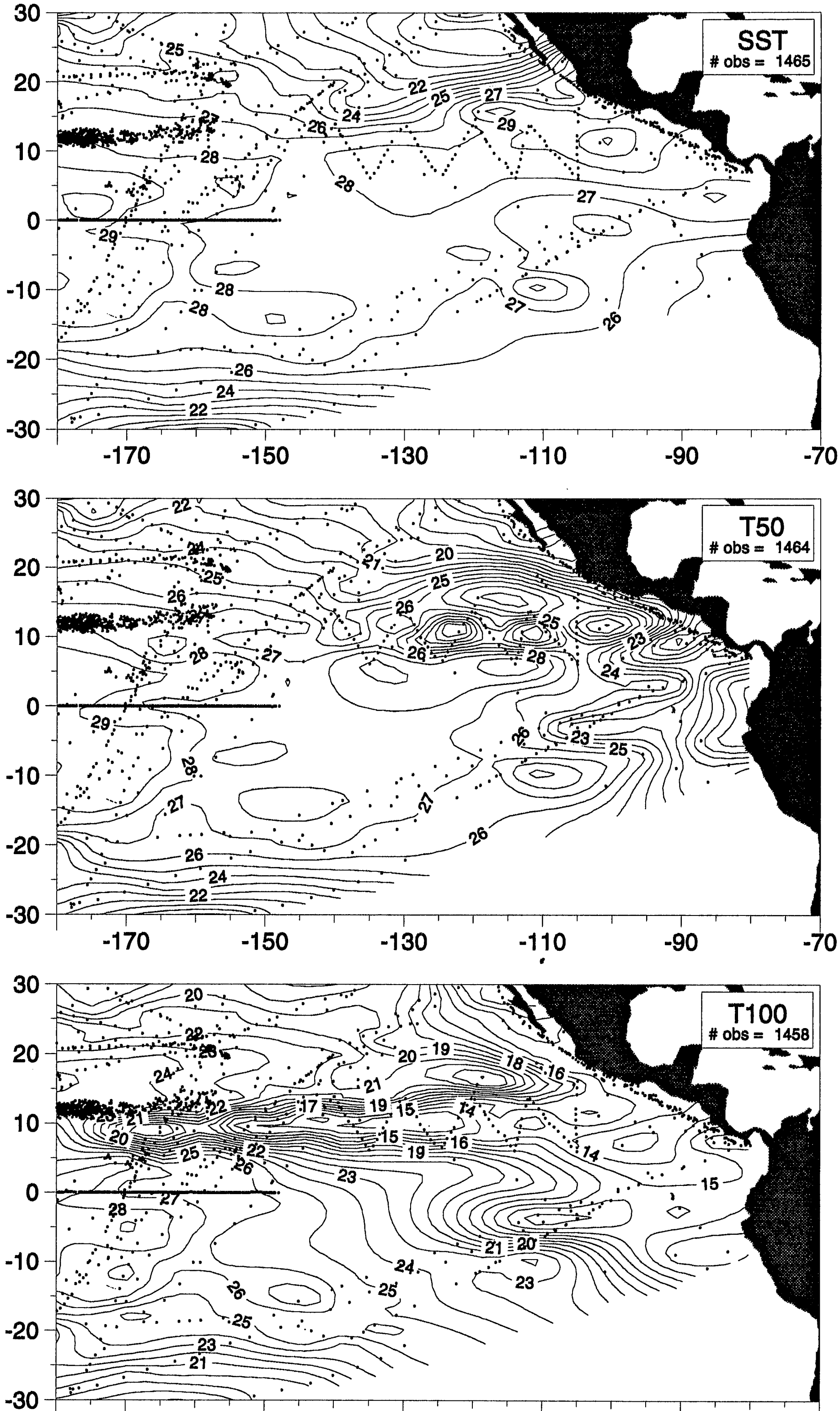

Plate 27. Bimonthly fields for May-June 1982.

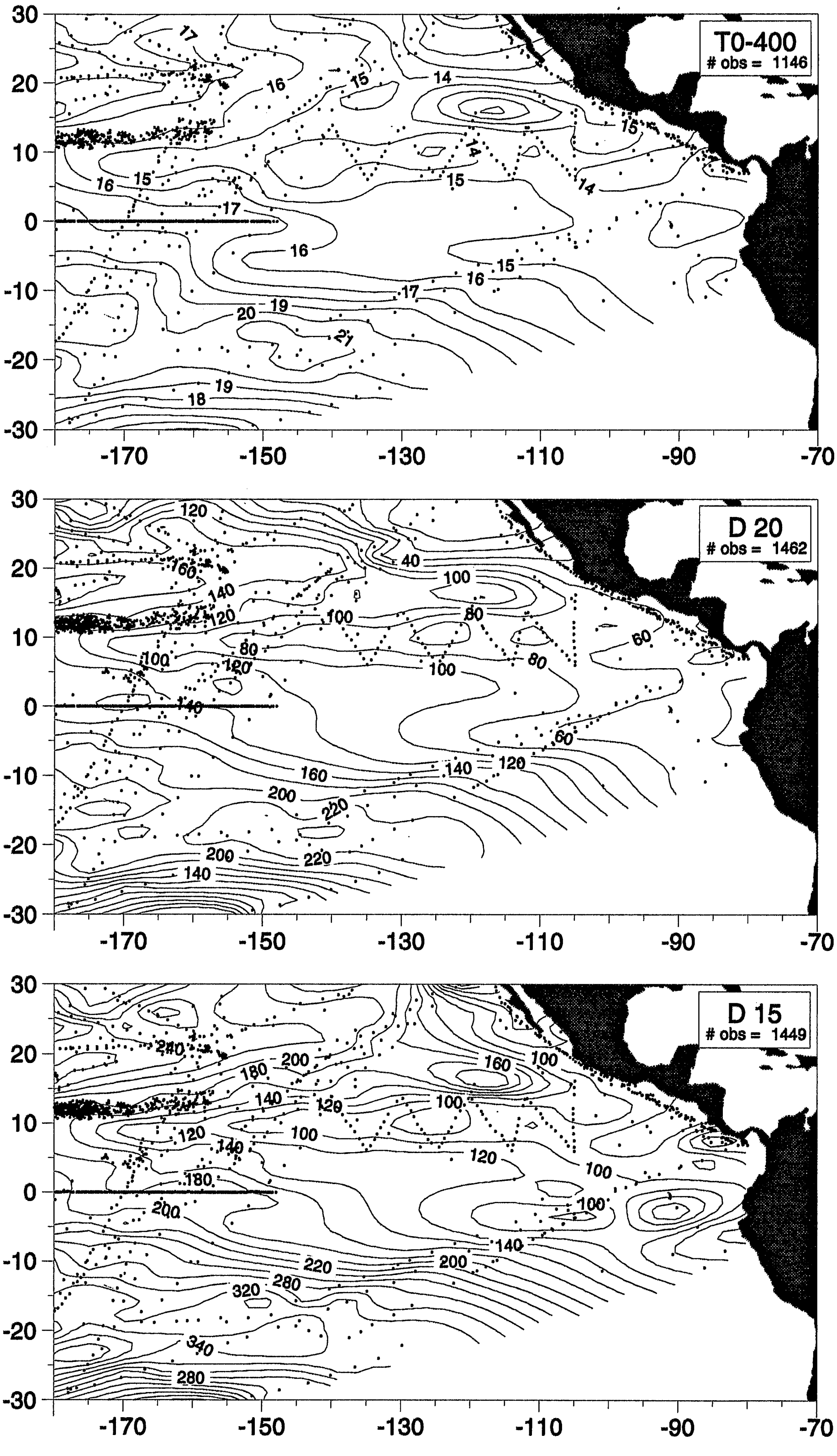

Plate 27 – *continued.* Bimonthly fields for May-June 1982.

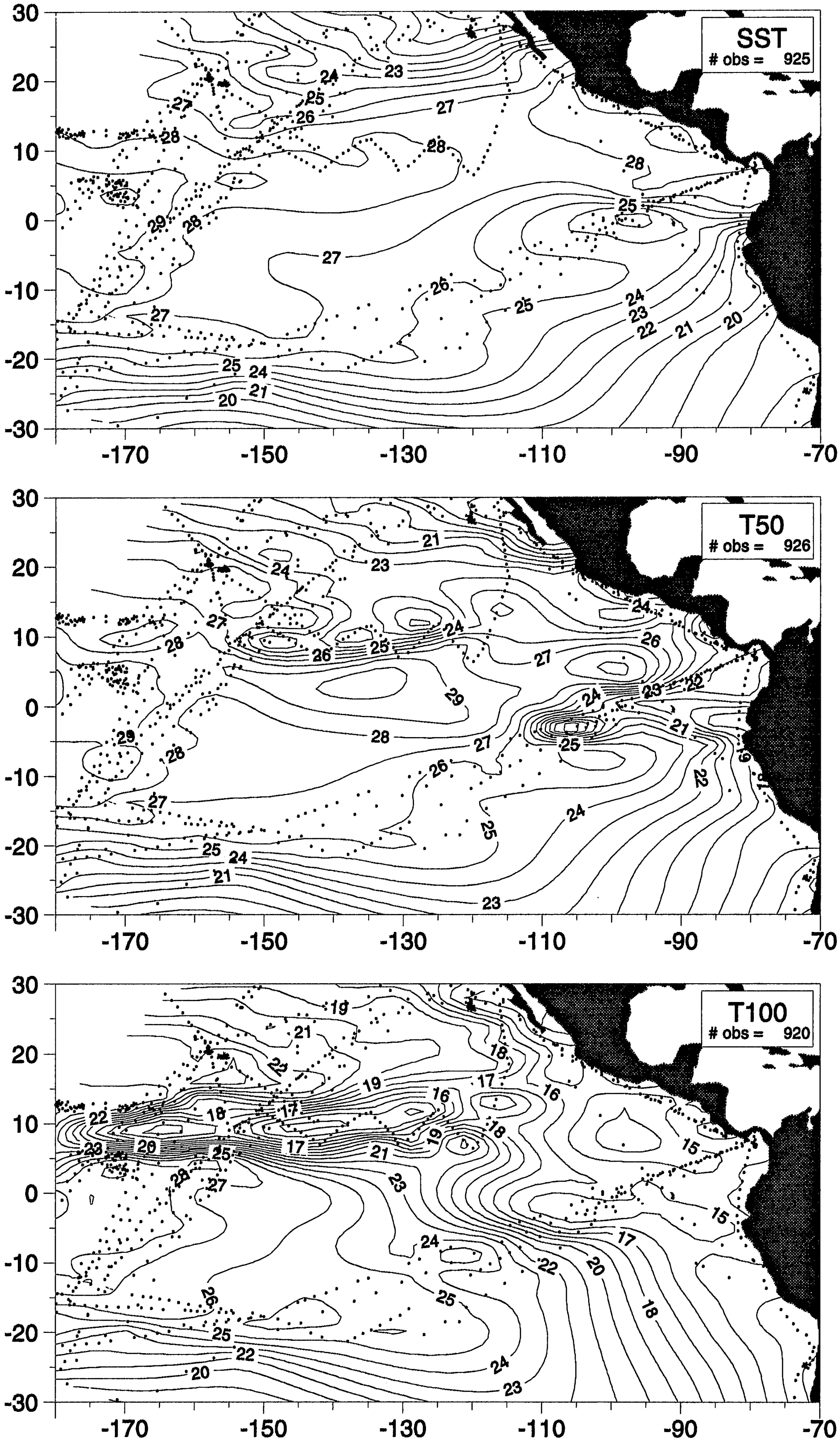

Plate 28. Bimonthly fields for July-August 1982.

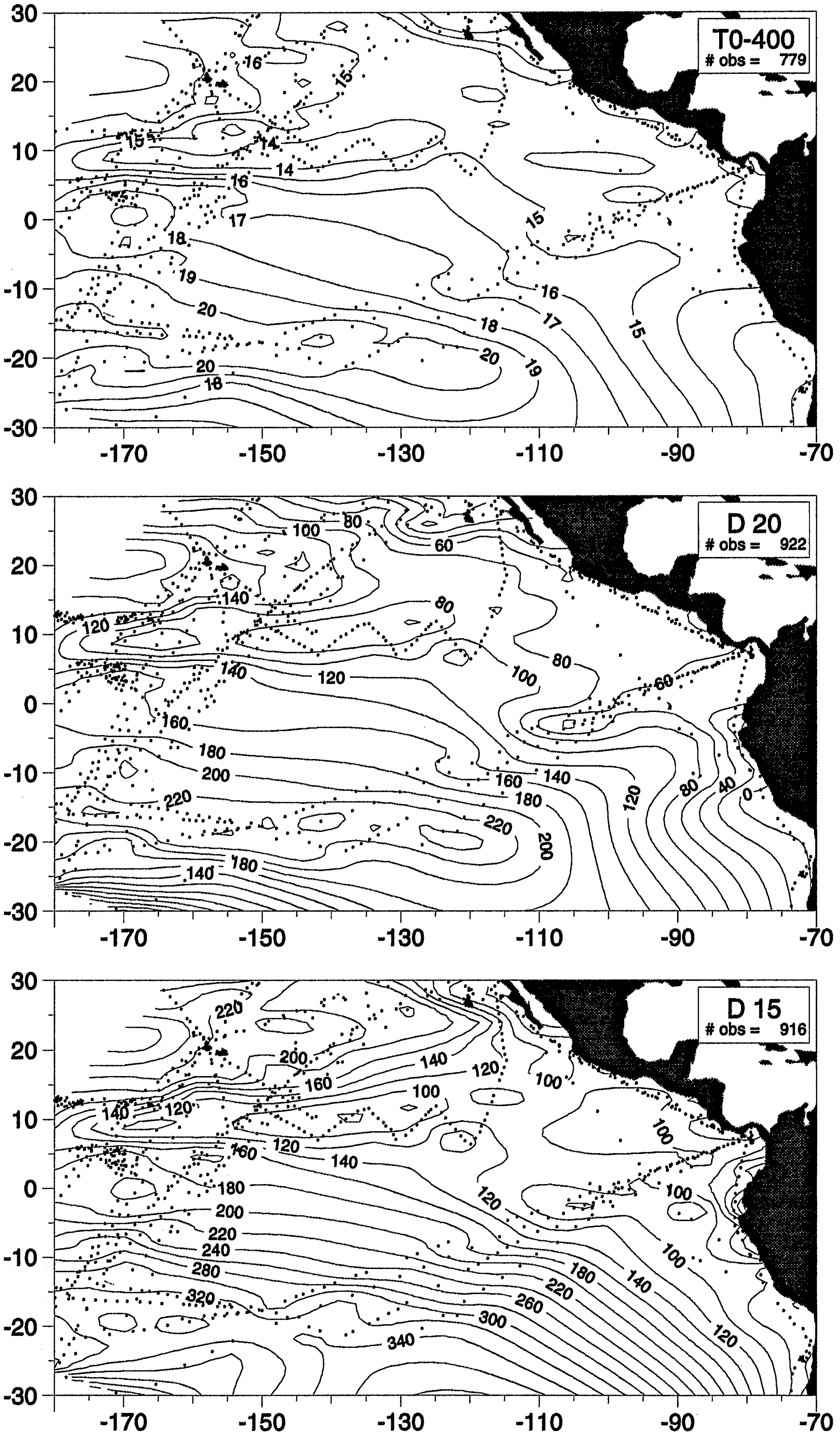

Plate 28 – *continued*. Bimonthly fields for July-August 1982.

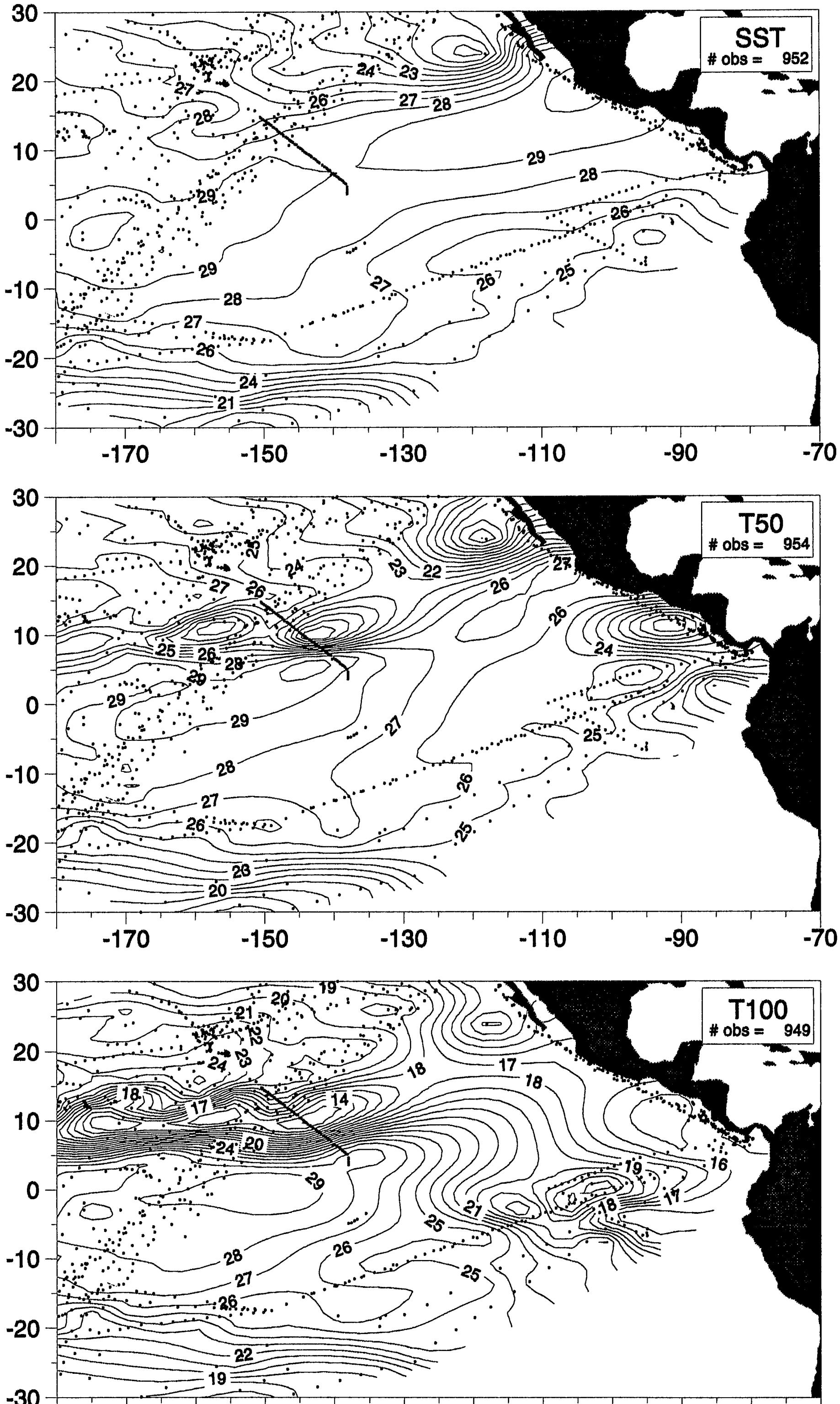

Plate 29. Bimonthly fields for September-October 1982.

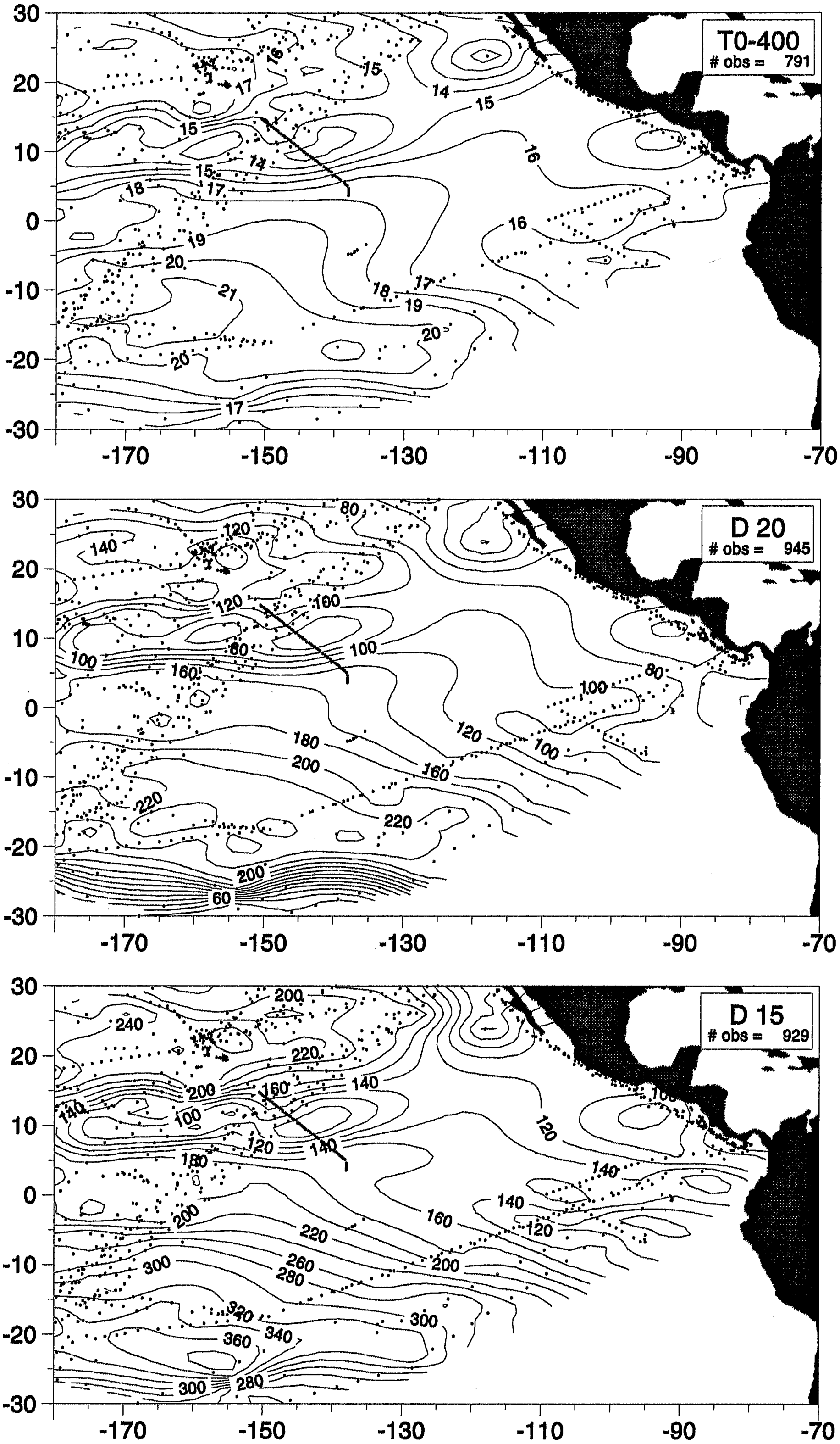

Plate 29 – *continued*. Bimonthly fields for September-October 1982.

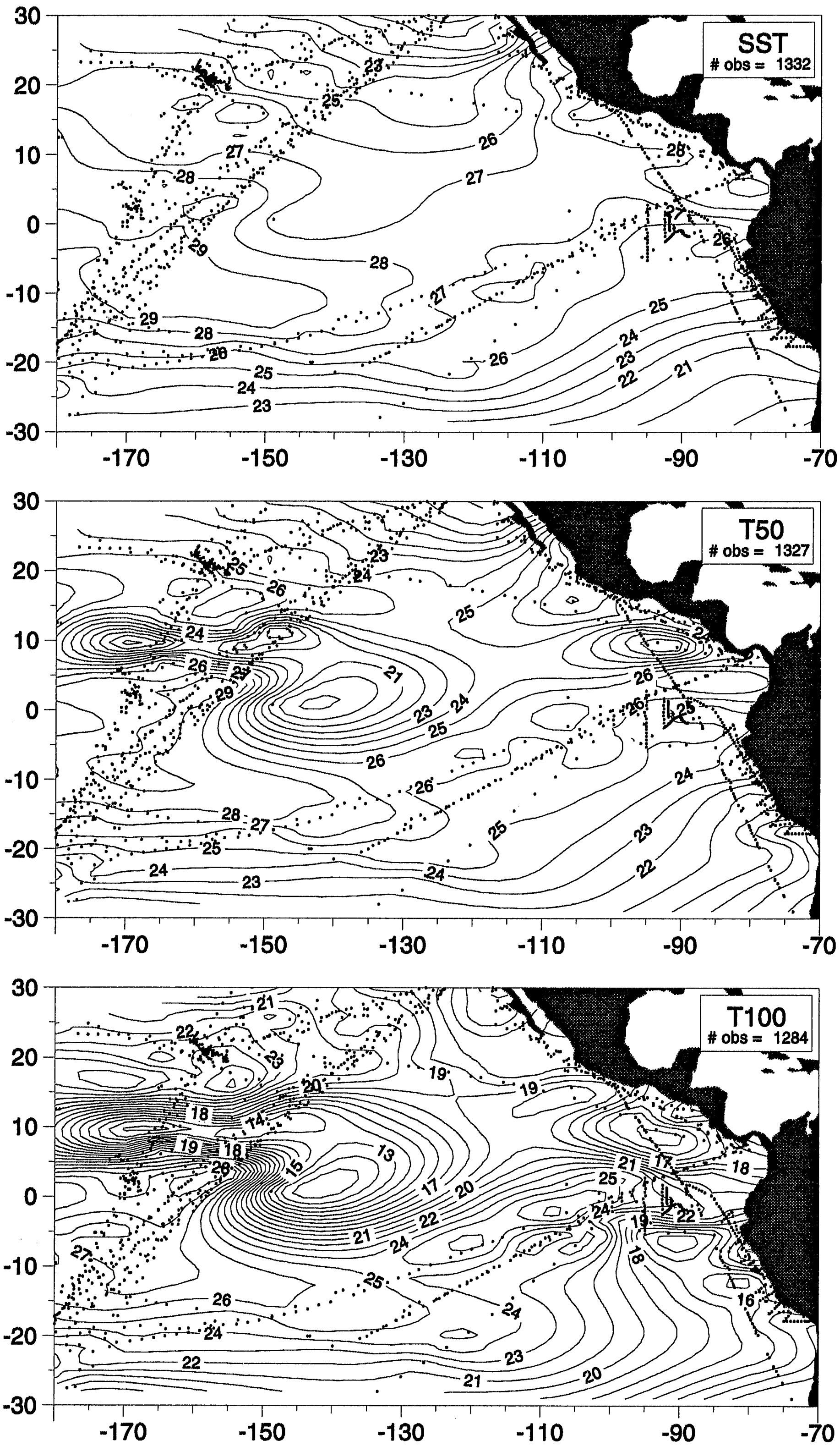

Plate 30. Bimonthly fields for November-December 1982.

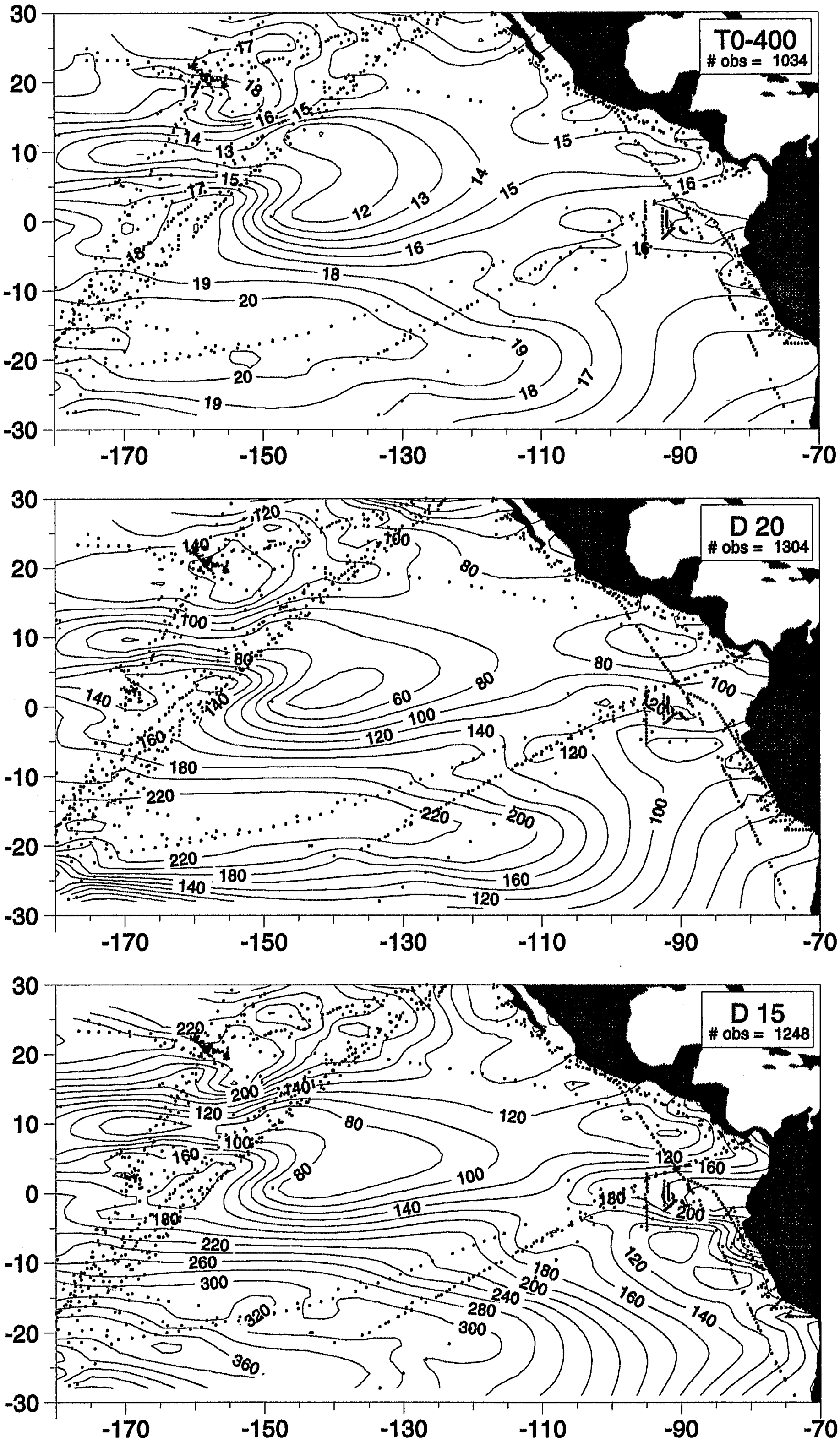

Plate 30 – *continued*. Bimonthly fields for November-December 1982.

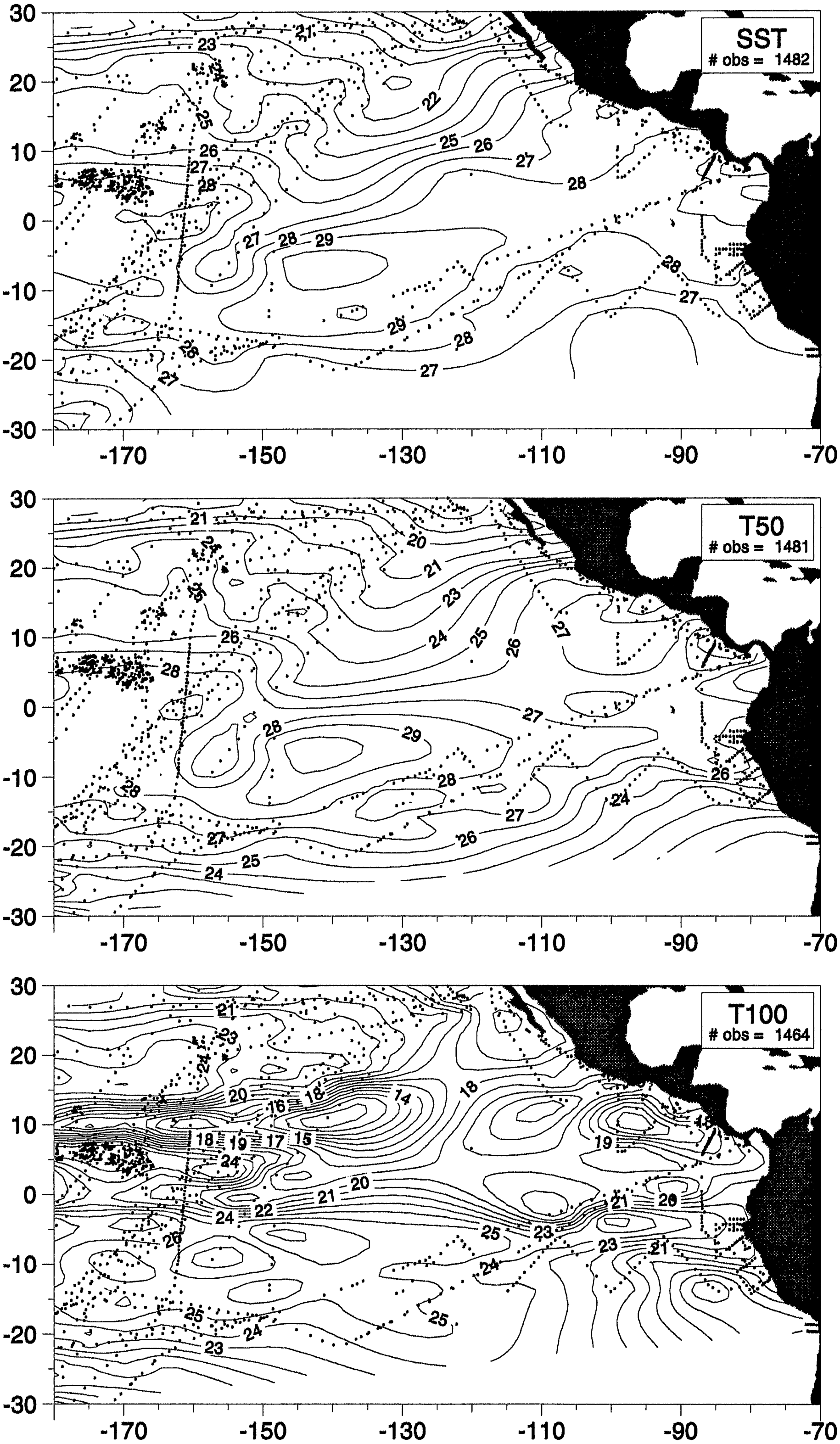

Plate 31. Bimonthly fields for January-February 1983.

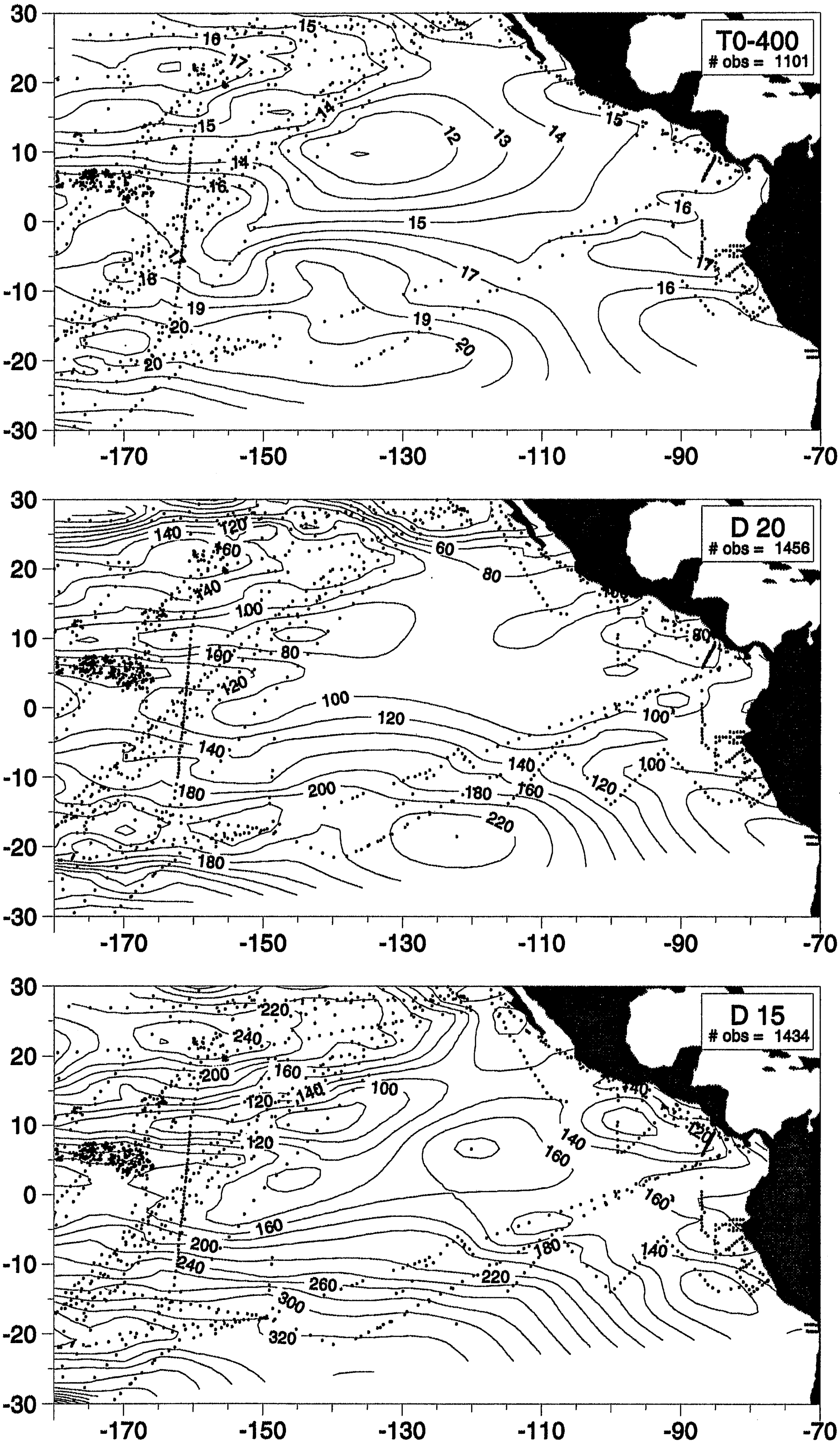

Plate 31 – *continued*. Bimonthly fields for January-February 1983.

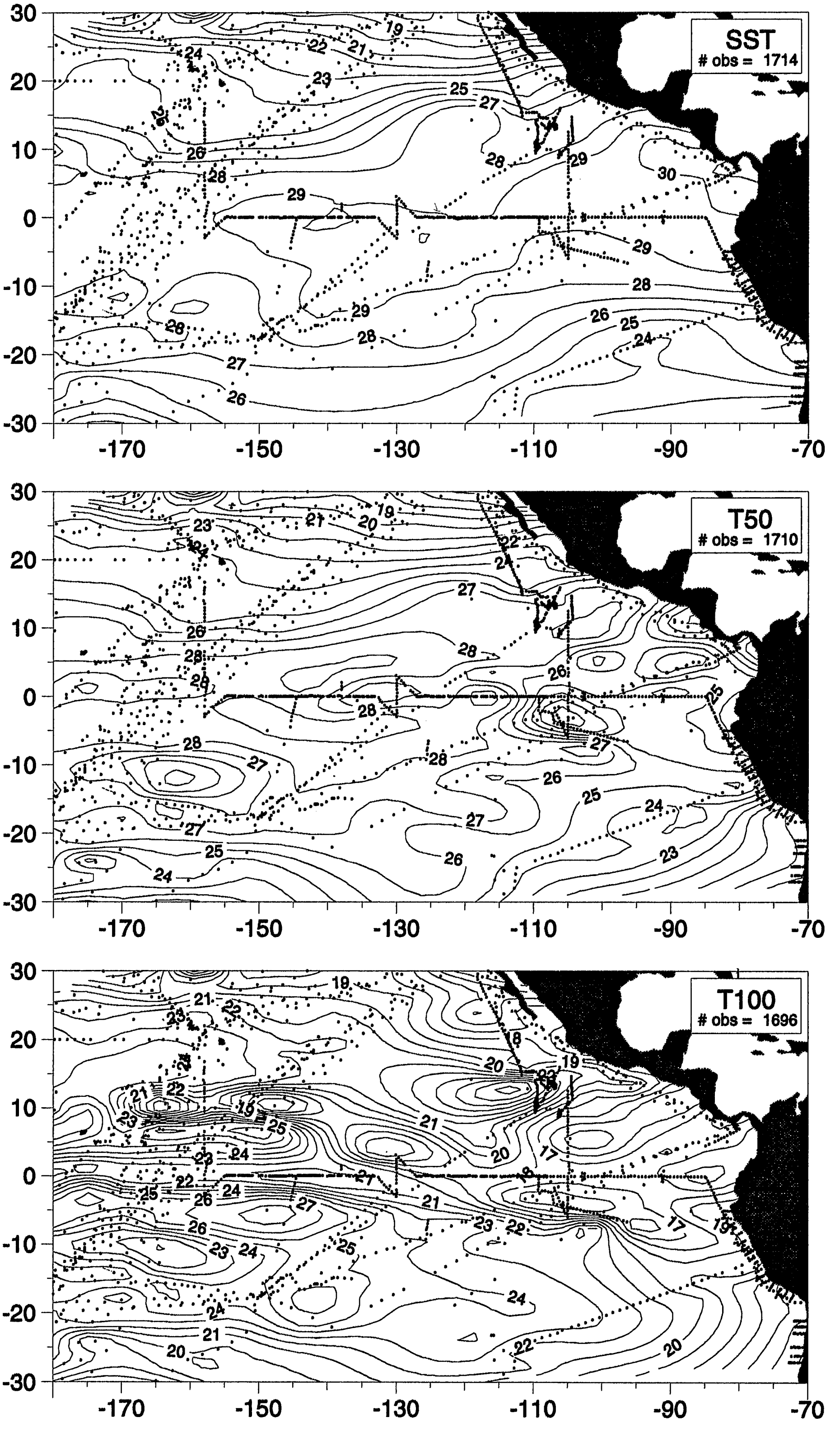

Plate 32. Bimonthly fields for March-April 1983.

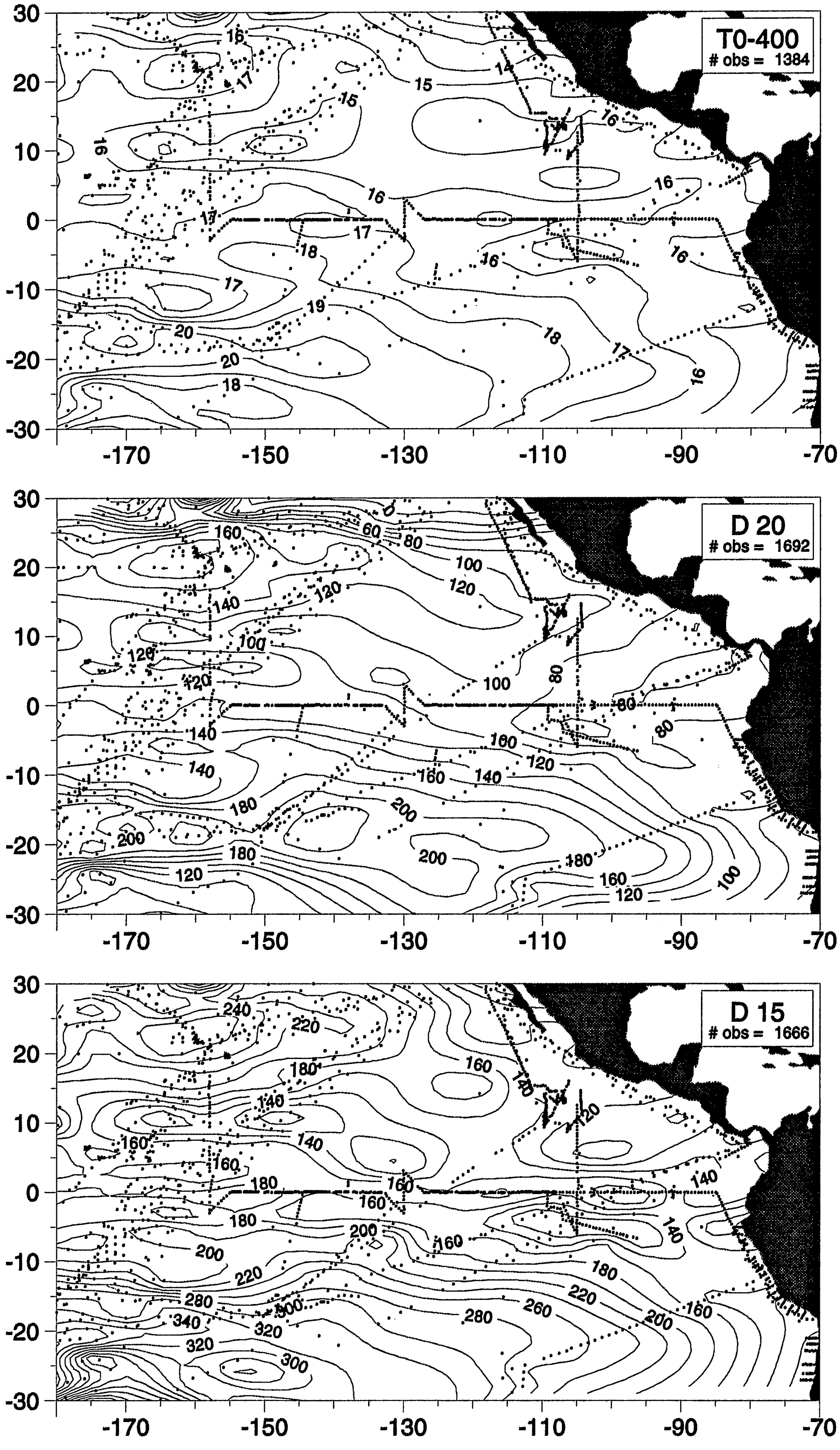

Plate 32 – *continued.* Bimonthly fields for March-April 1983.

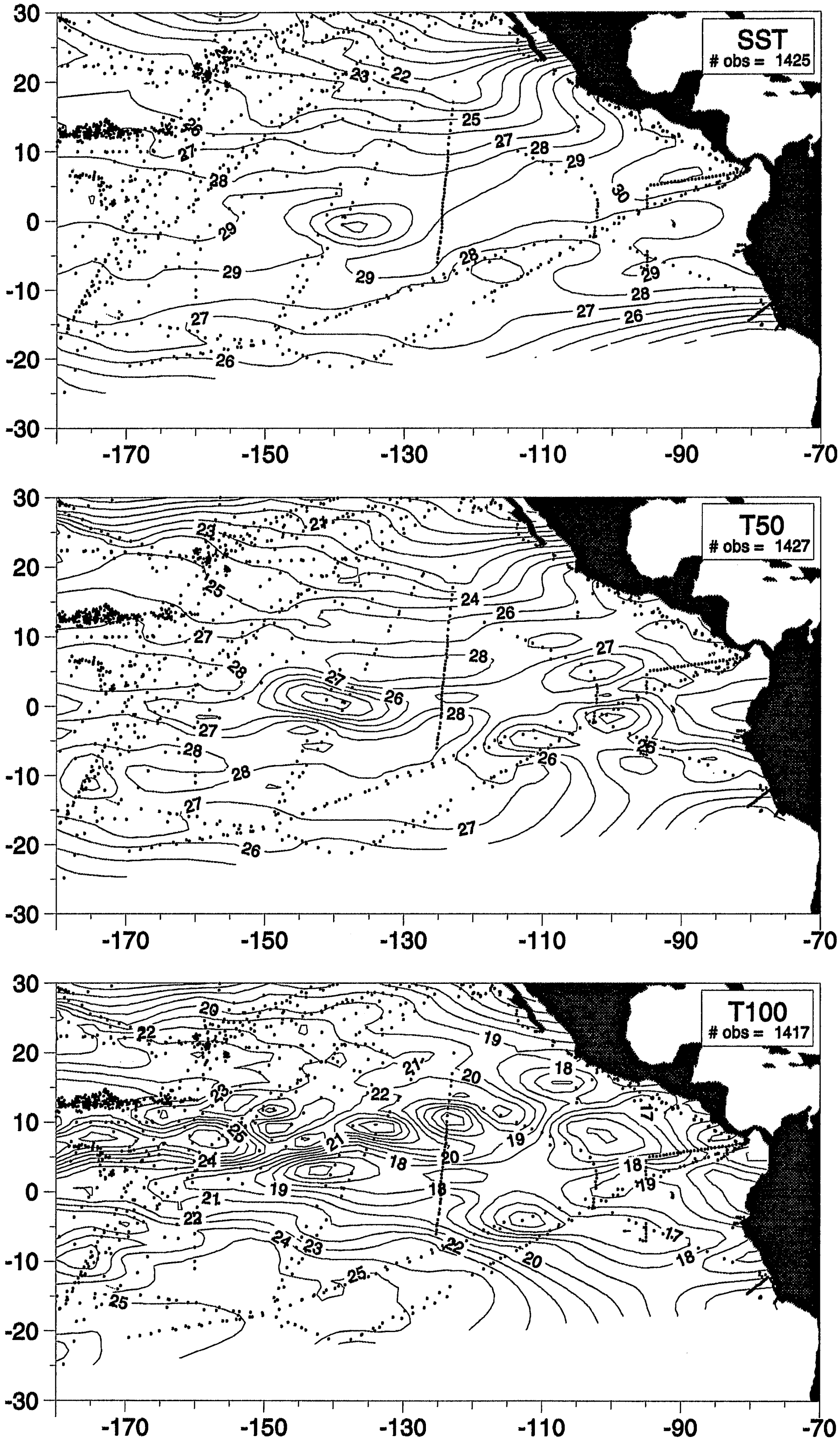

Plate 33. Bimonthly fields for May-June 1983.

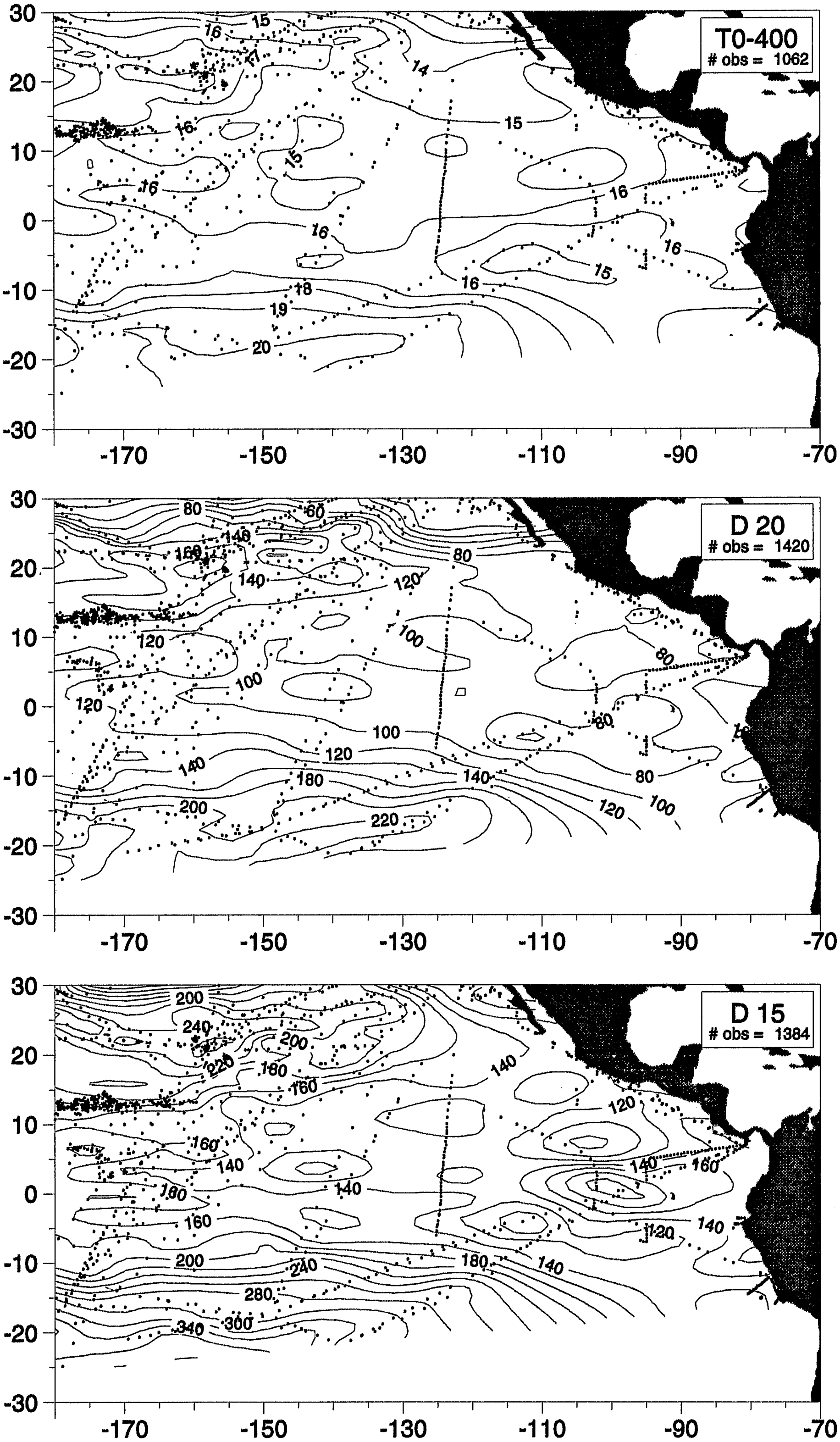

Plate 33 – *continued*. Bimonthly fields for May-June 1983.

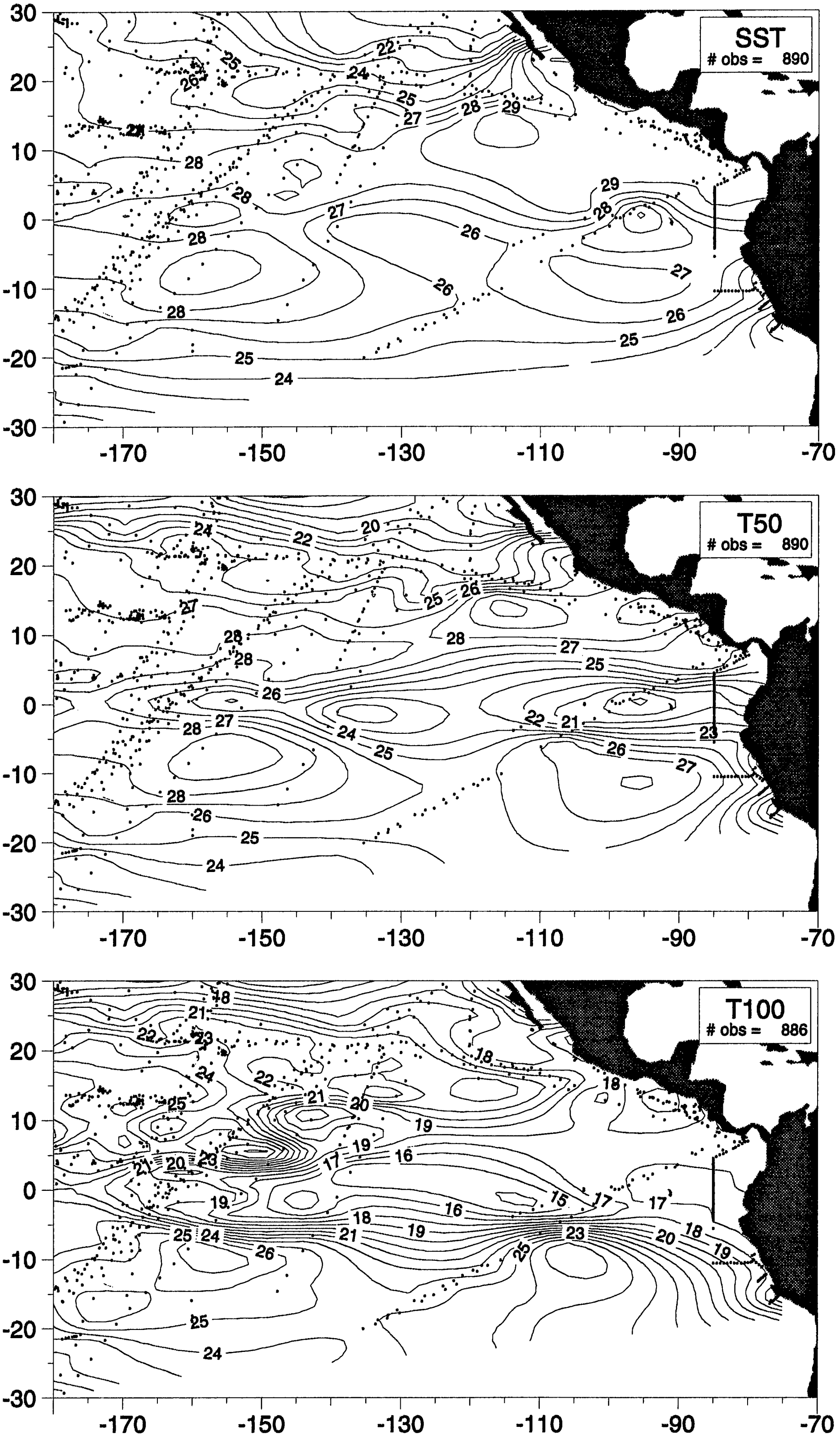

Plate 34. Bimonthly fields for July-August 1983.

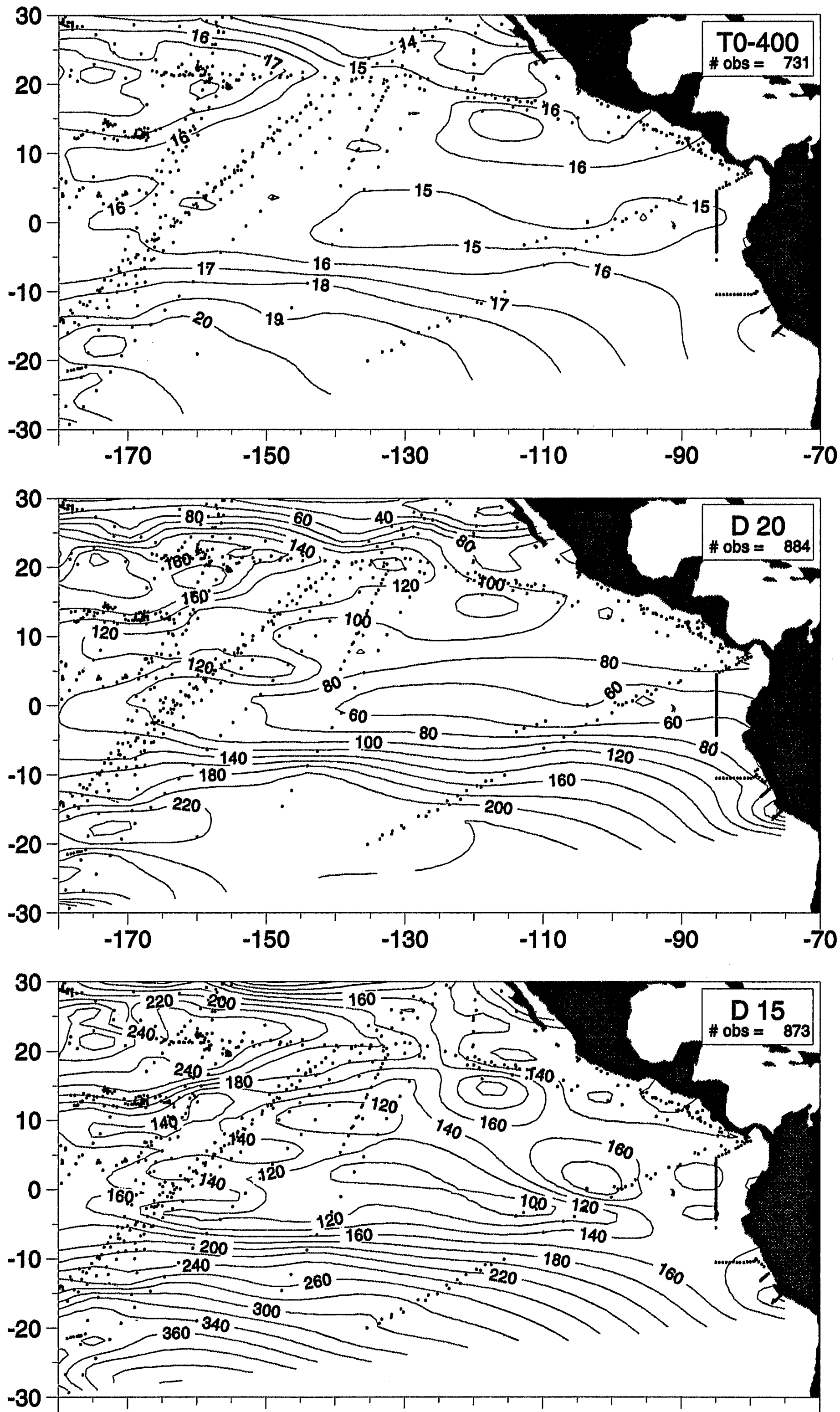

Plate 34 – *continued*. Bimonthly fields for July-August 1983.

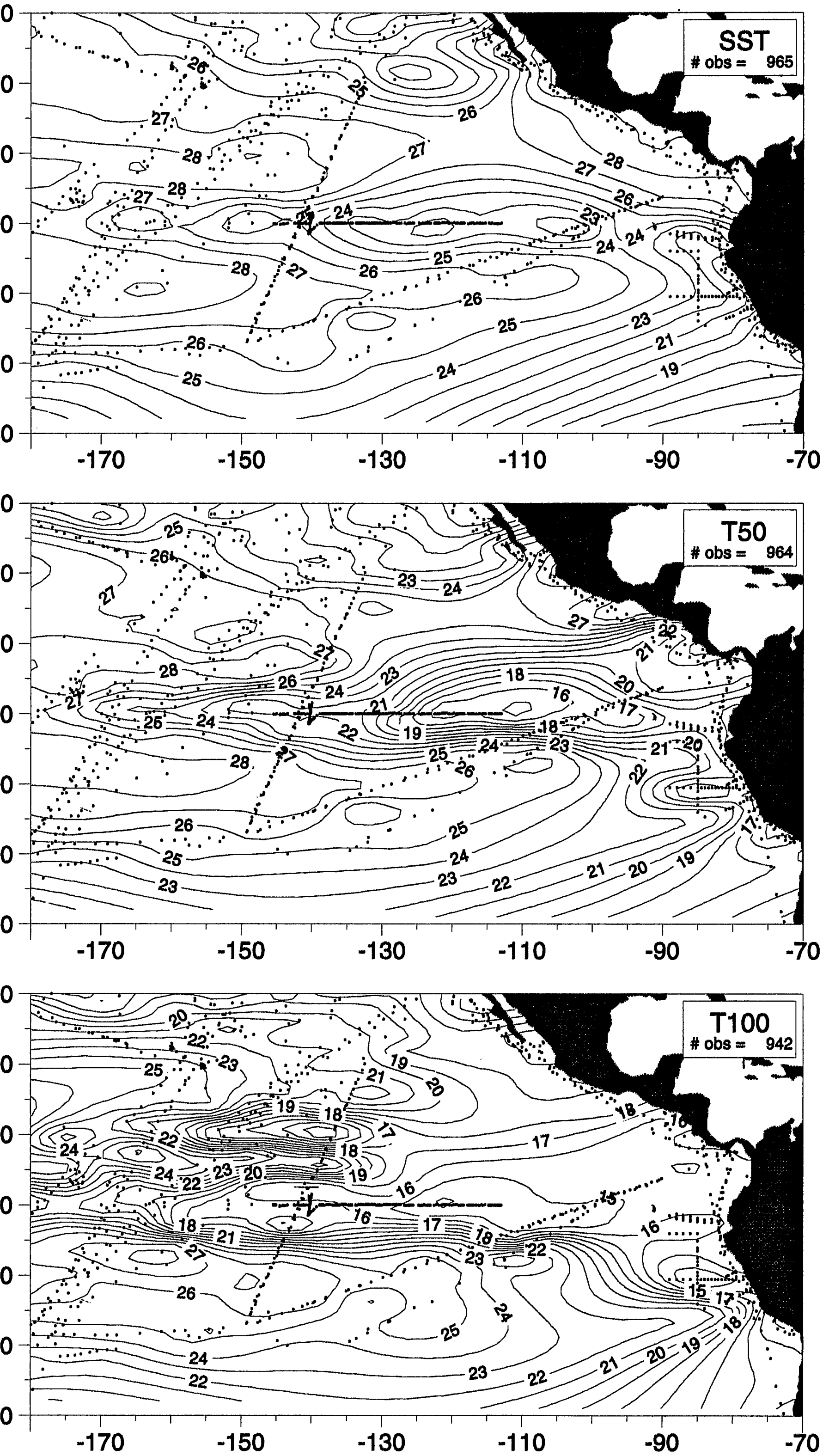

Plate 35. Bimonthly fields for September-October 1983.

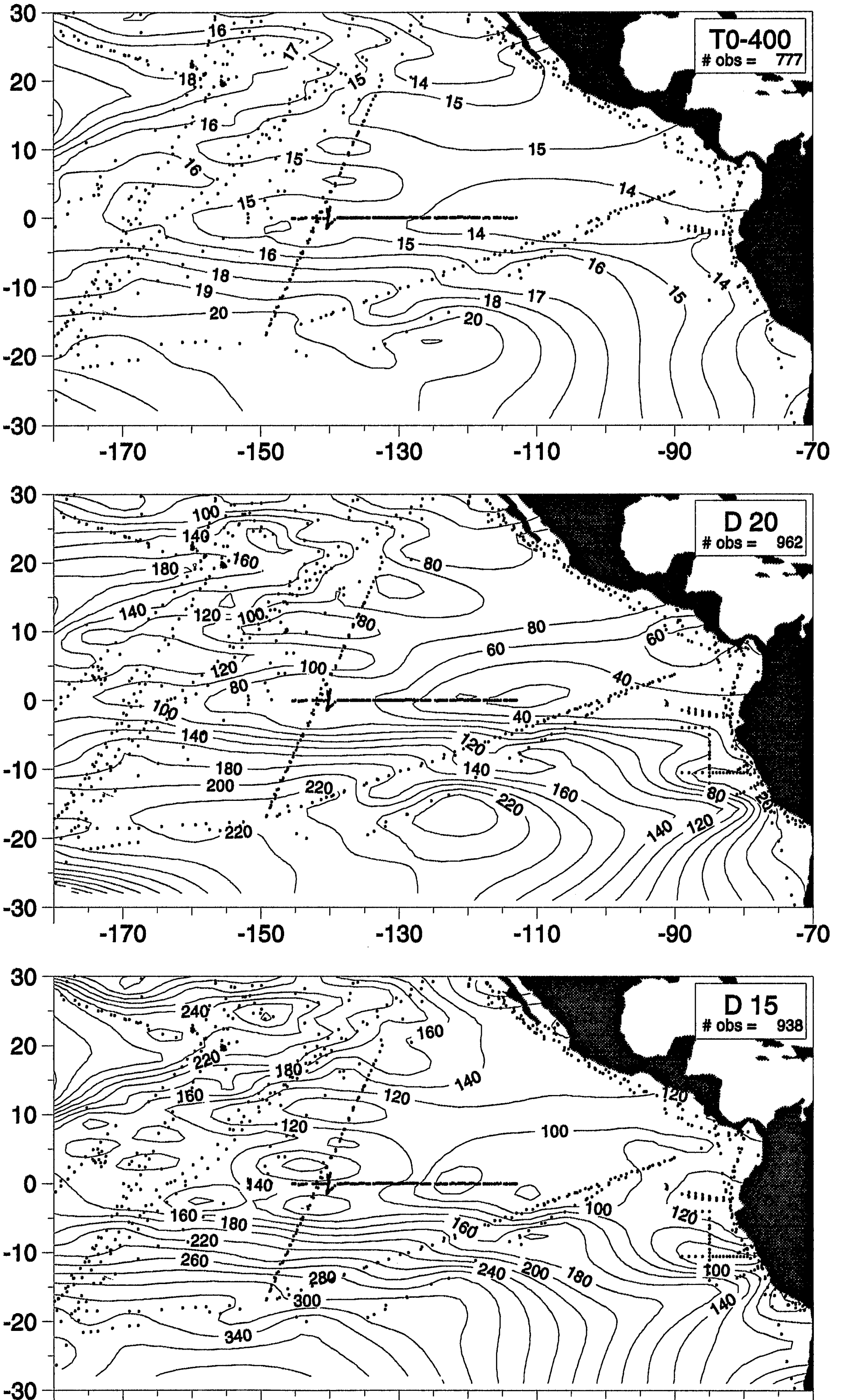

Plate 35 – *continued*. Bimonthly fields for September-October 1983.

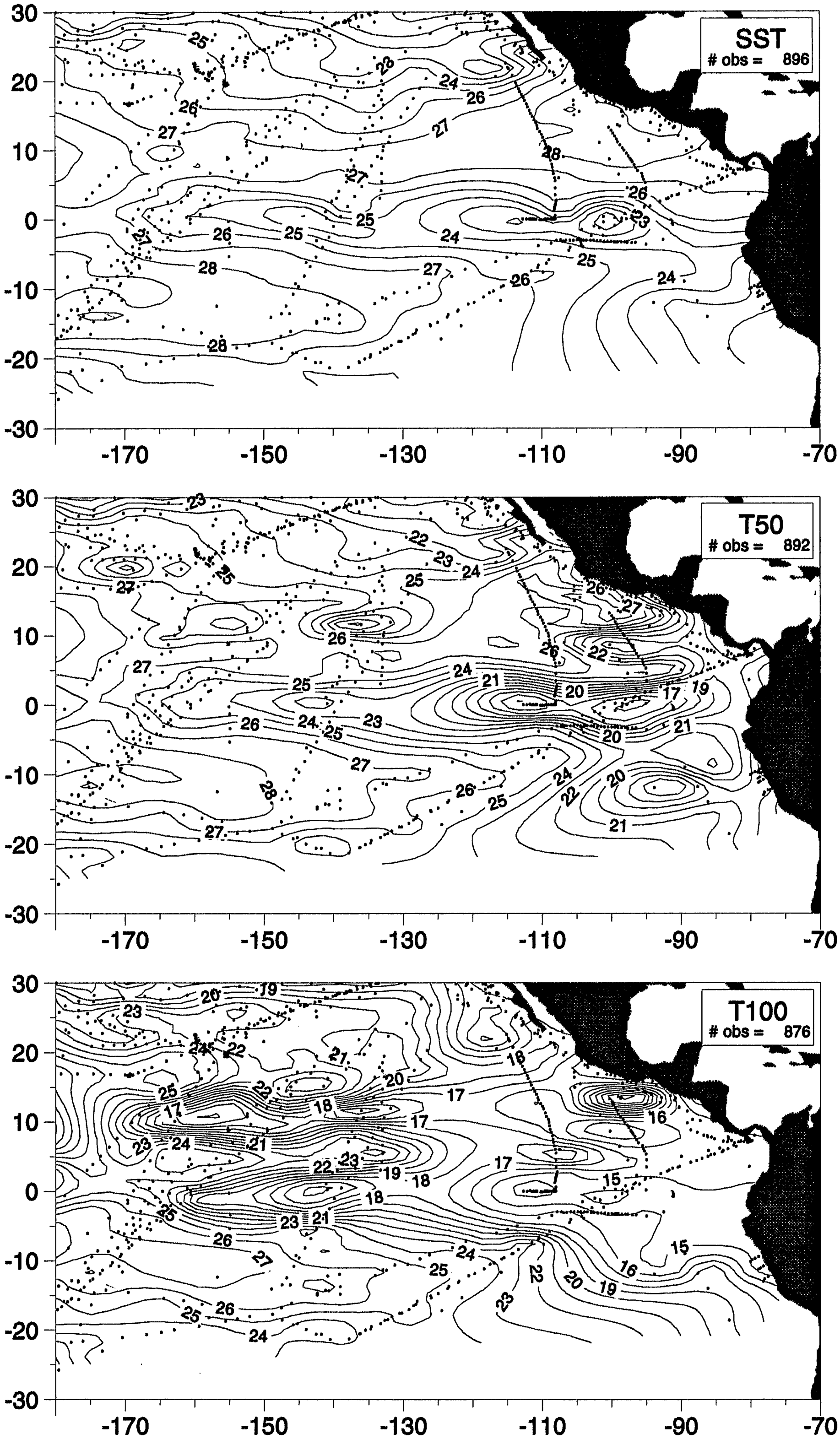

Plate 36. Bimonthly fields for November-December 1983.

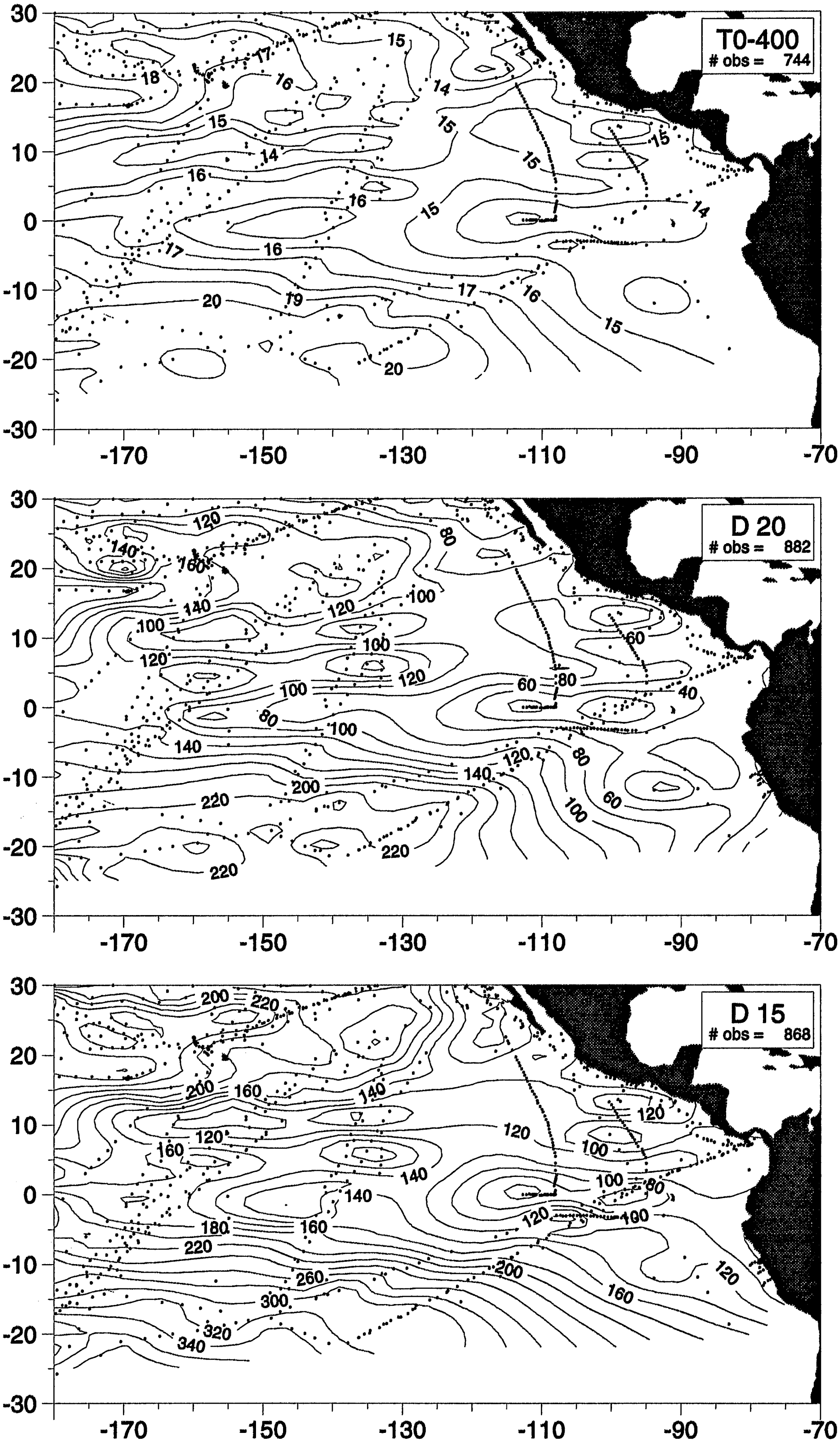

Plate 36 – *continued.* Bimonthly fields for November-December 1983.

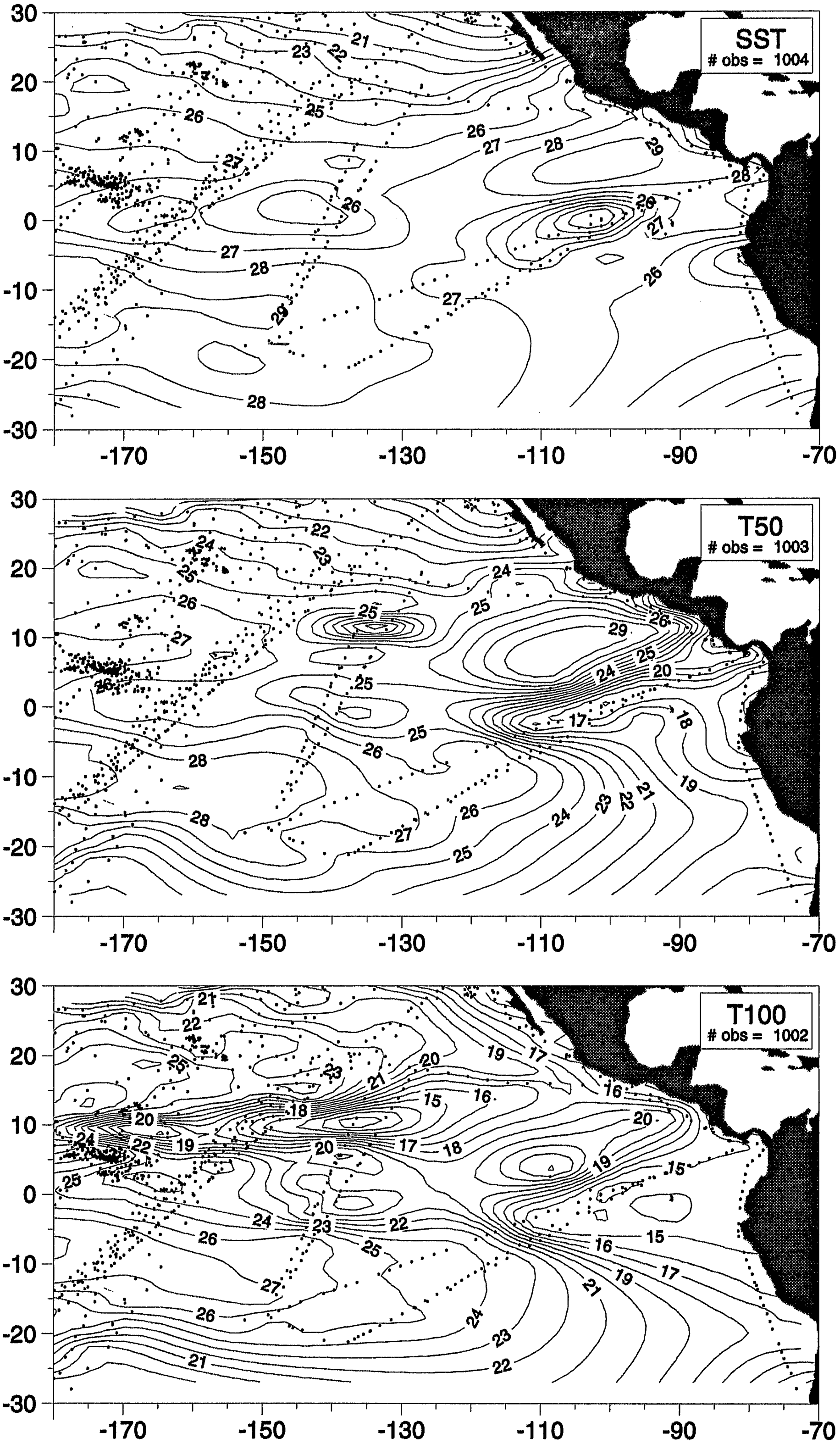

Plate 37. Bimonthly fields for January-February 1984.

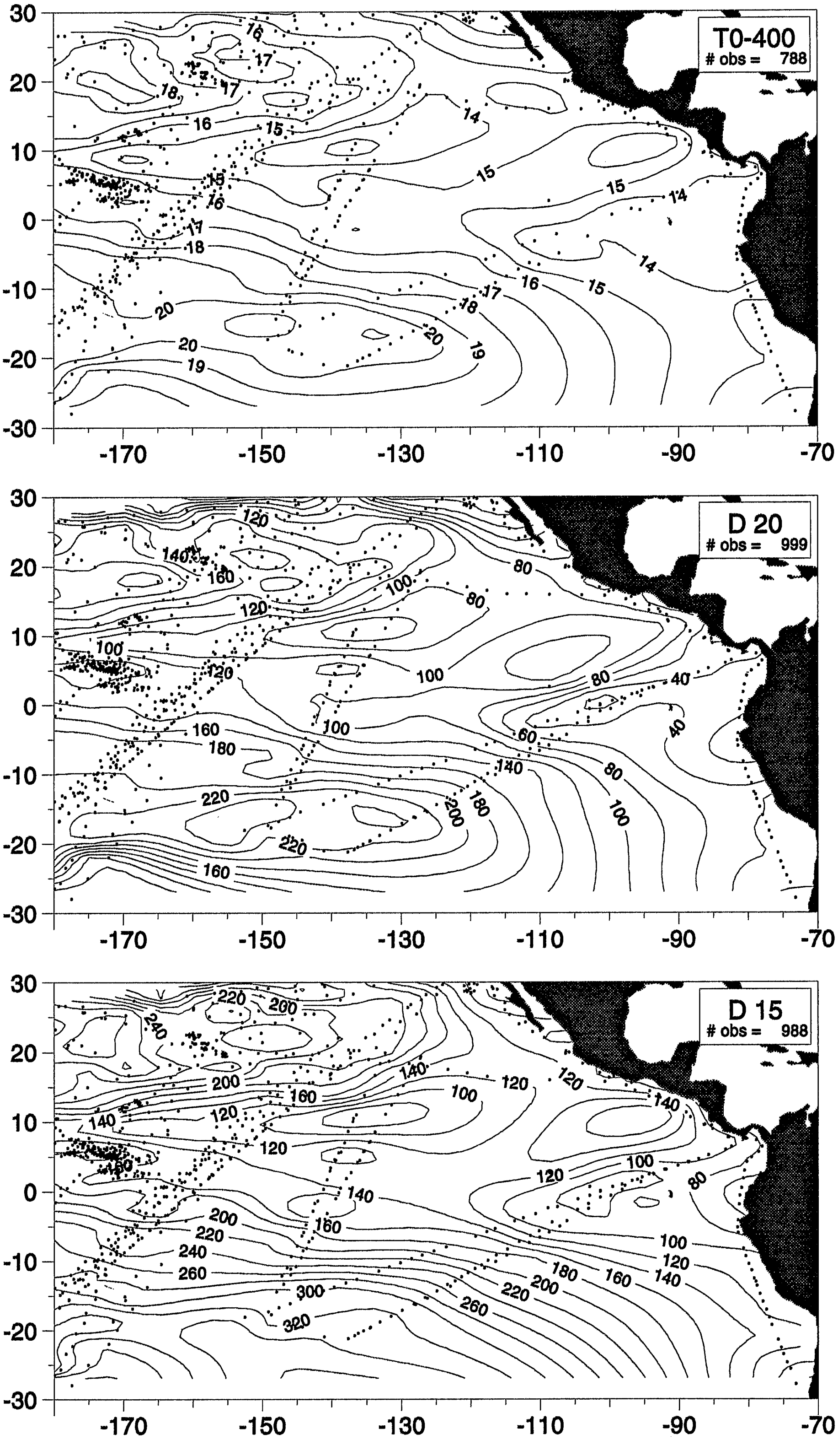

Plate 37 – *continued*. Bimonthly fields for January-February 1984.

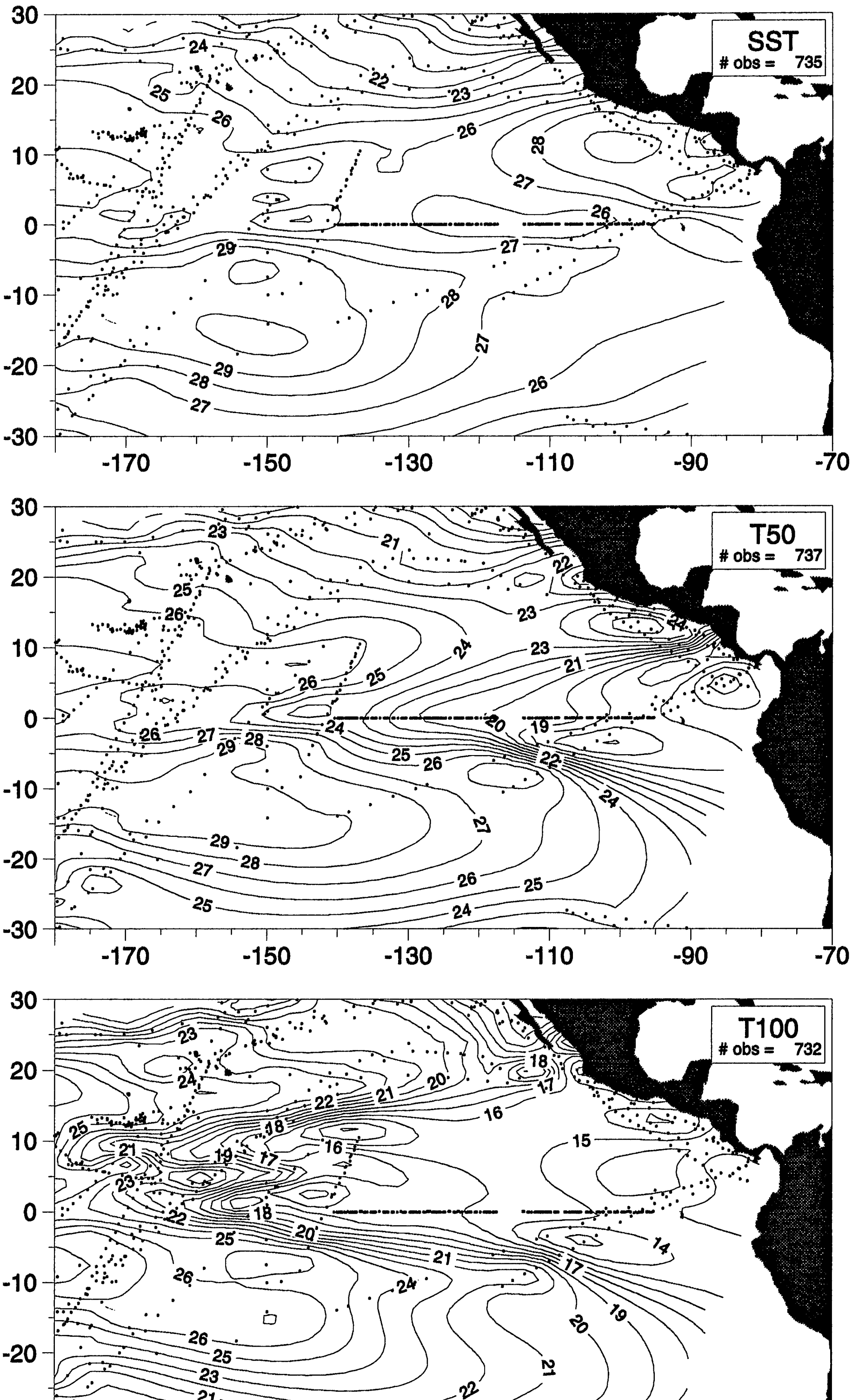

Plate 38. Bimonthly fields for March-April 1984.

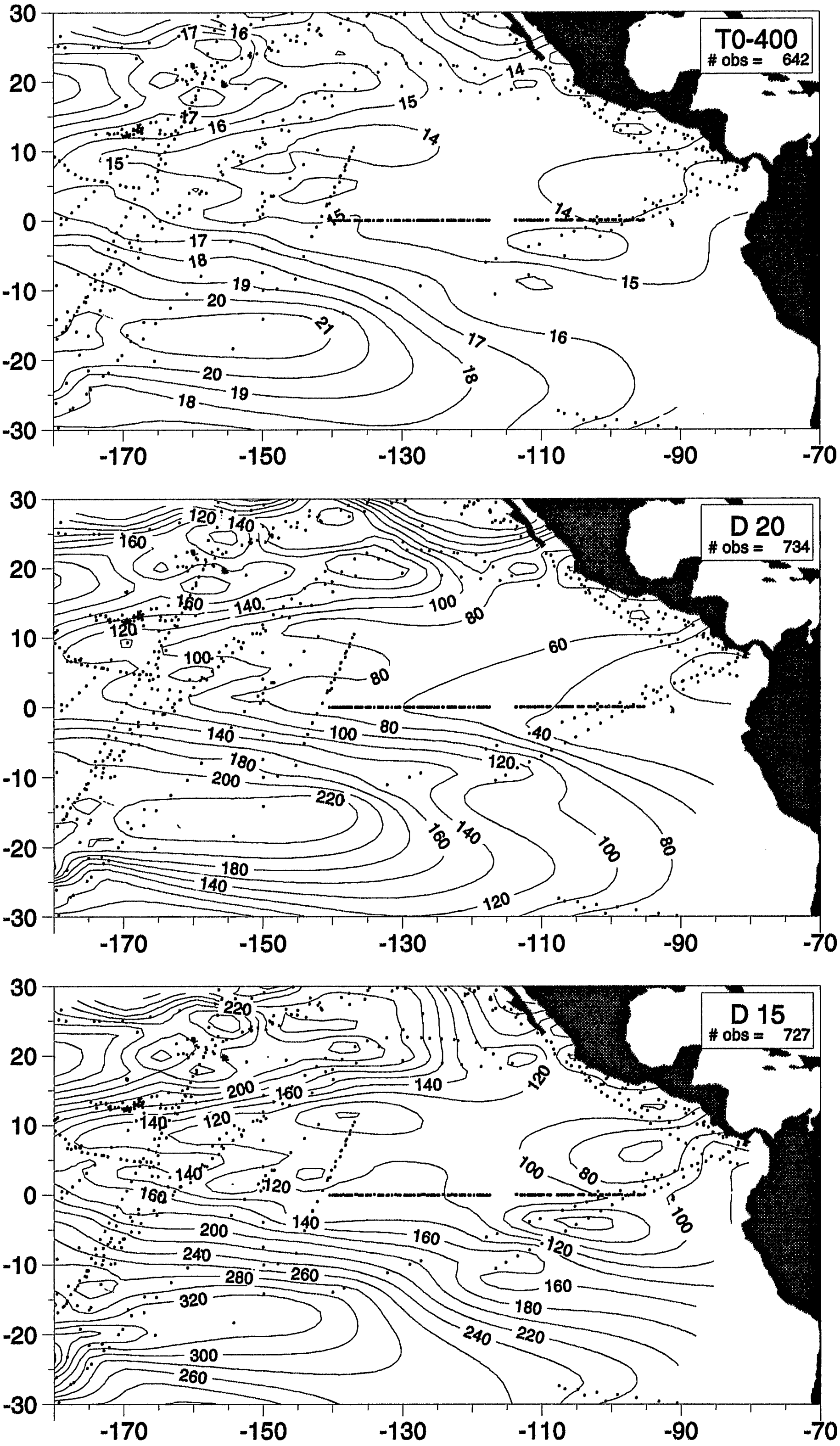

Plate 38 – *continued*. Bimonthly fields for March-April 1984.

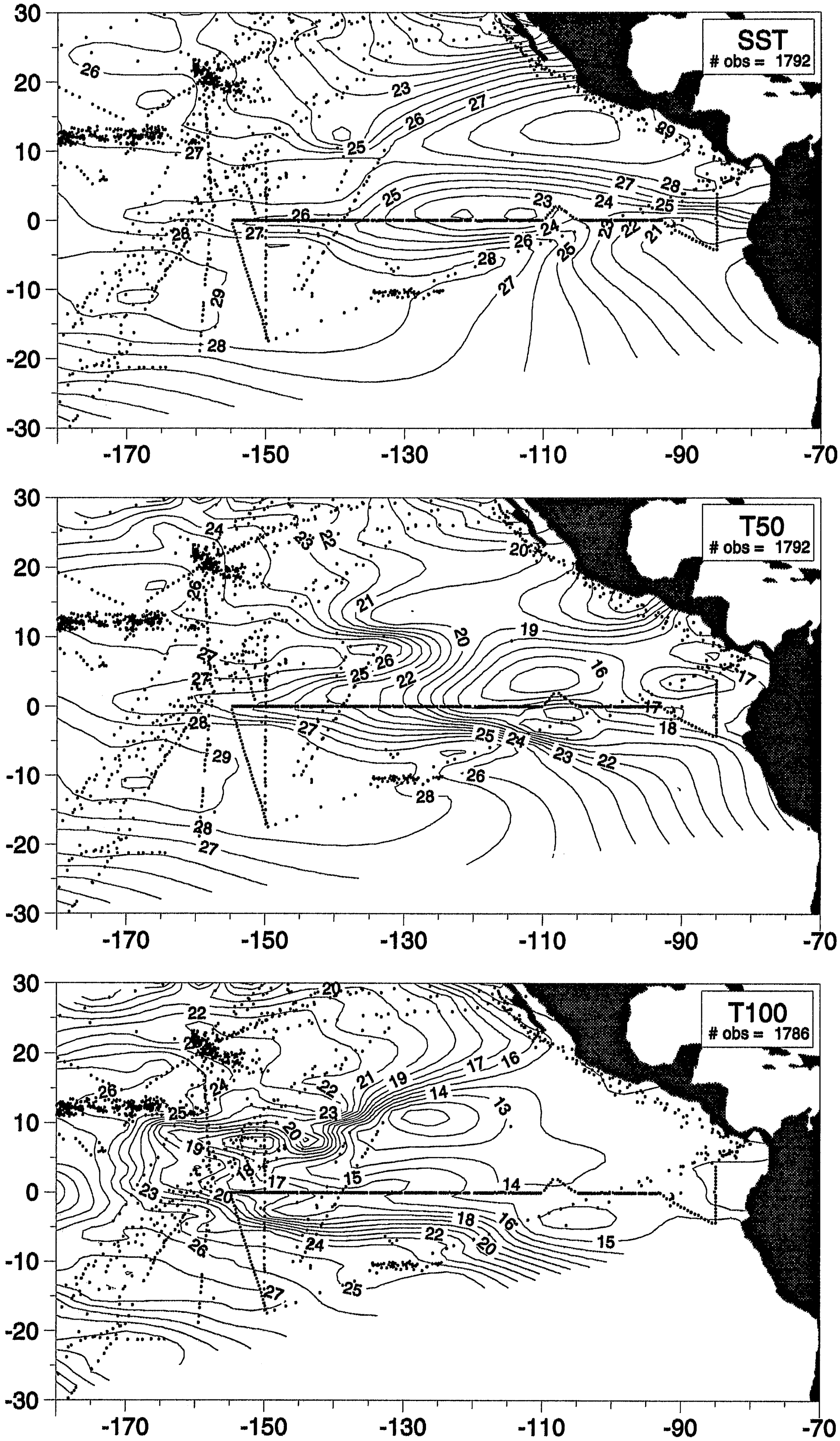

Plate 39. Bimonthly fields for May-June 1984.

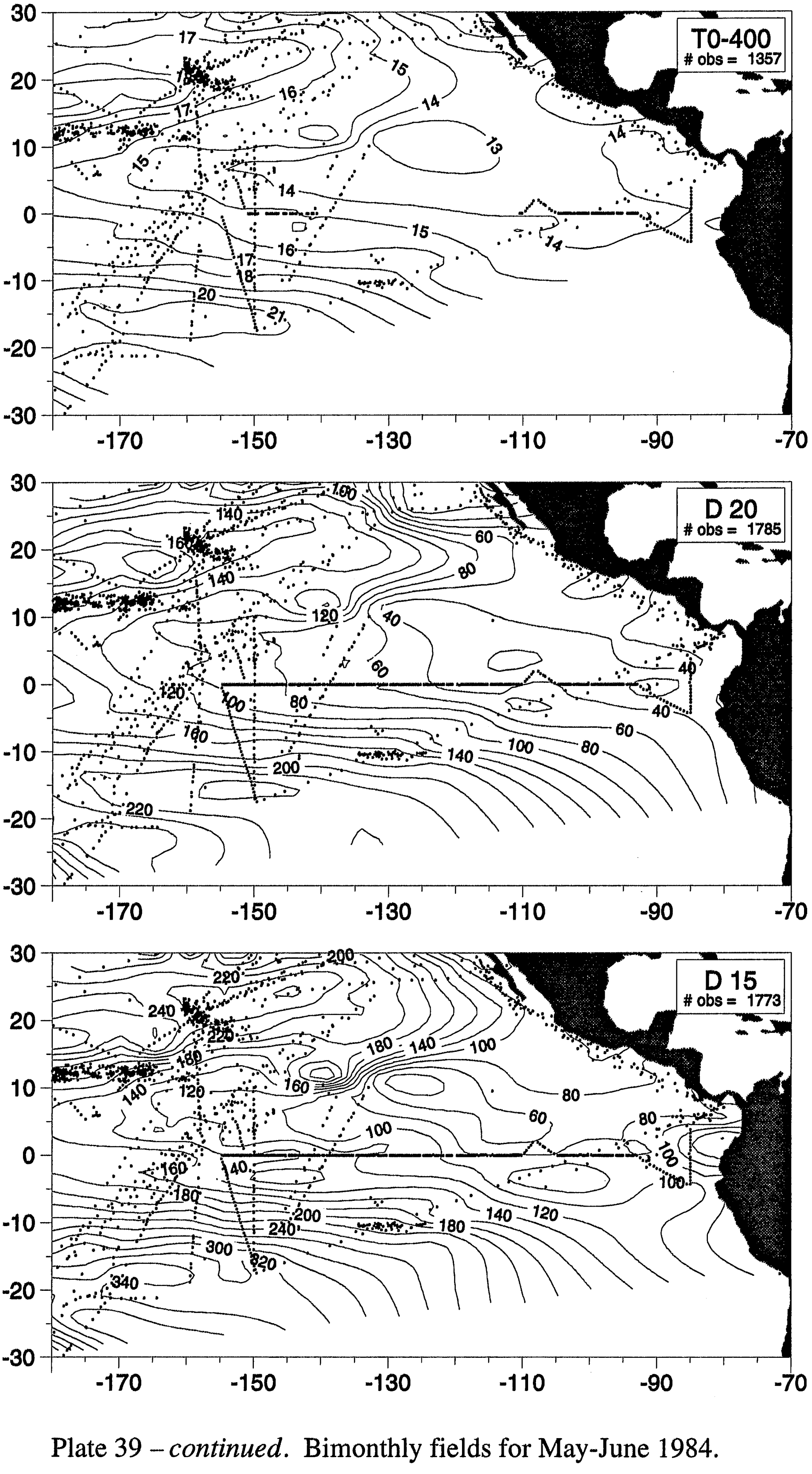

Plate 39 – *continued*. Bimonthly fields for May-June 1984.

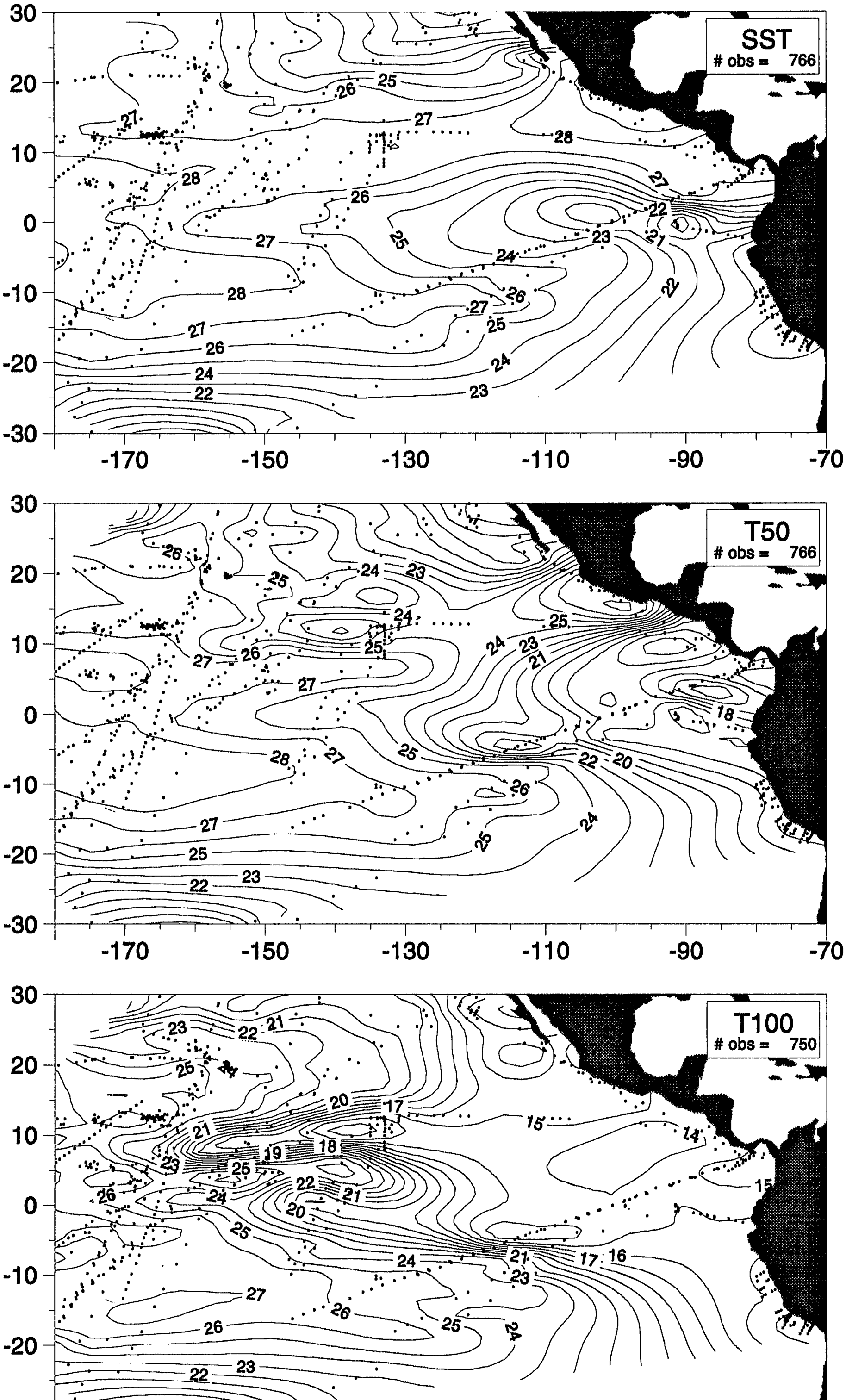

Plate 40. Bimonthly fields for July-August 1984.

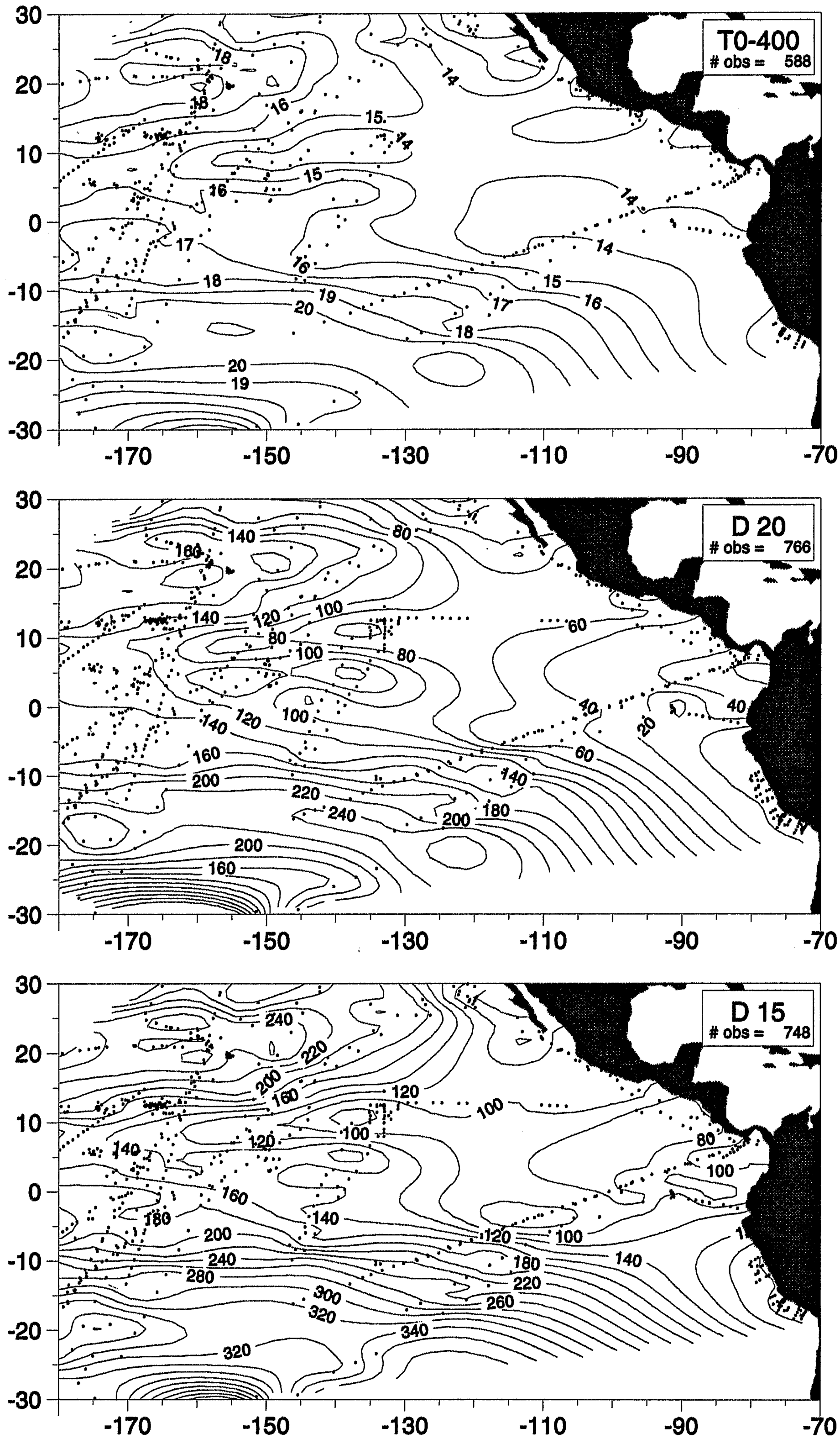

Plate 40 – *continued*. Bimonthly fields for July-August 1984.

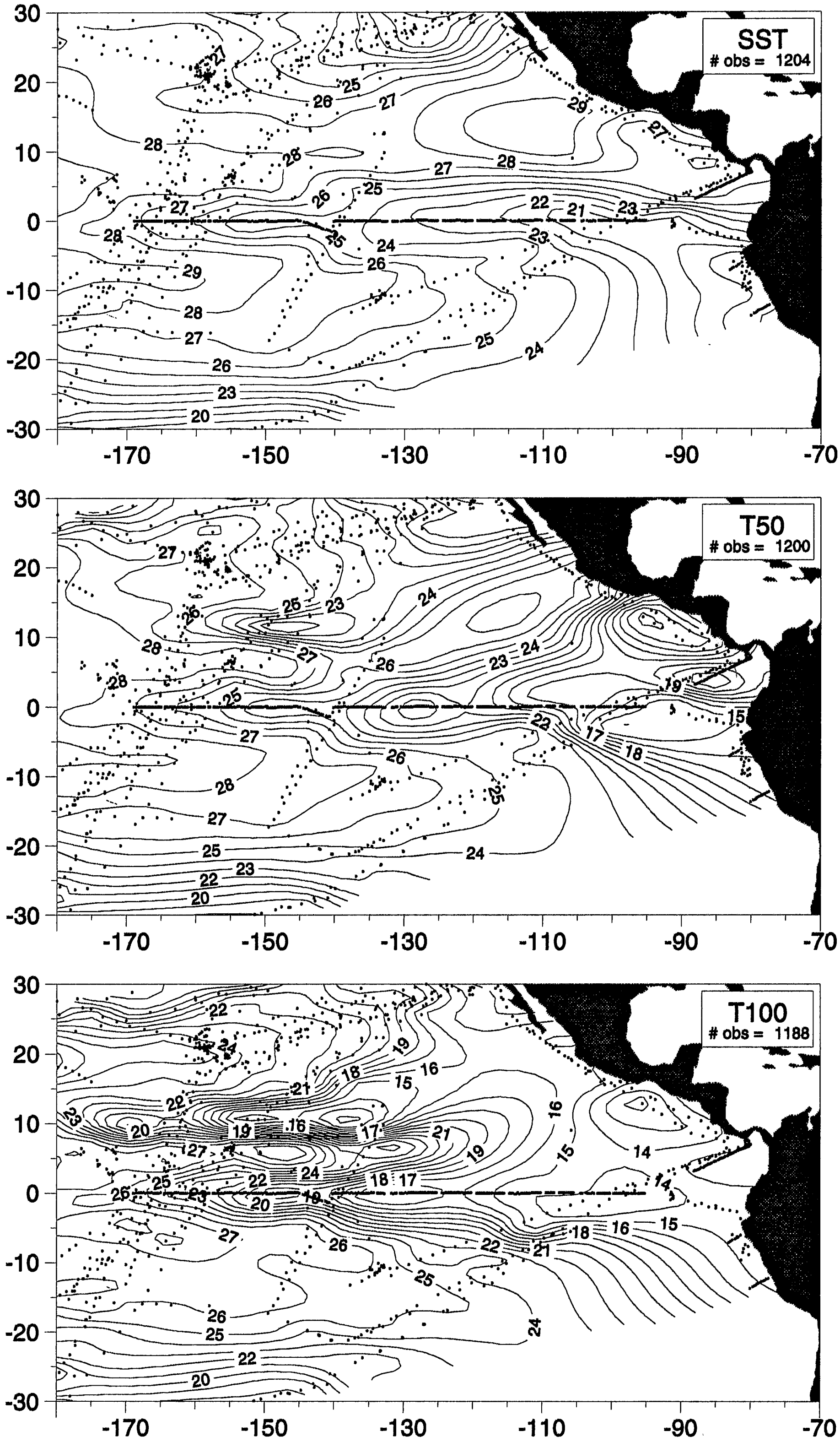

Plate 41. Bimonthly fields for September-October 1984.

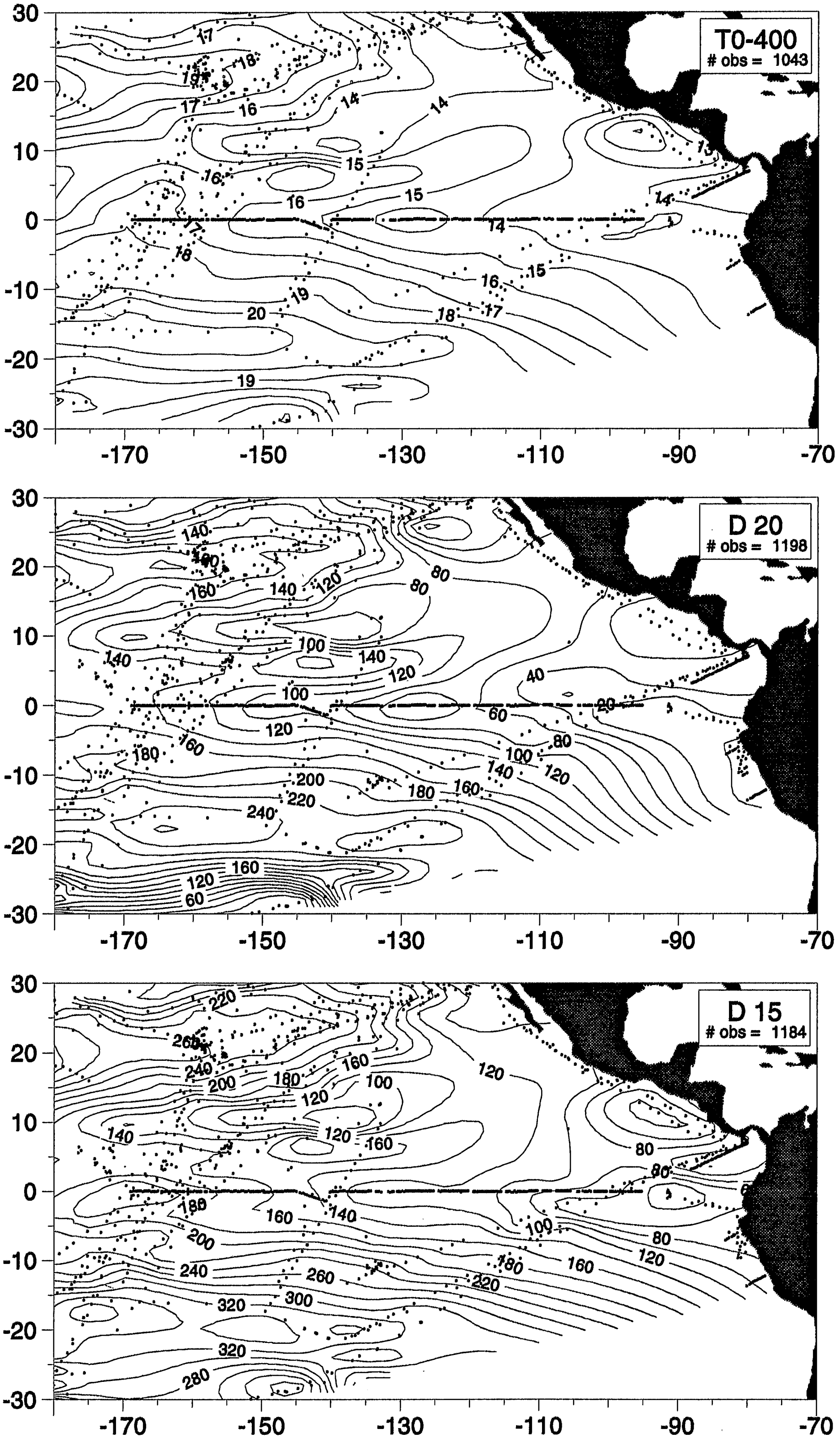

Plate 41 – *continued*. Bimonthly fields for September-October 1984.

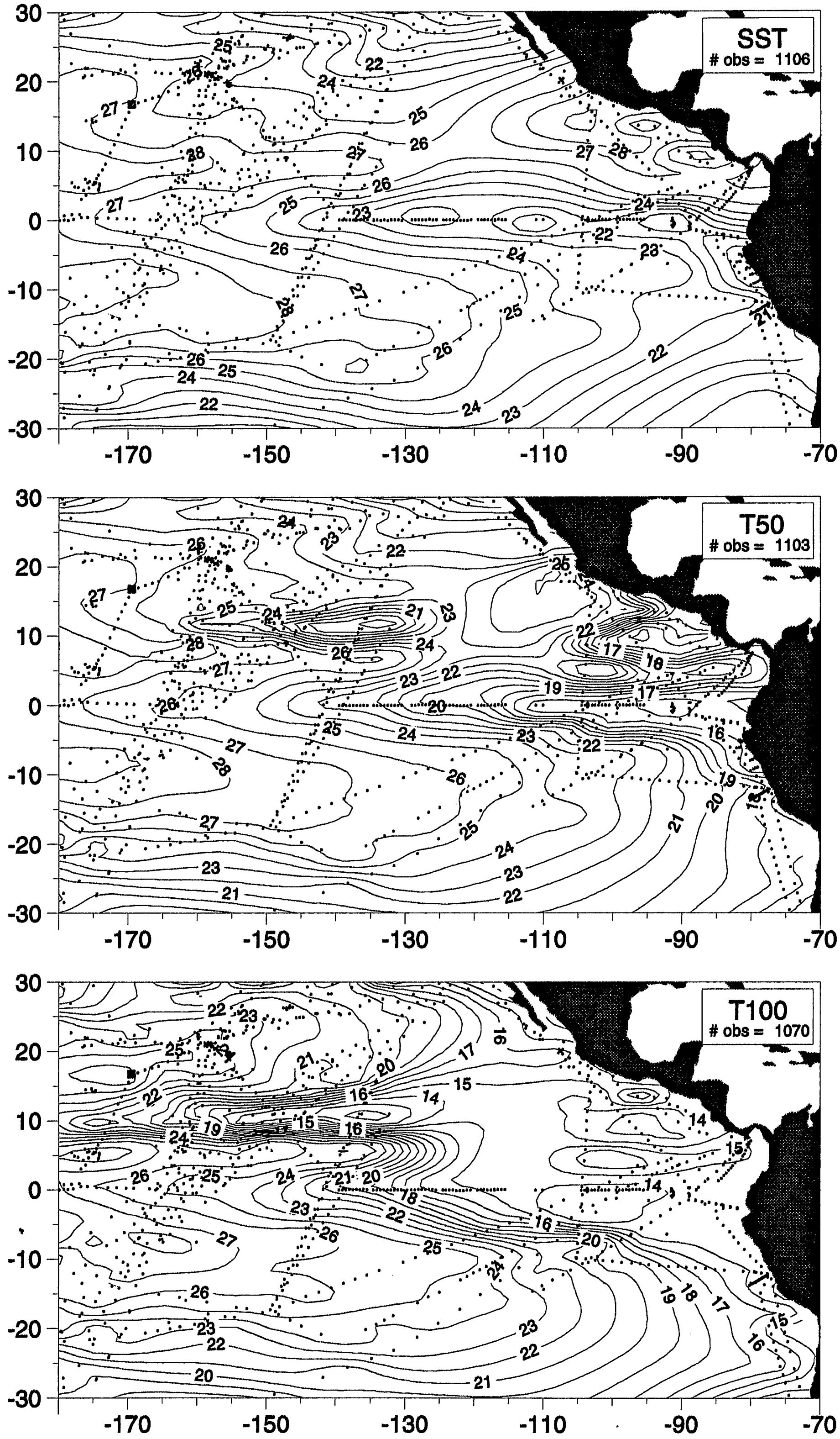

Plate 42. Bimonthly fields for November-December 1984.

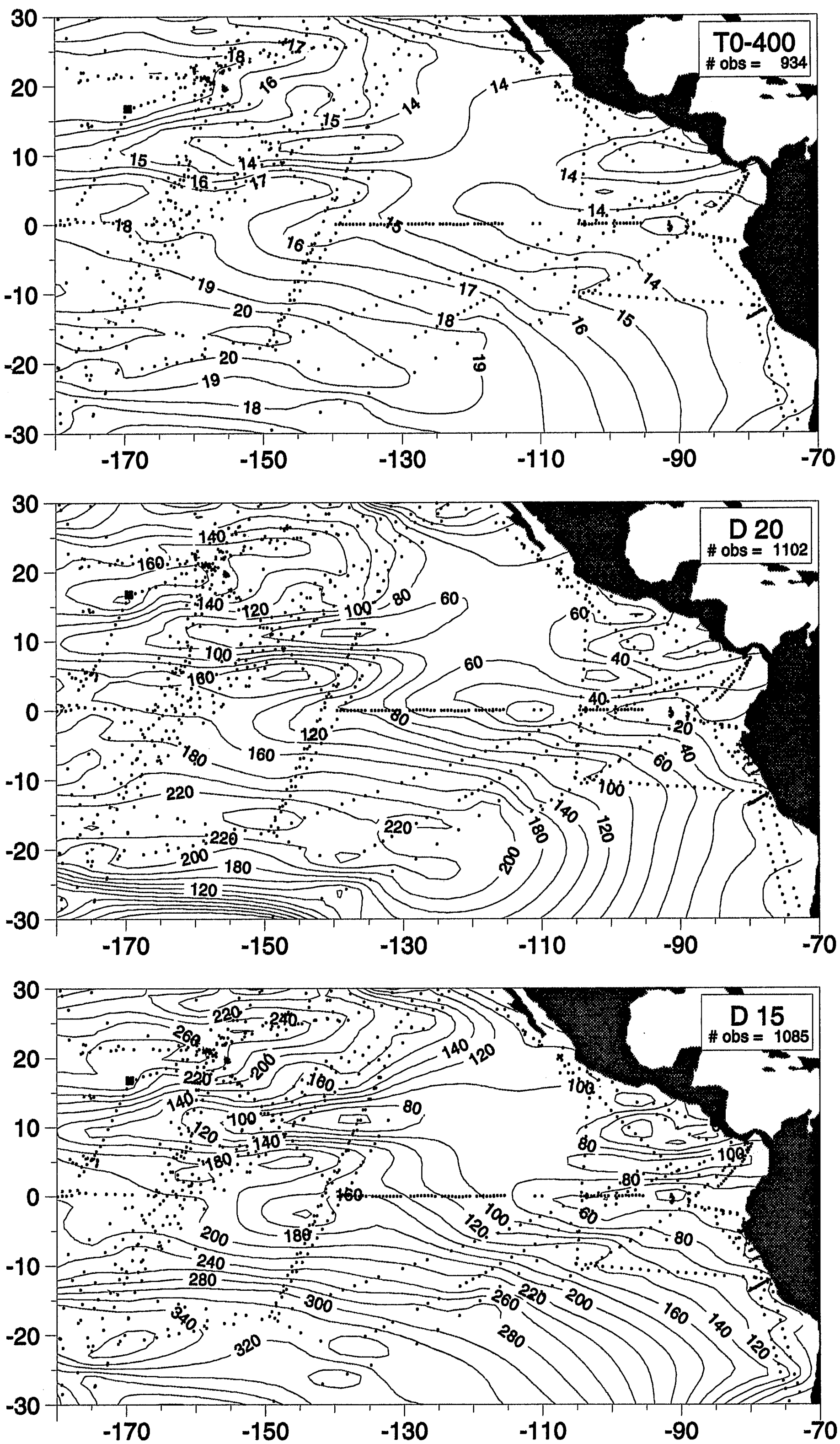

Plate 42 – *continued*. Bimonthly fields for November-December 1984.

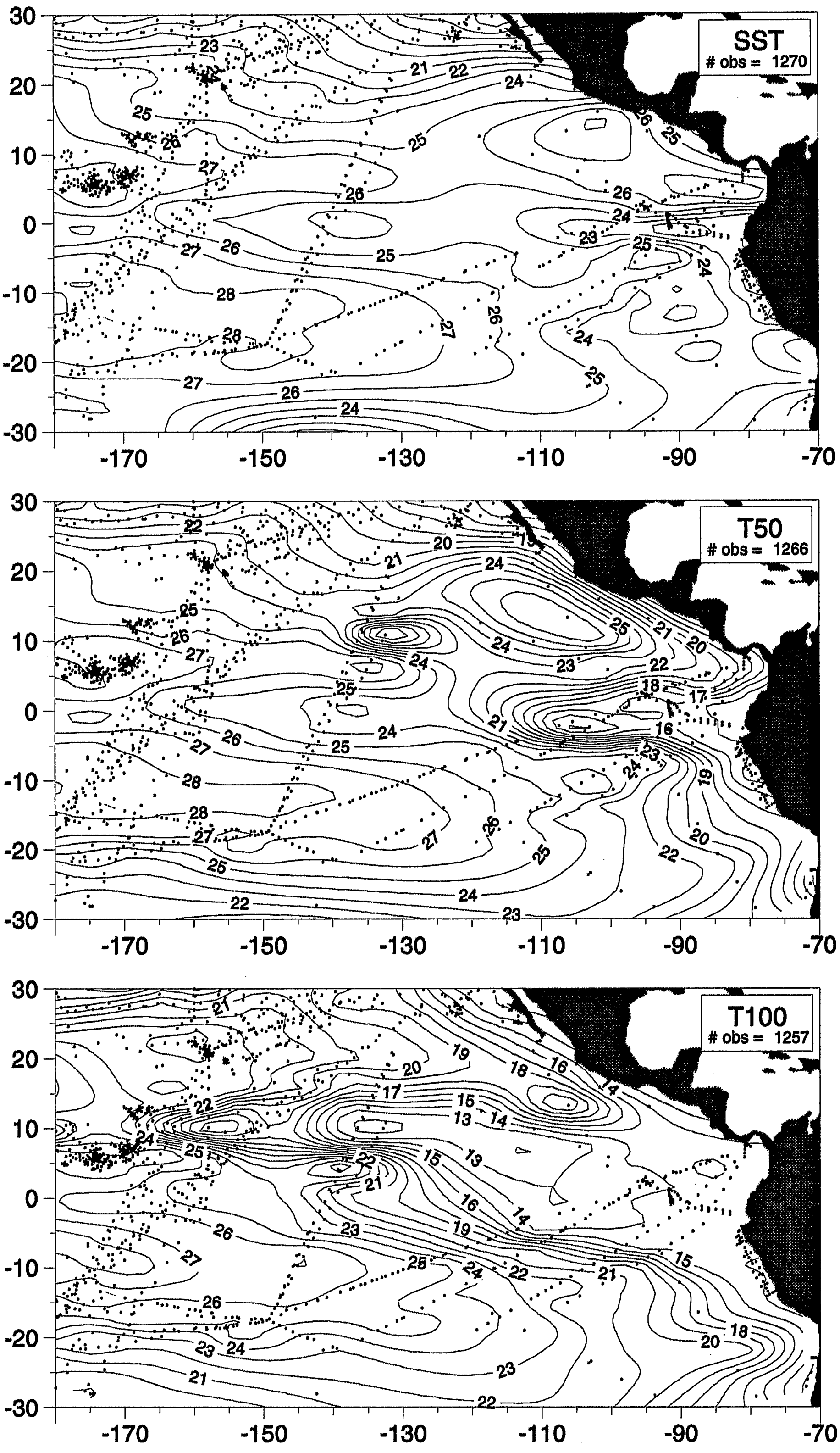

Plate 43. Bimonthly fields for January-February 1985.

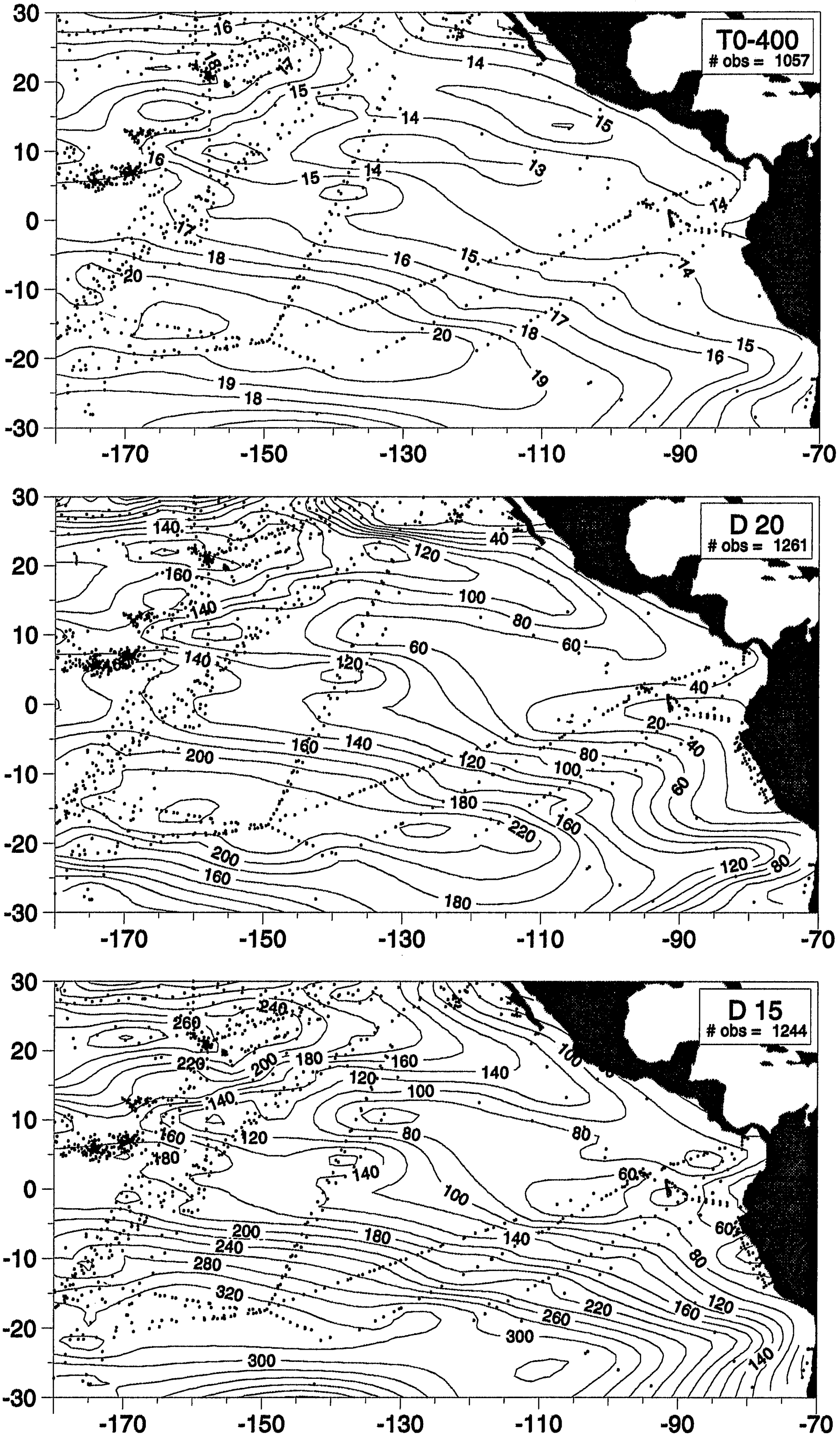

Plate 43 – *continued.* Bimonthly fields for January-February 1985.

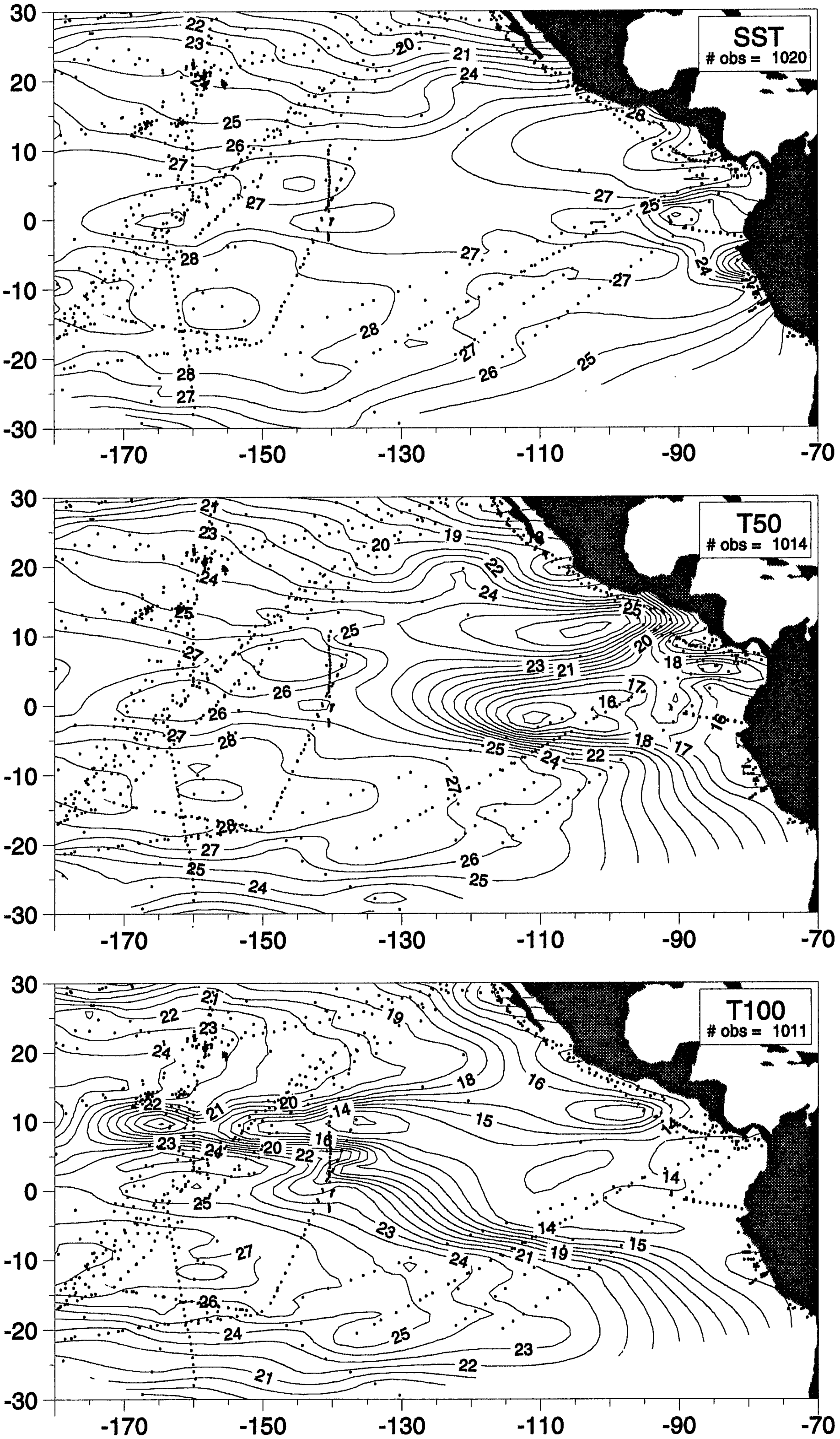

Plate 44. Bimonthly fields for March-April 1985.

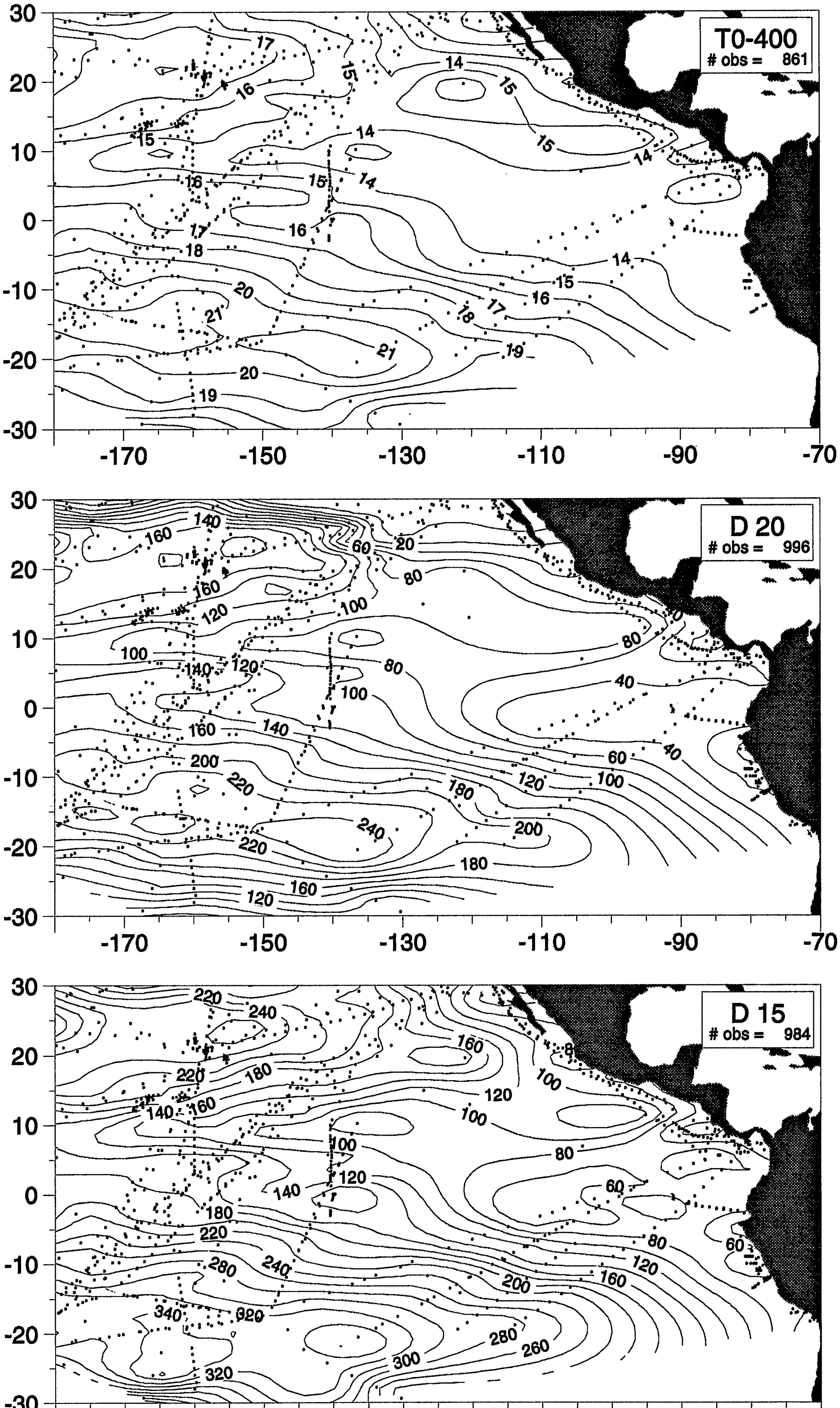

Plate 44 – *continued*. Bimonthly fields for March-April 1985.

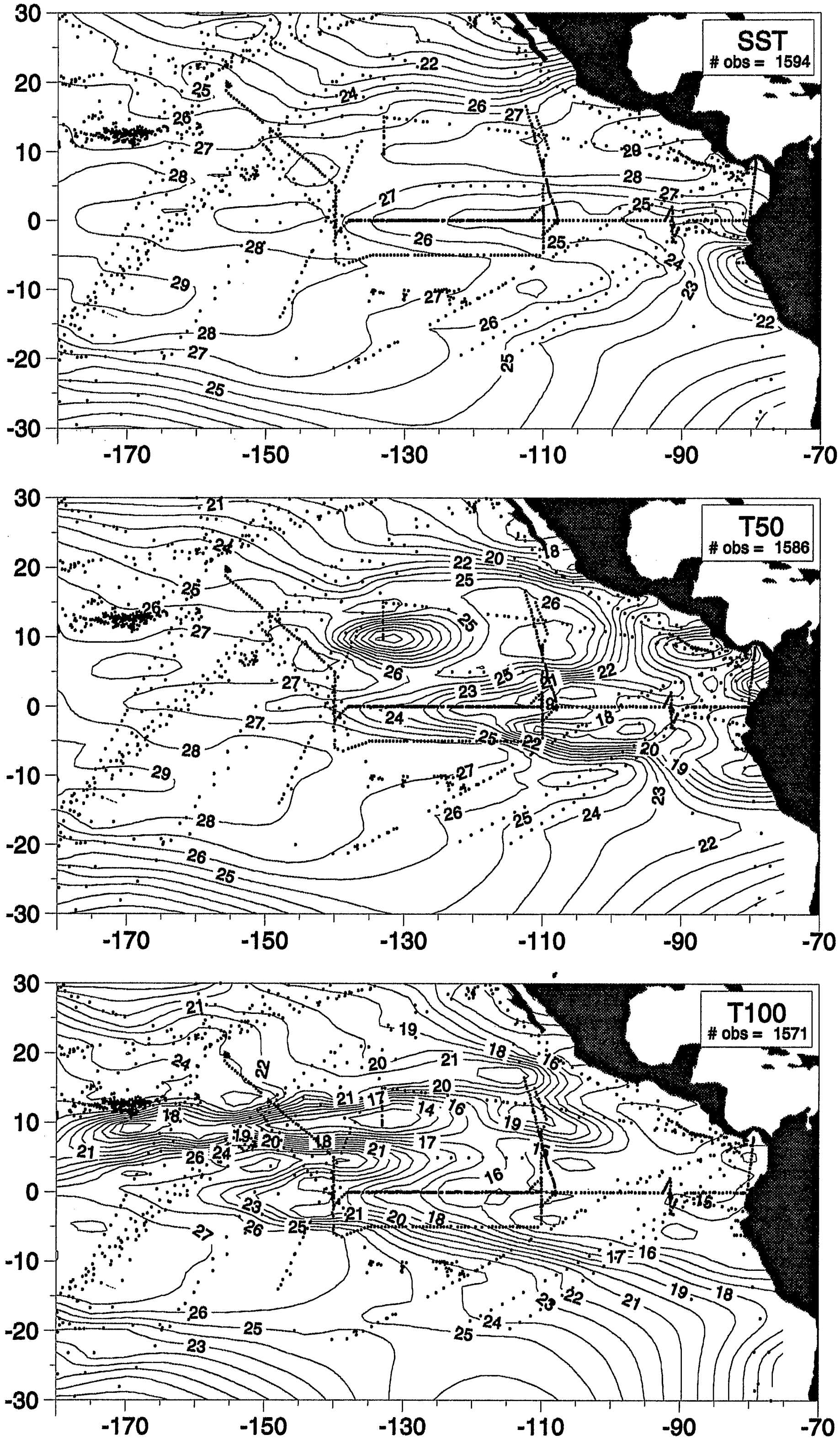

Plate 45. Bimonthly fields for May-June 1985.

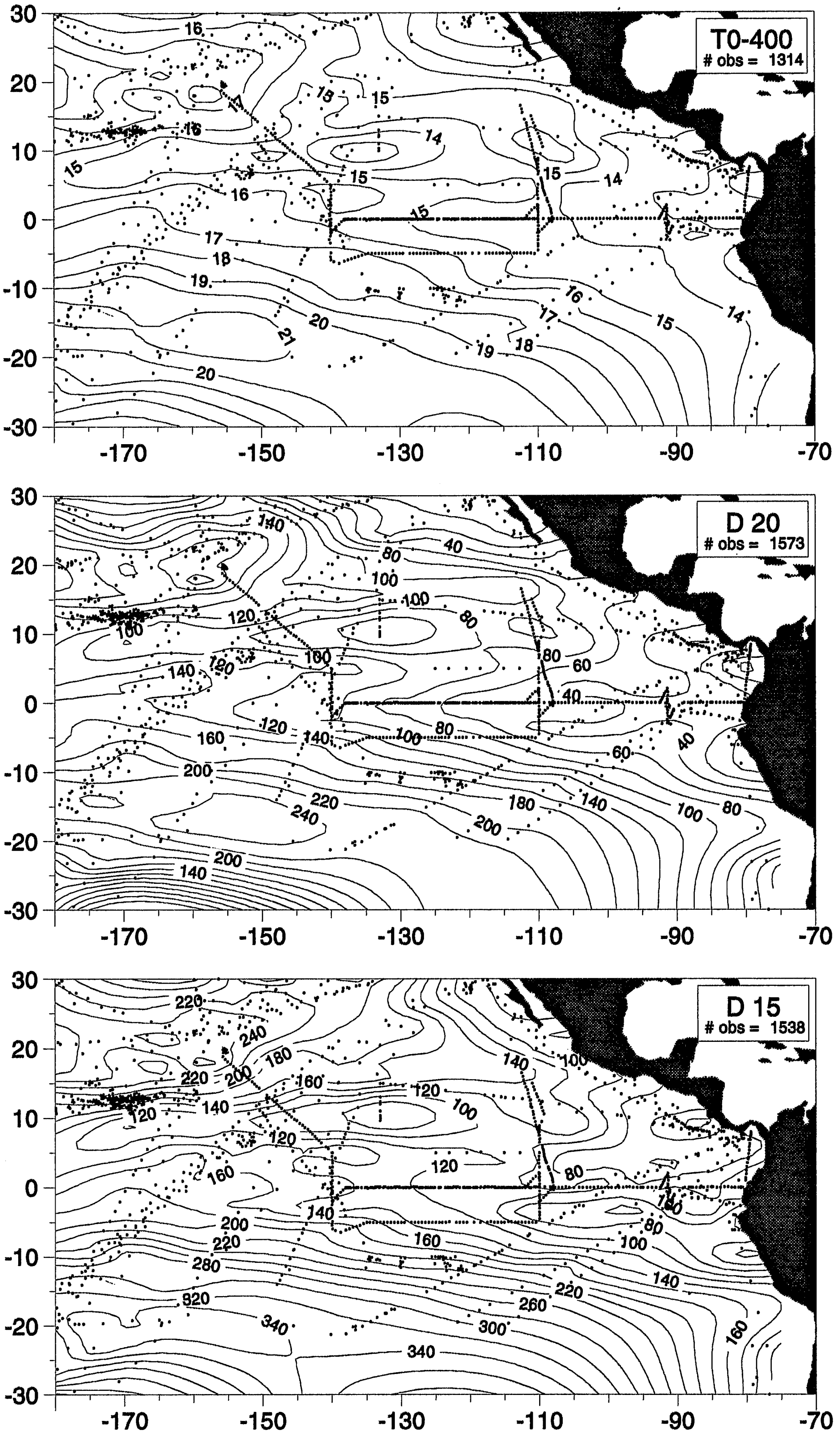

Plate 45 – *continued*. Bimonthly fields for May-June 1985.

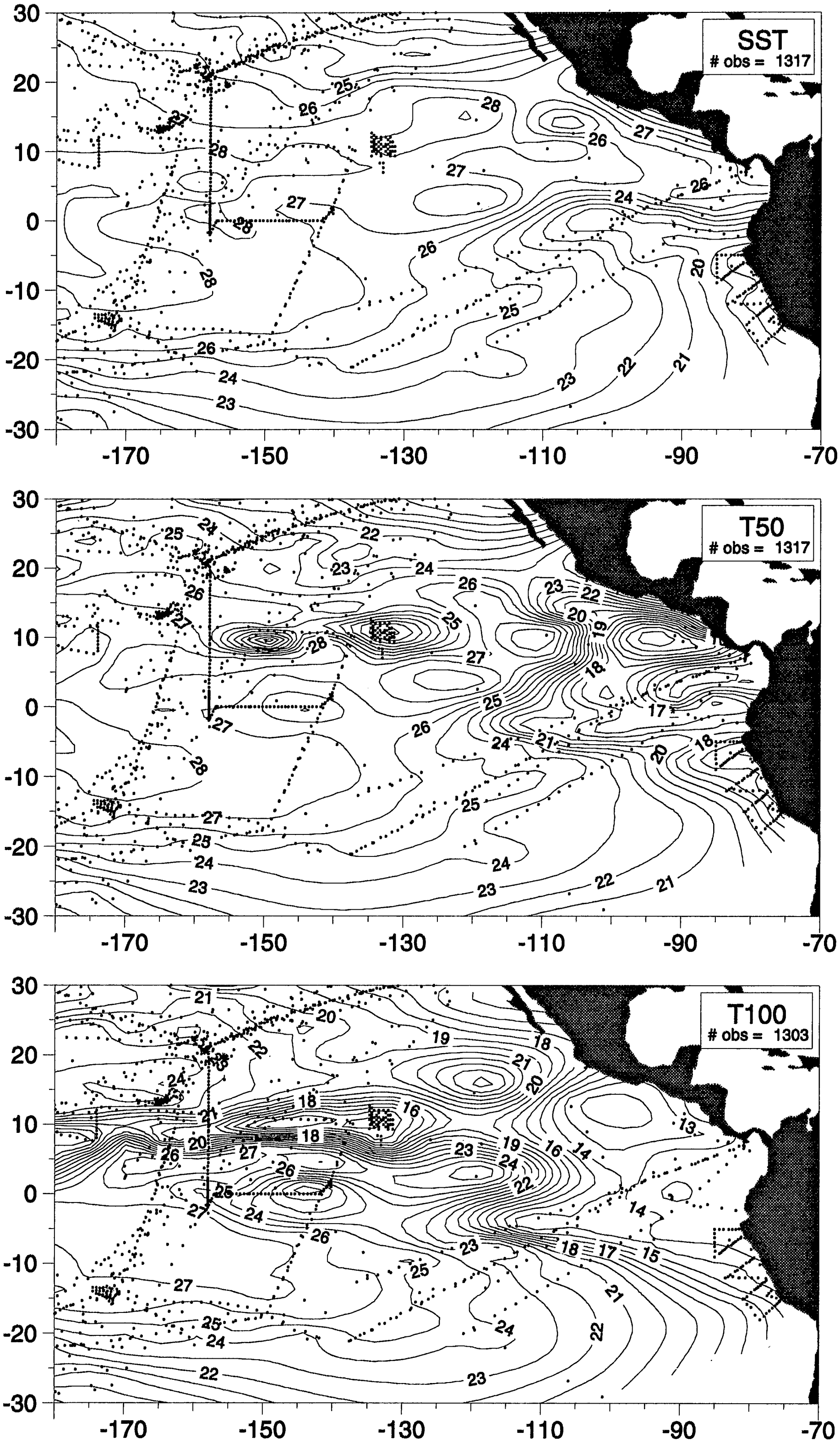

Plate 46. Bimonthly fields for July-August 1985.

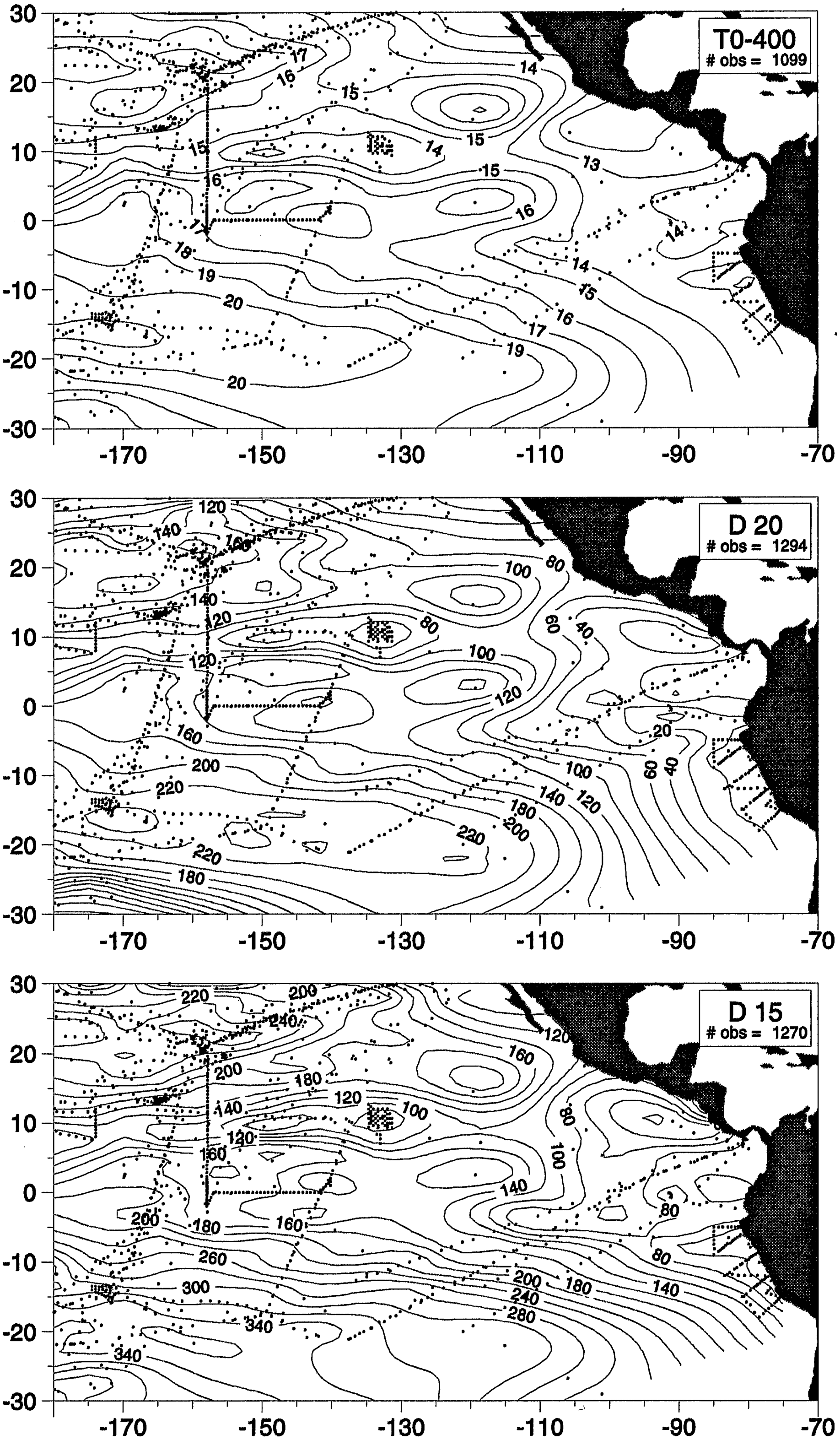

Plate 46 – *continued*. Bimonthly fields for July-August 1985.

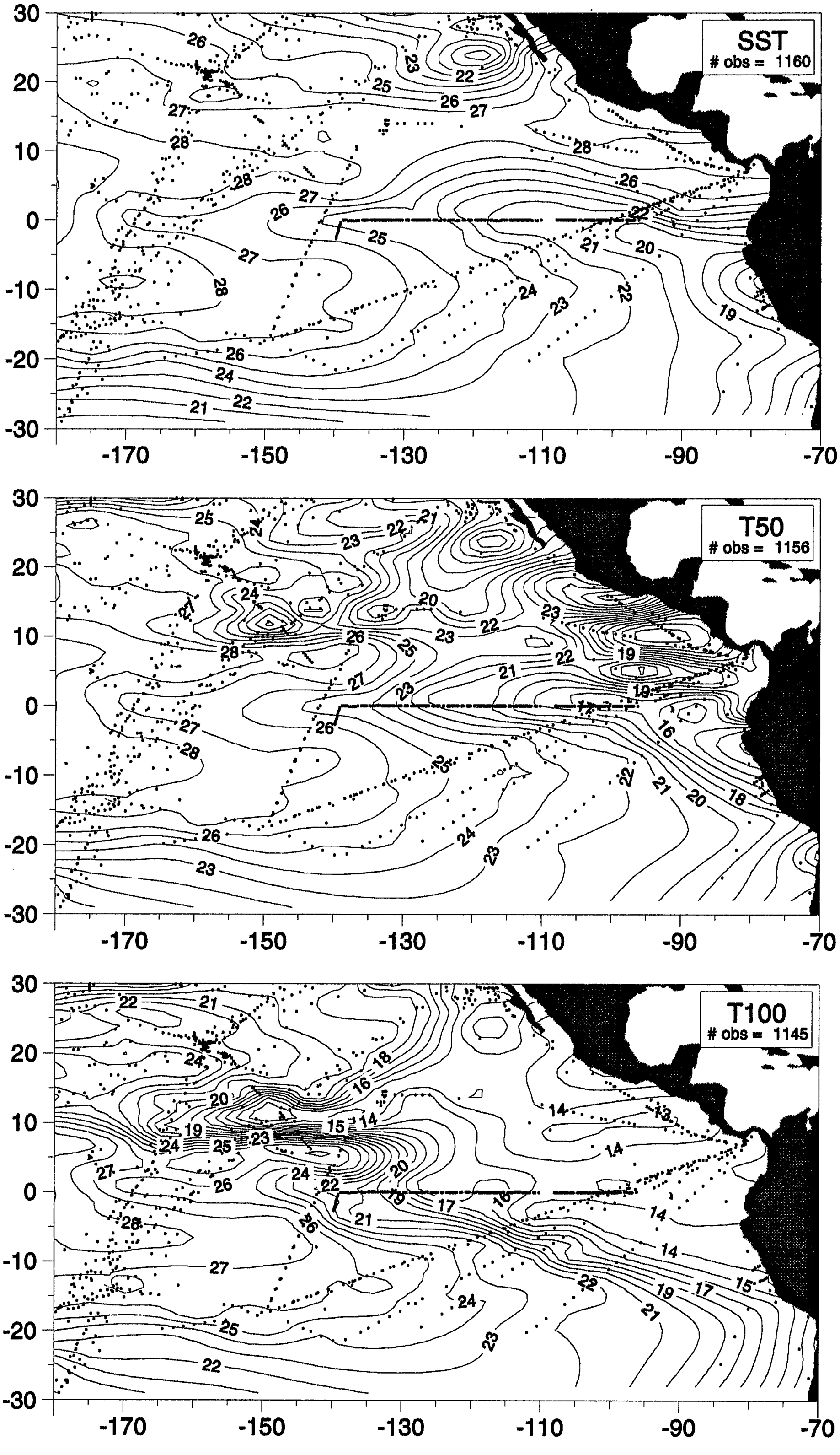

Plate 47. Bimonthly fields for September-October 1985.

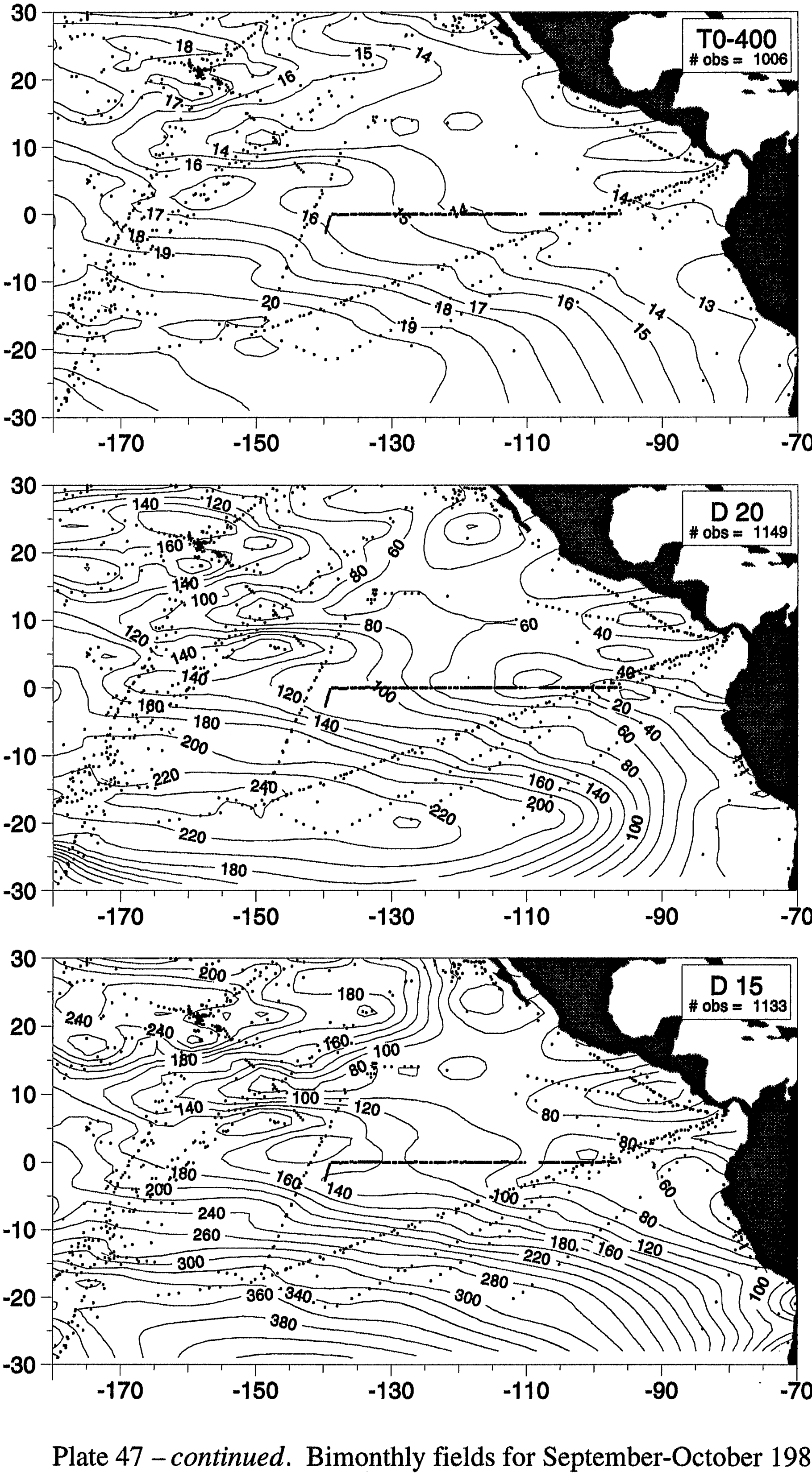

Plate 47 – *continued*. Bimonthly fields for September-October 1985.

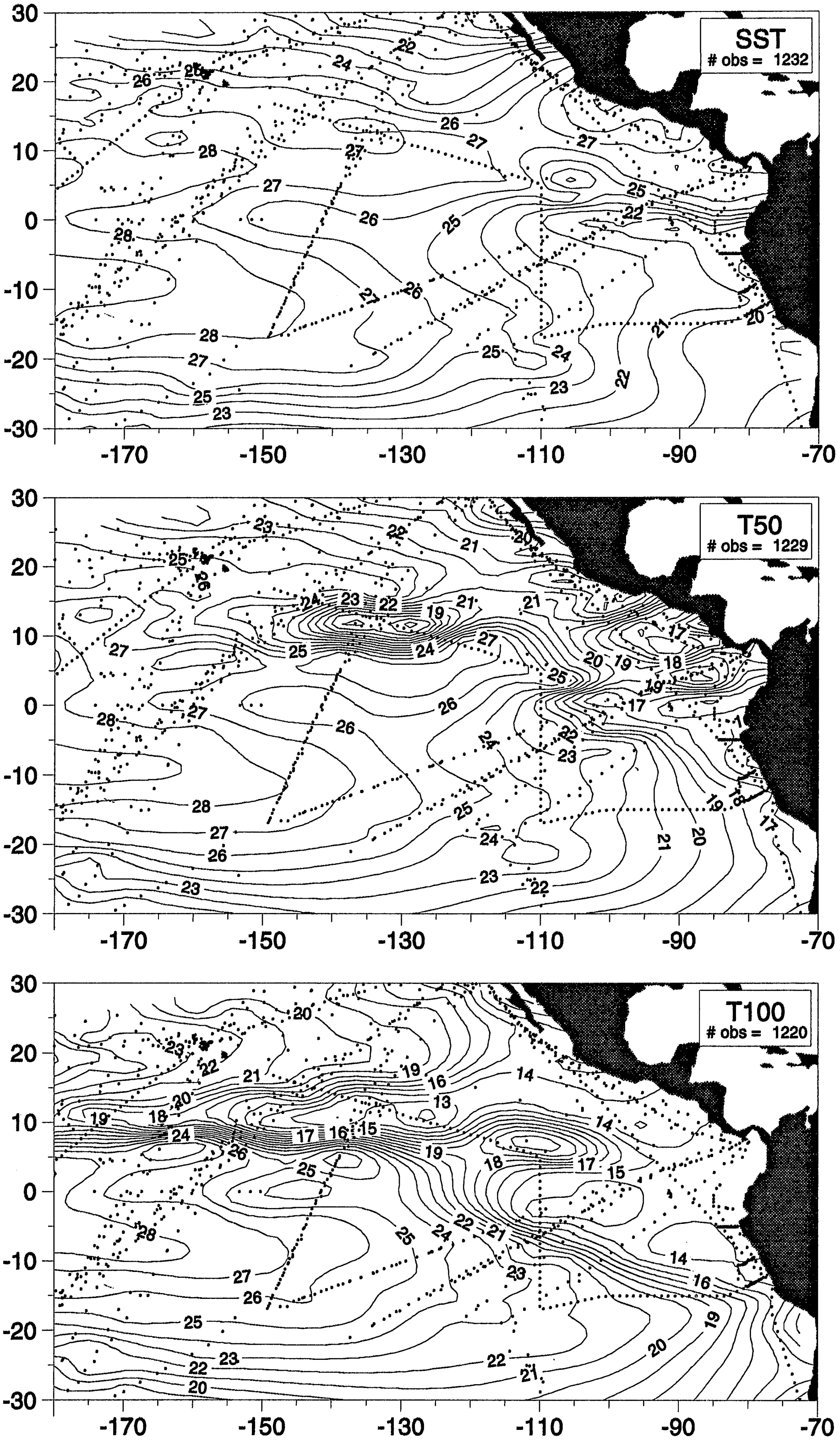

Plate 48. Bimonthly fields for November-December 1985.

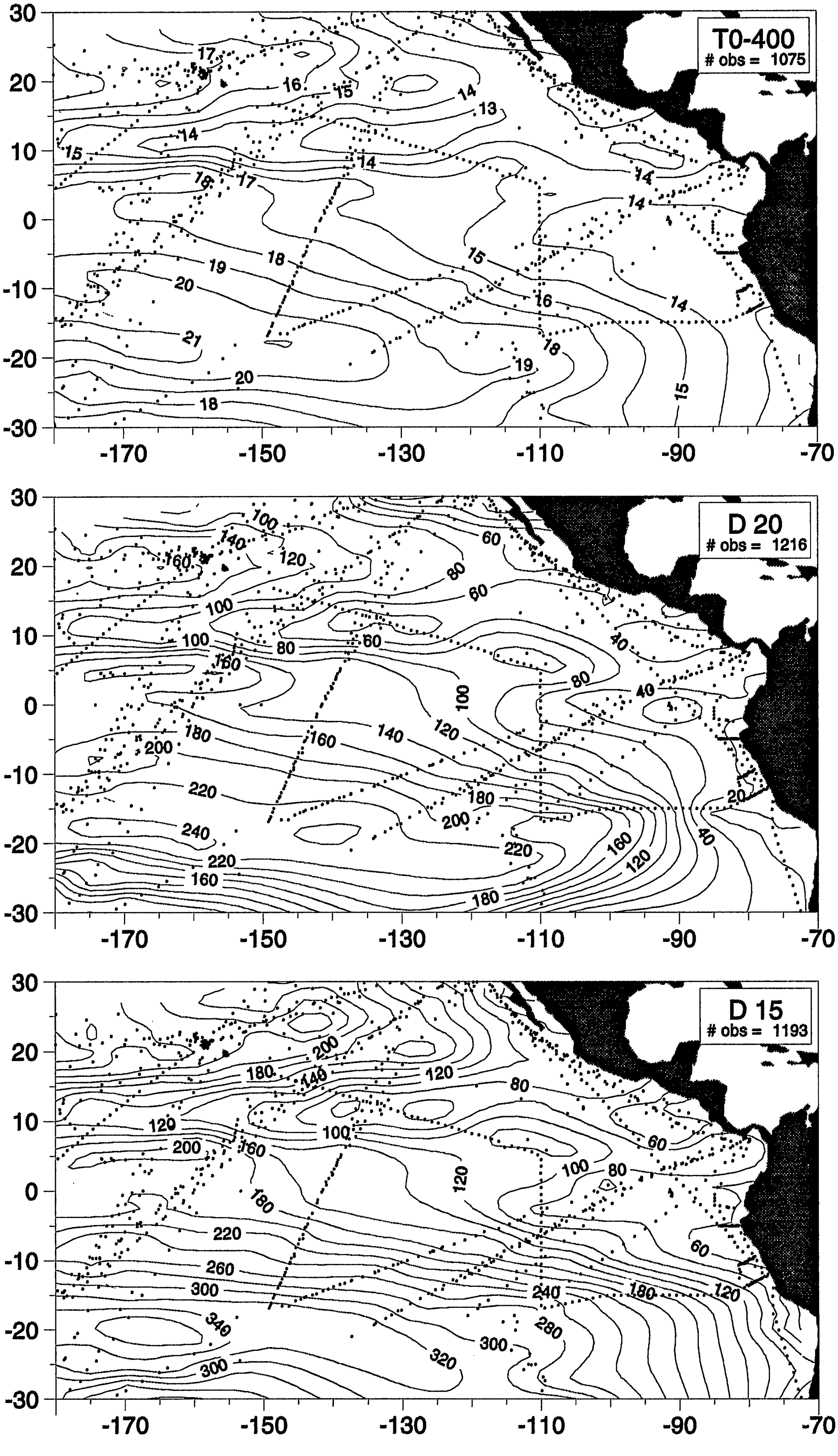

Plate 48 – *continued*. Bimonthly fields for November-December 1985.

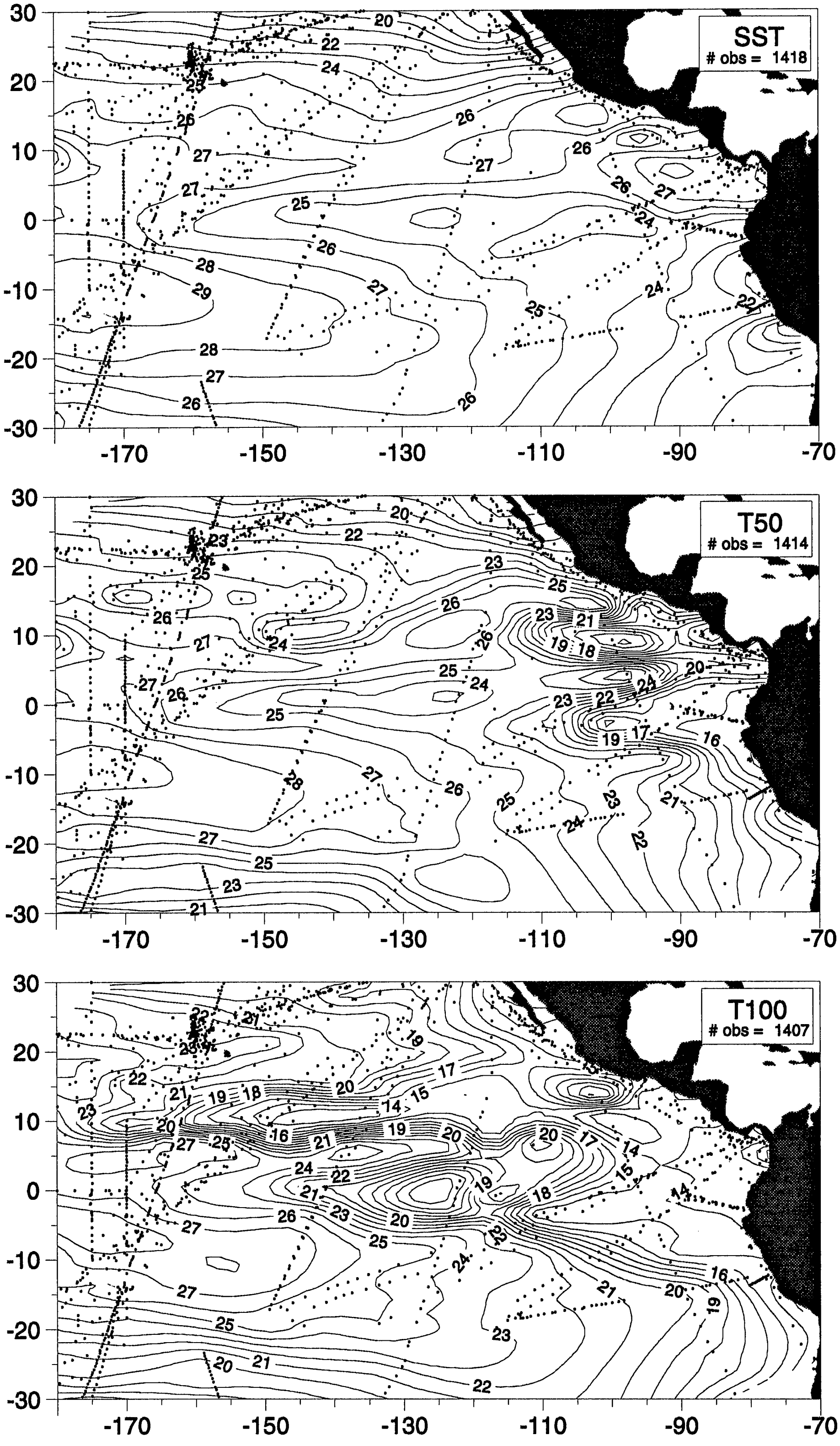

Plate 49. Bimonthly fields for January-February 1986.

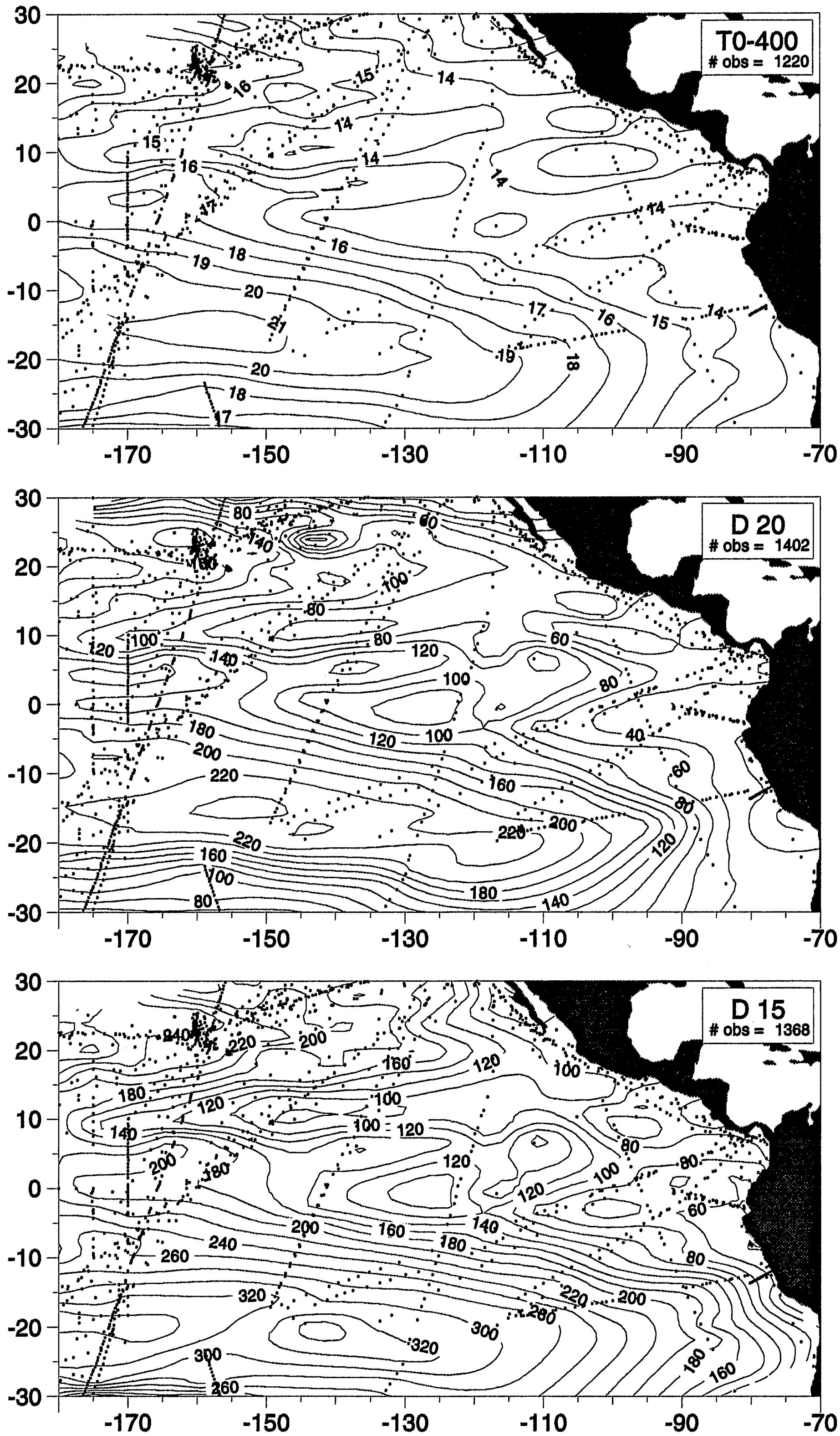

Plate 49 – *continued*. Bimonthly fields for January-February 1986.

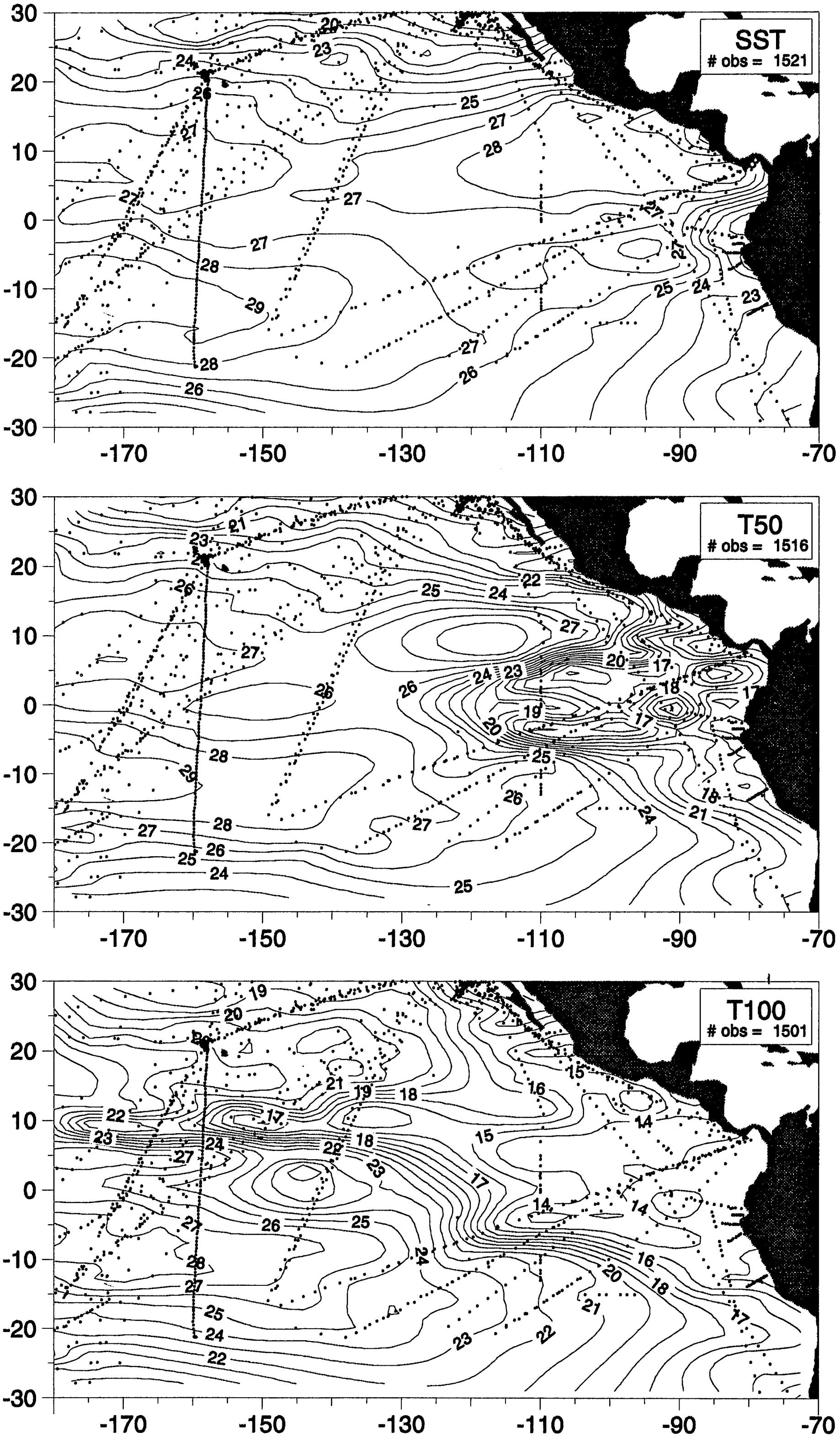

Plate 50. Bimonthly fields for March-April 1986.

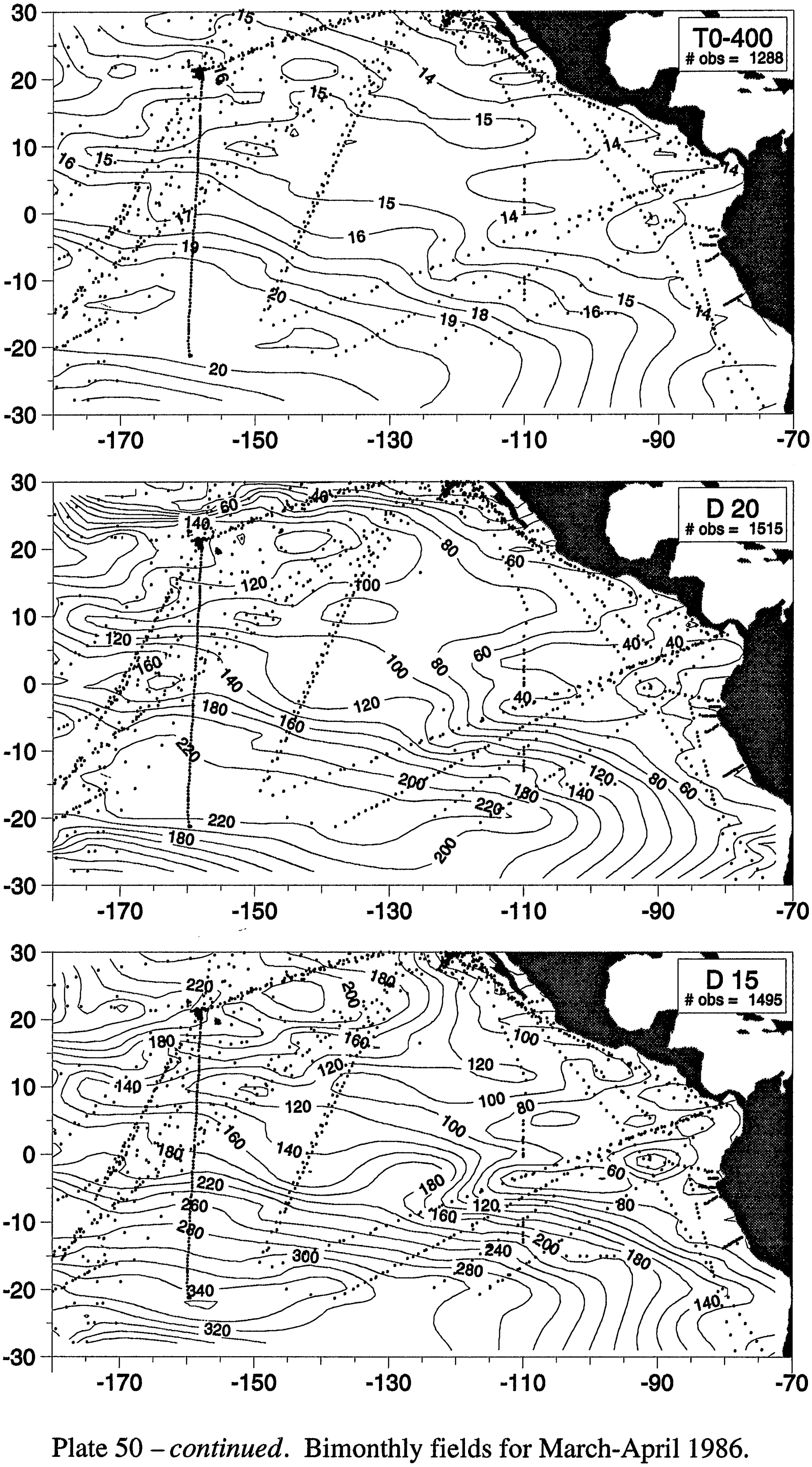

Plate 50 – *continued*. Bimonthly fields for March-April 1986.

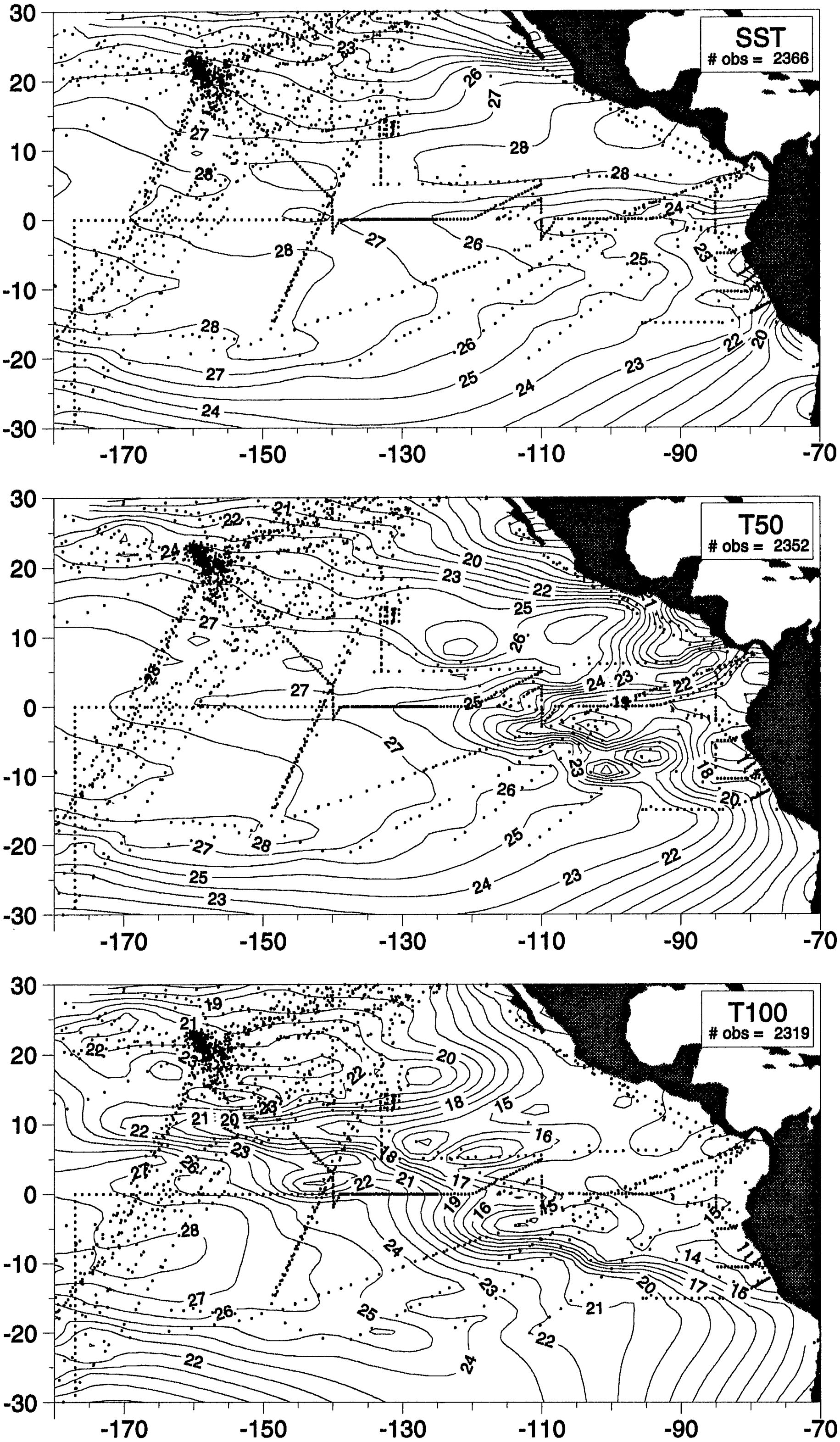

Plate 51. Bimonthly fields for May-June 1986.

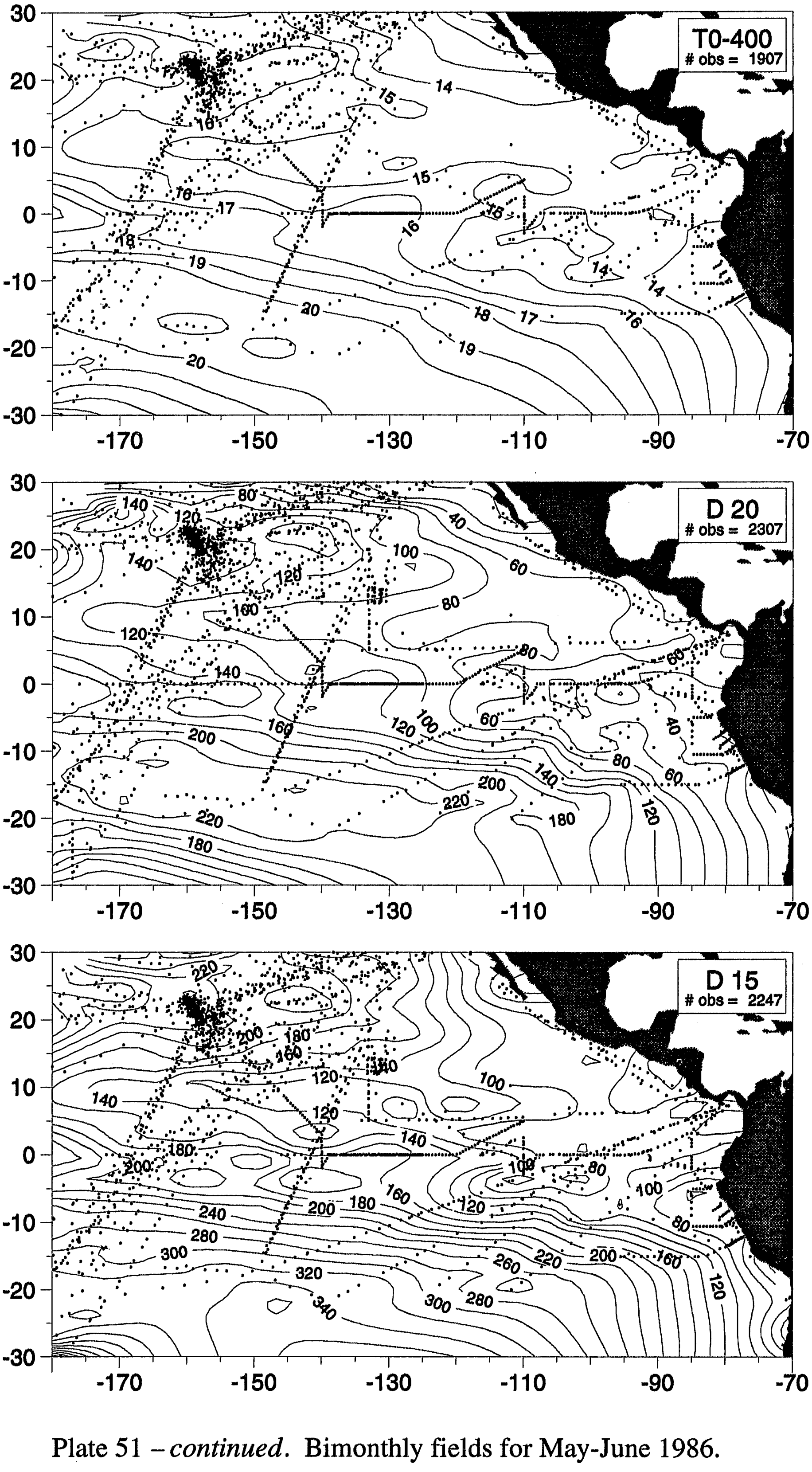

Plate 51 – *continued*. Bimonthly fields for May-June 1986.

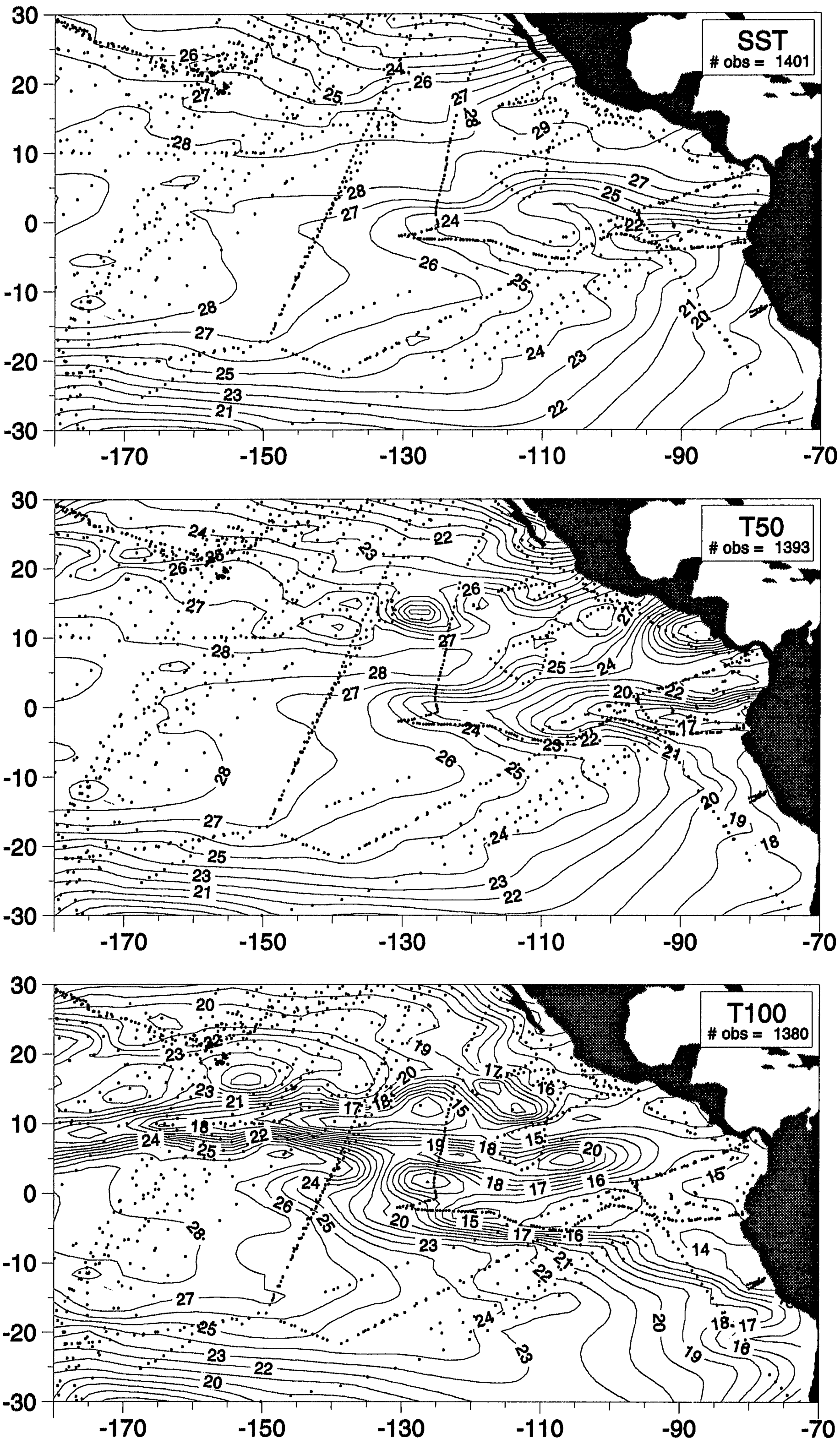

Plate 52. Bimonthly fields for July-August 1986.

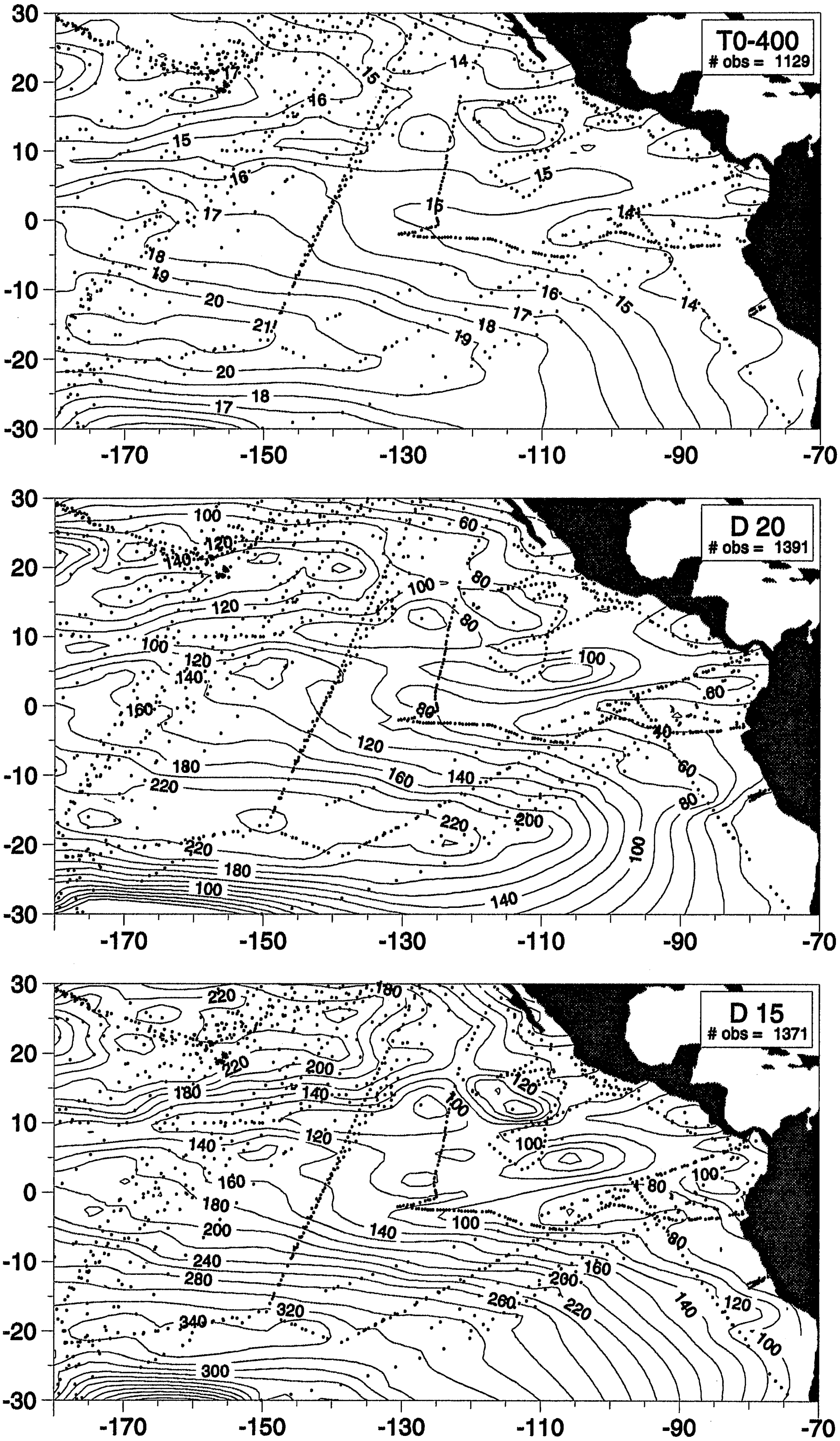

Plate 52 – *continued*. Bimonthly fields for July-August 1986.

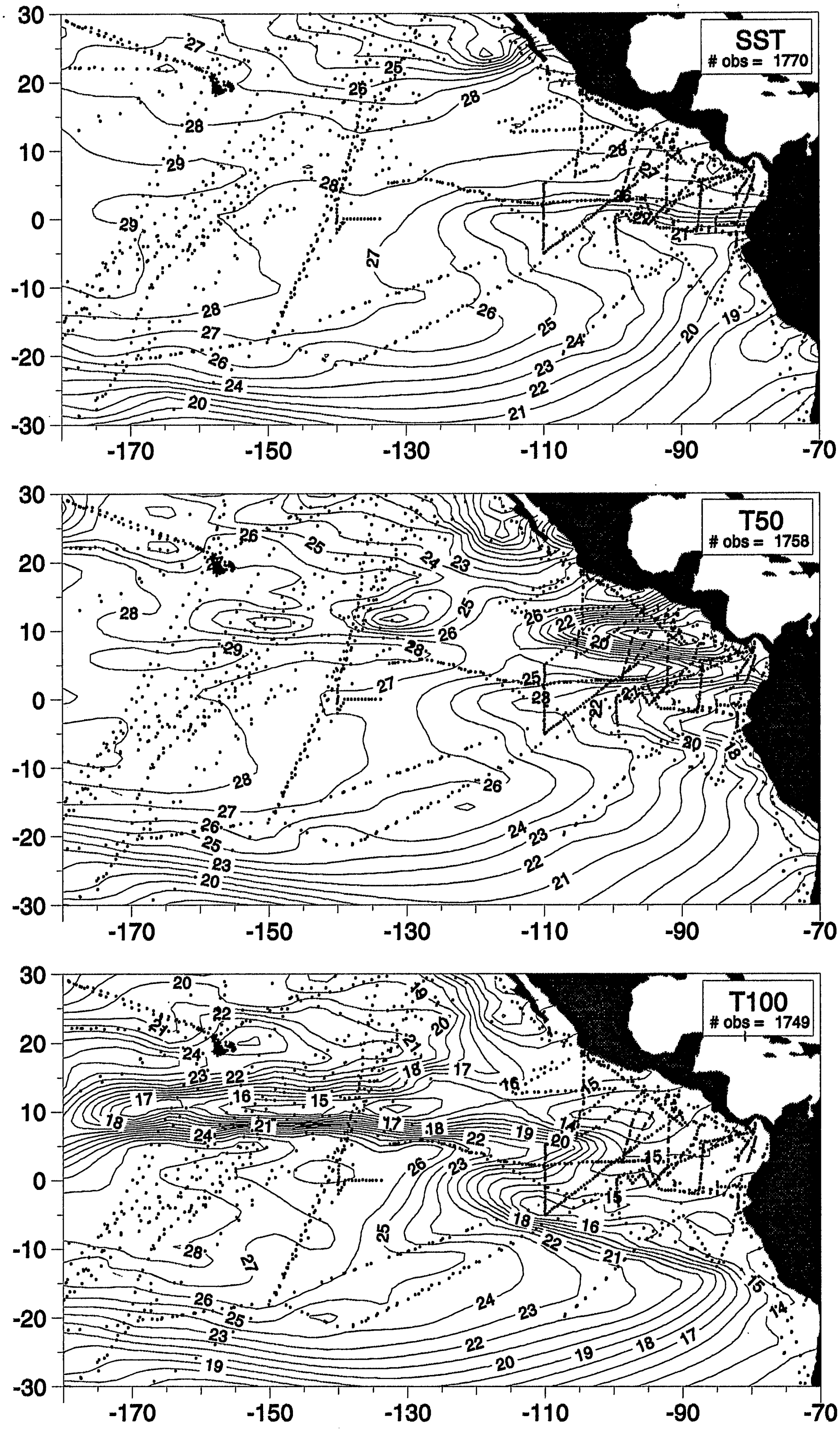

Plate 53. Bimonthly fields for September-October 1986.

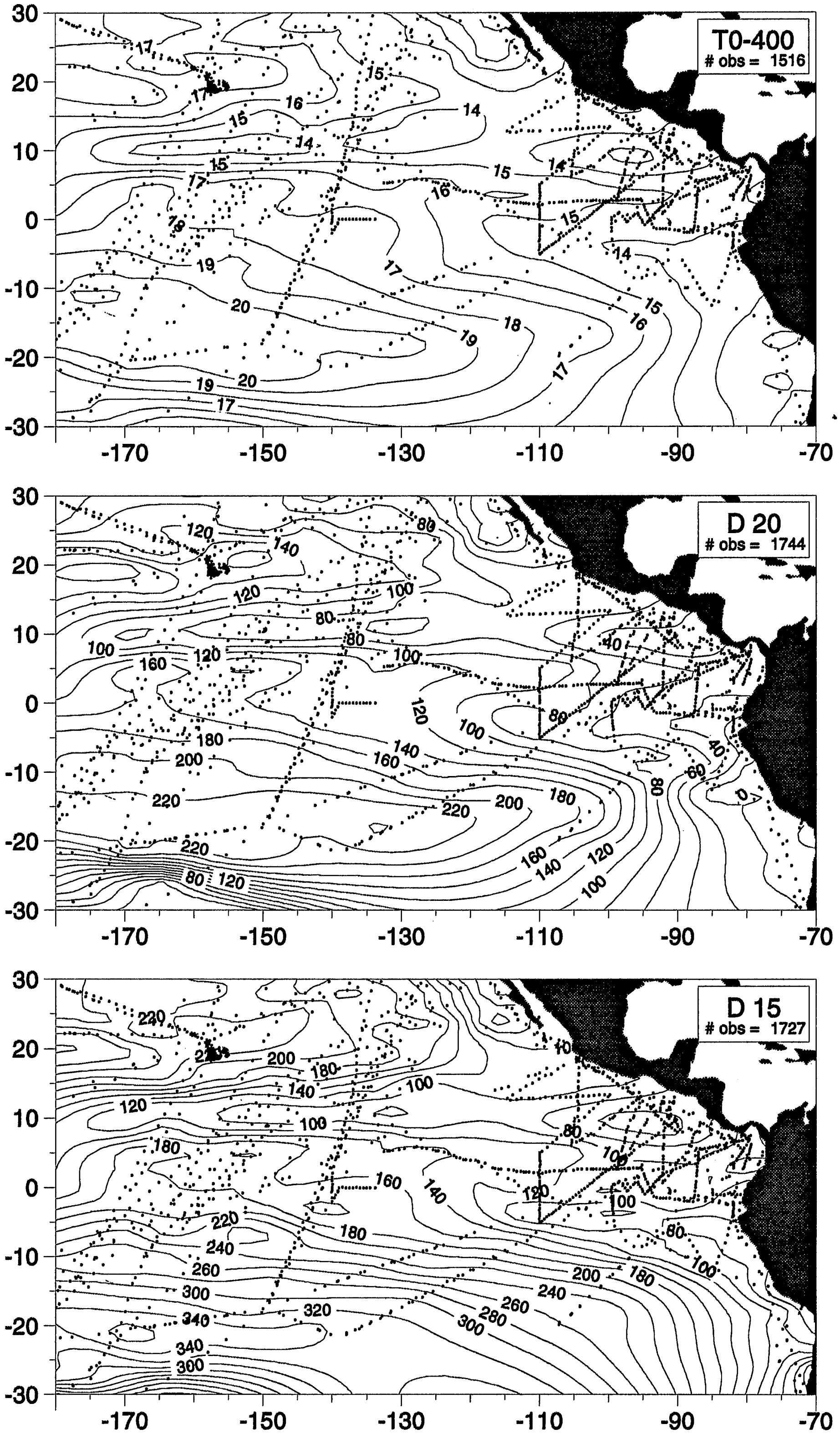

Plate 53 – *continued.* Bimonthly fields for September-October 1986.

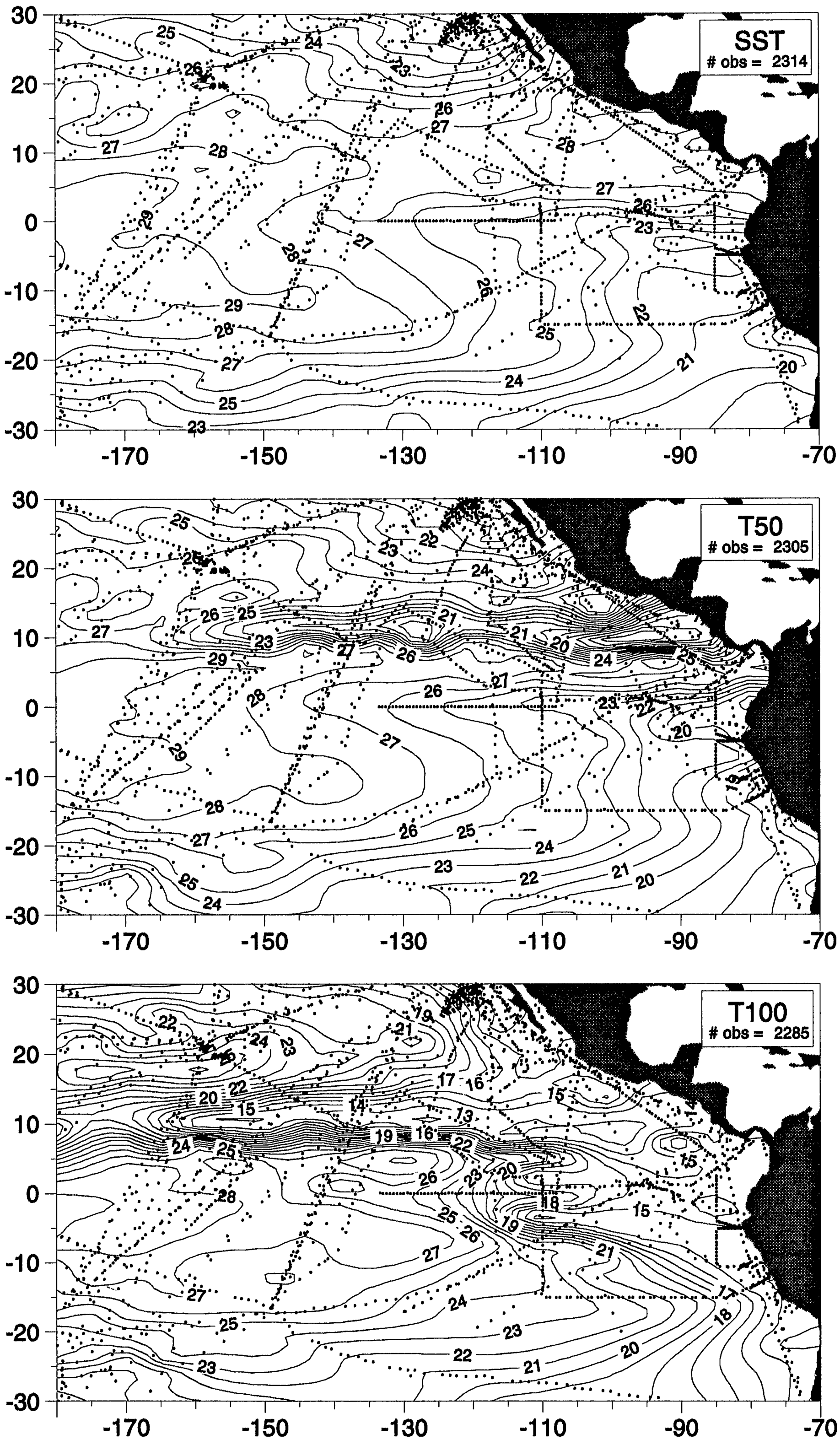

Plate 54. Bimonthly fields for November-December 1986.

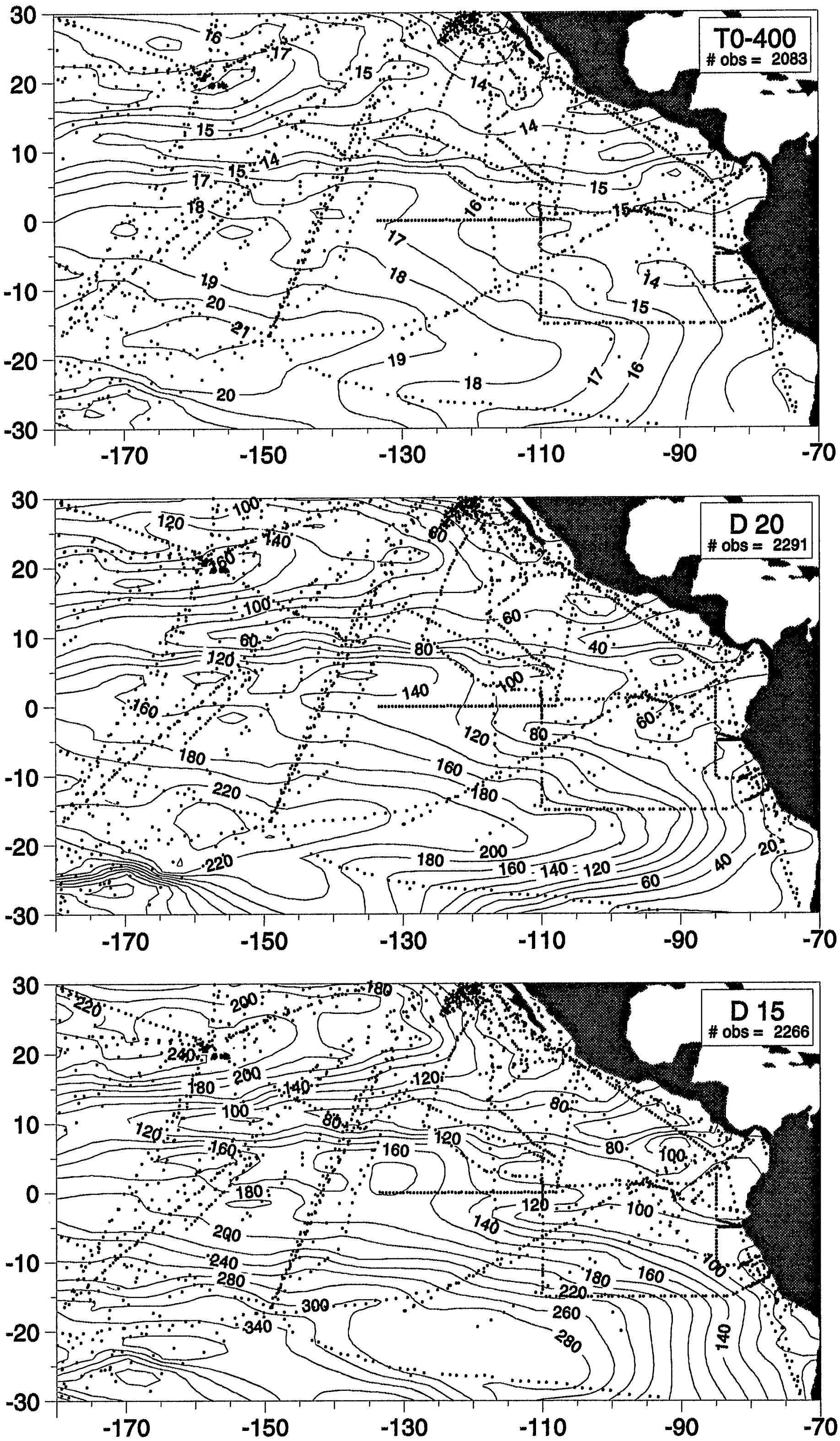

Plate 54 – *continued*. Bimonthly fields for November-December 1986.

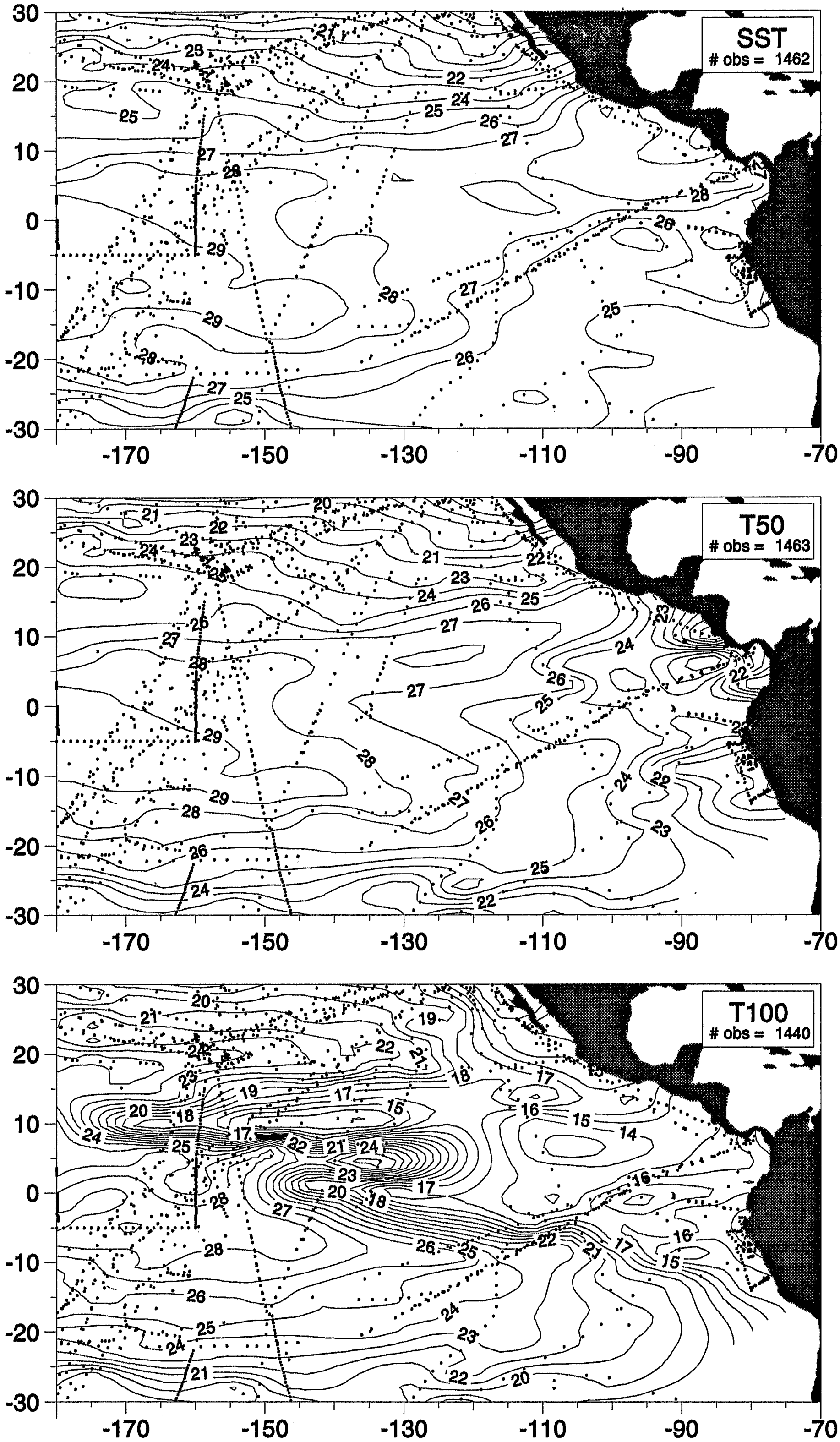

Plate 55. Bimonthly fields for January-February 1987.

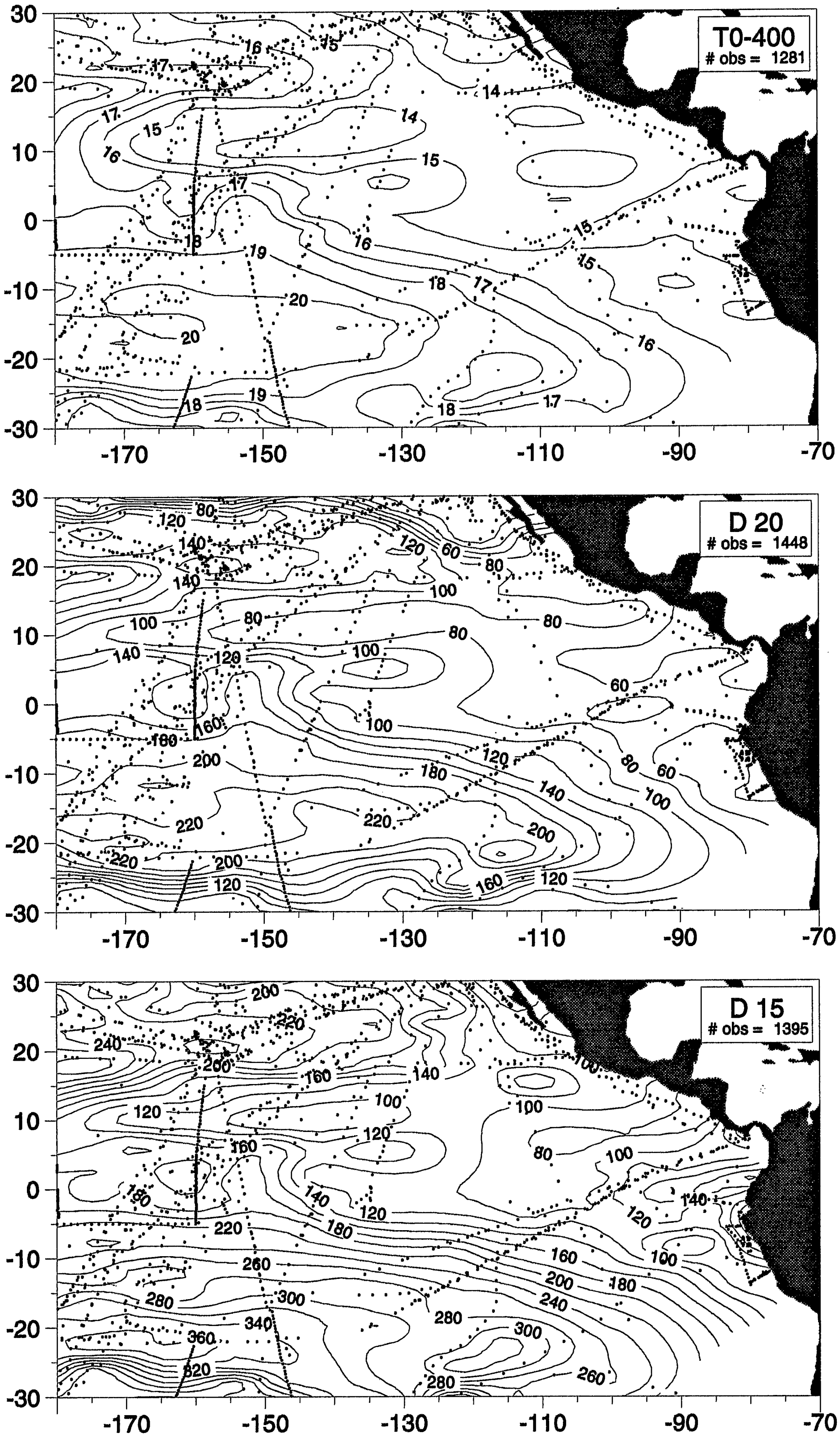

Plate 55 – *continued*. Bimonthly fields for January-February 1987.

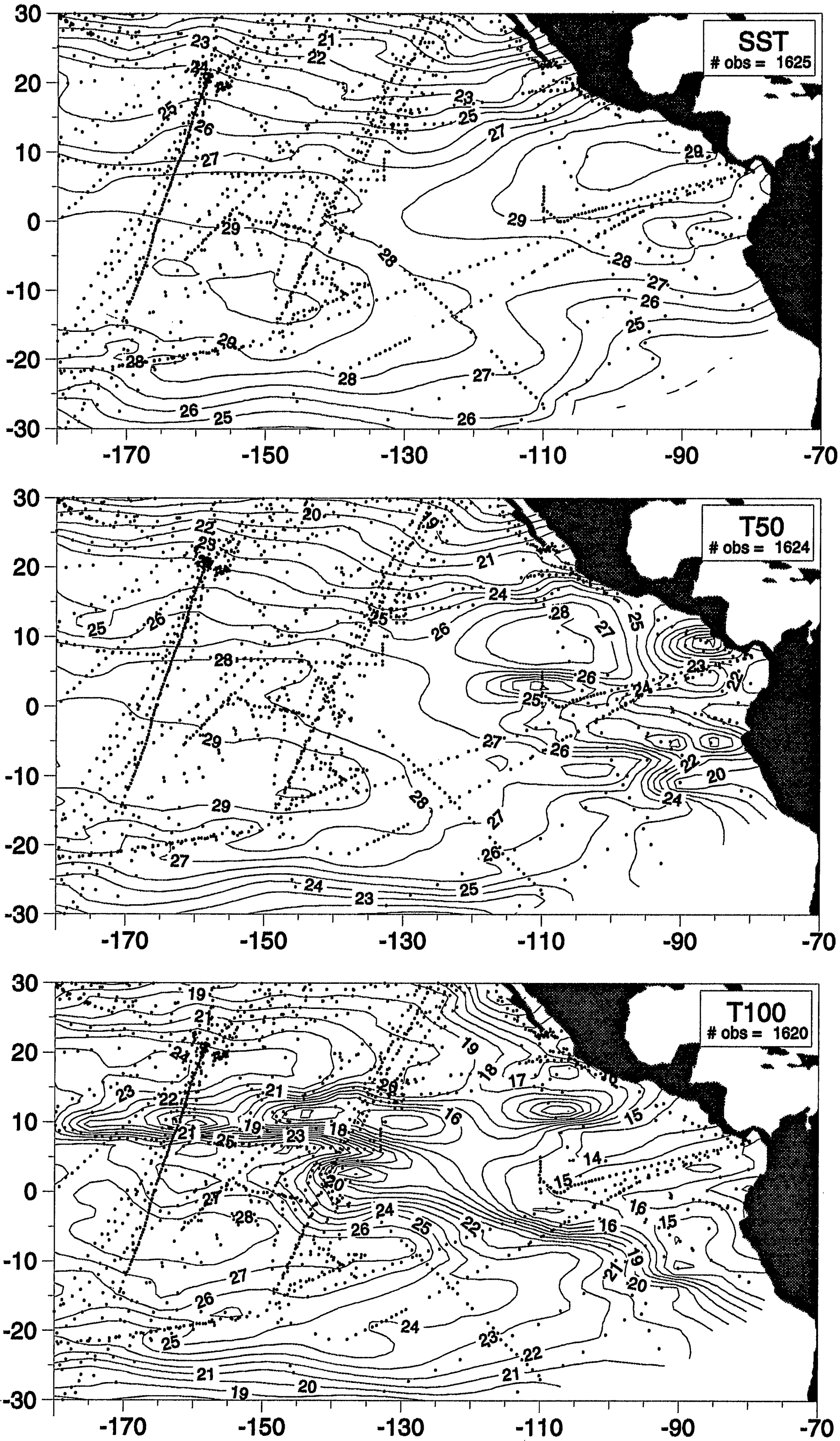

Plate 56. Bimonthly fields for March-April 1987.

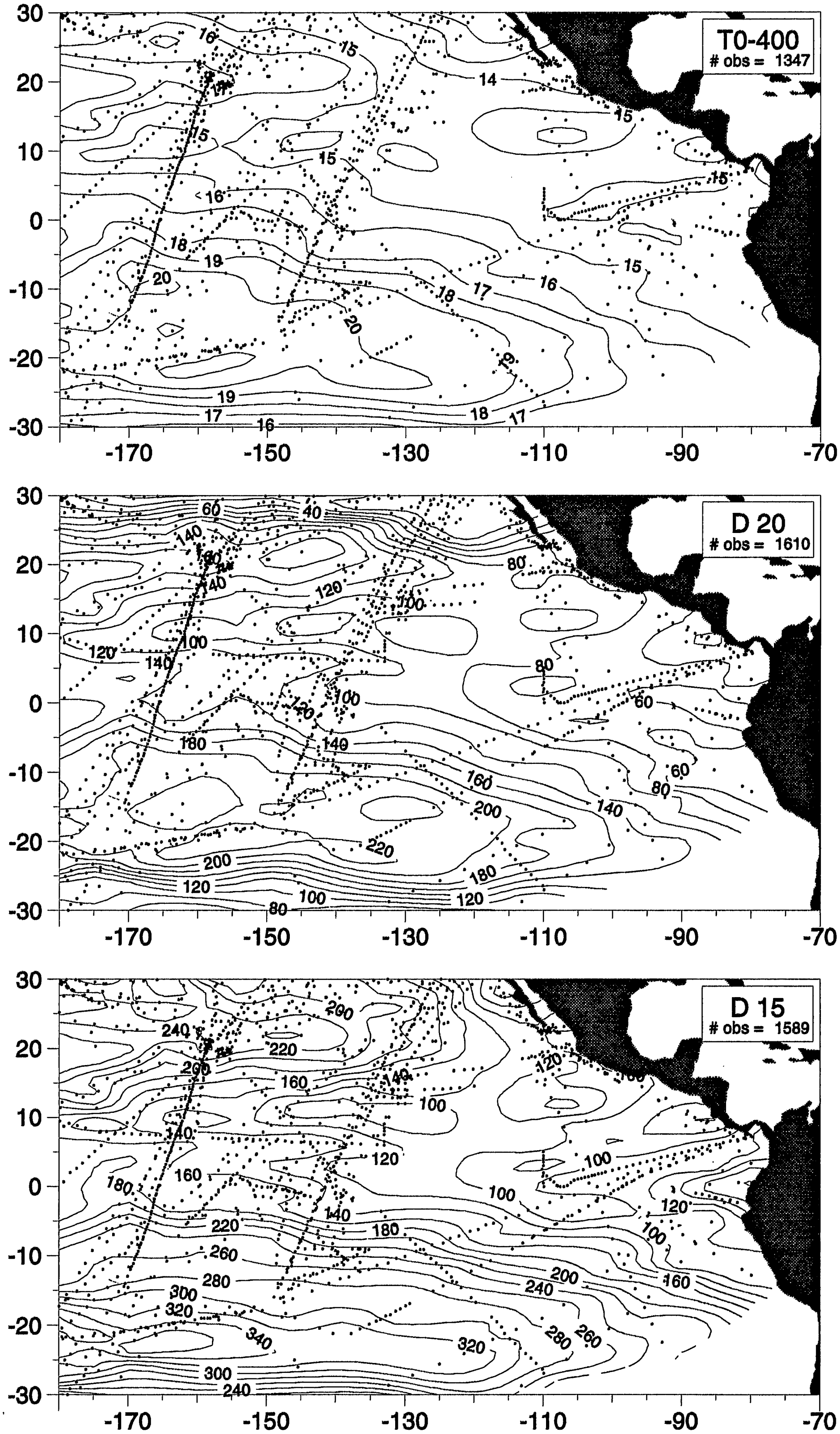

Plate 56 – *continued*. Bimonthly fields for March-April 1987.

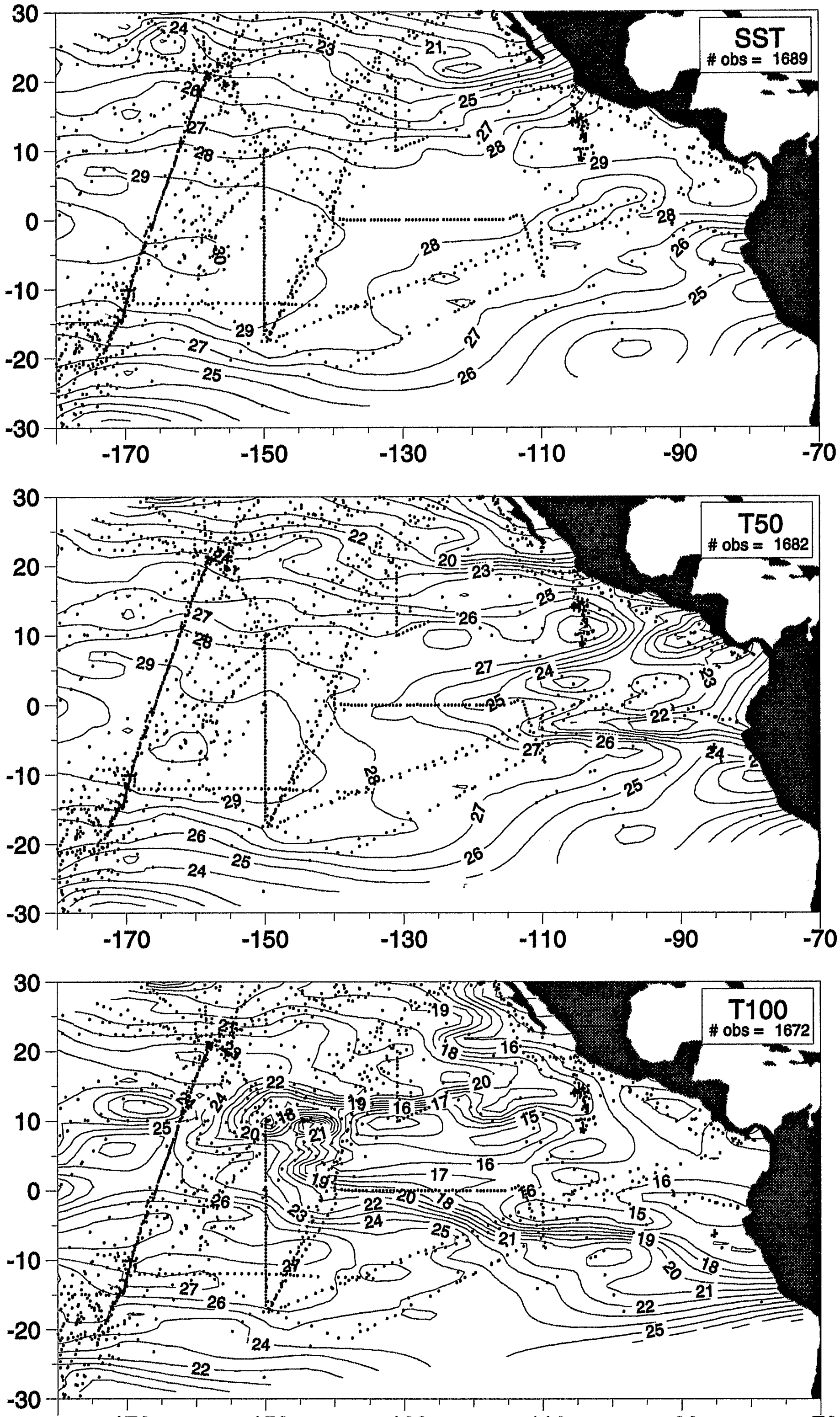

Plate 57. Bimonthly fields for May-June 1987.

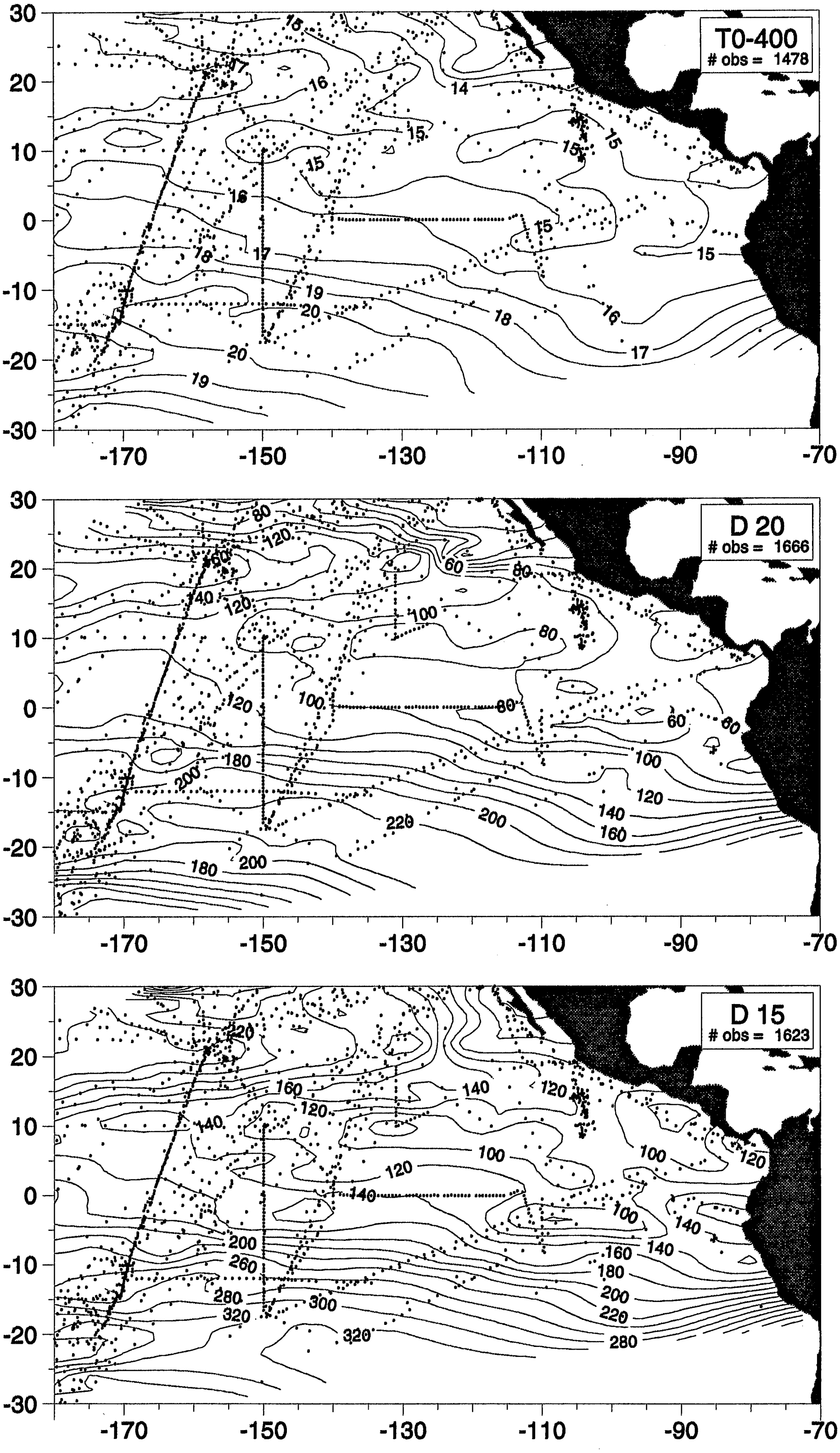

Plate 57 – *continued.* Bimonthly fields for May-June 1987.

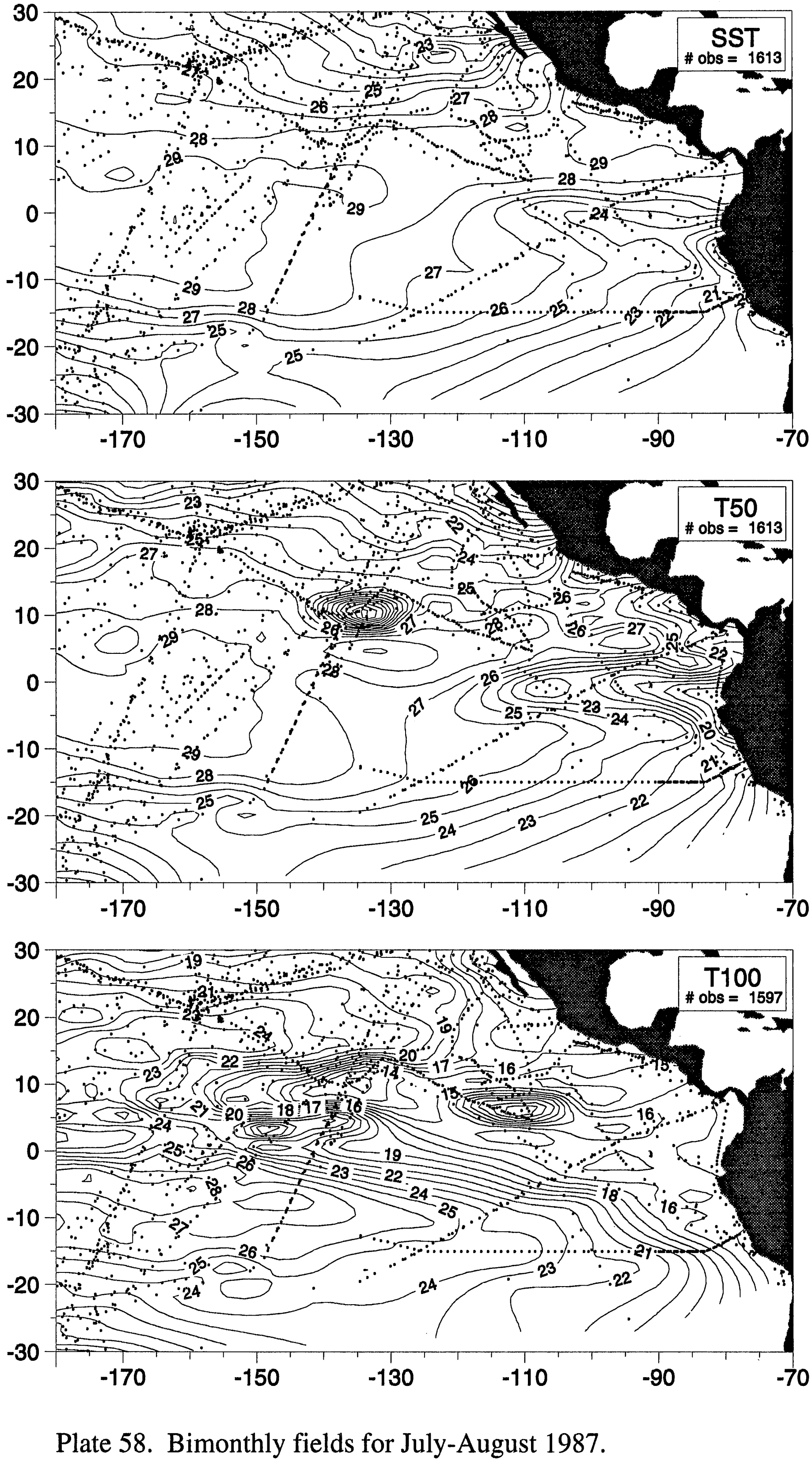

Plate 58. Bimonthly fields for July-August 1987.

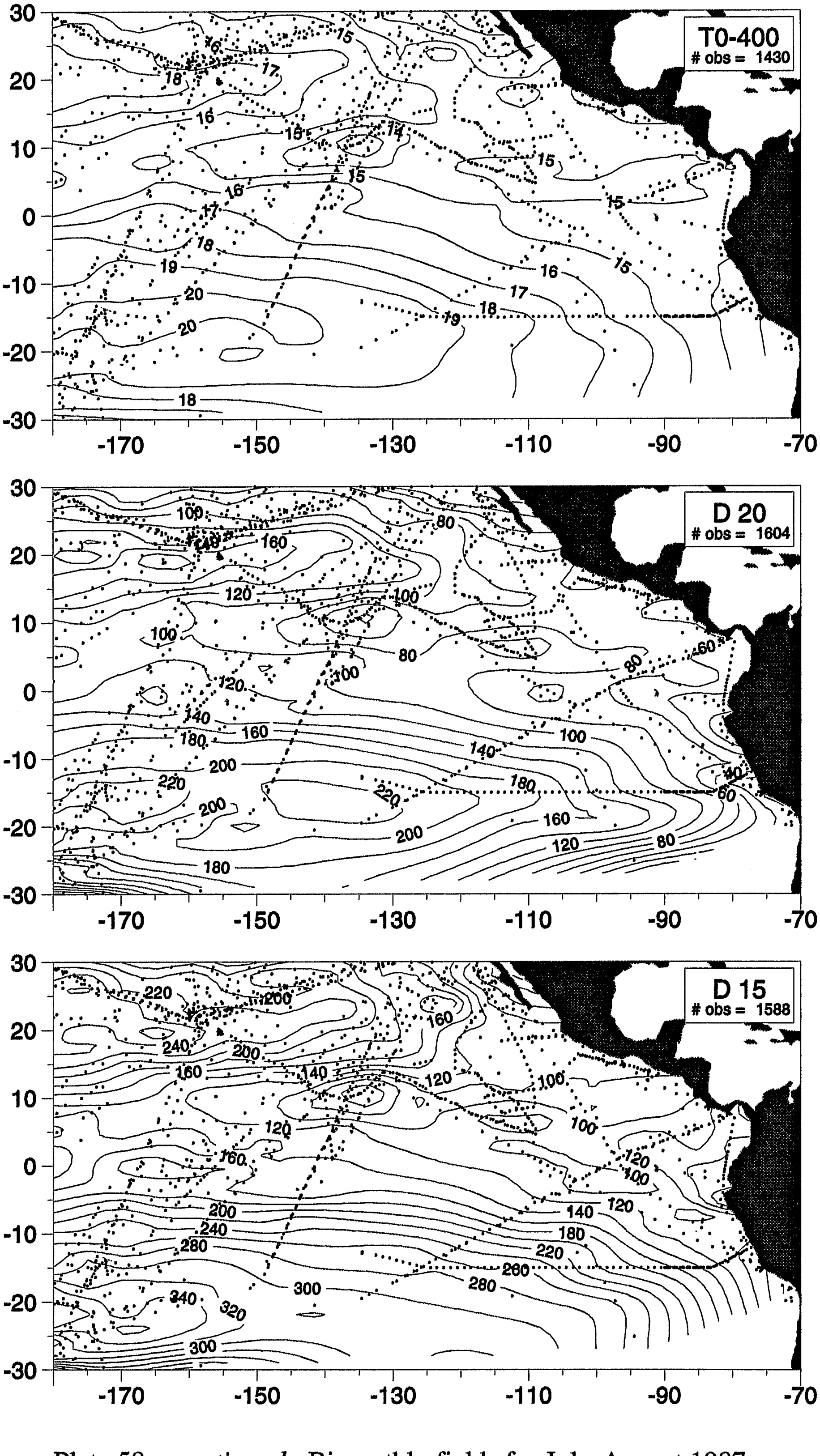

Plate 58 – *continued*. Bimonthly fields for July-August 1987.

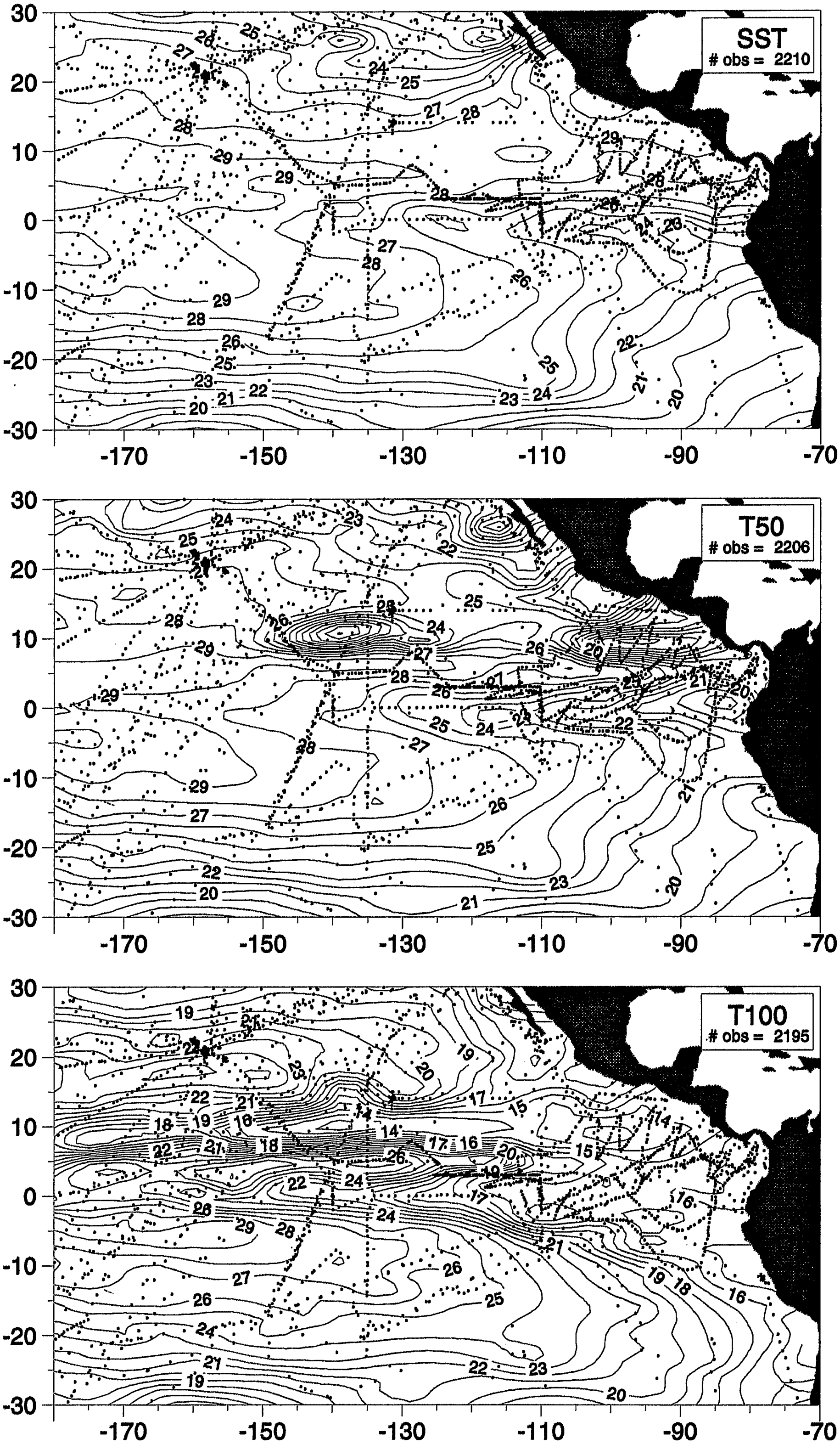

Plate 59. Bimonthly fields for September-October 1987.

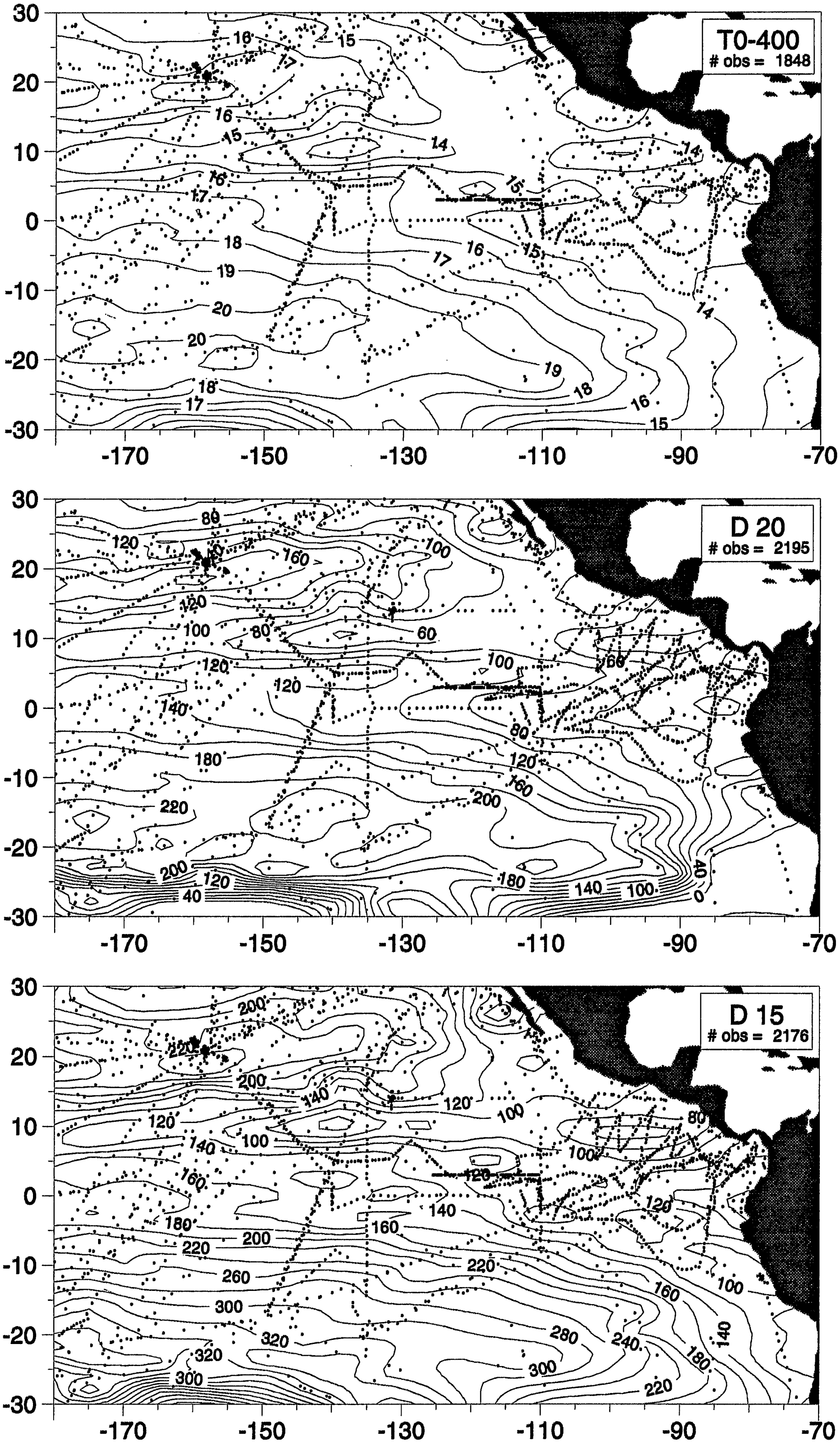

Plate 59 – *continued*. Bimonthly fields for September-October 1987.

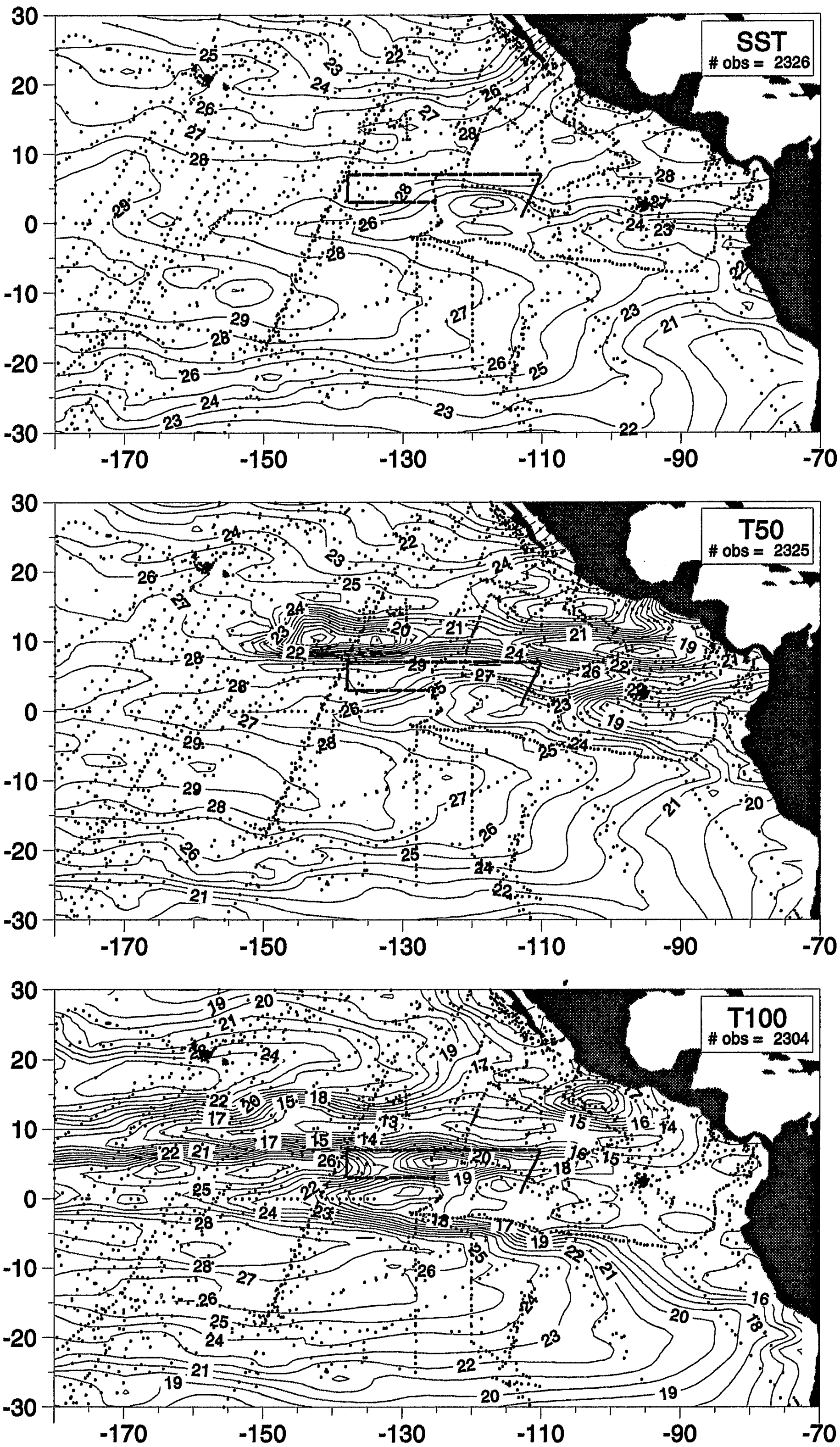

Plate 60. Bimonthly fields for November-December 1987.

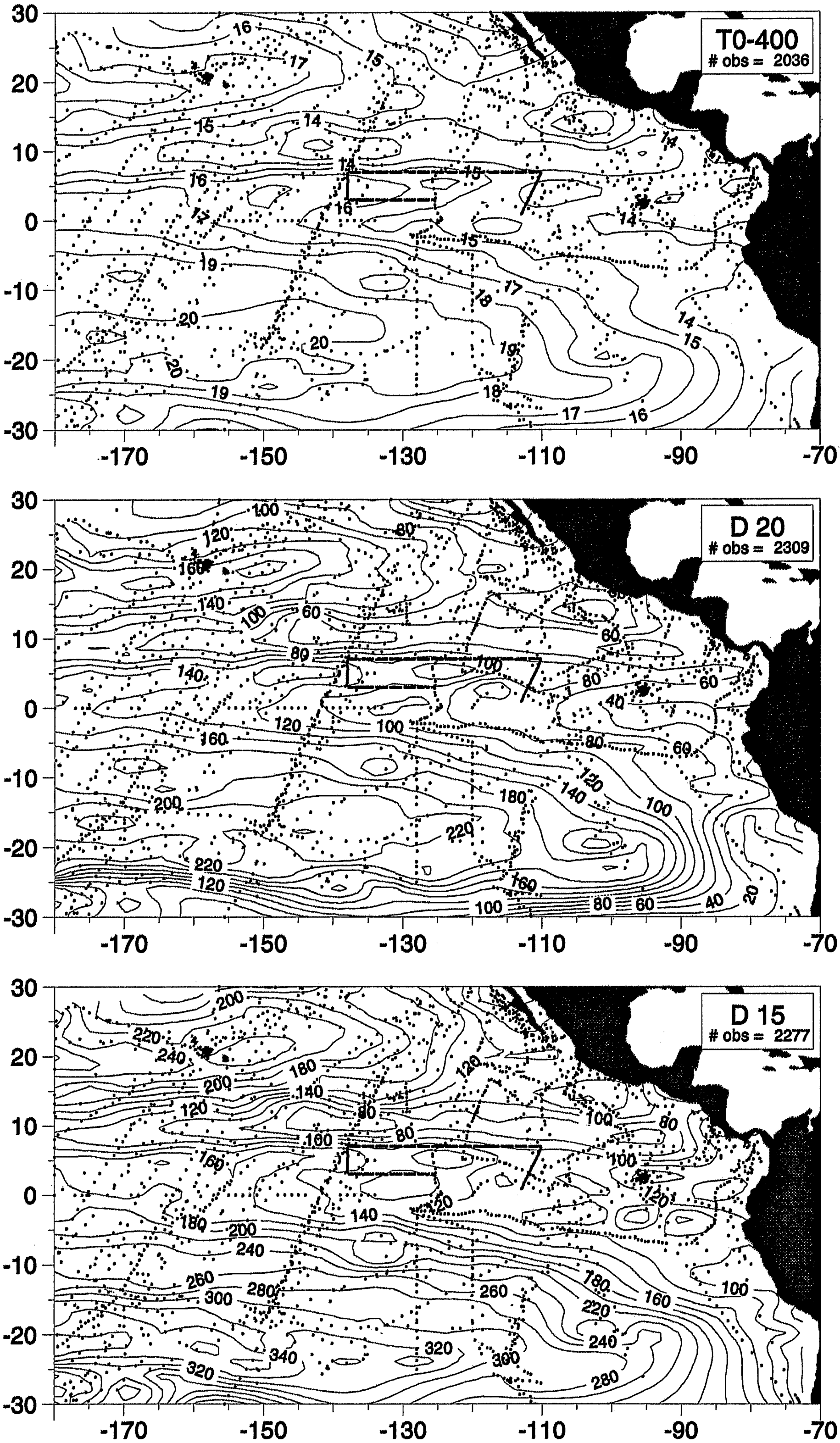

Plate 60 – *continued.* Bimonthly fields for November-December 1987.

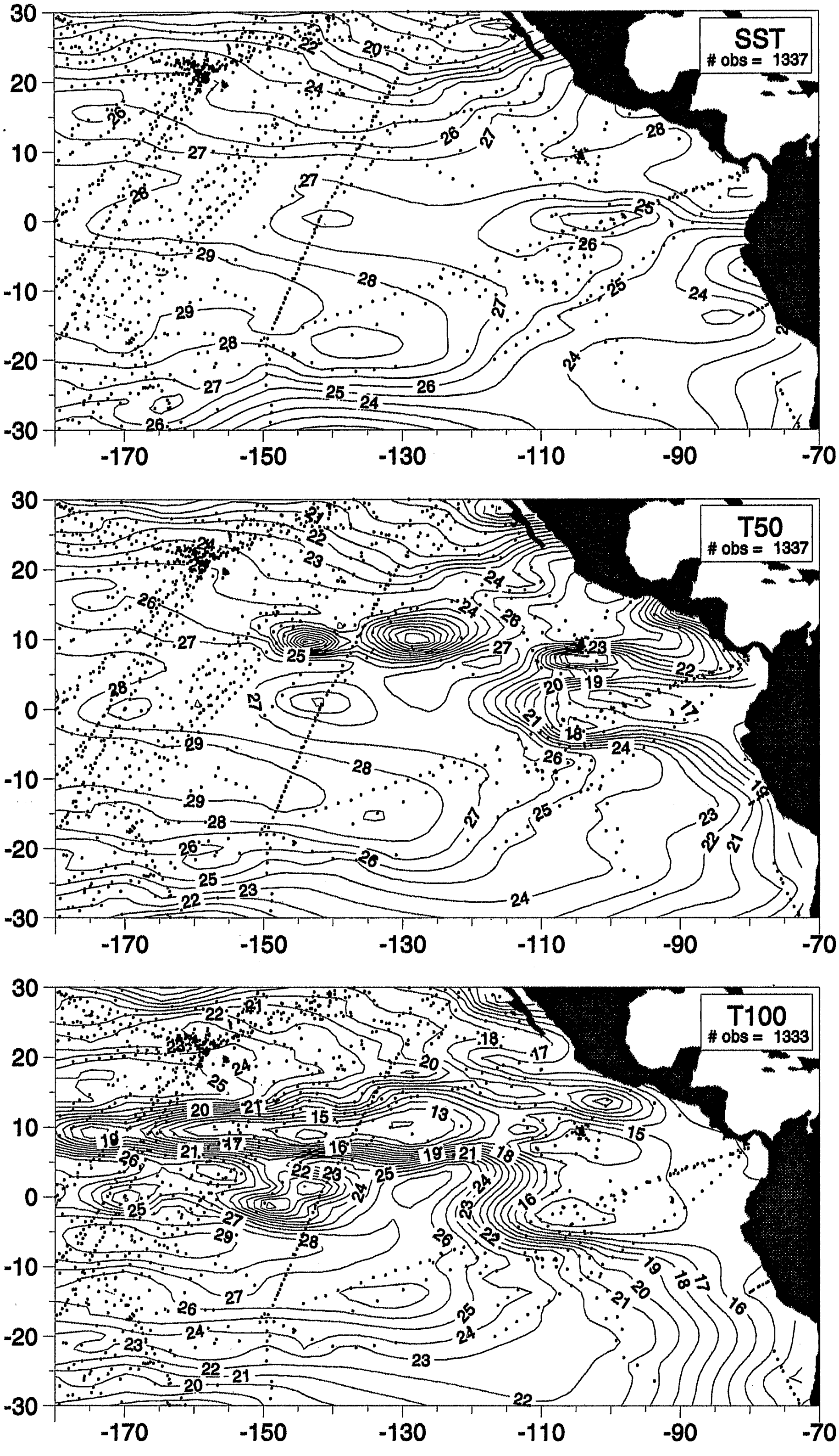

Plate 61. Bimonthly fields for January-February 1988.

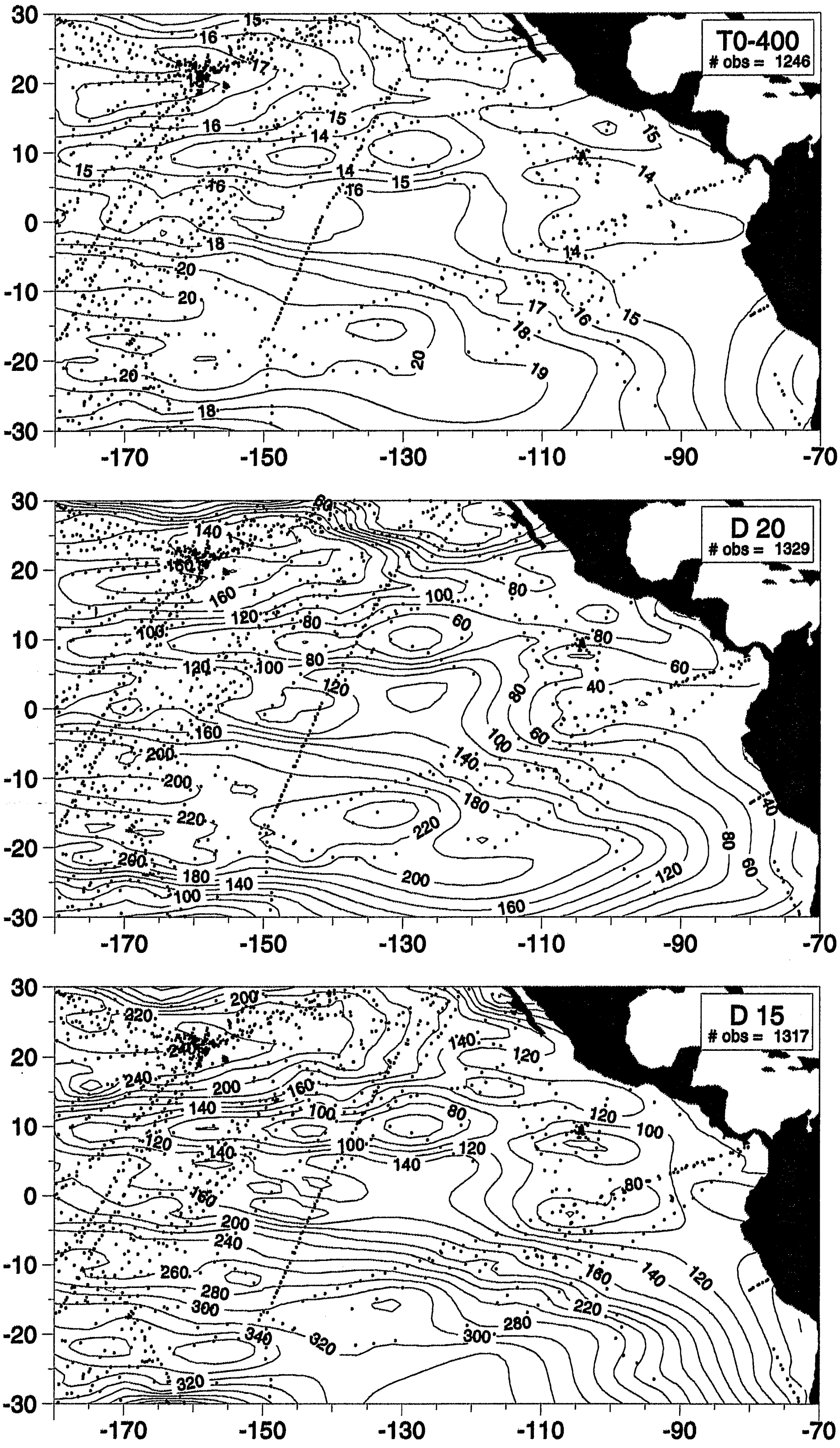

Plate 61 – *continued*. Bimonthly fields for January-February 1988.

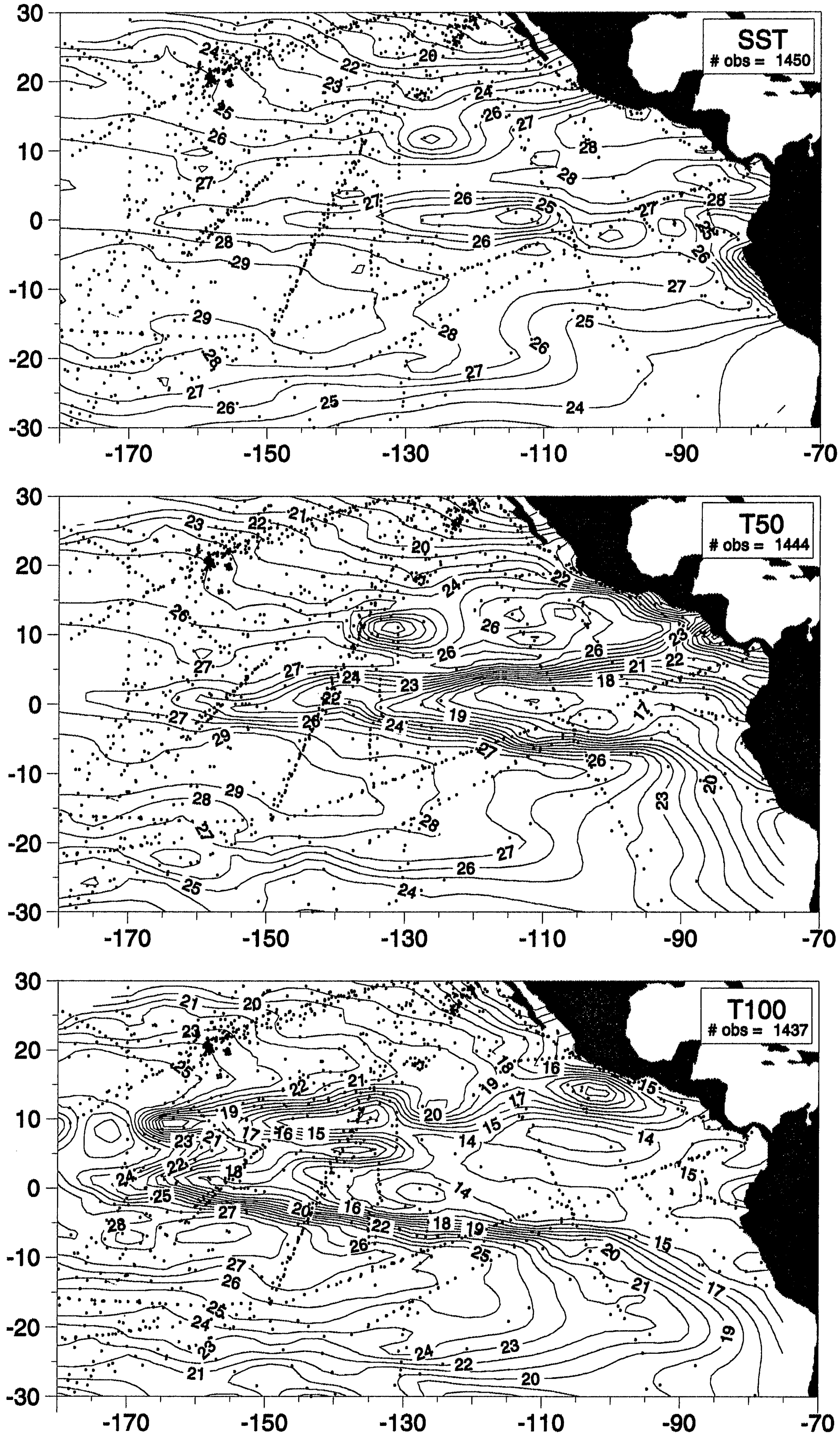

Plate 62. Bimonthly fields for March-April 1988.

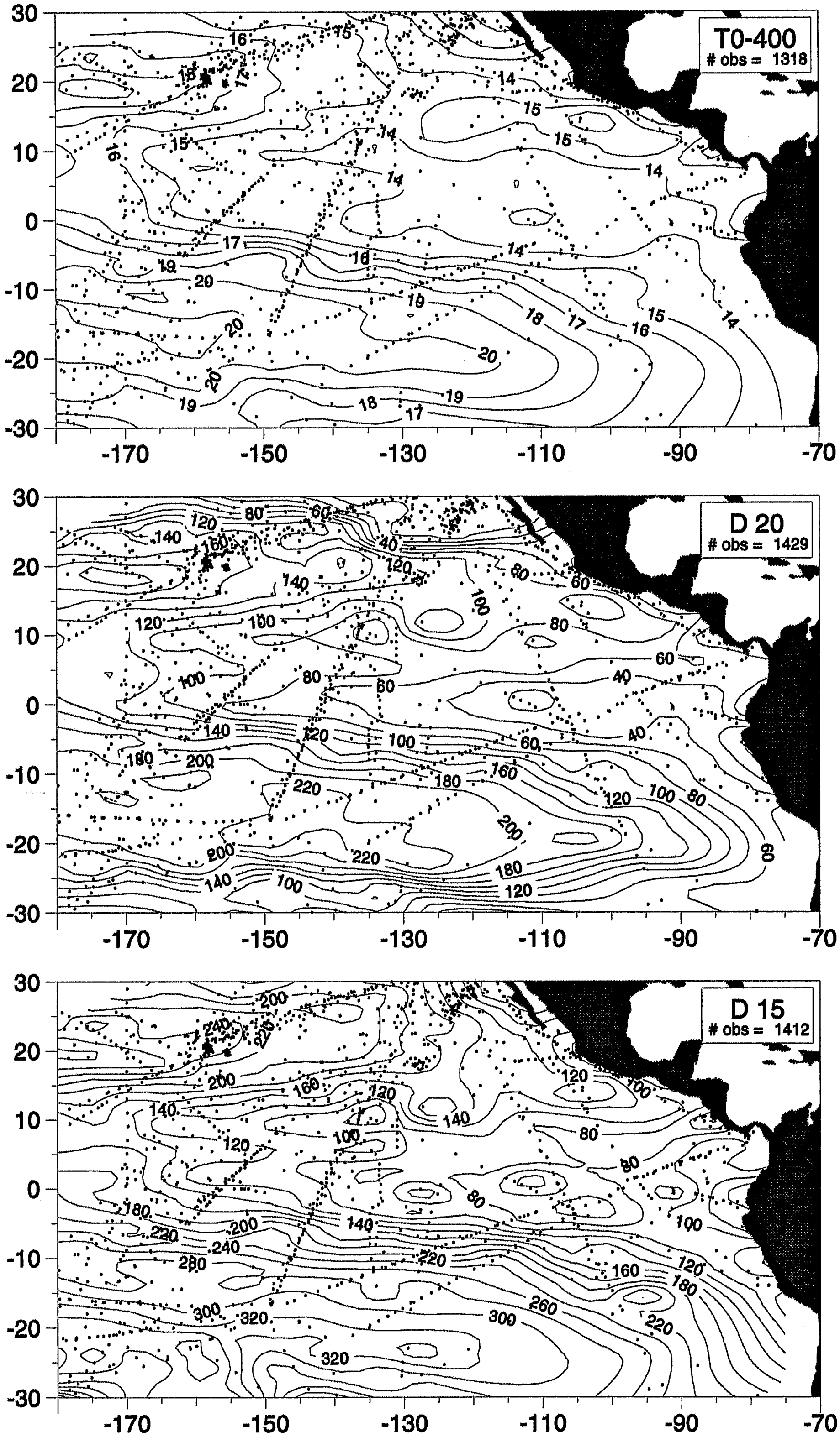

Plate 62 – *continued*. Bimonthly fields for March-April 1988.

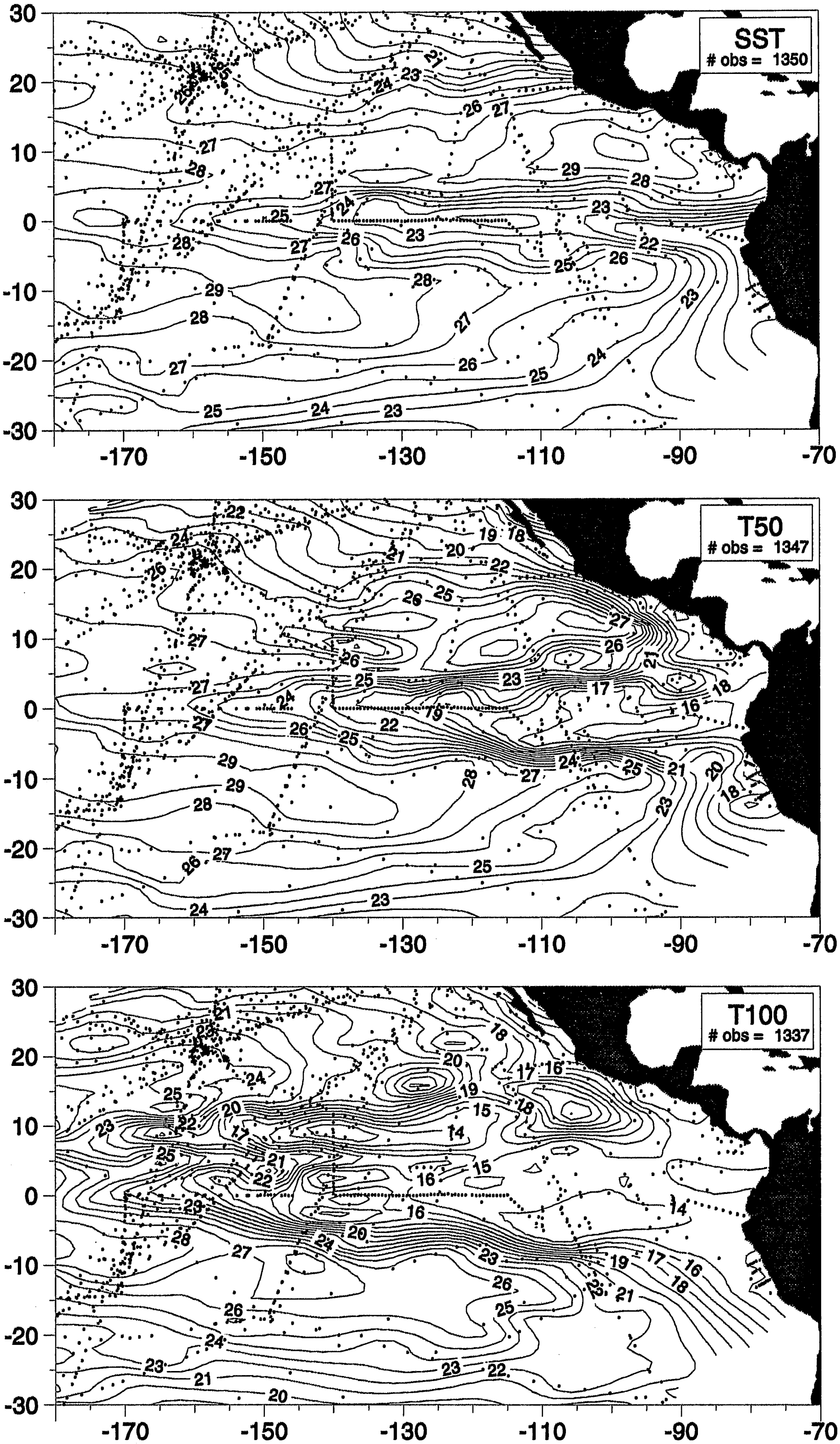

Plate 63. Bimonthly fields for May-June 1988.

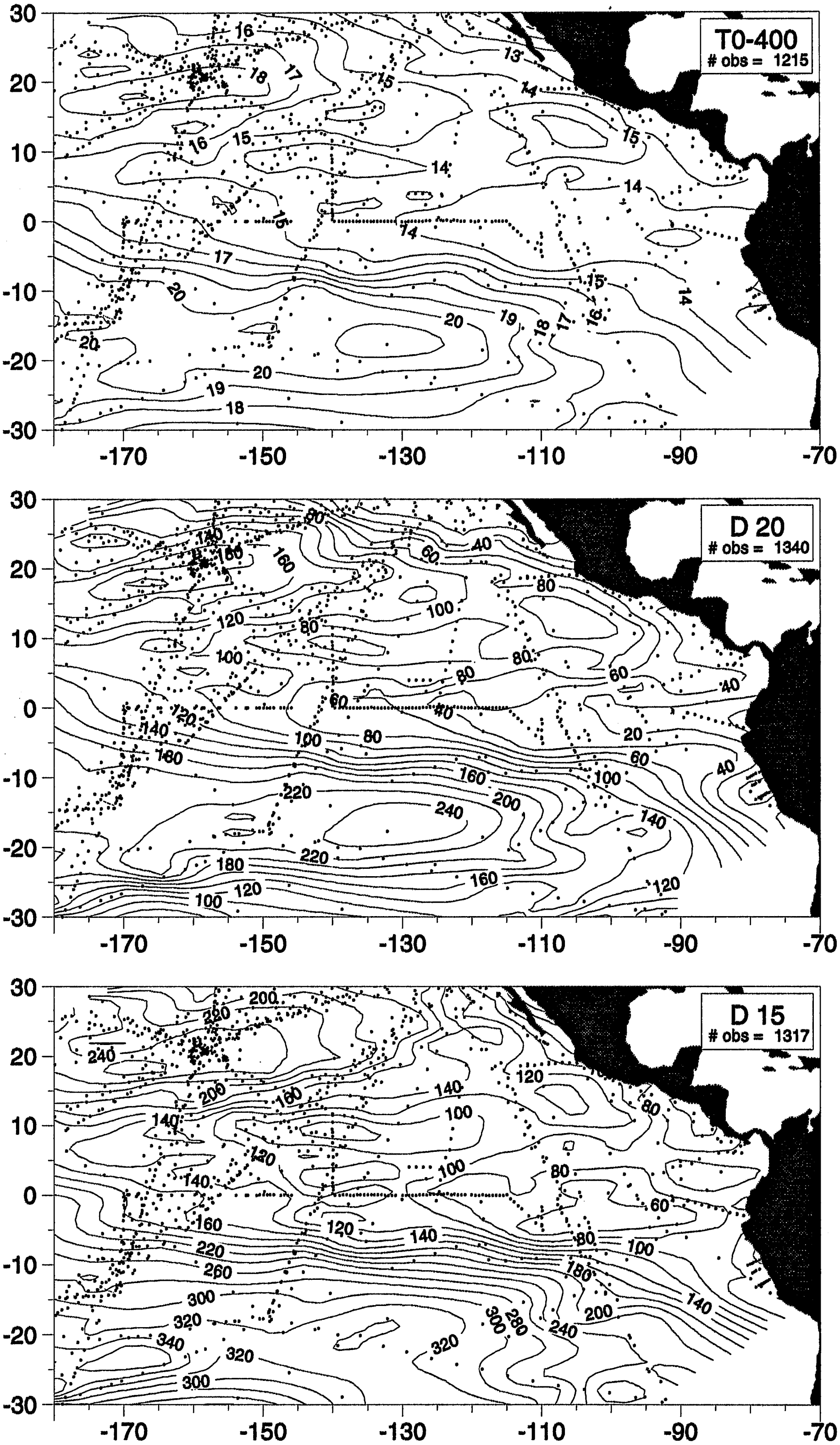

Plate 63 – *continued*. Bimonthly fields for May-June 1988.

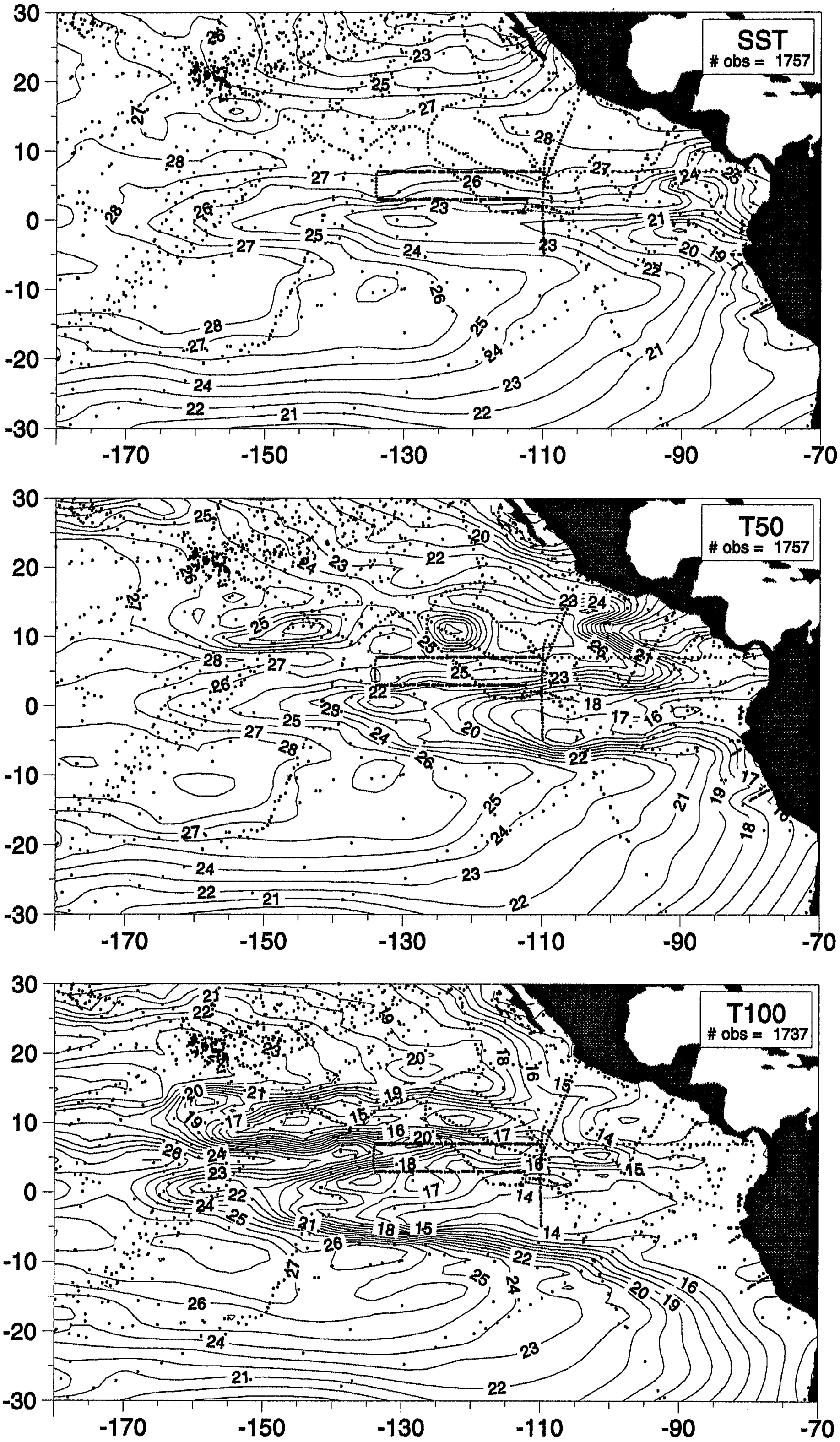

Plate 64. Bimonthly fields for July-August 1988.

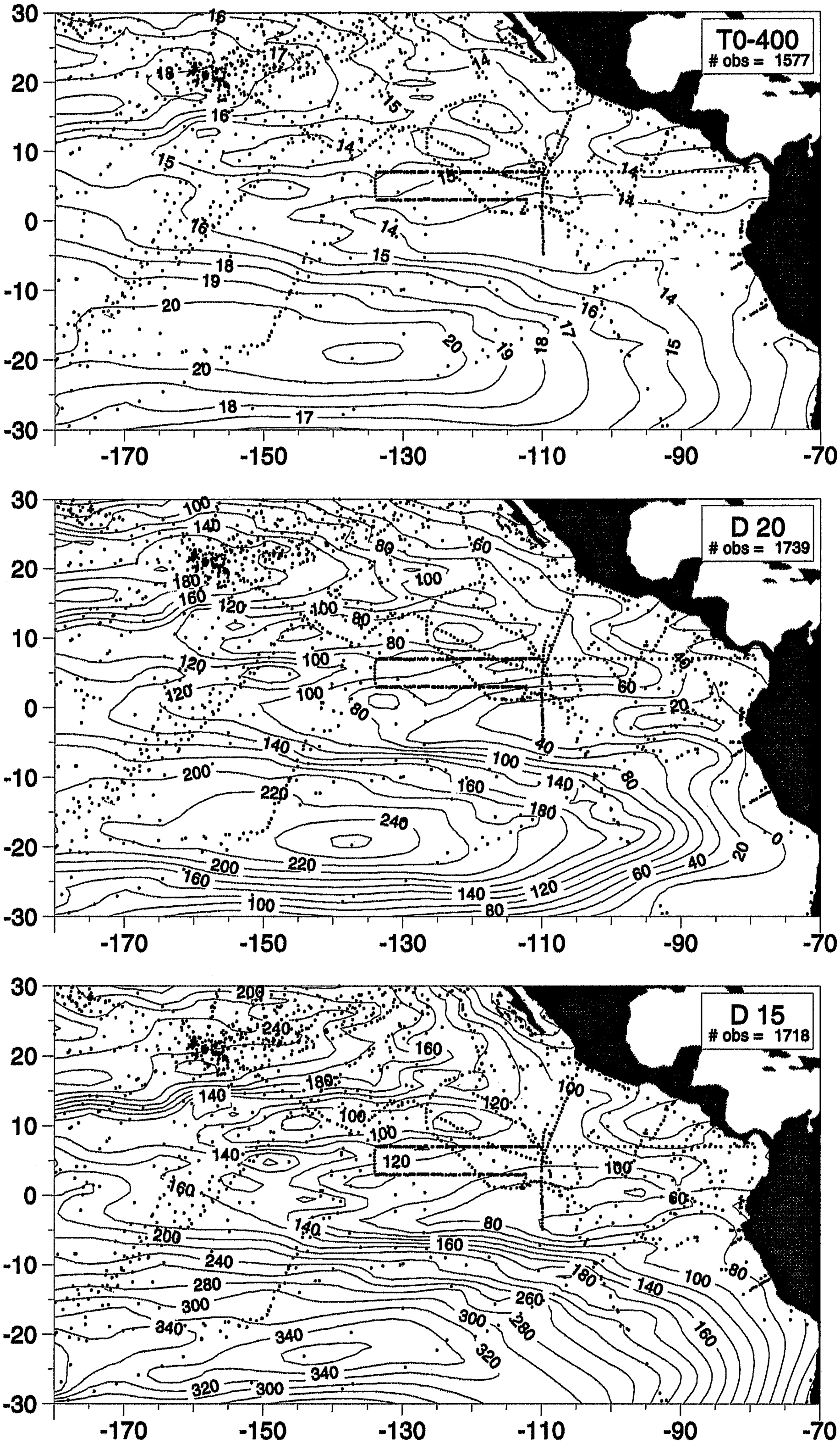

Plate 64 – *continued.* Bimonthly fields for July-August 1988.

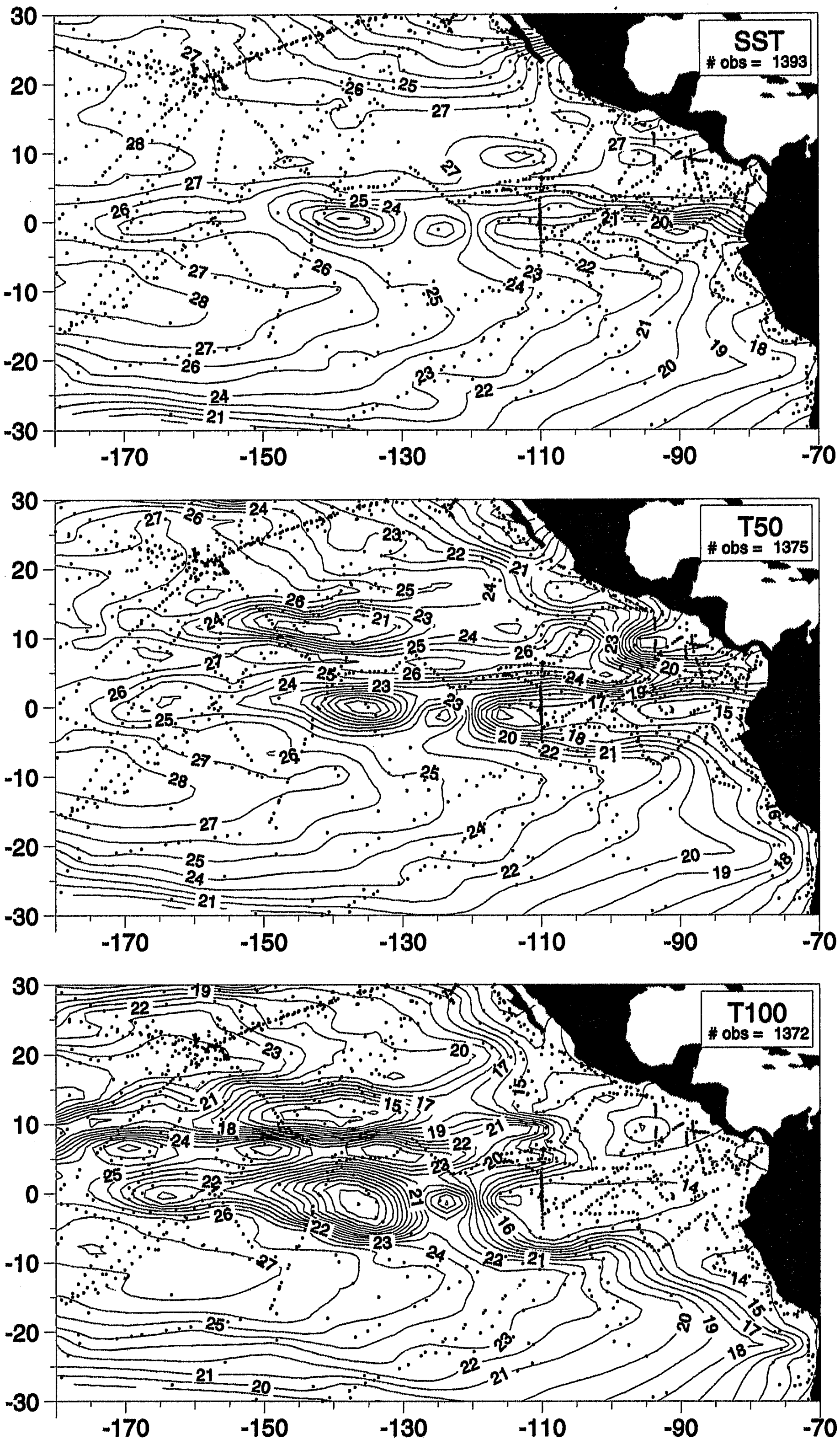

Plate 65. Bimonthly fields for September-October 1988.

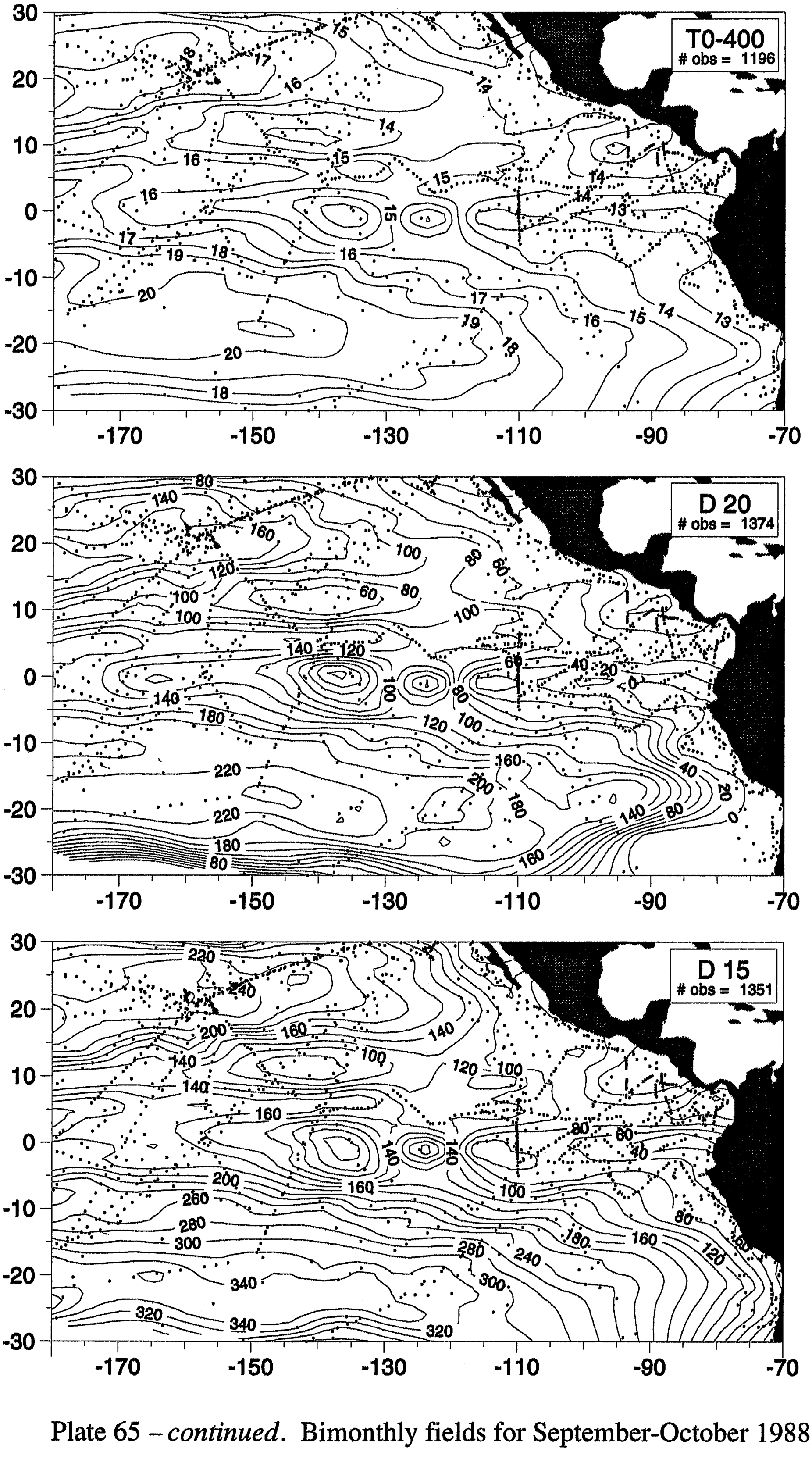

Plate 65 – *continued*. Bimonthly fields for September-October 1988.

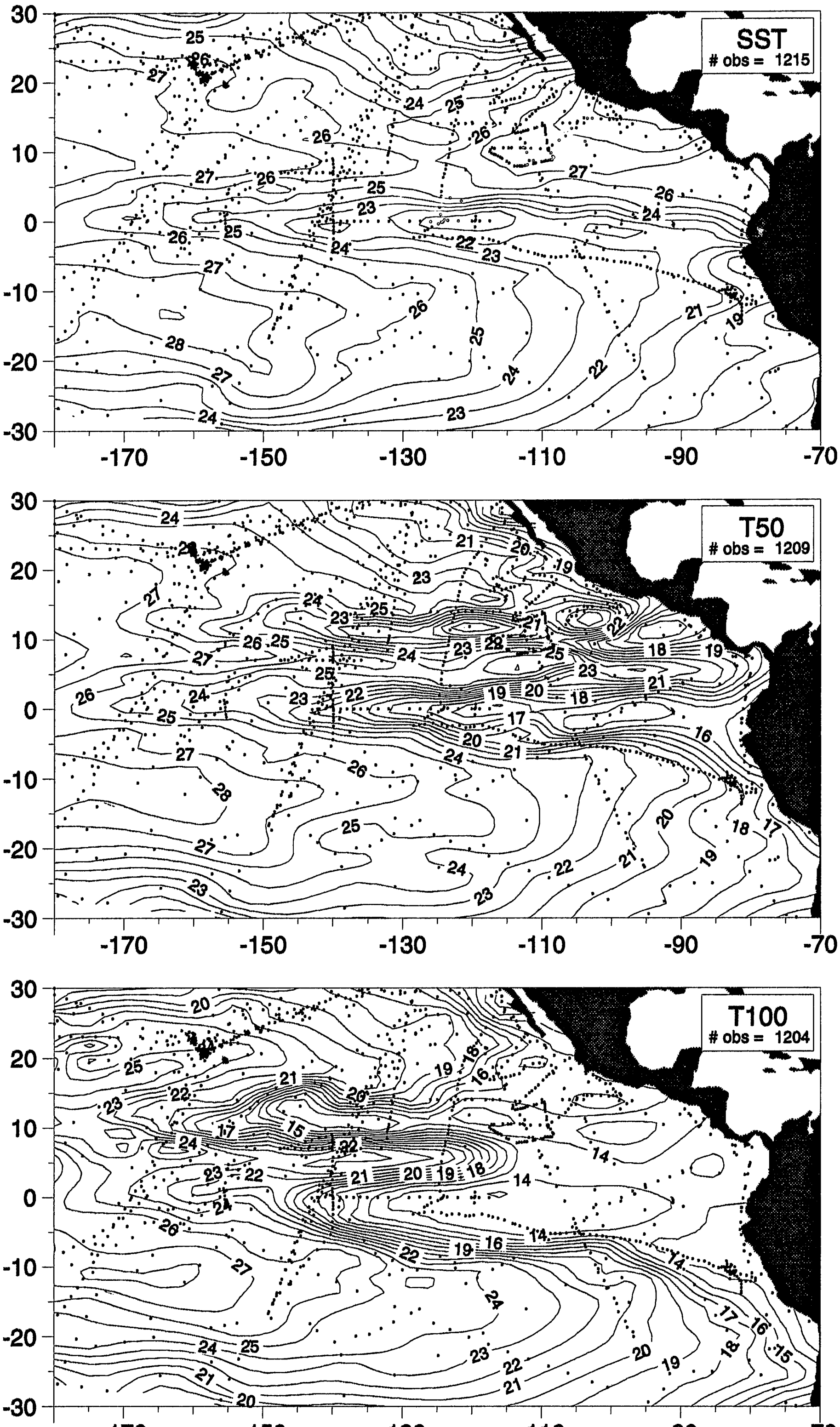

Plate 66. Bimonthly fields for November-December 1988.

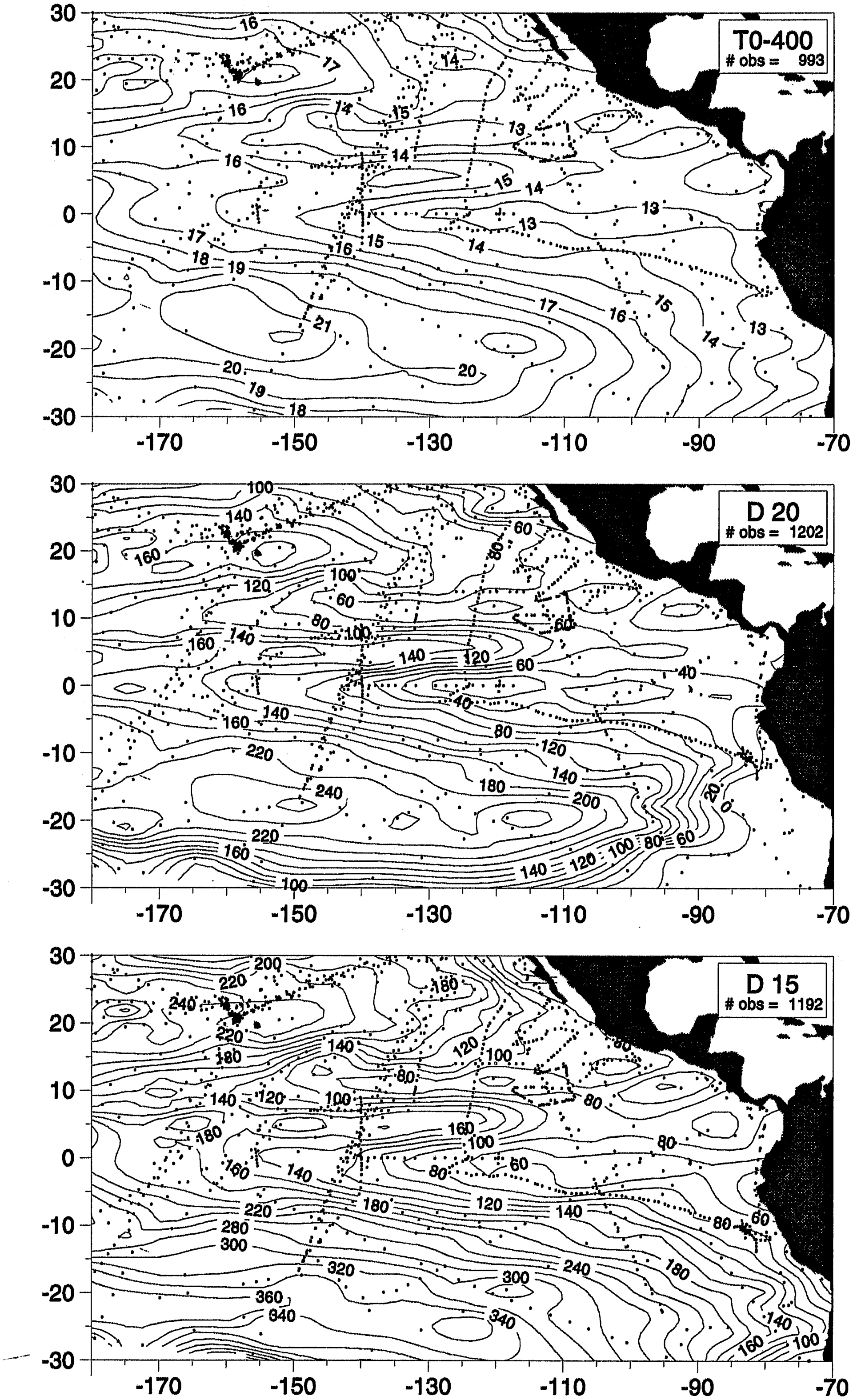

Plate 66 – *continued.* Bimonthly fields for November-December 1988.

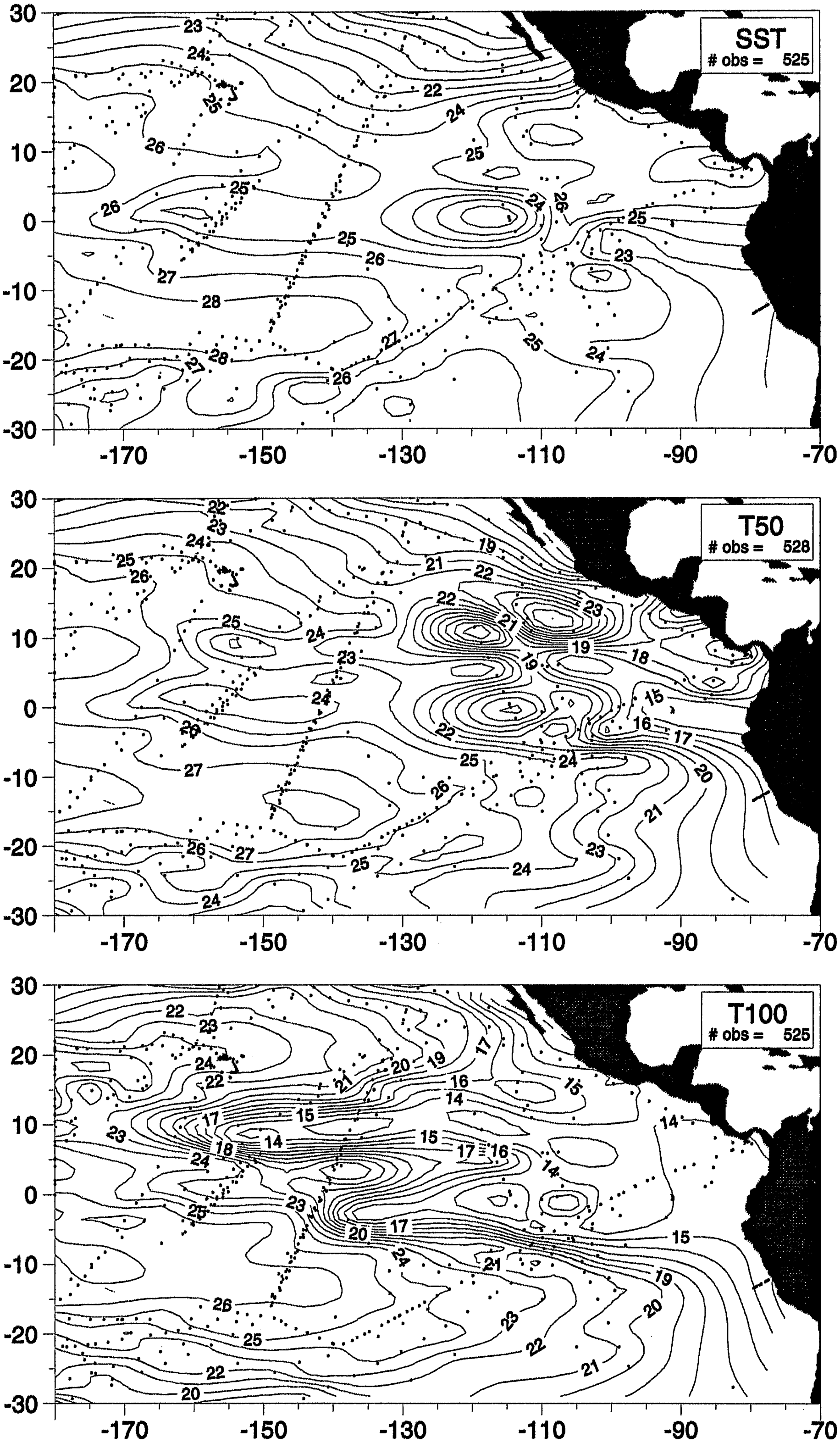

Plate 67. Bimonthly fields for January-February 1989.

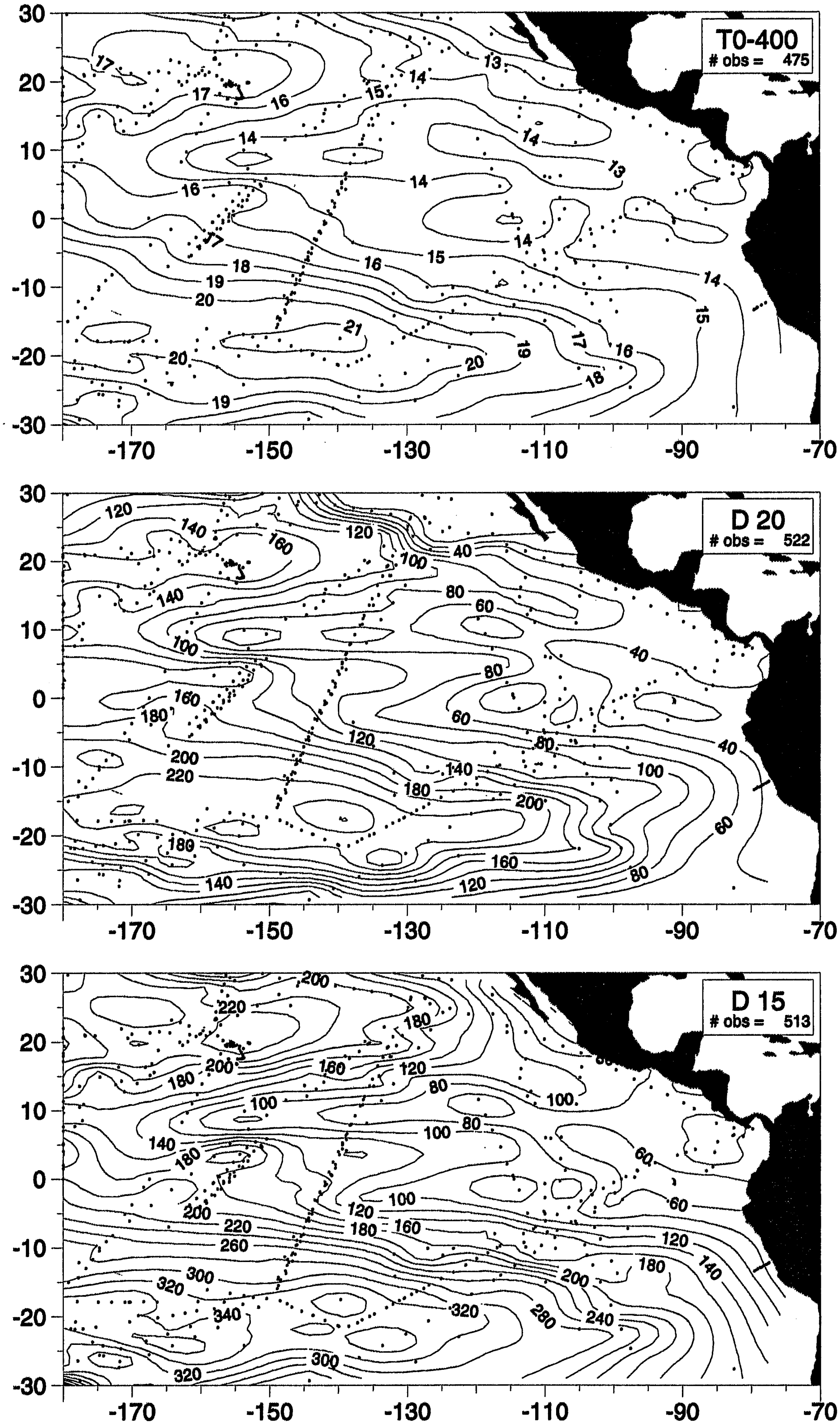

Plate 67 – *continued*. Bimonthly fields for January-February 1989.

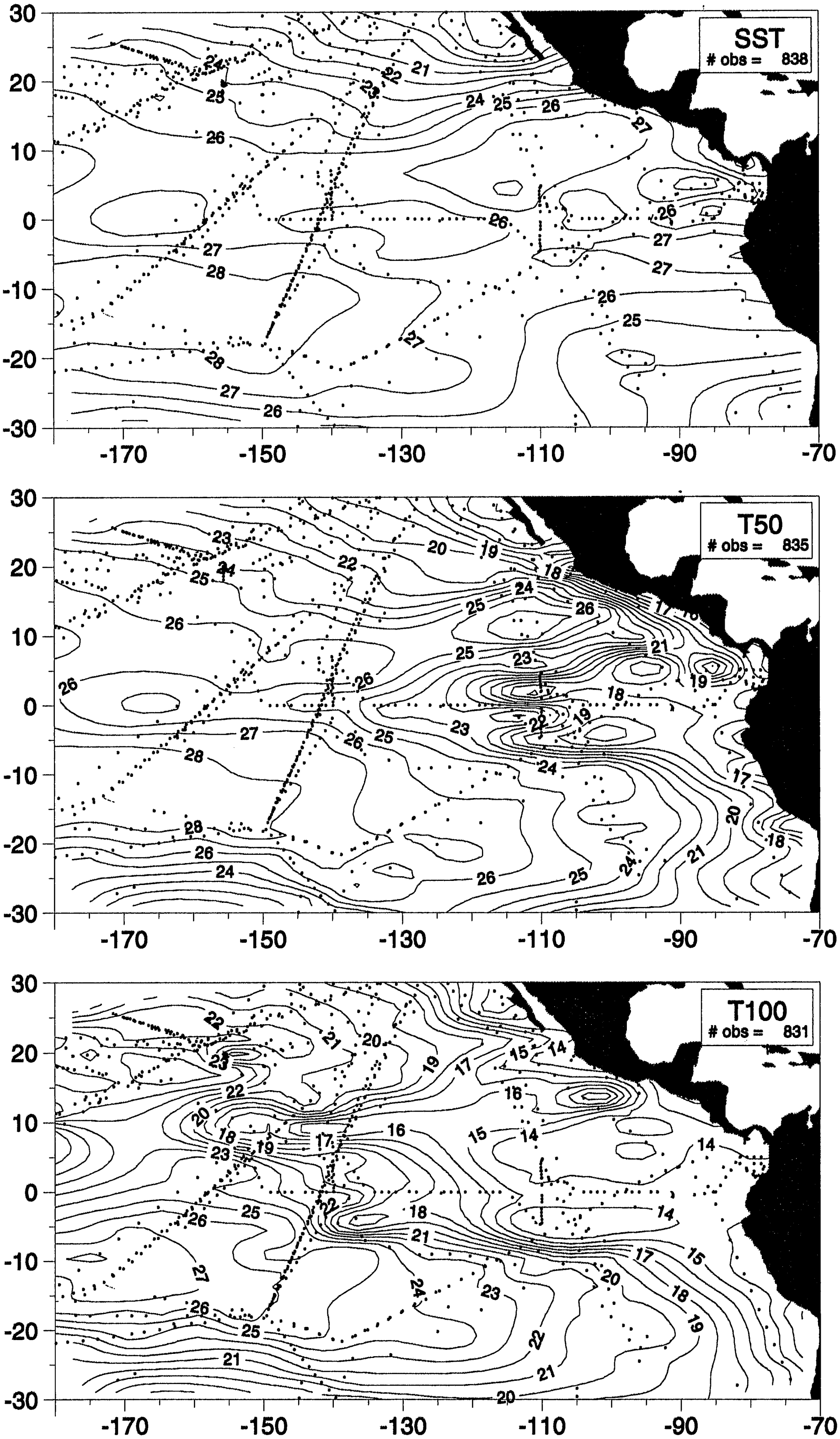

Plate 68. Bimonthly fields for March-April 1989.

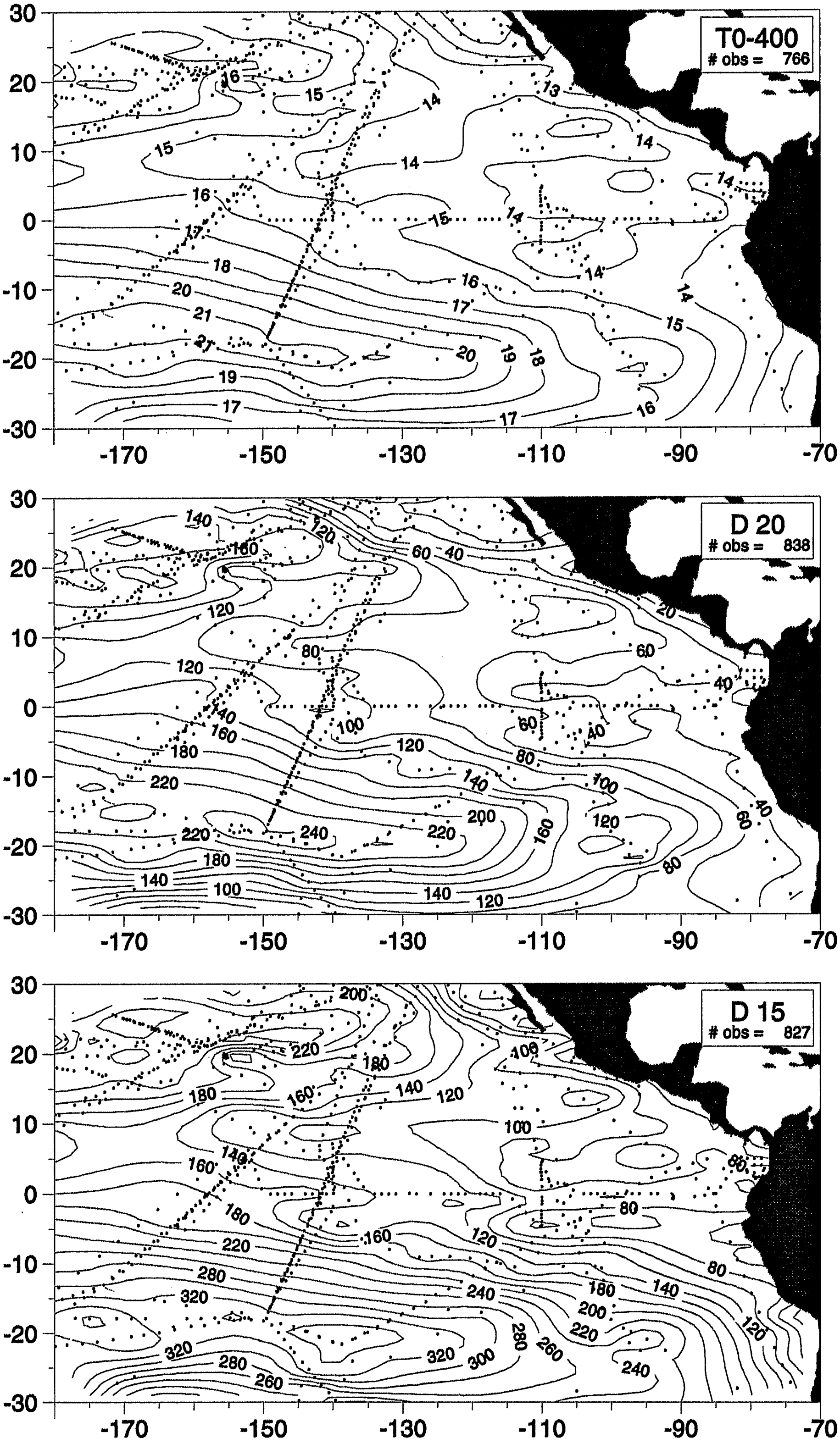

Plate 68 – *continued*. Bimonthly fields for March-April 1989.

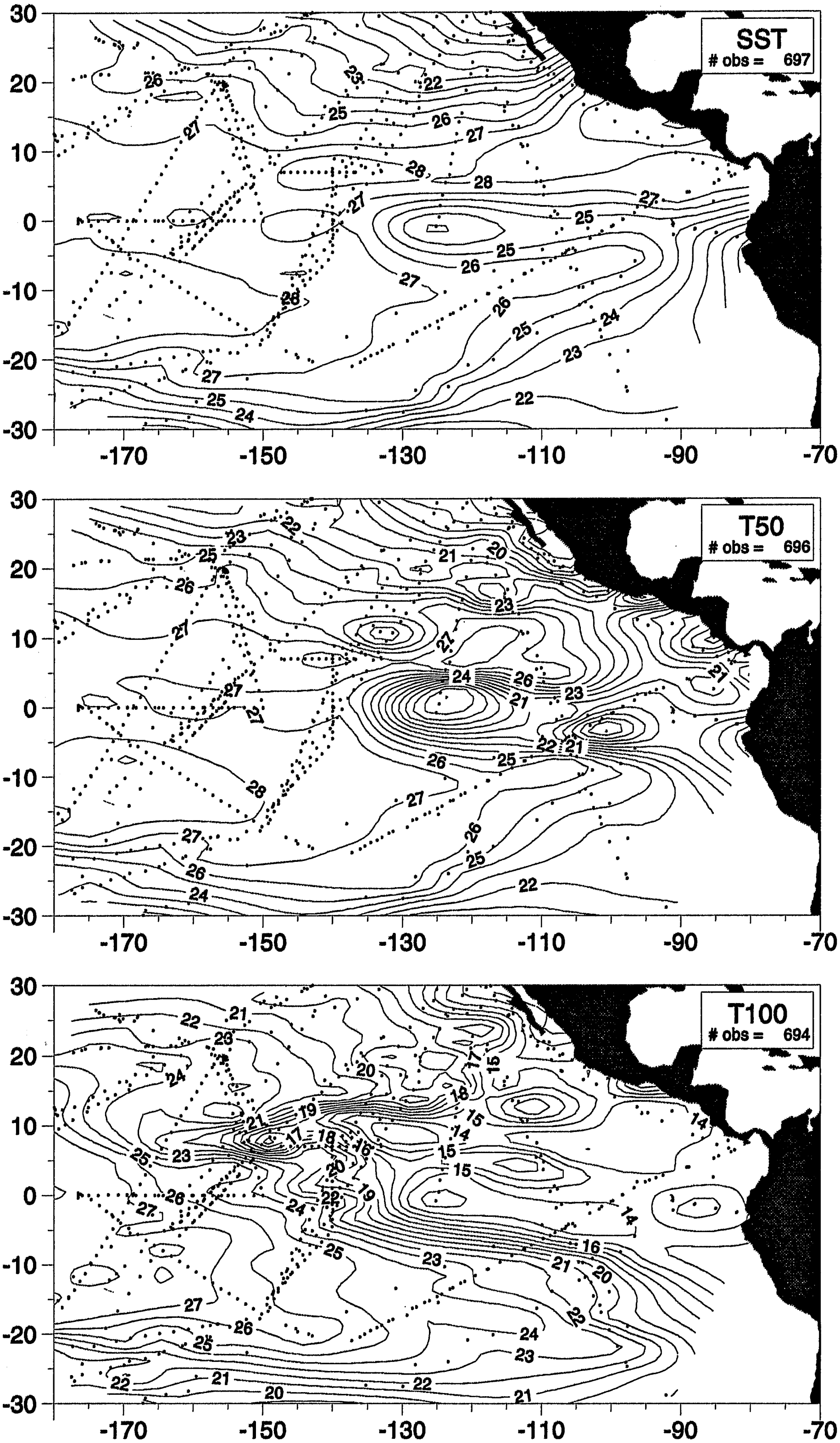

Plate 69. Bimonthly fields for May-June 1989.

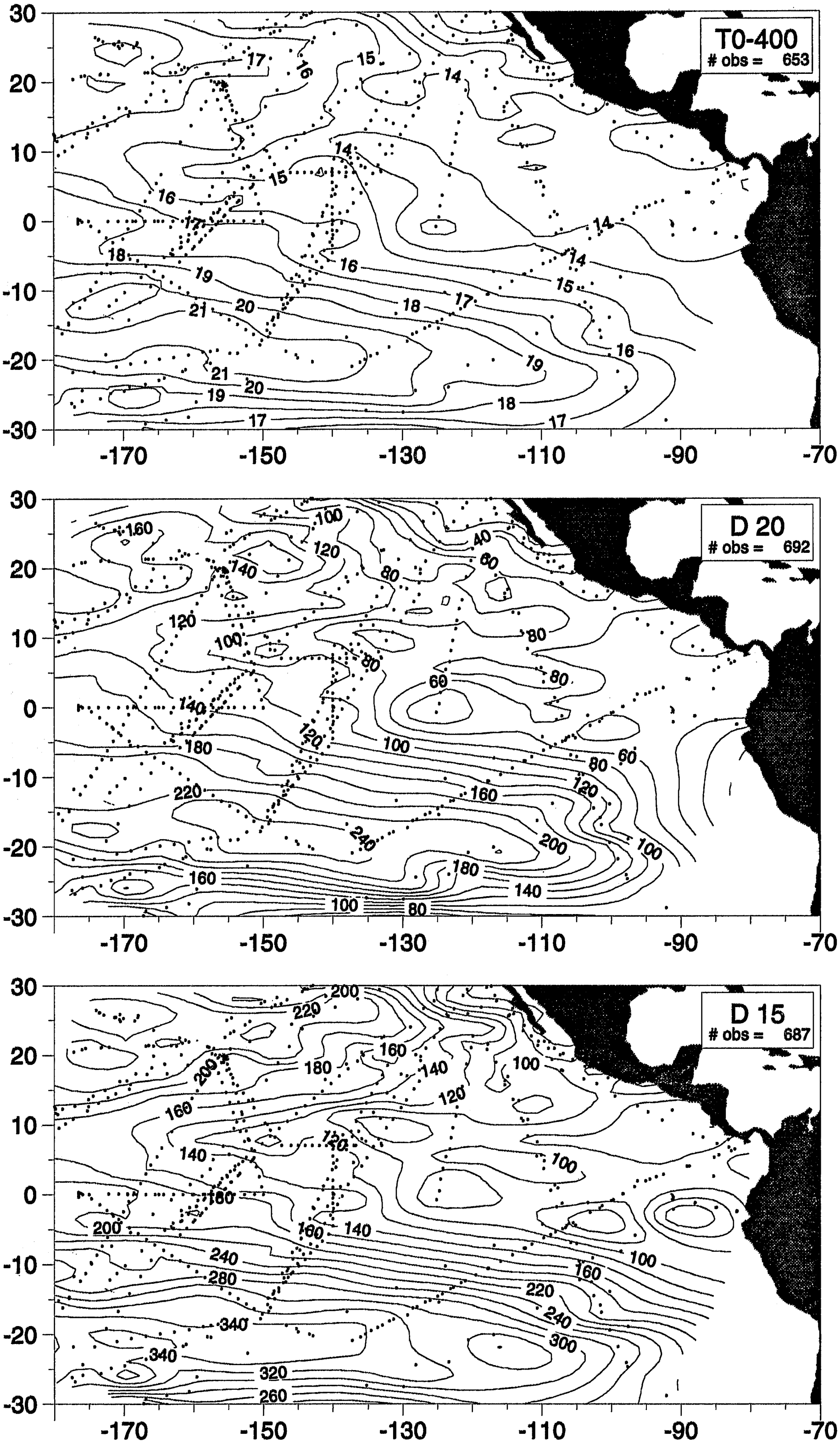

Plate 69 – *continued*. Bimonthly fields for May-June 1989.

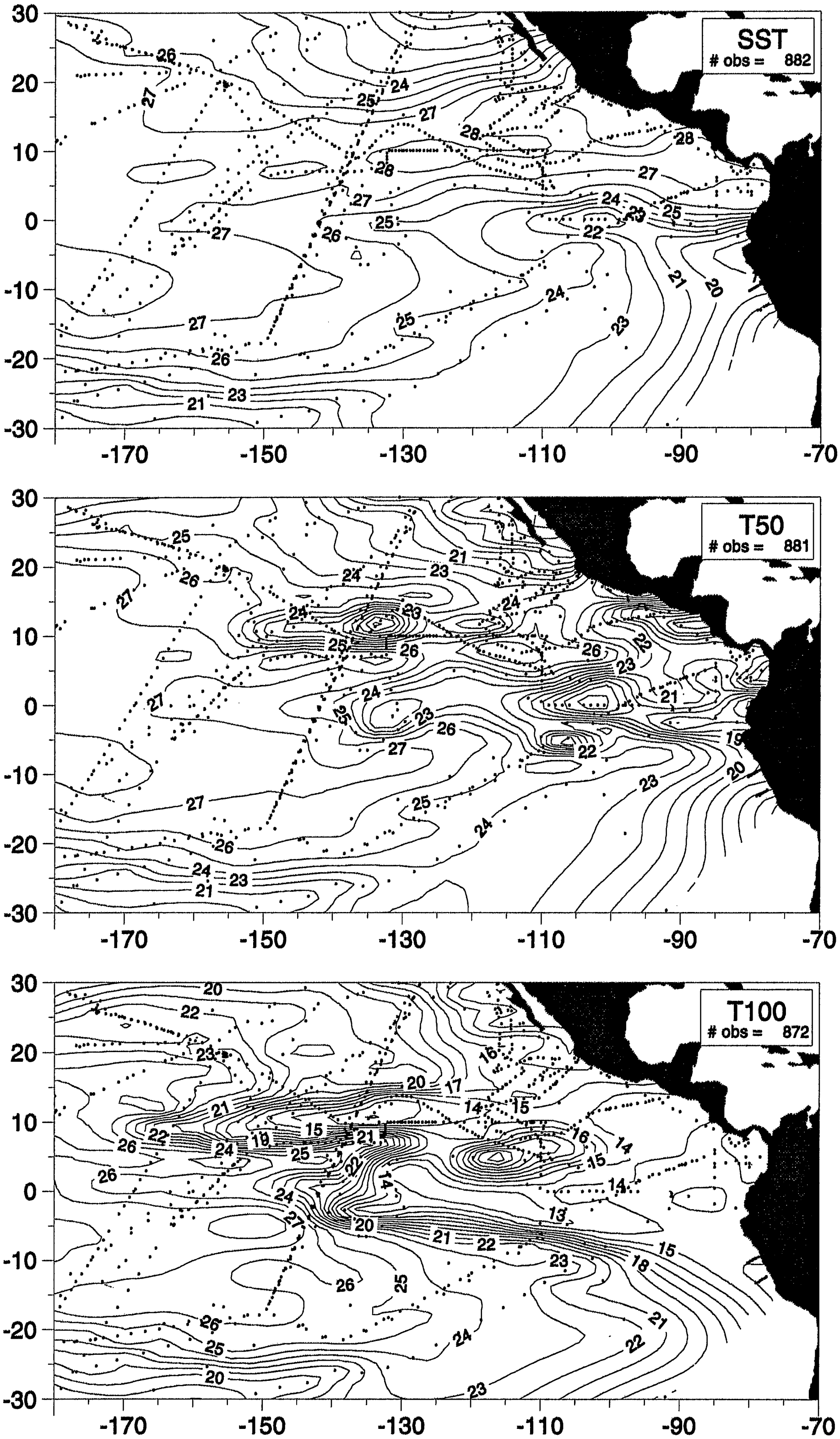

Plate 70. Bimonthly fields for July-August 1989.

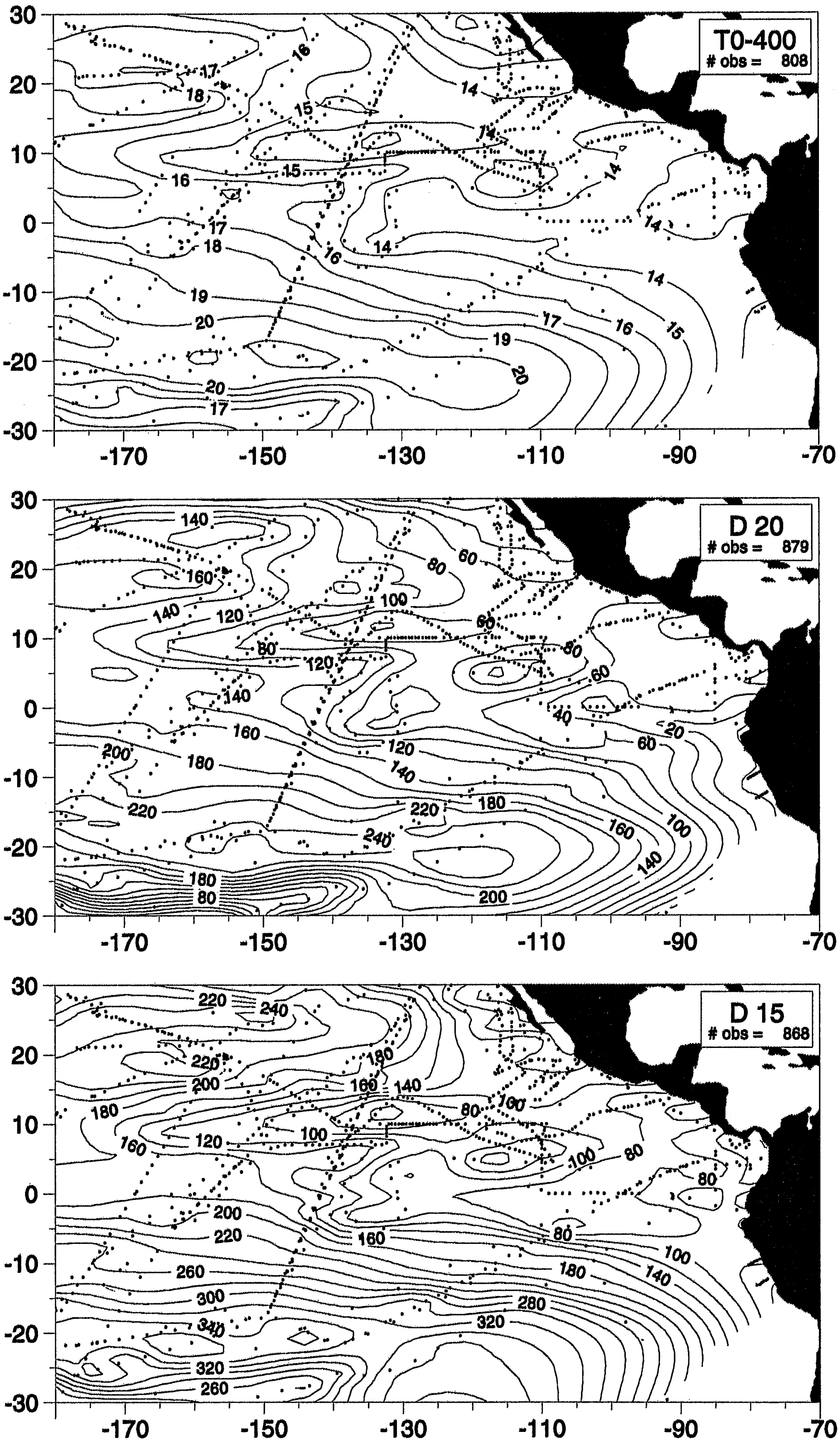

Plate 70 – *continued*. Bimonthly fields for July-August 1989.

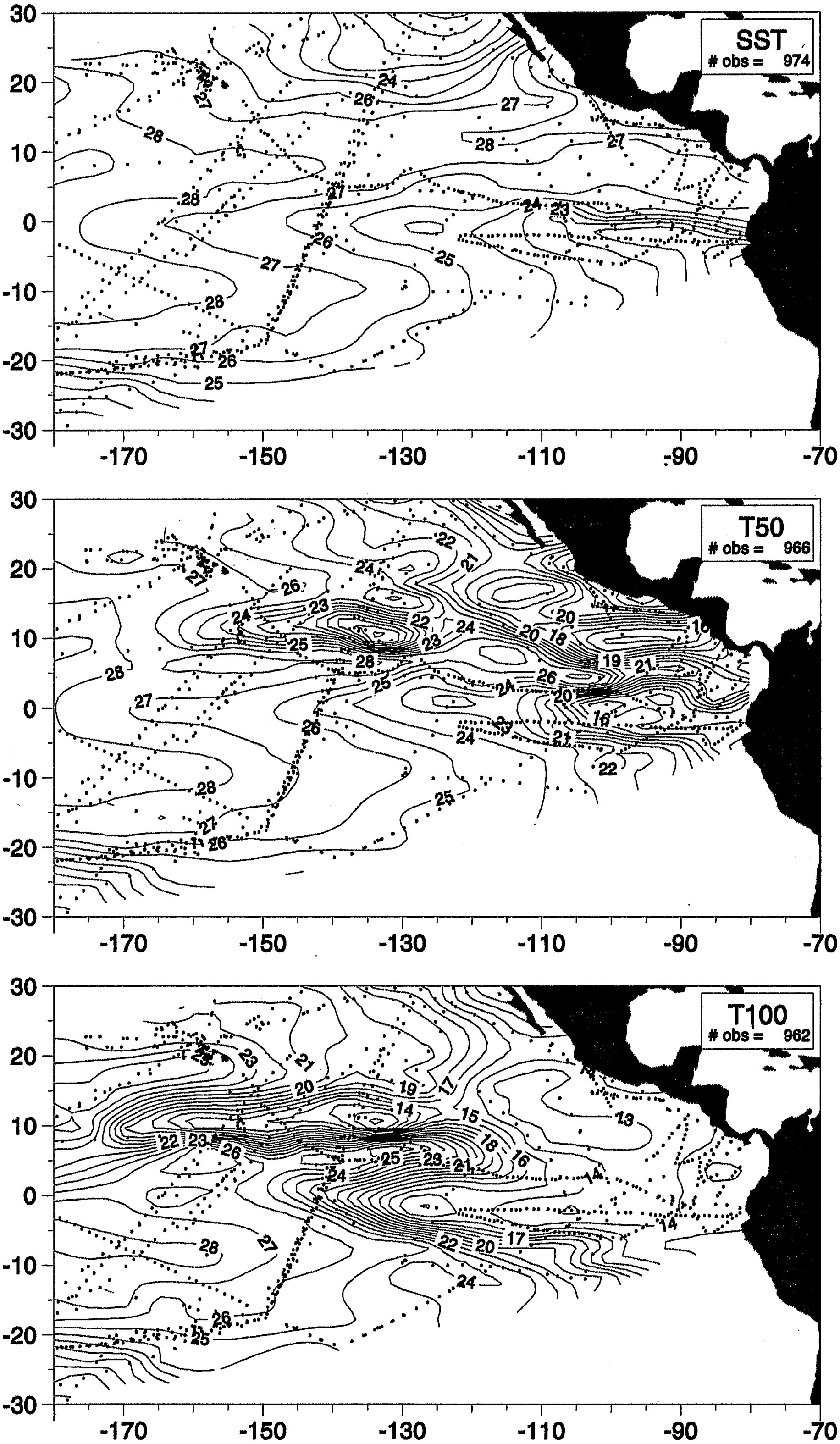

Plate 71. Bimonthly fields for September-October 1989.

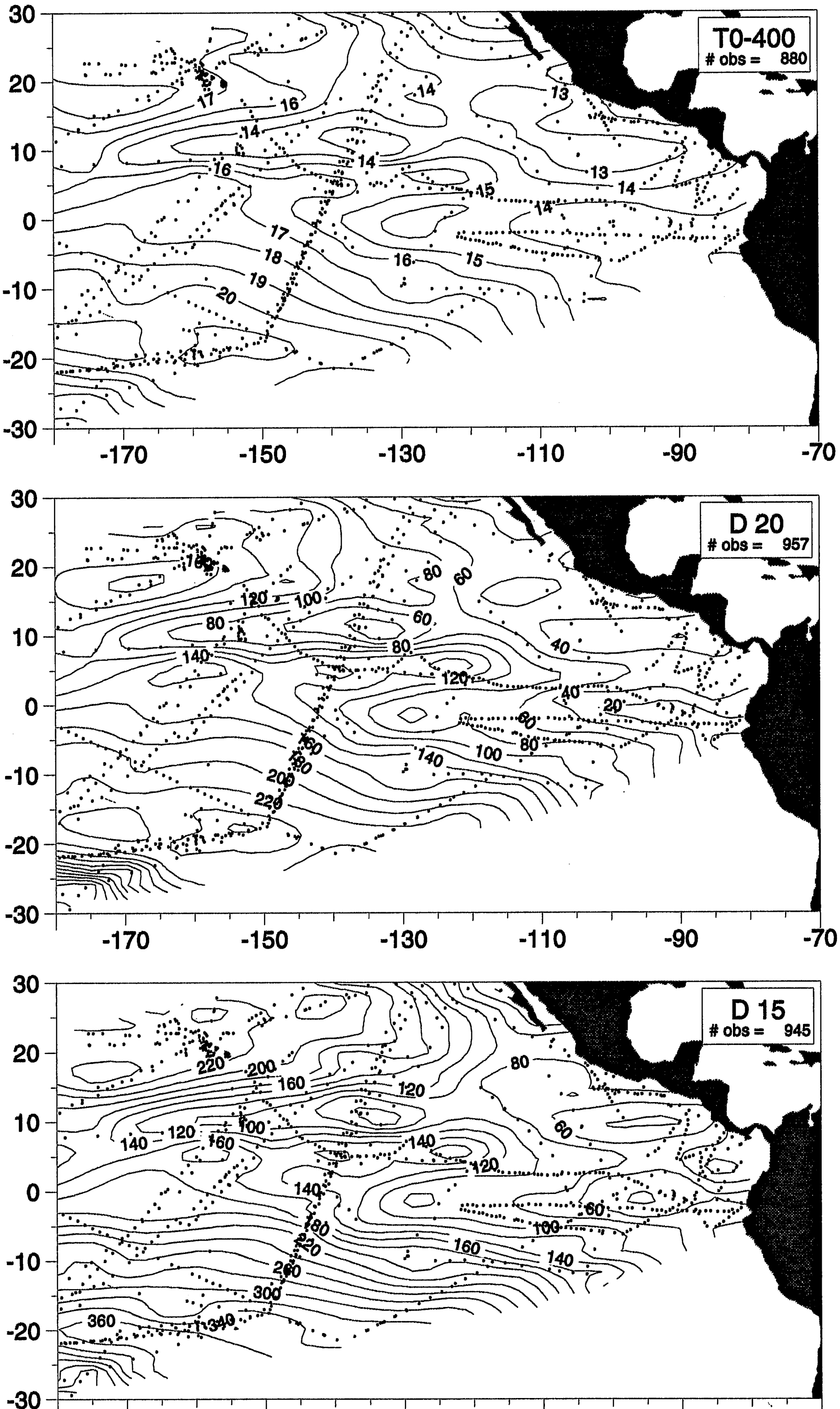

Plate 71 – *continued*. Bimonthly fields for September-October 1989.

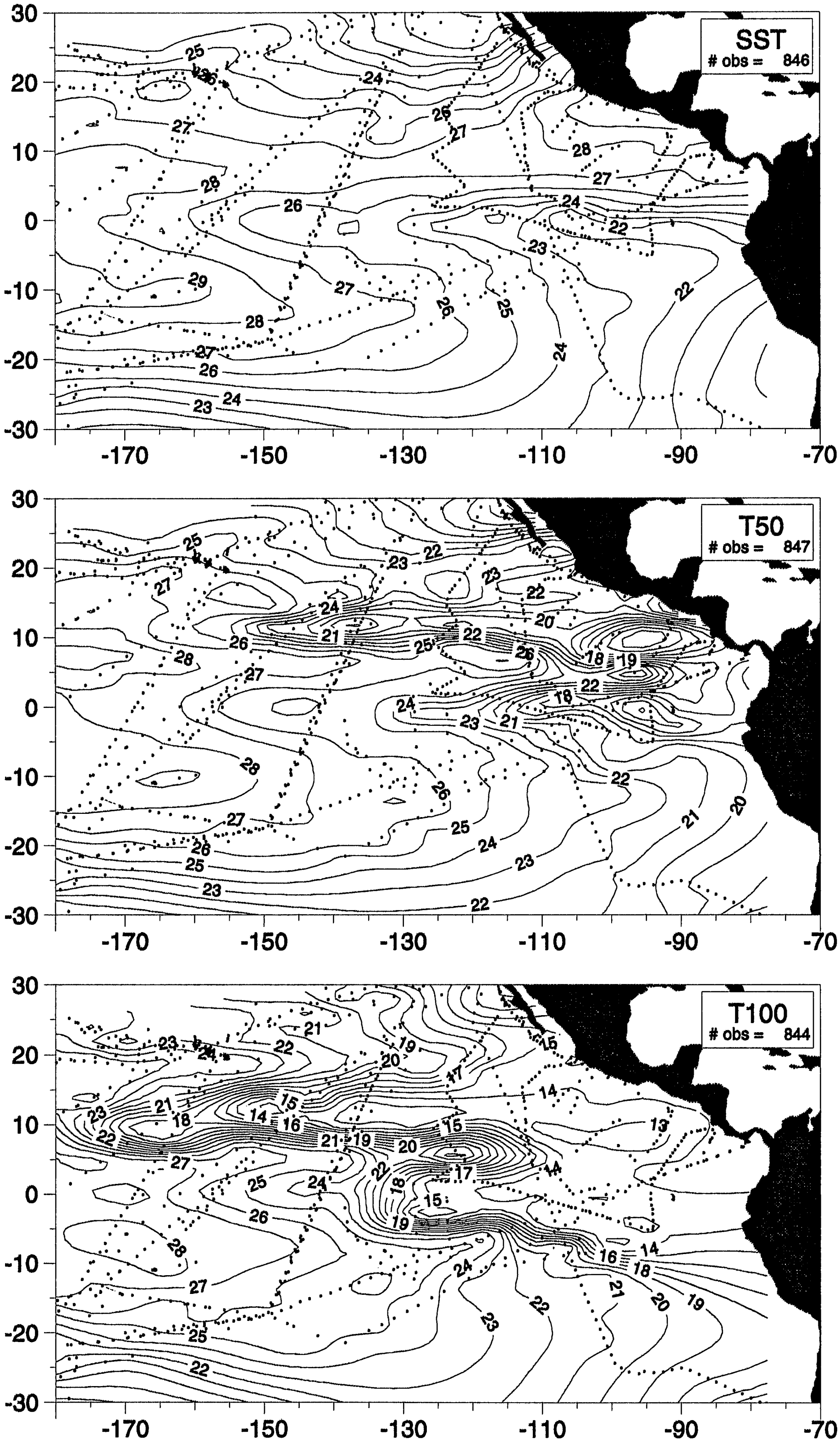

Plate 72. Bimonthly fields for November-December 1989.

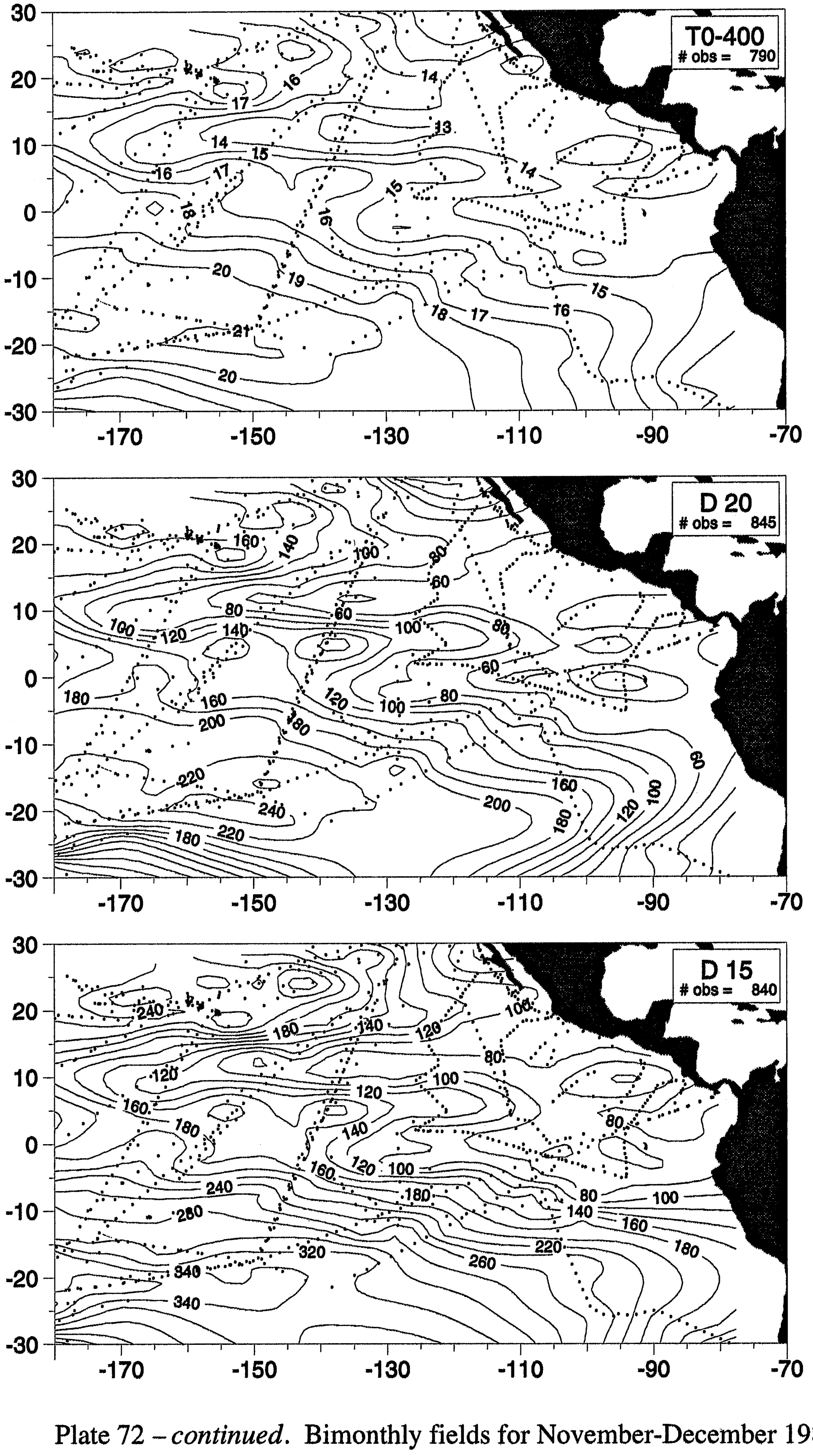

Plate 72 – *continued*. Bimonthly fields for November-December 1989.

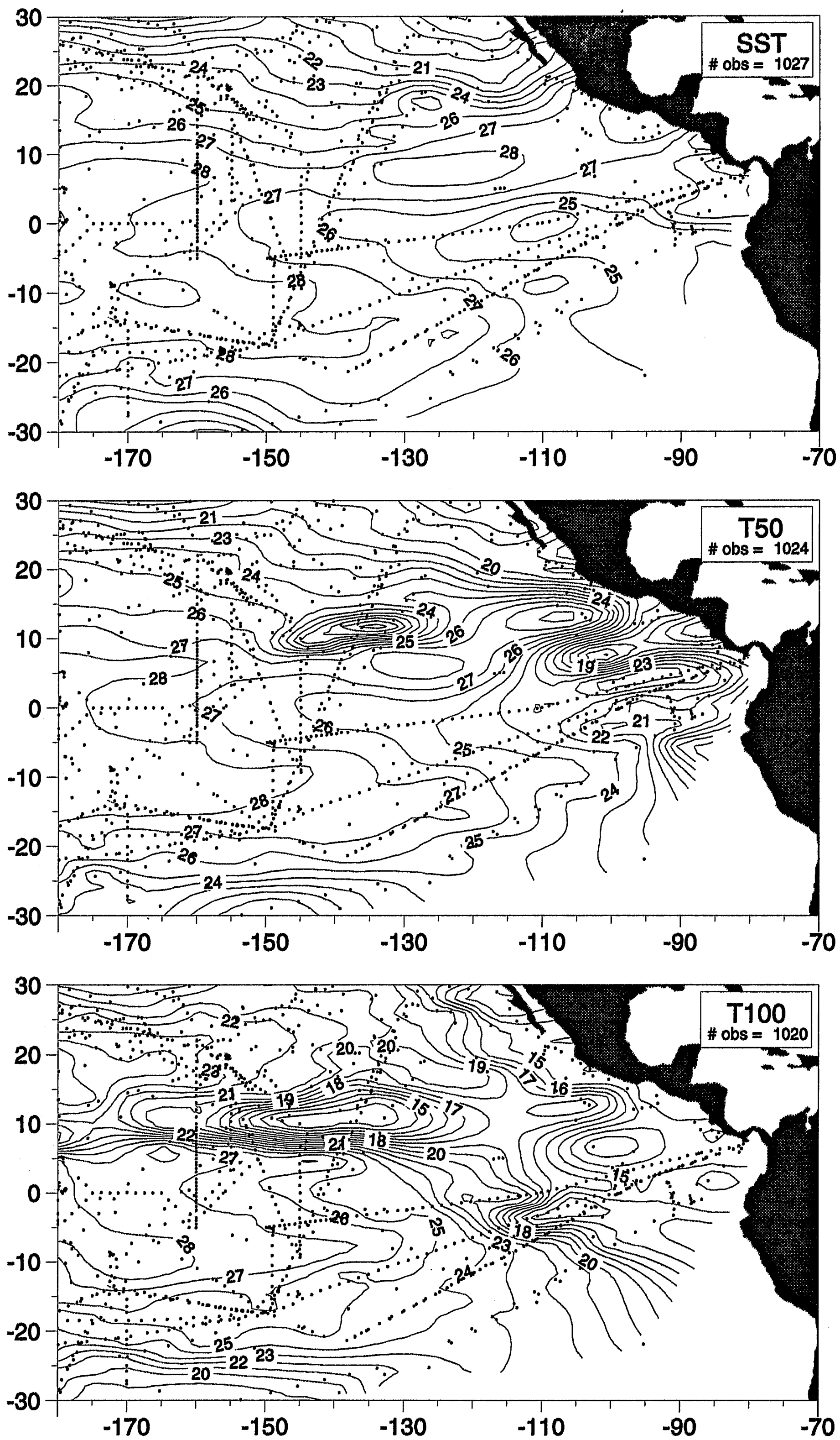

Plate 73. Bimonthly fields for January-February 1990.

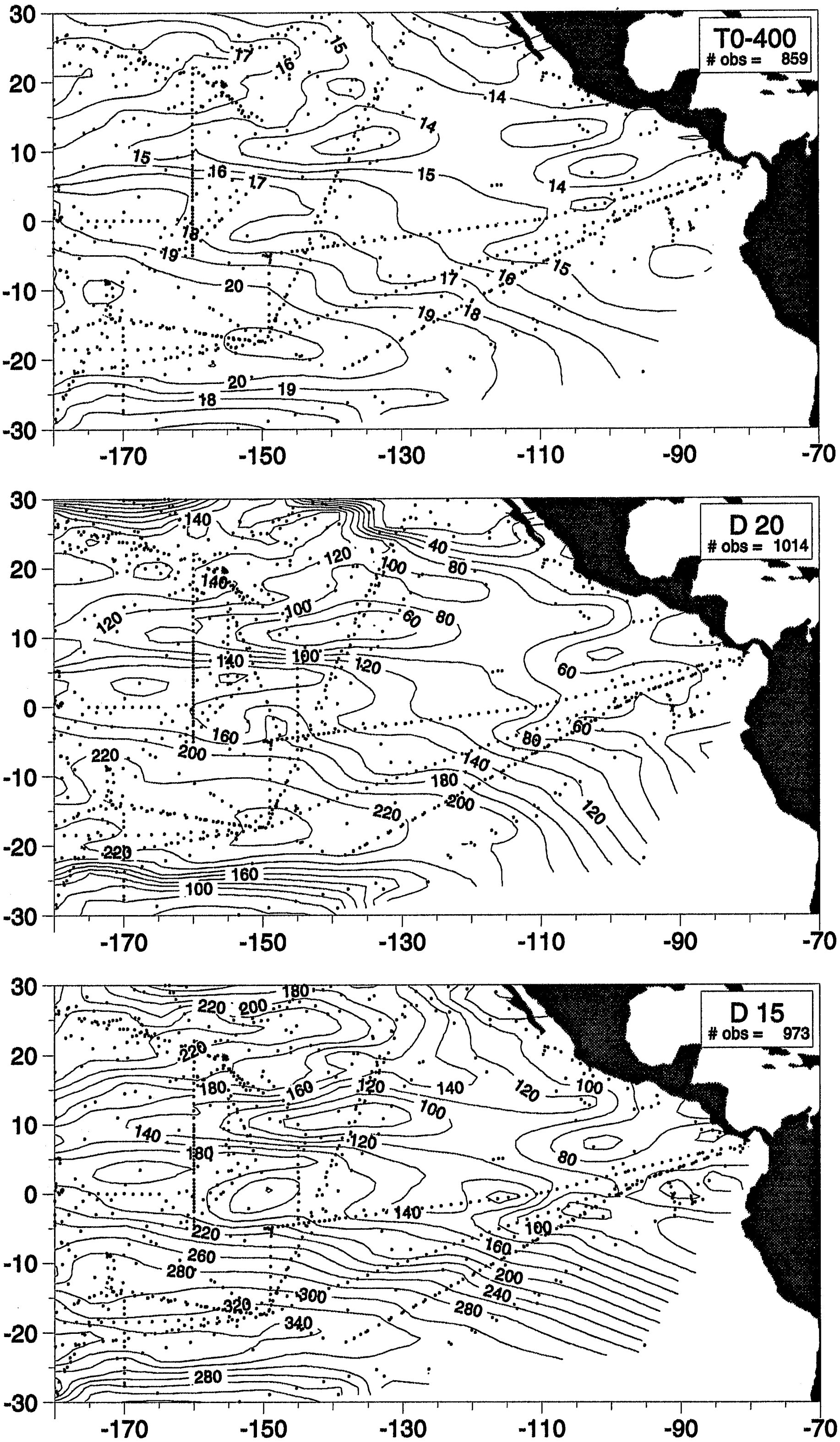

Plate 73 – *continued.* Bimonthly fields for January-February 1990.

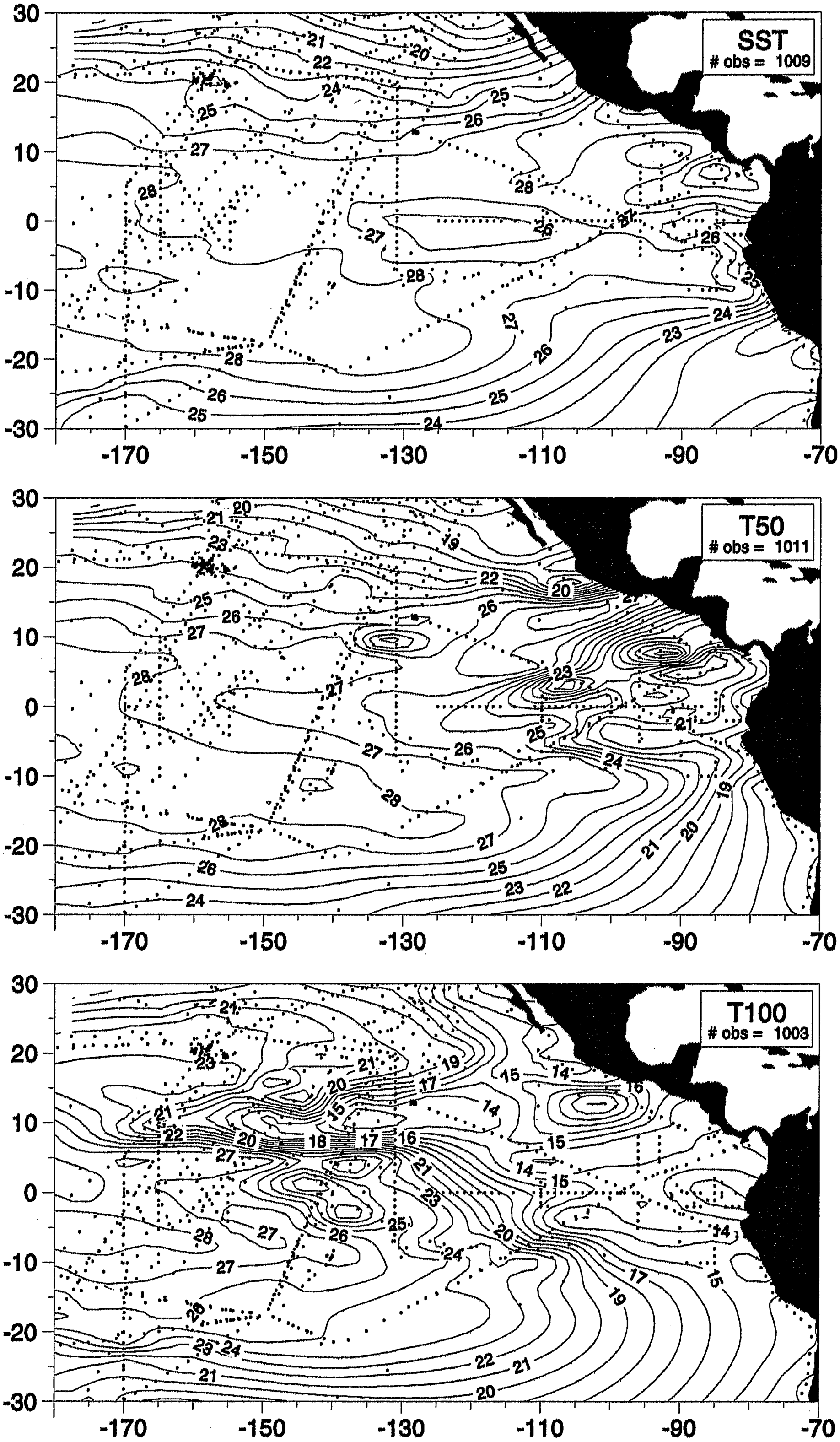

Plate 74. Bimonthly fields for March-April 1990.

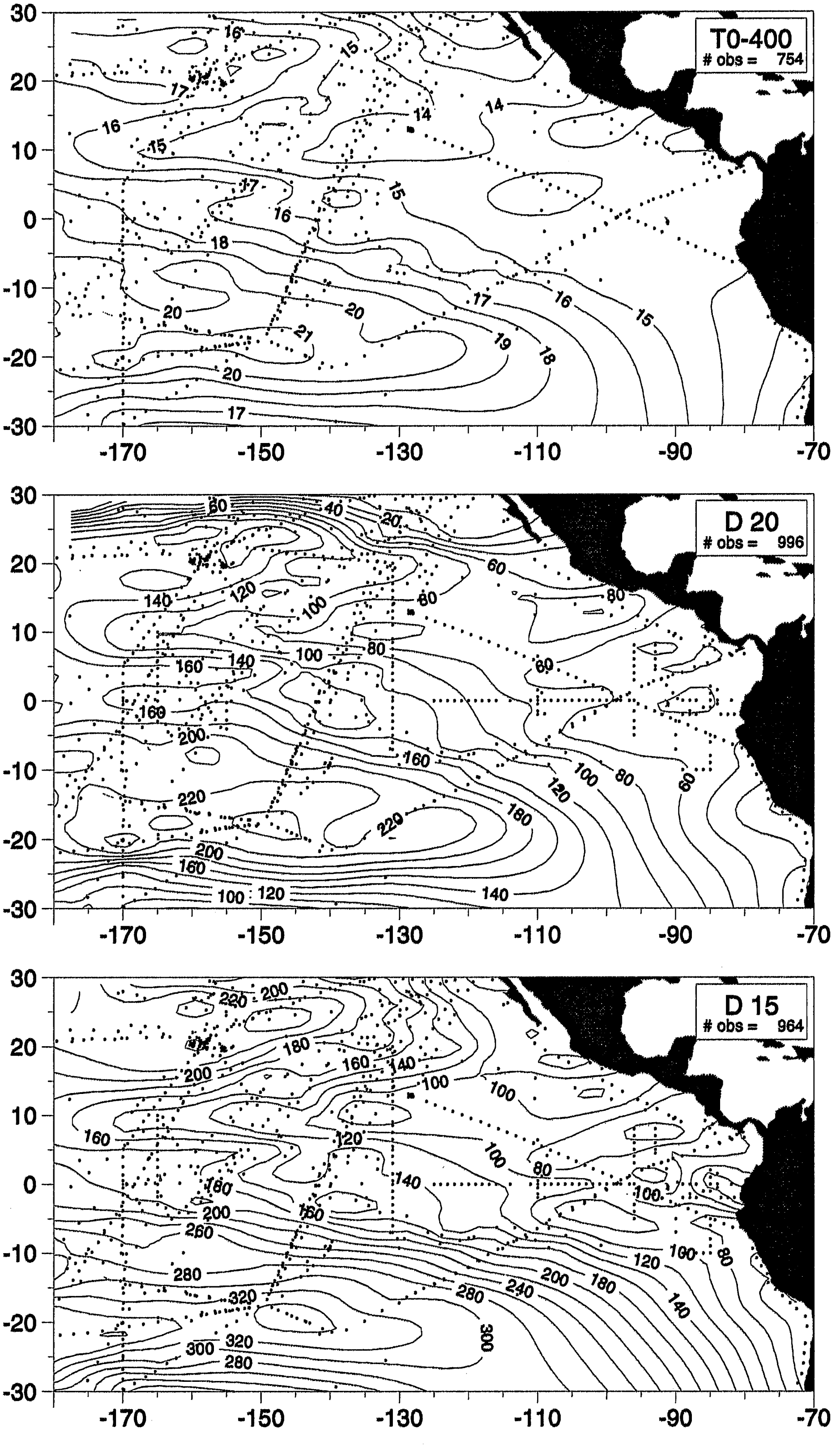

Plate 74 – *continued*. Bimonthly fields for March-April 1990.

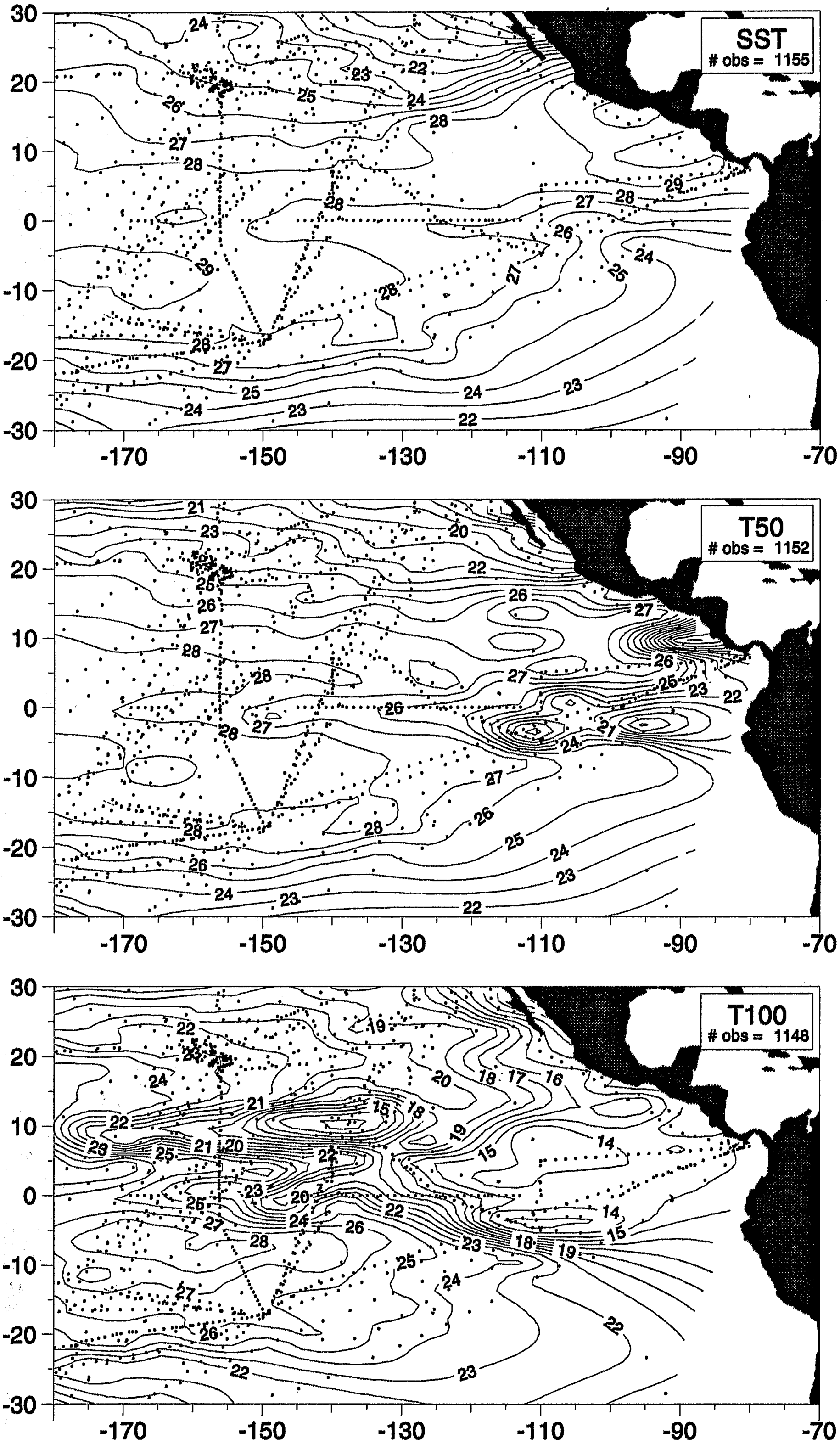

Plate 75. Bimonthly fields for May-June 1990.

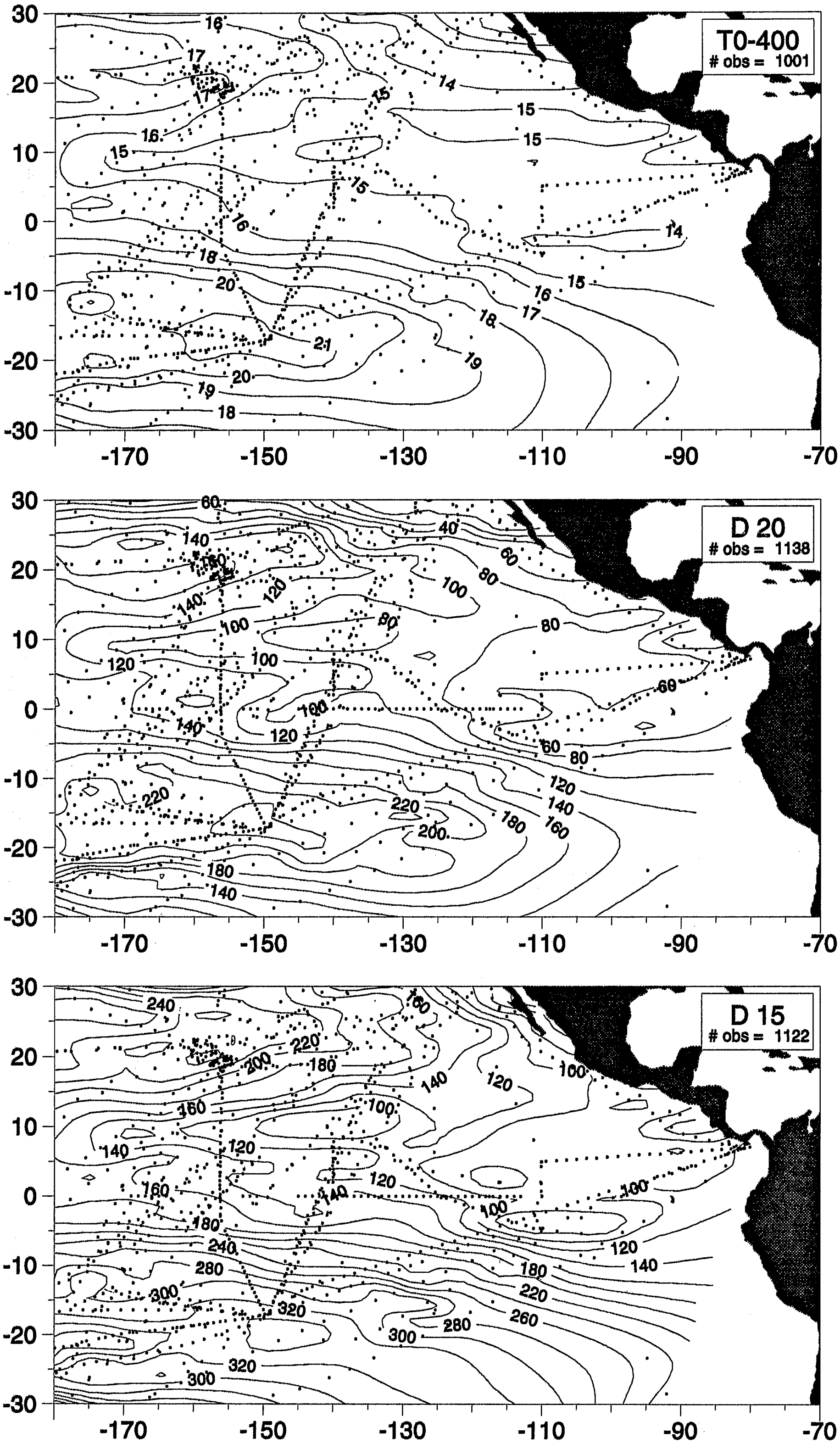

Plate 75 – *continued*. Bimonthly fields for May-June 1990.

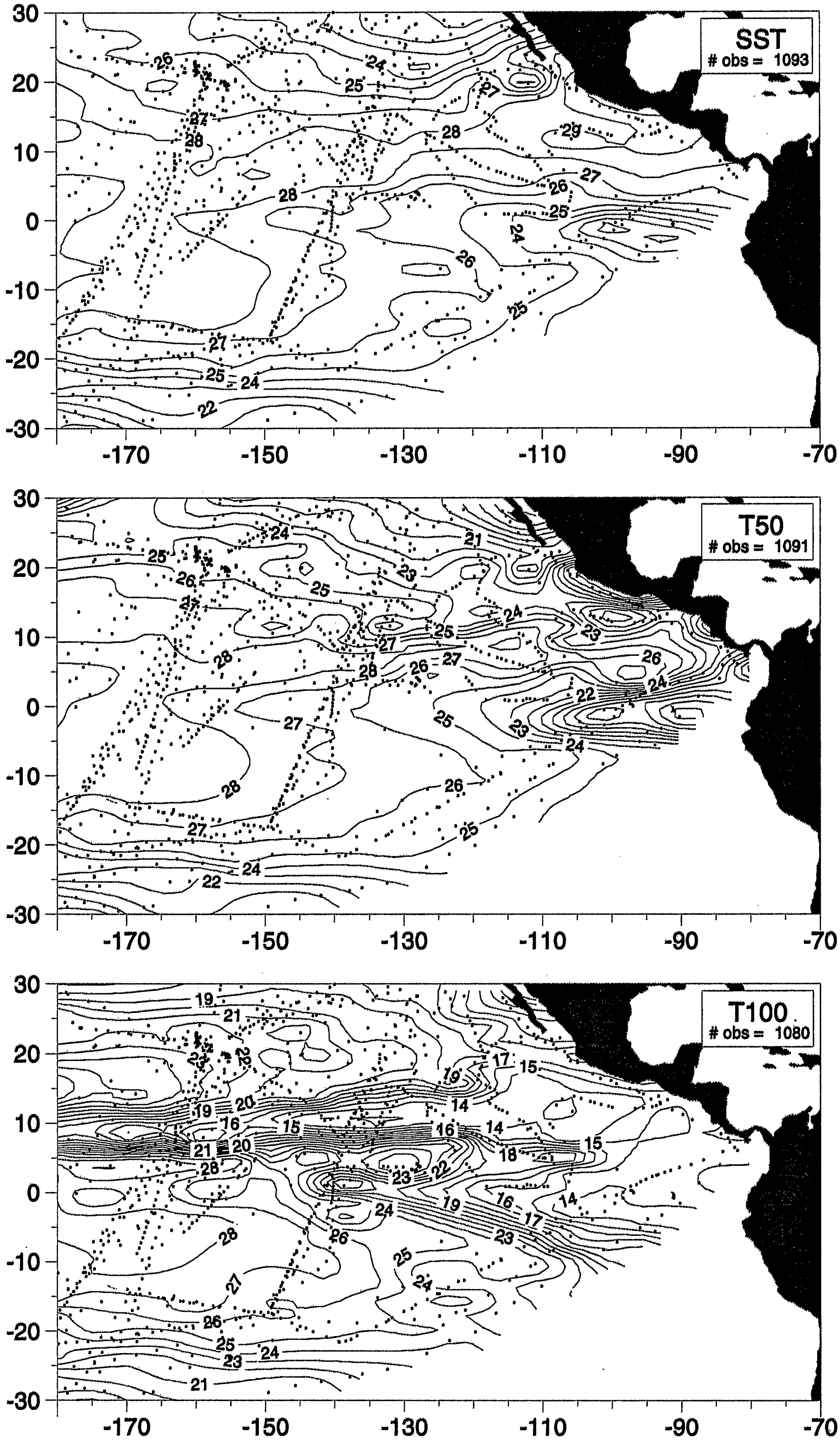

Plate 76. Bimonthly fields for July-August 1990.

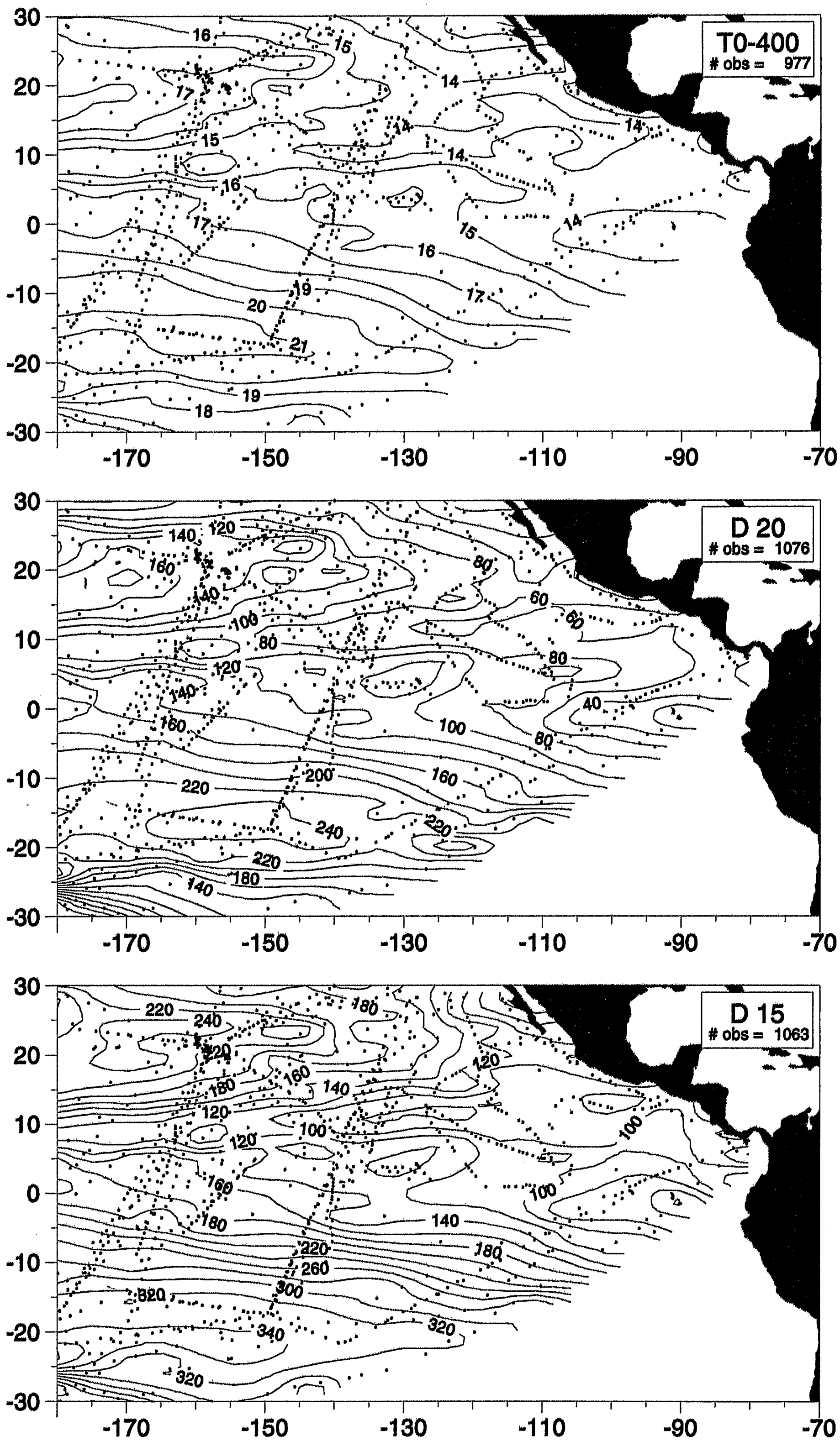

Plate 76 – *continued.* Bimonthly fields for July-August 1990.

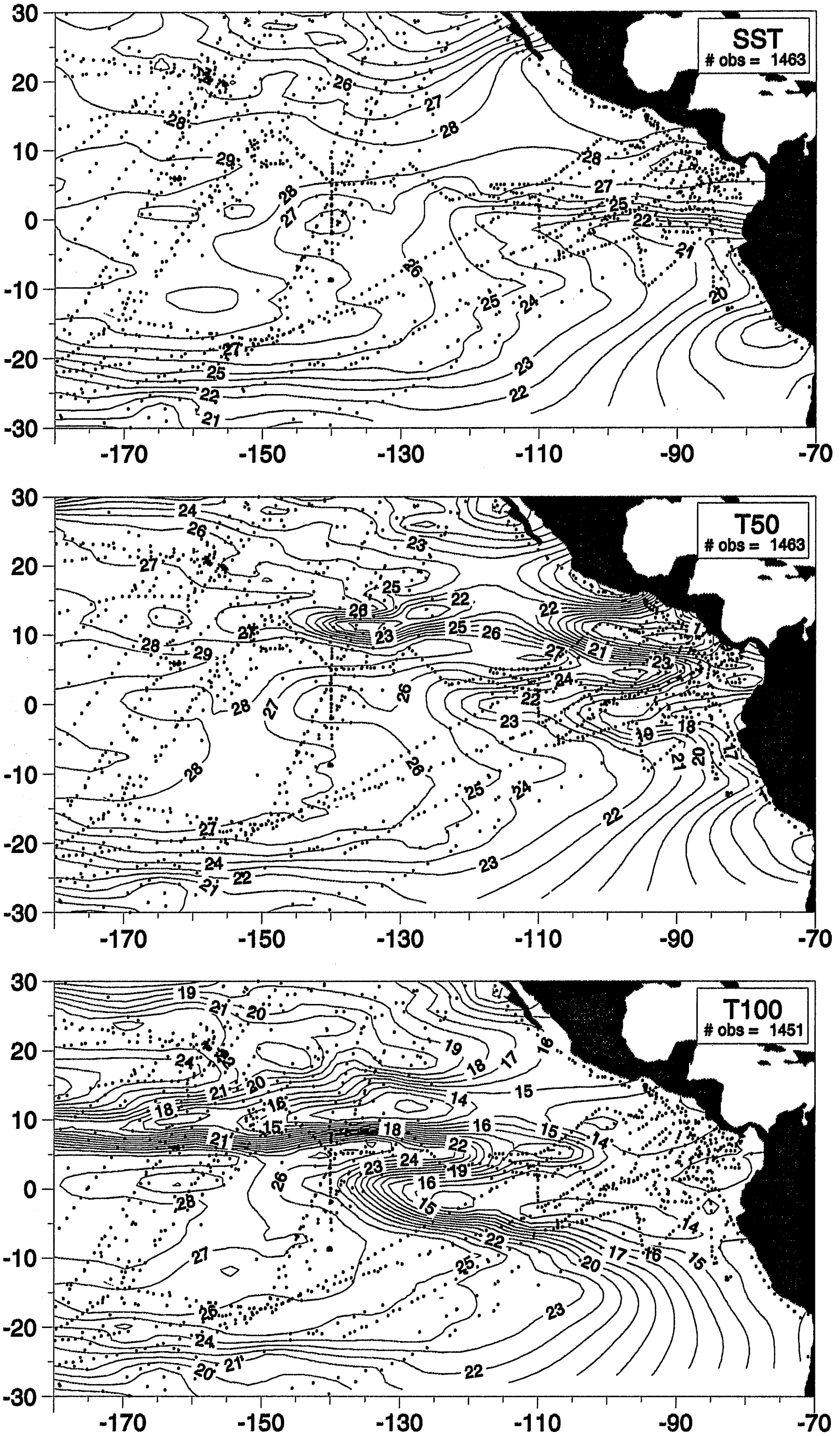

Plate 77. Bimonthly fields for September-October 1990.

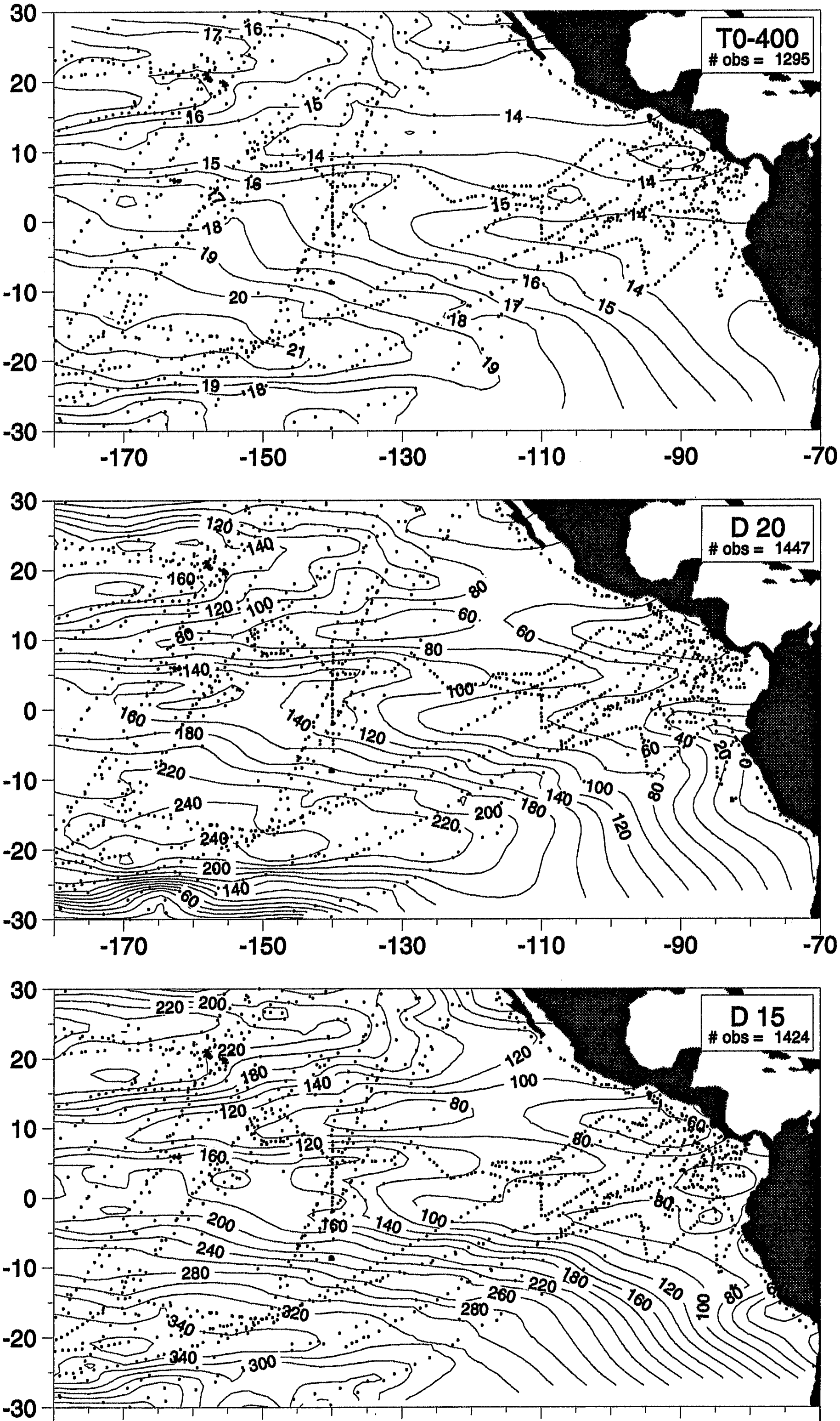

Plate 77 – *continued*. Bimonthly fields for September-October 1990.

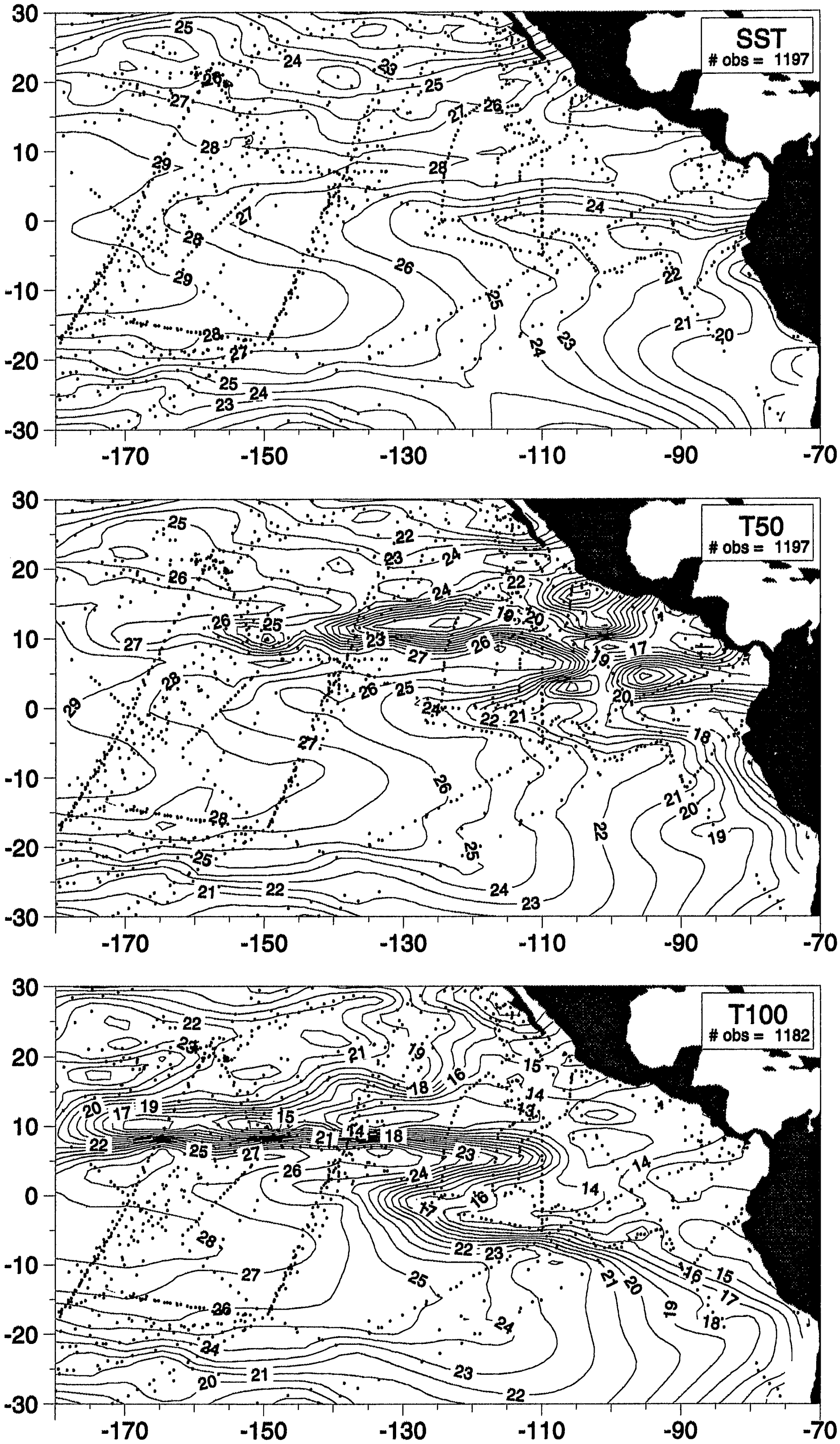

Plate 78. Bimonthly fields for November-December 1990.

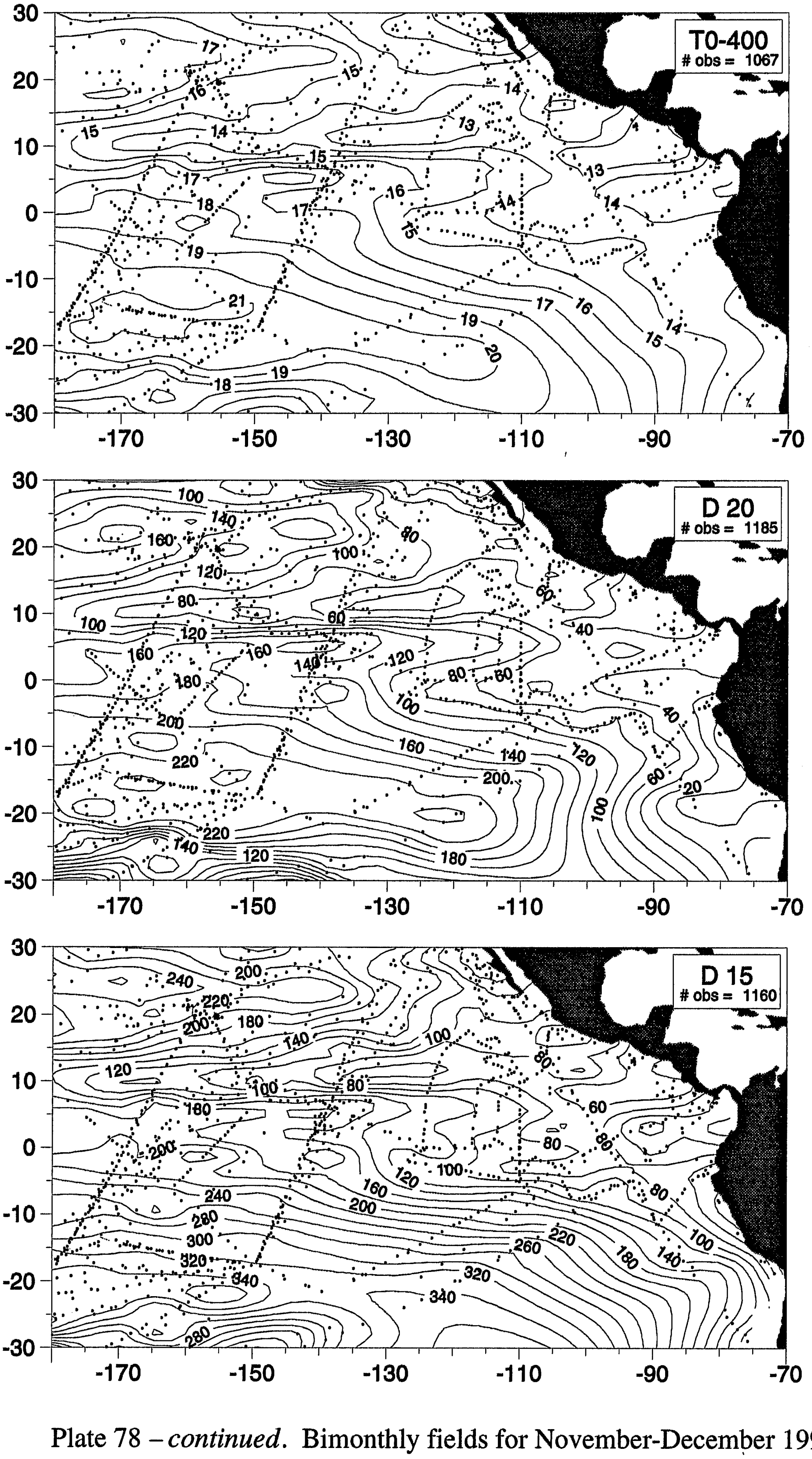

Plate 78 – *continued.* Bimonthly fields for November-December 1990.

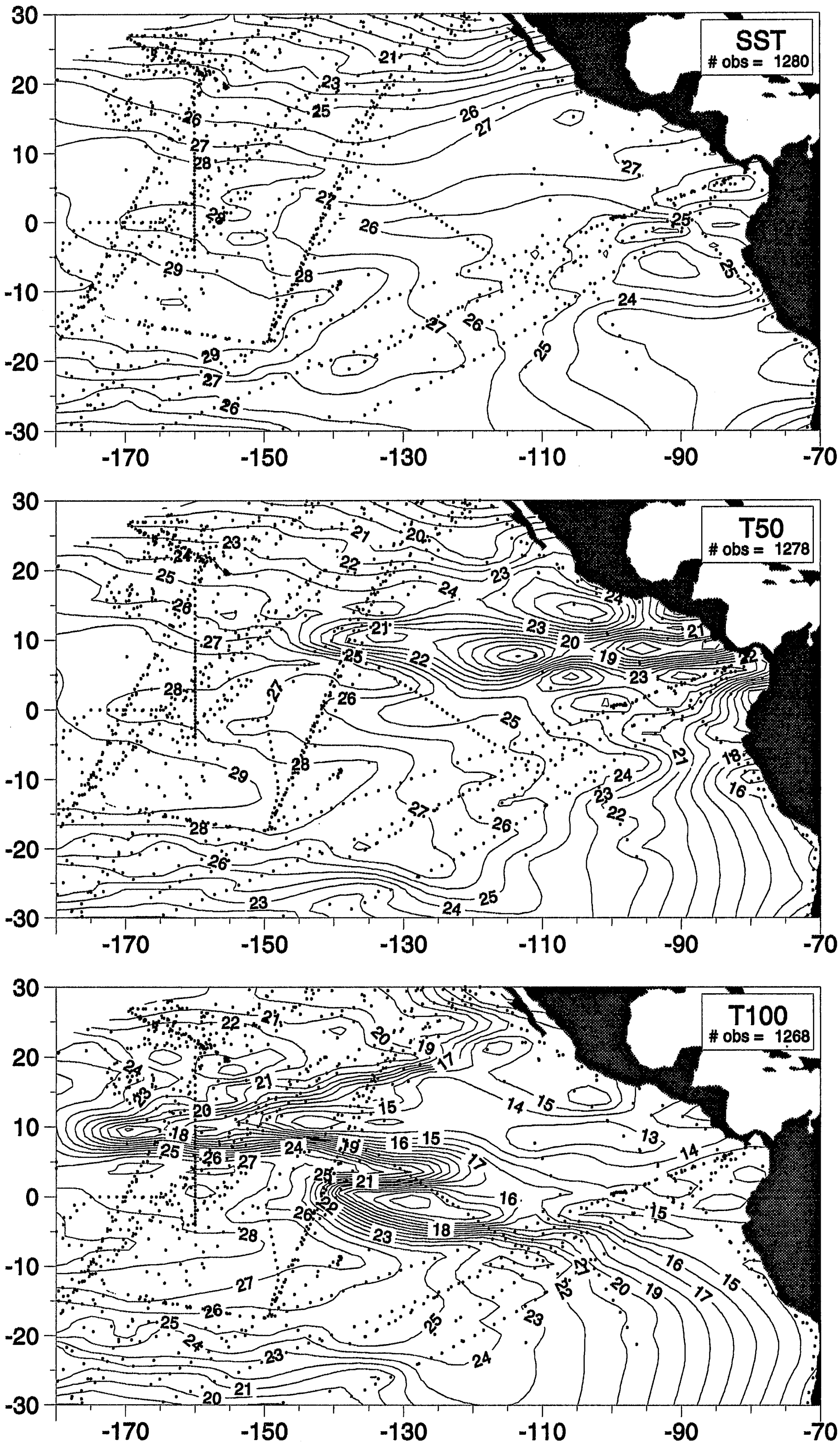

Plate 79. Bimonthly fields for January-February 1991.

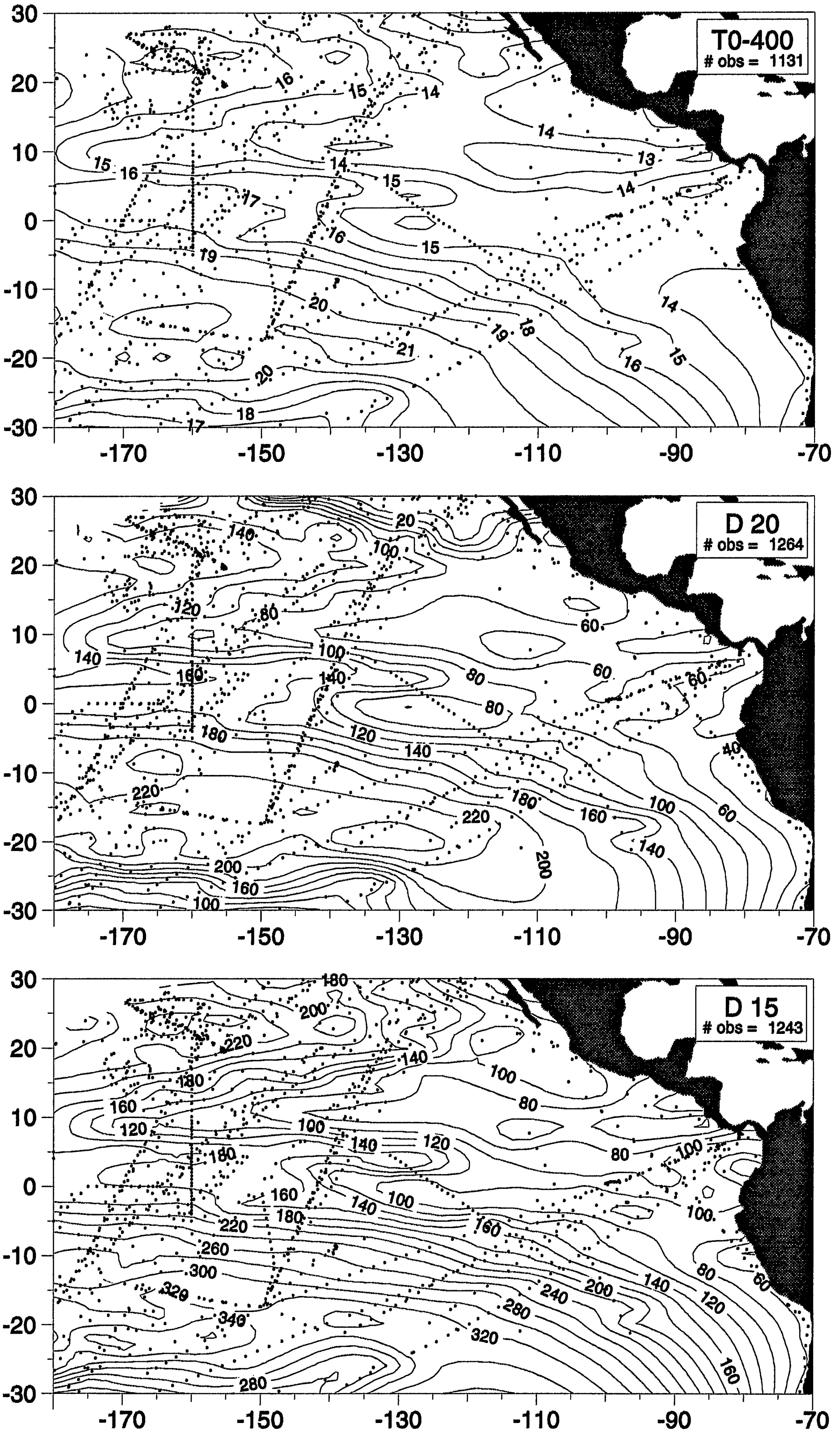

Plate 79 – *continued*. Bimonthly fields for January-February 1991.

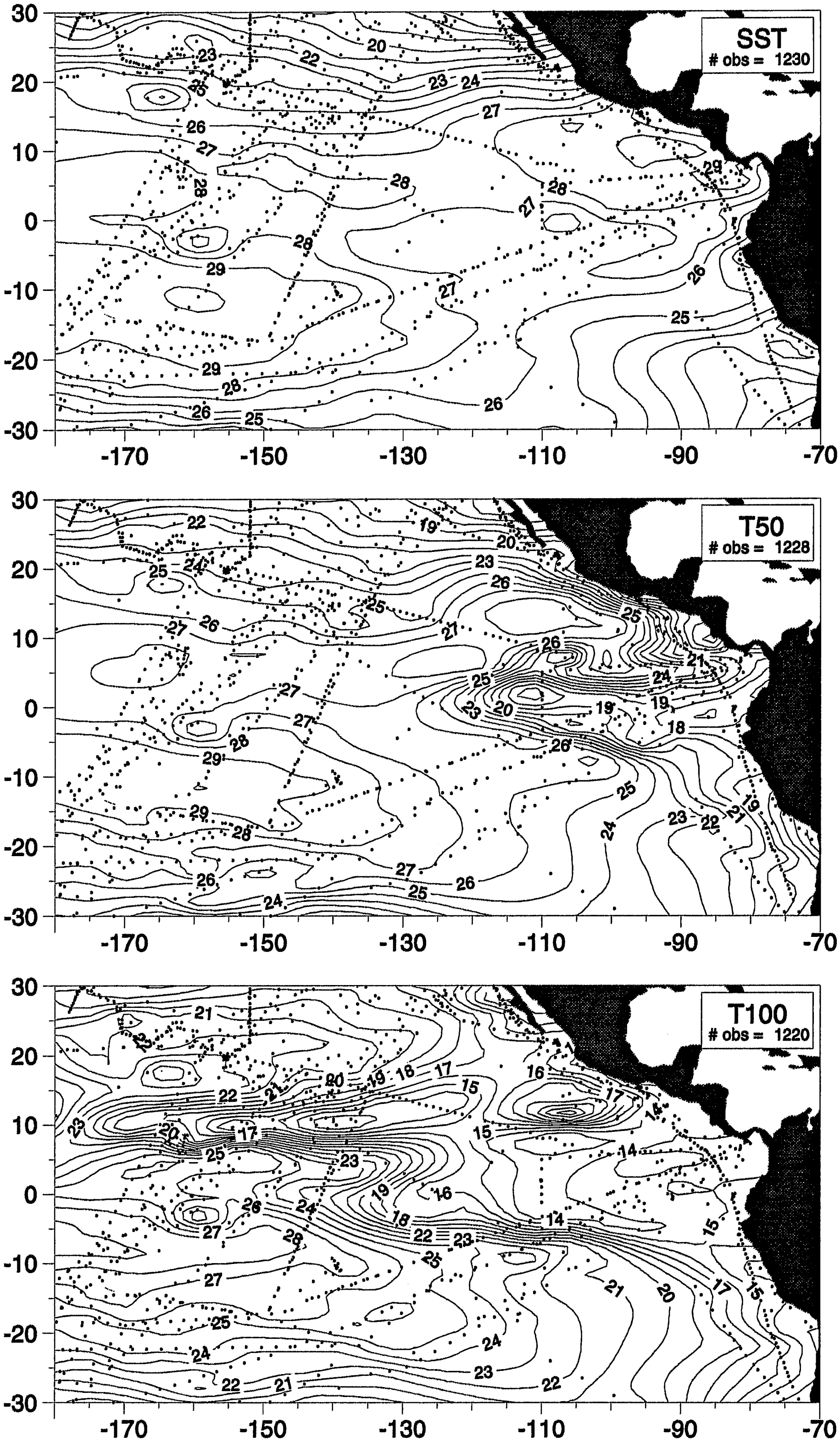

Plate 80. Bimonthly fields for March-April 1991.

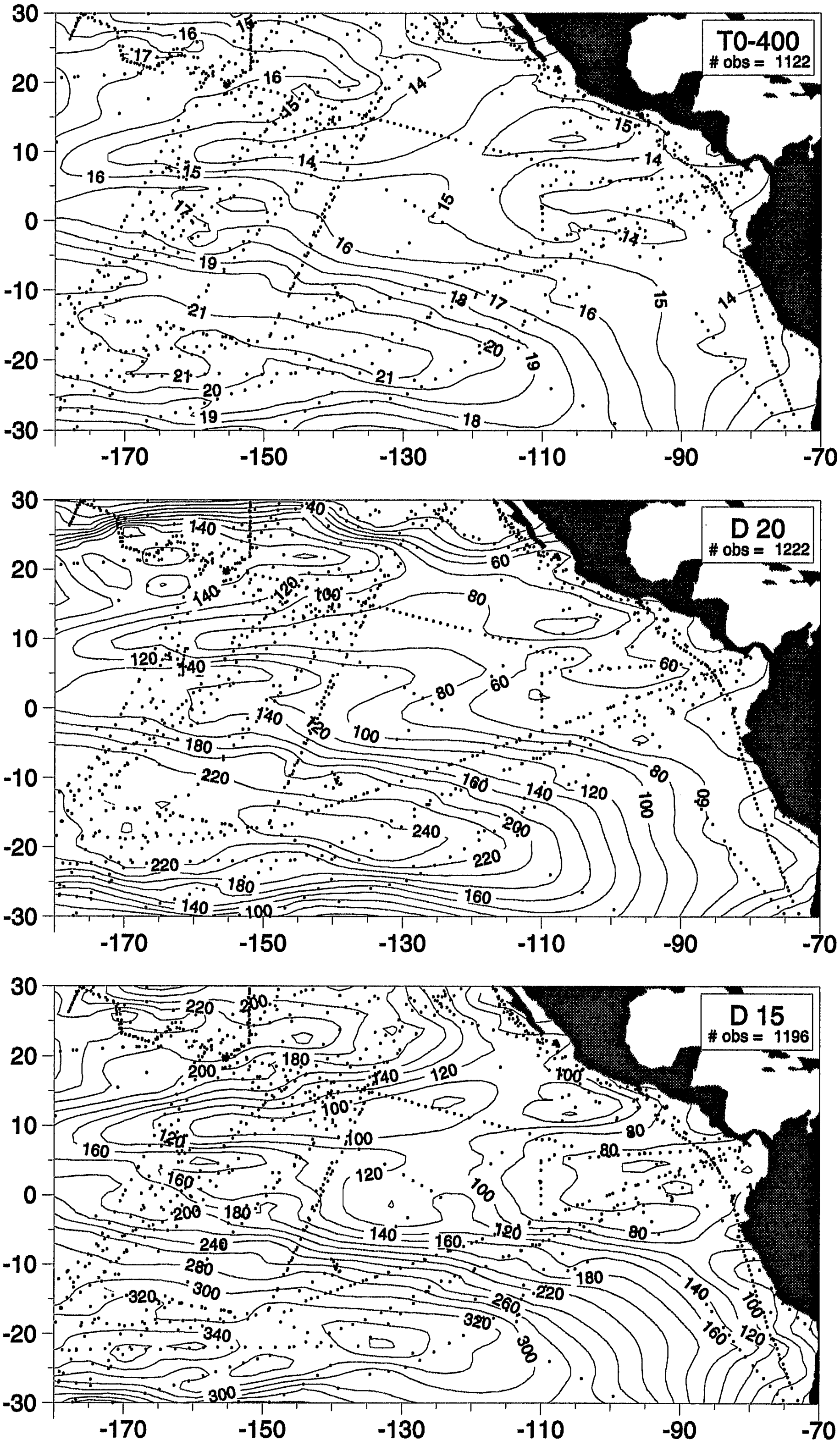

Plate 80 – *continued*. Bimonthly fields for March-April 1991.

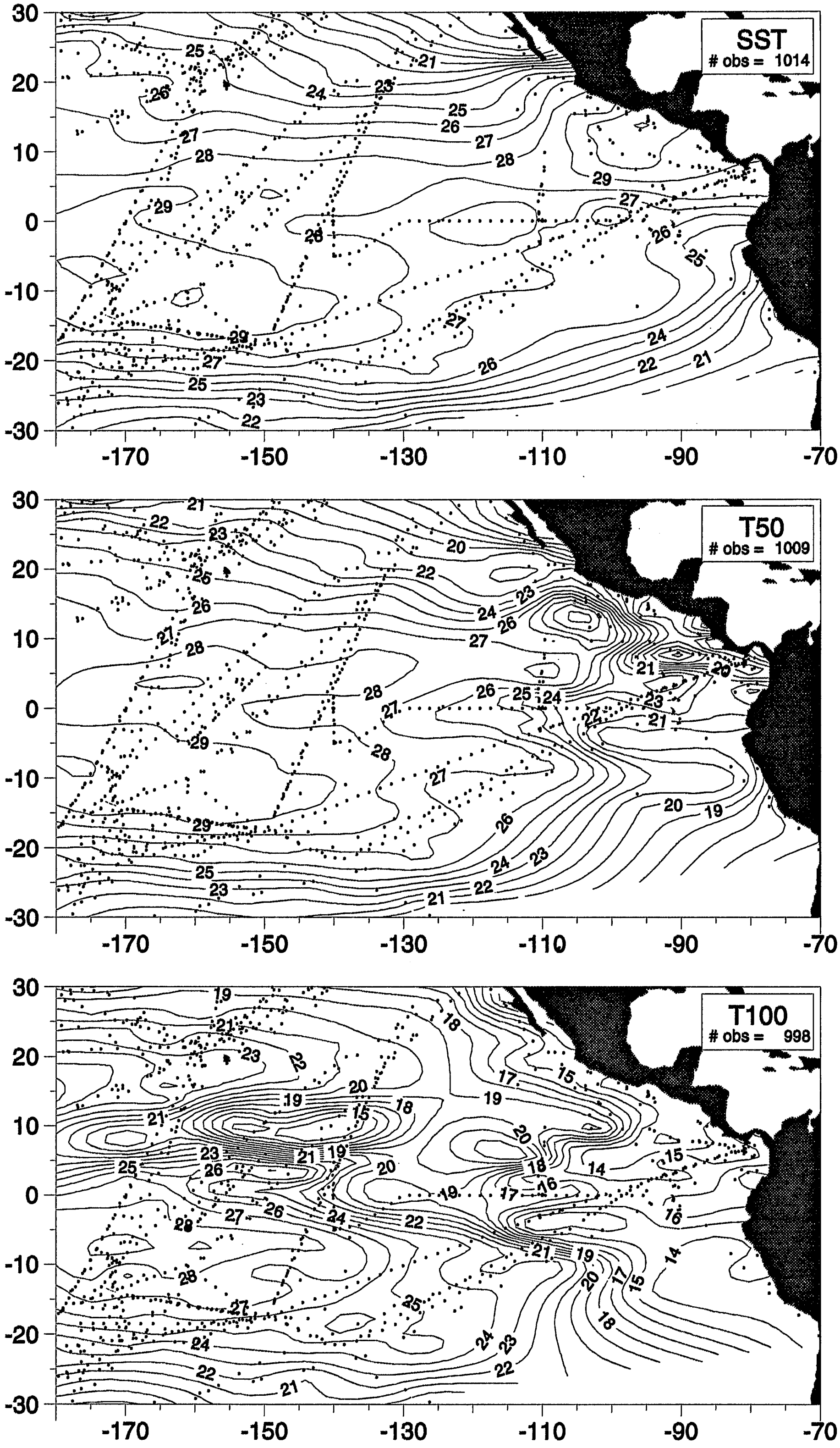

Plate 81. Bimonthly fields for May-June 1991.

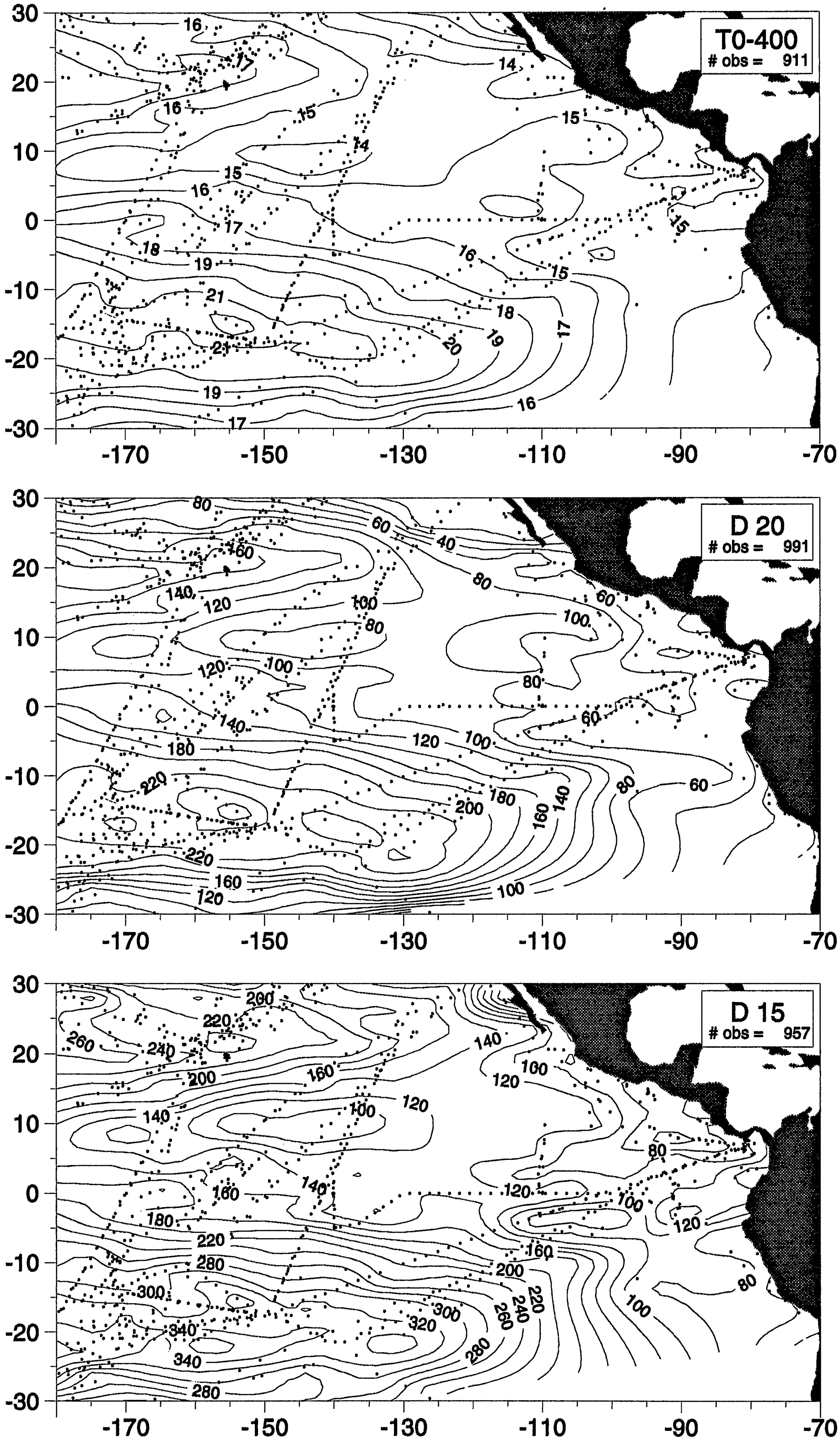

Plate 81 – *continued*. Bimonthly fields for May-June 1991.

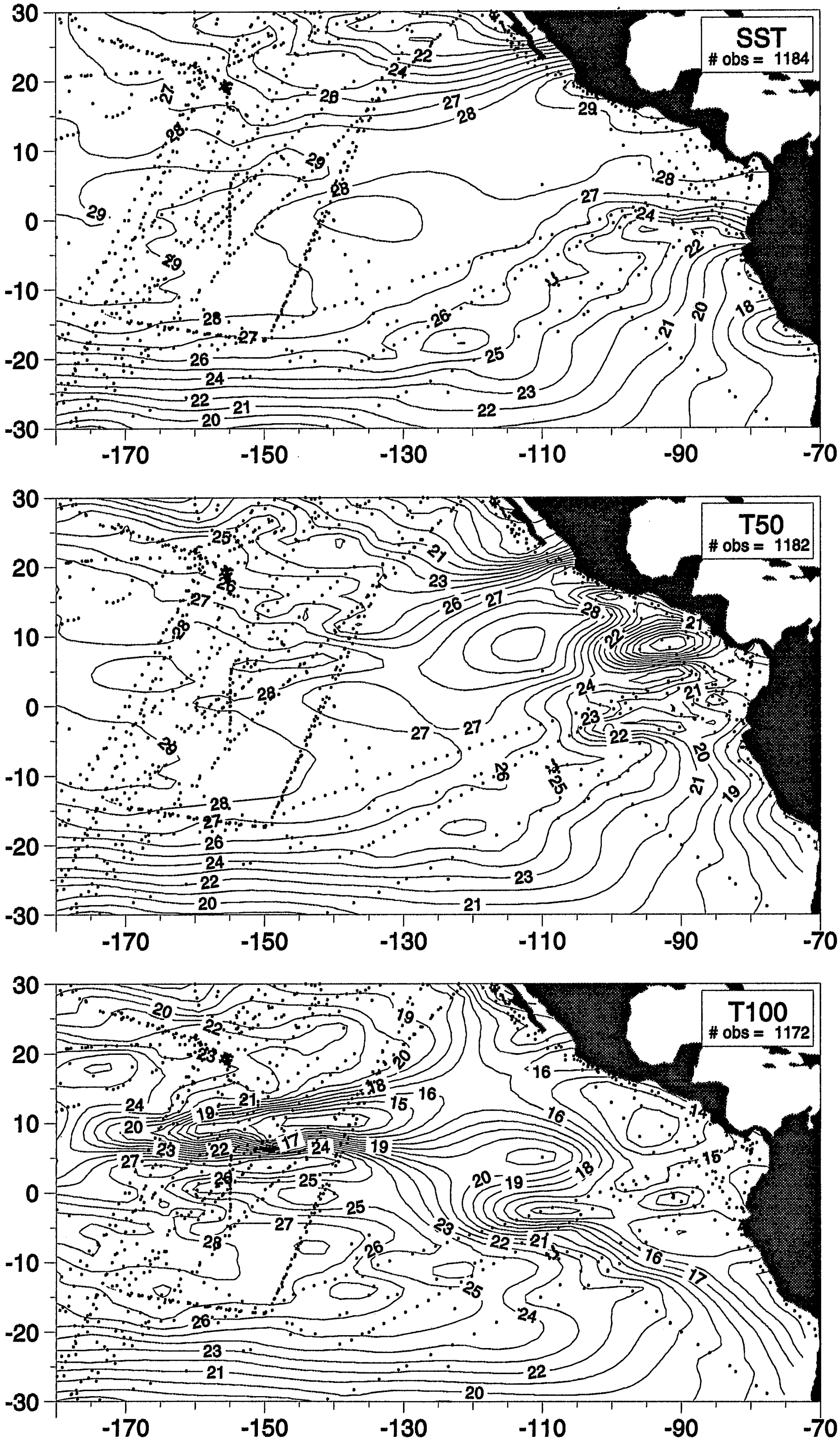

Plate 82. Bimonthly fields for July-August 1991.

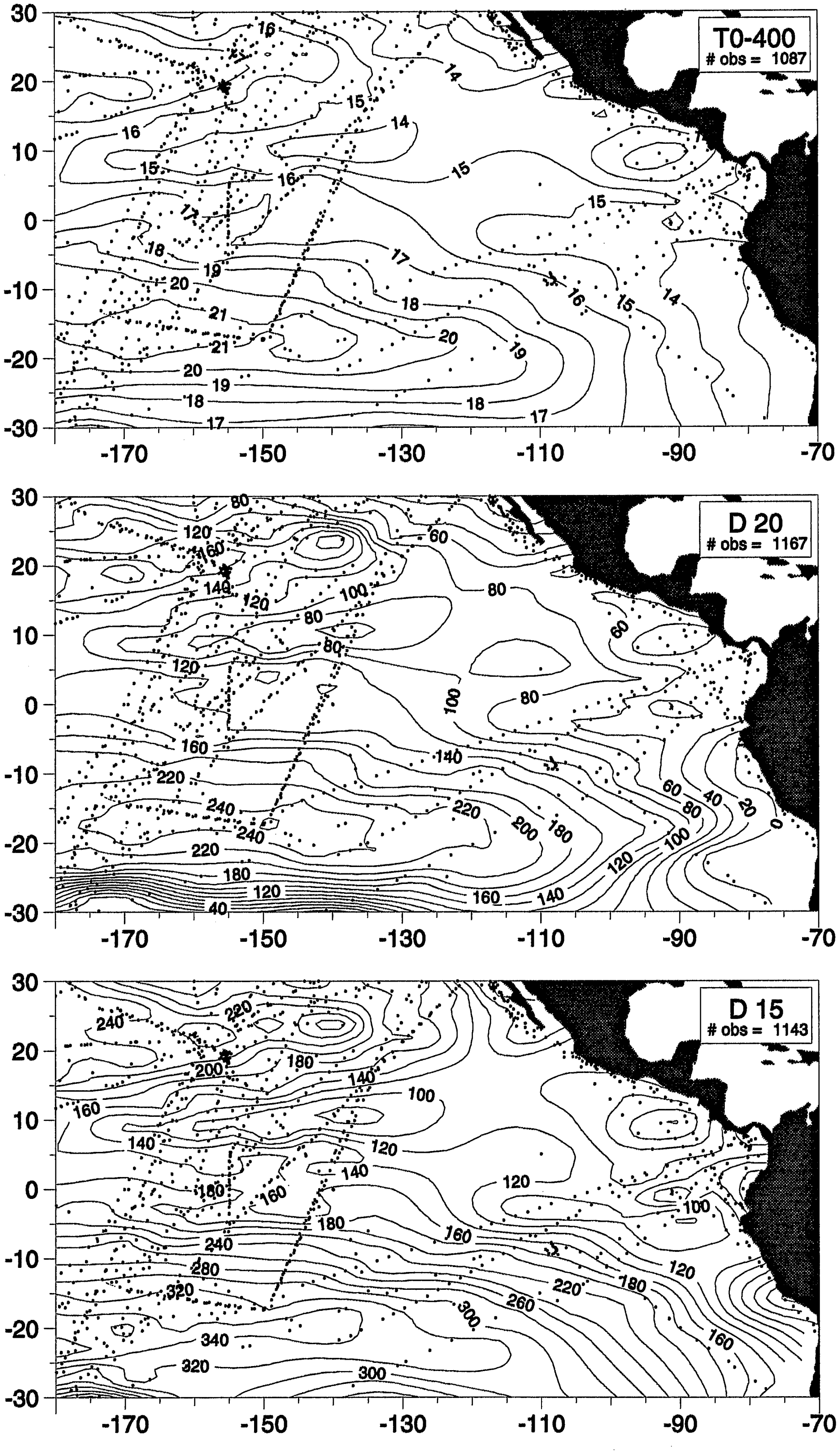

Plate 82 – *continued*. Bimonthly fields for July-August 1991.

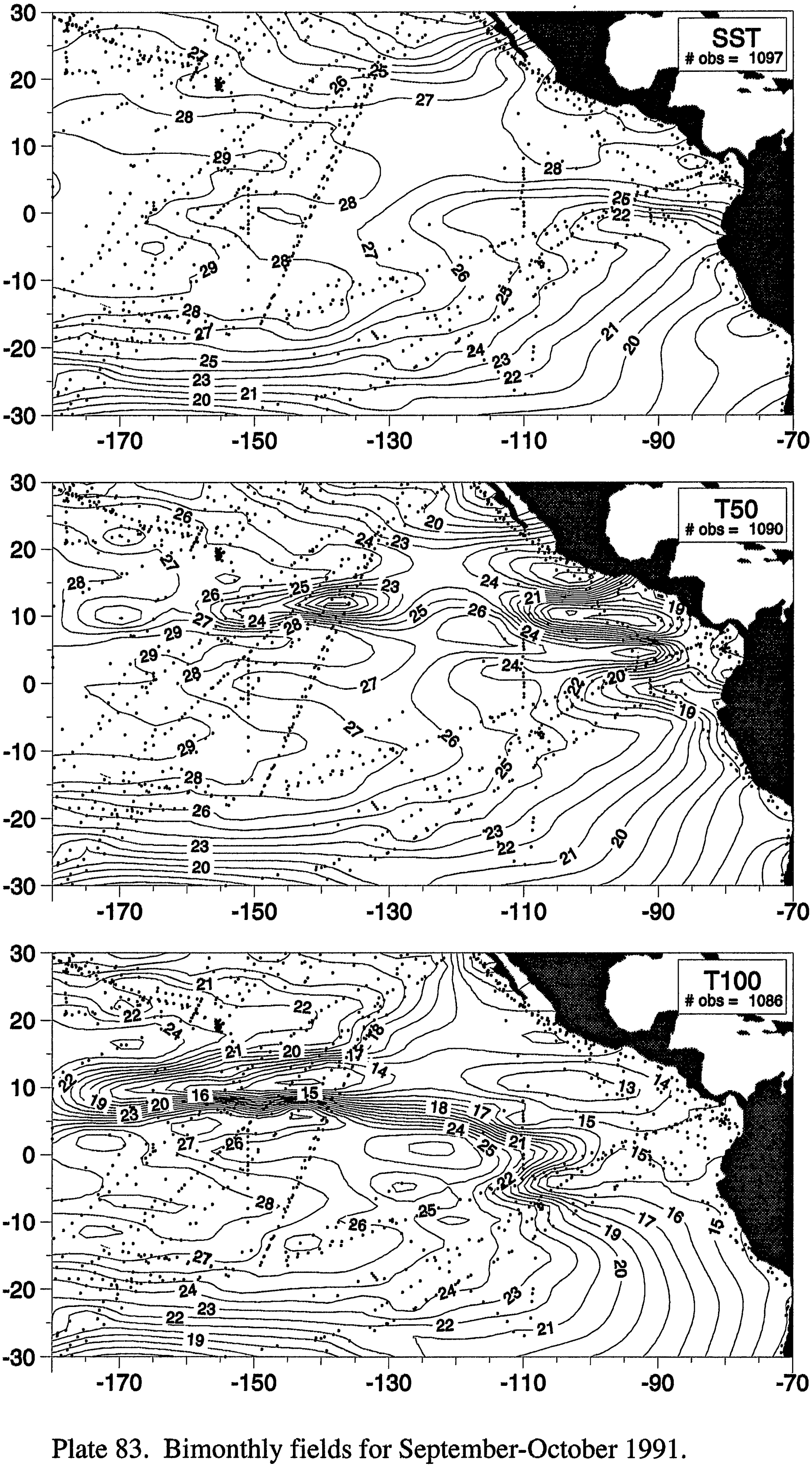

Plate 83. Bimonthly fields for September-October 1991.

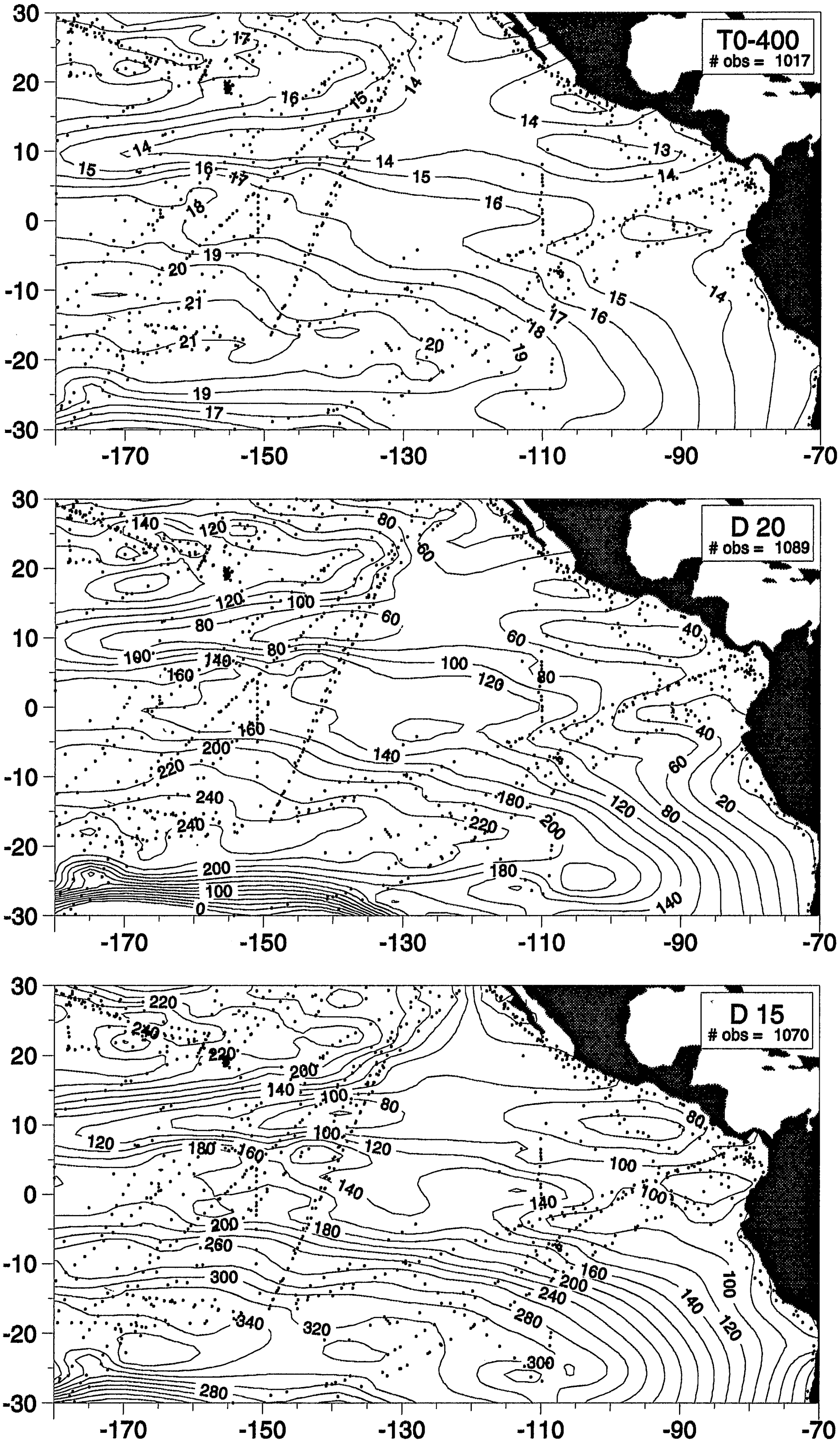

Plate 83 – *continued*. Bimonthly fields for September-October 1991.

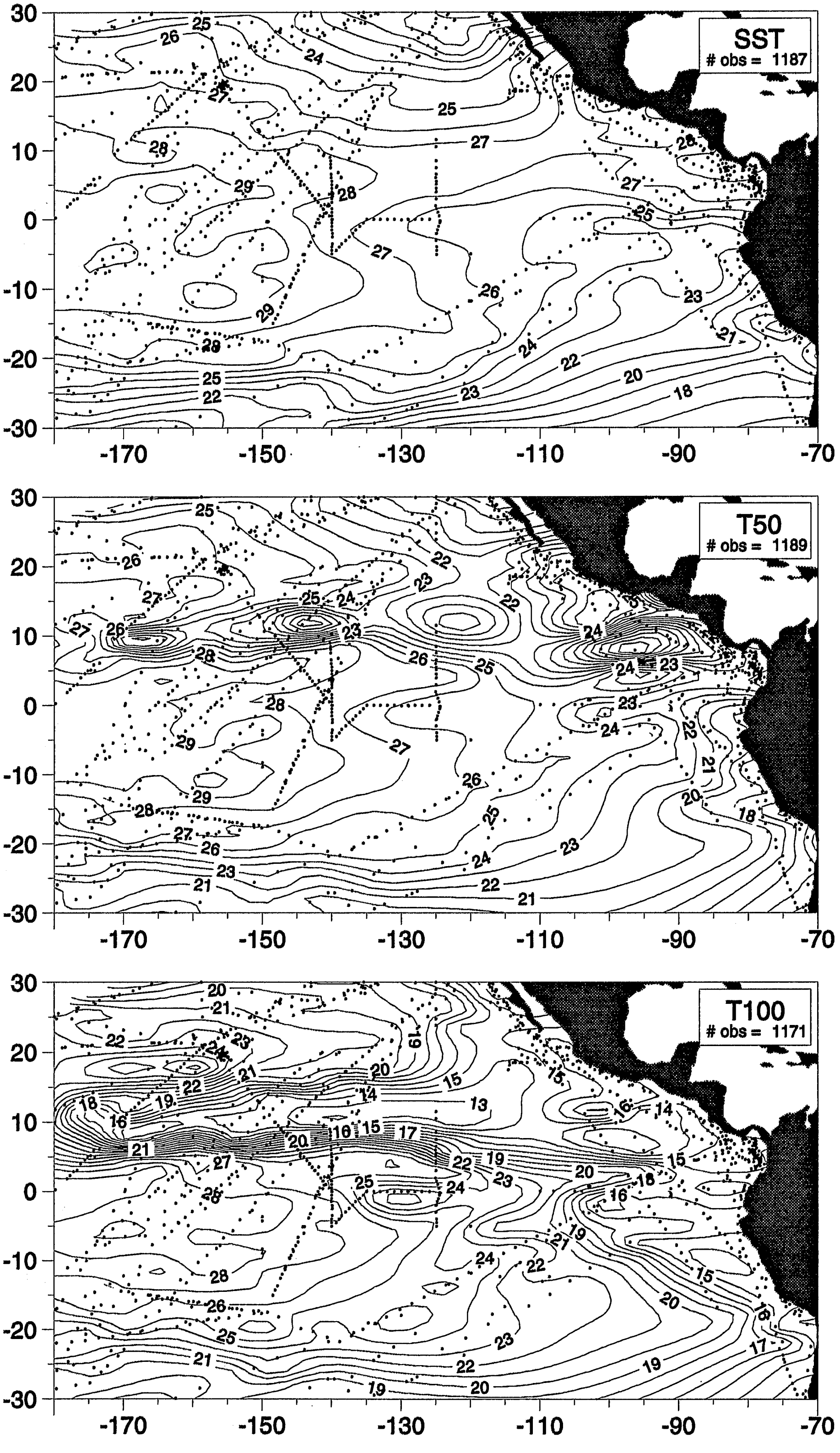

Plate 84. Bimonthly fields for November-December 1991.

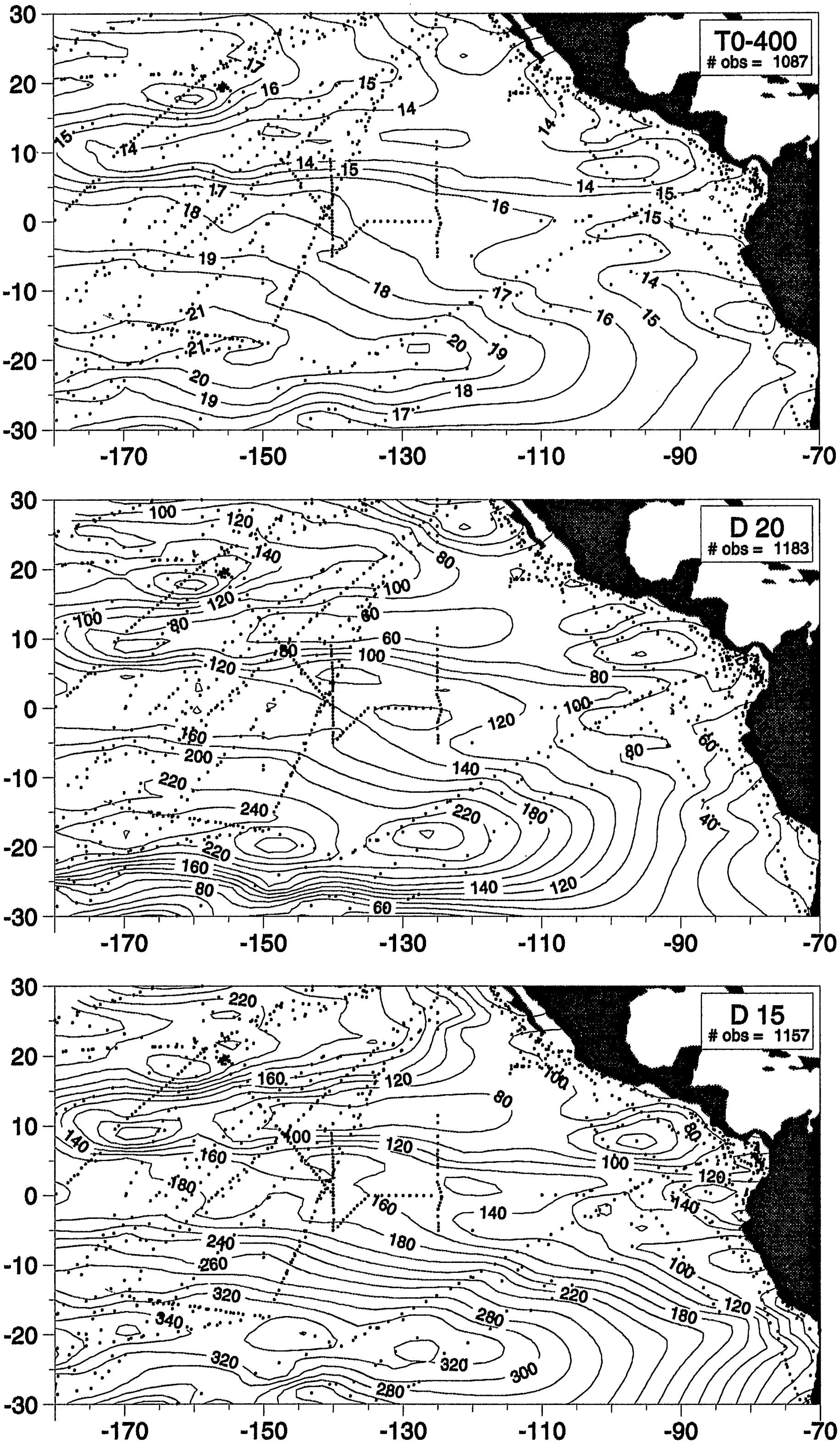

Plate 84 – *continued*. Bimonthly fields for November-December 1991.

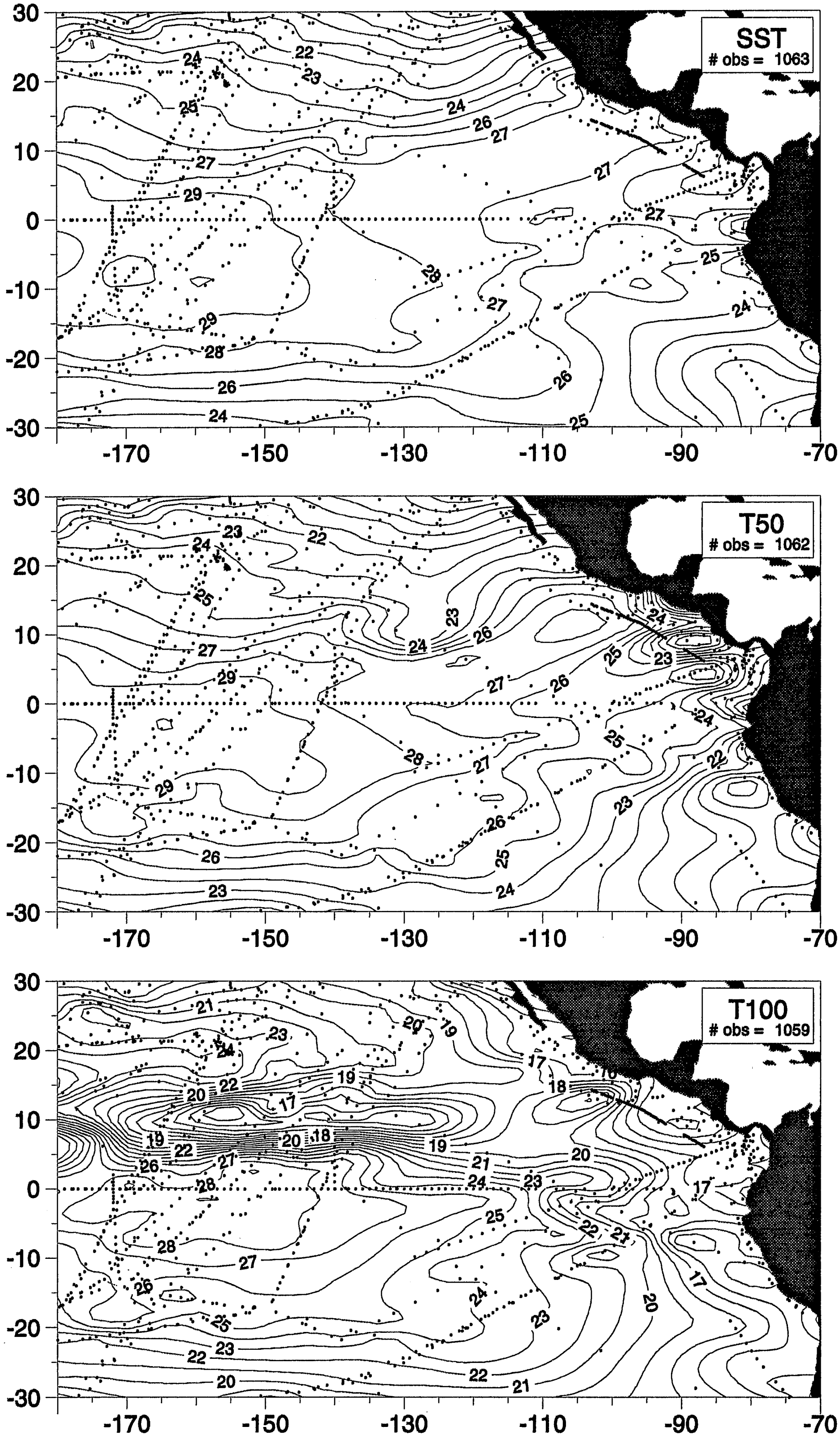

Plate 85. Bimonthly fields for January-February 1992.

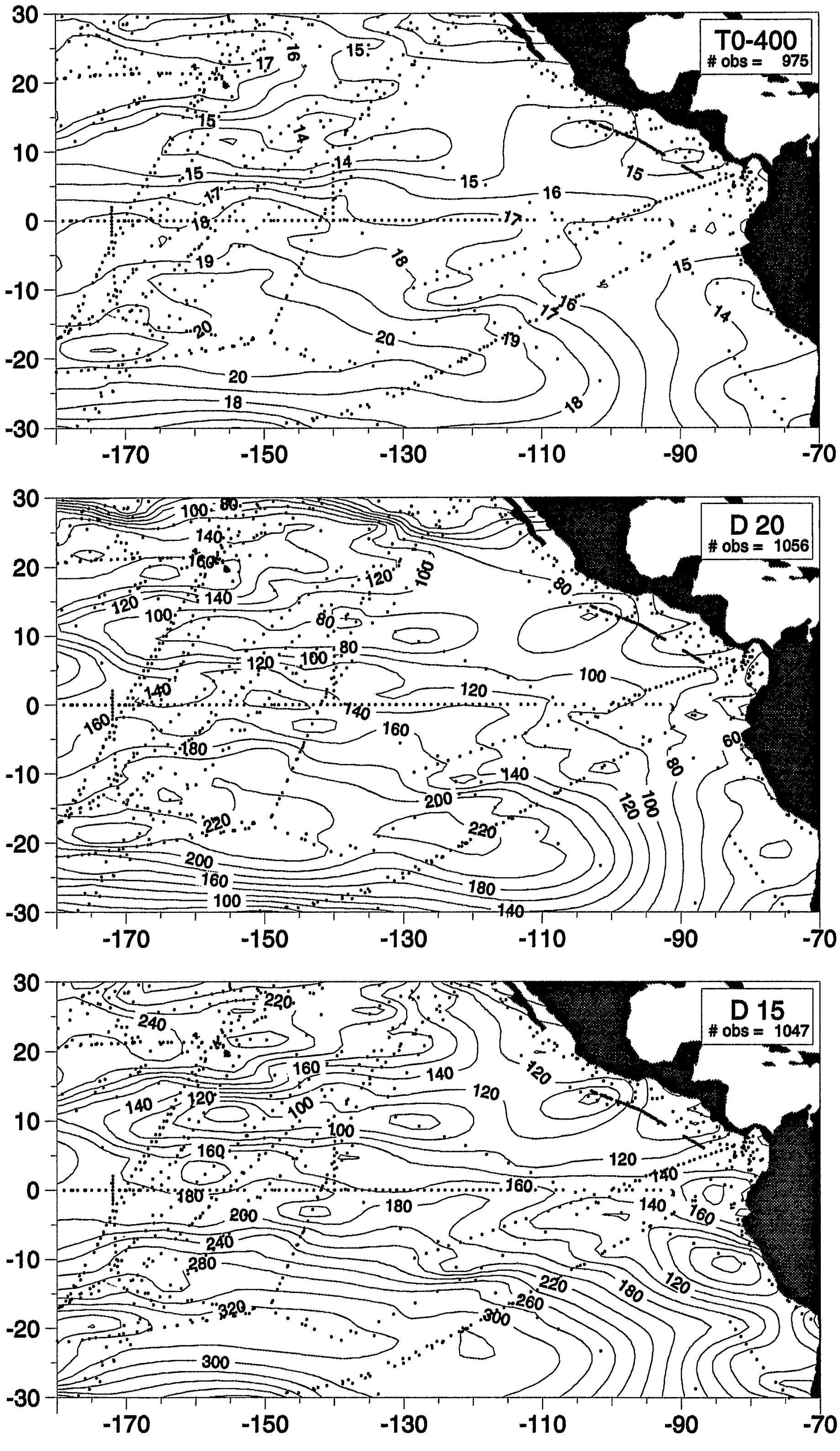

Plate 85 – *continued*. Bimonthly fields for January-February 1992.

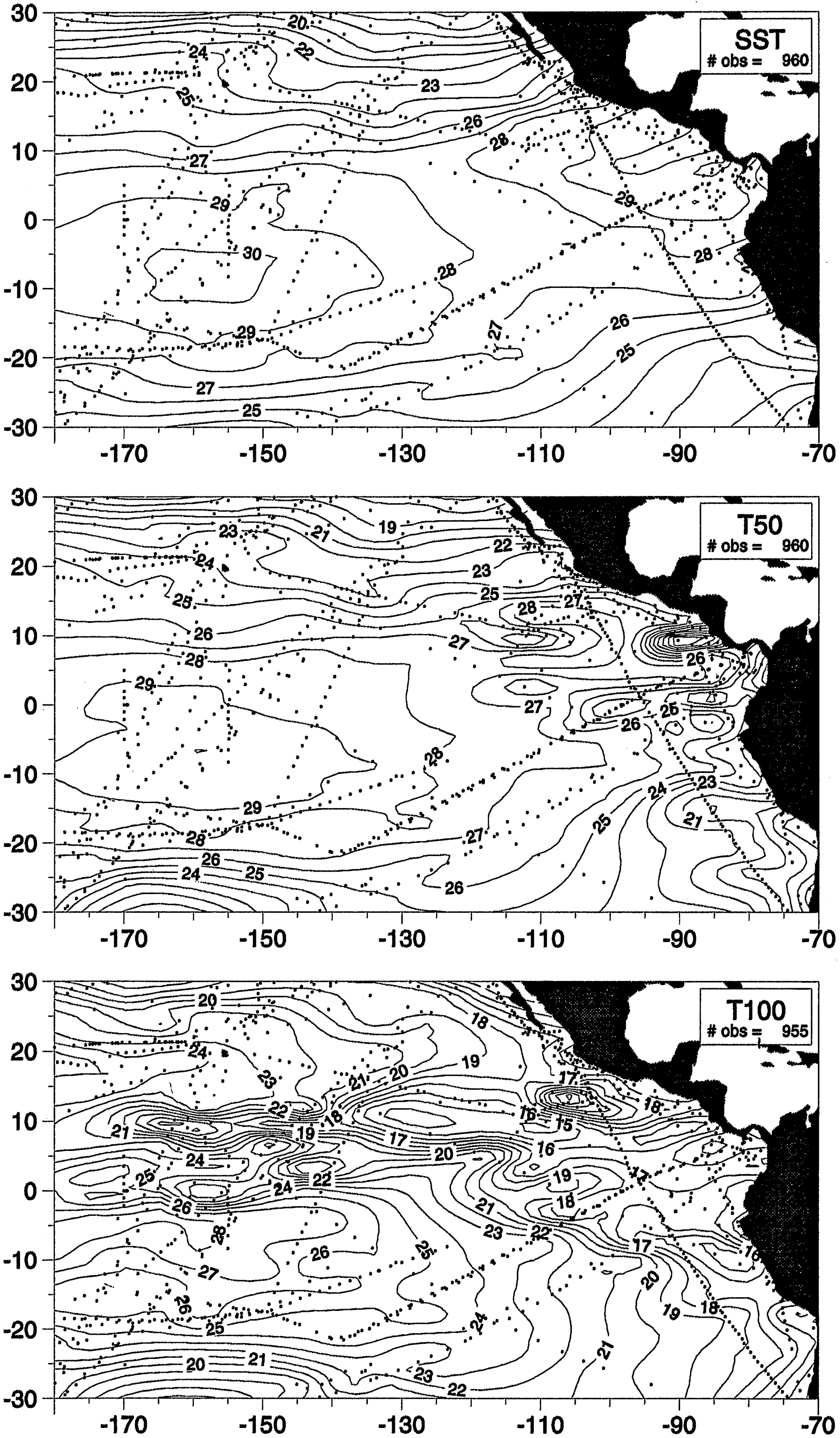

Plate 86. Bimonthly fields for March-April 1992.

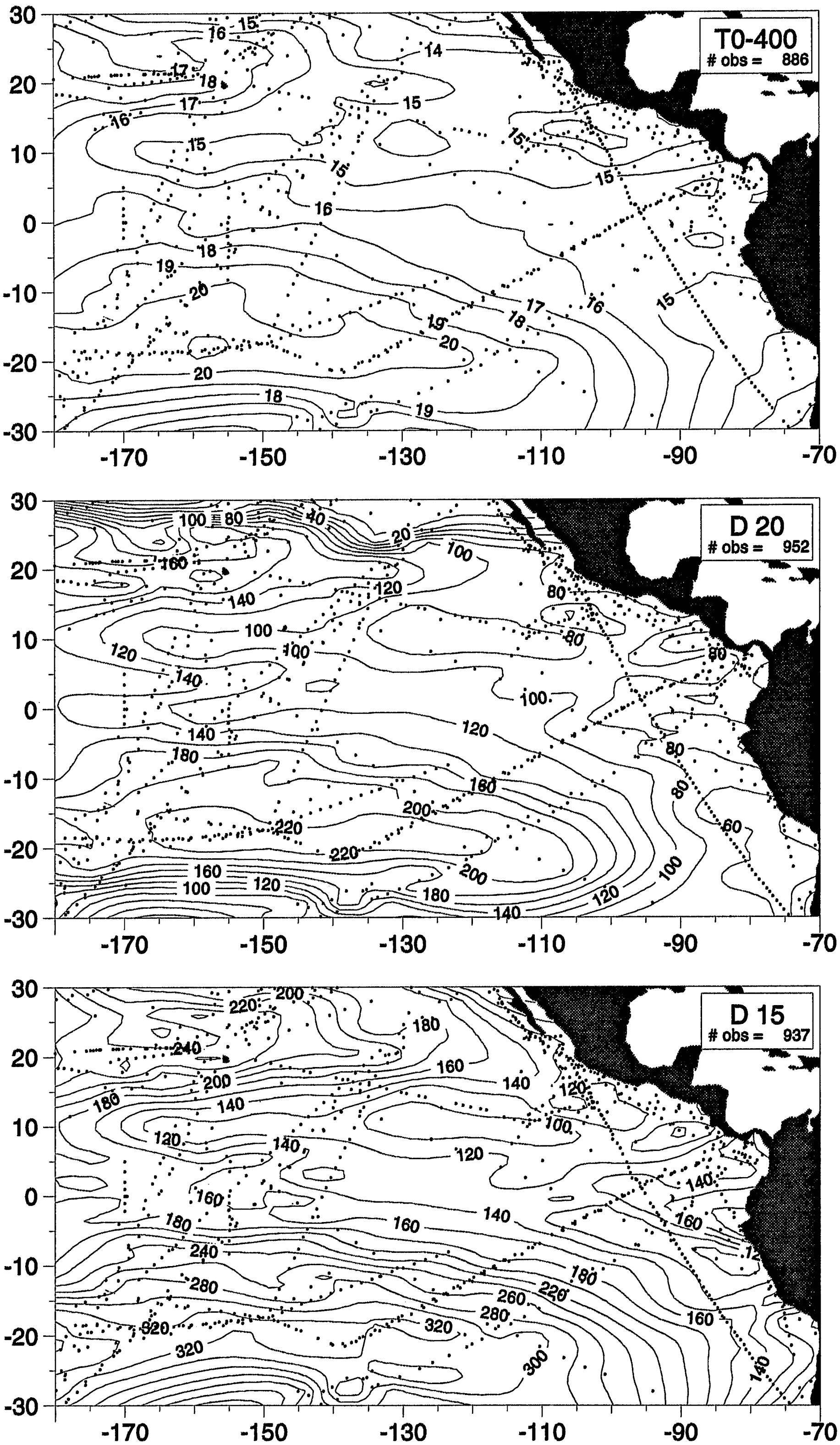

Plate 86 – *continued*. Bimonthly fields for March-April 1992.

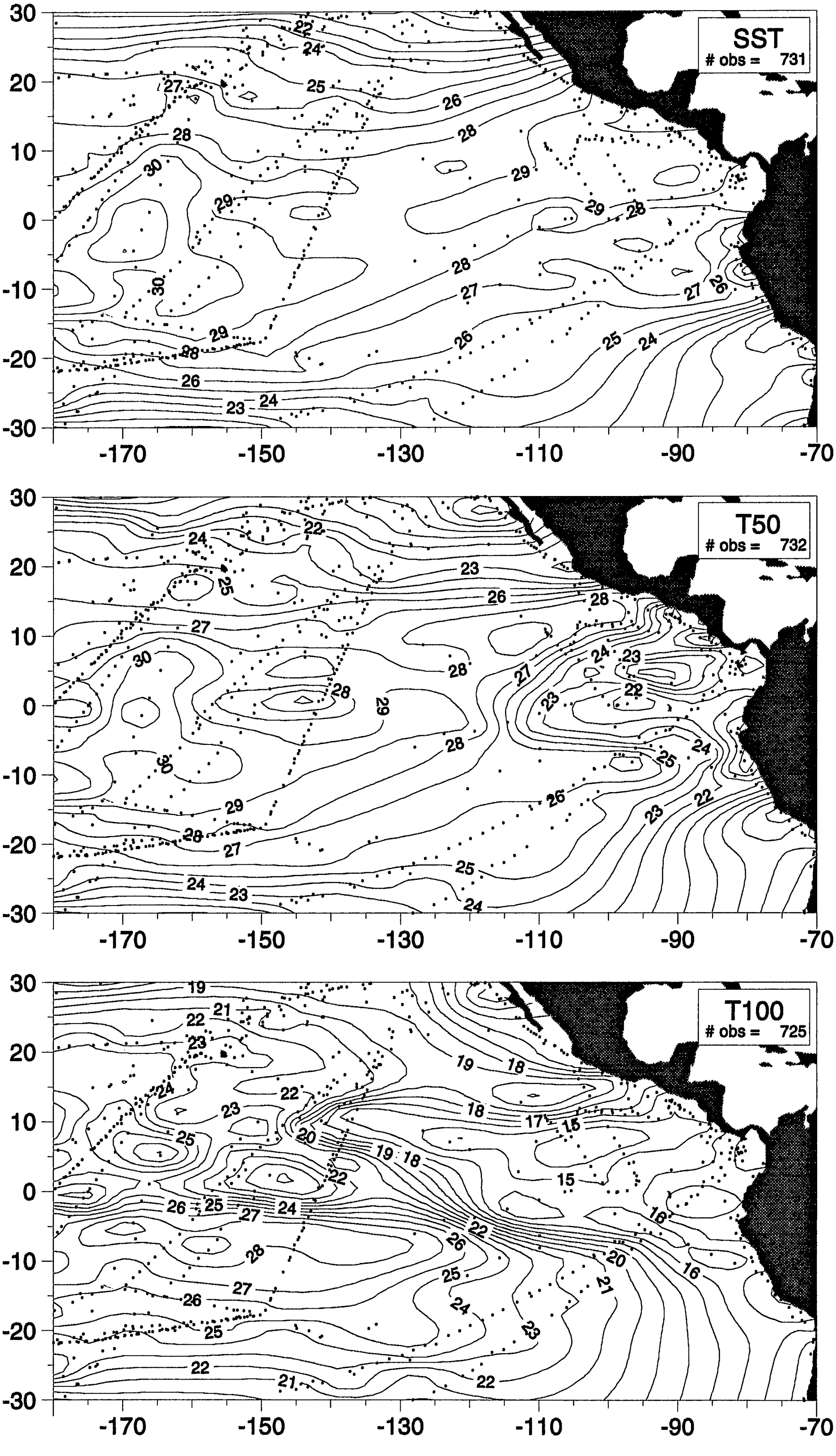

Plate 87. Bimonthly fields for May-June 1992.

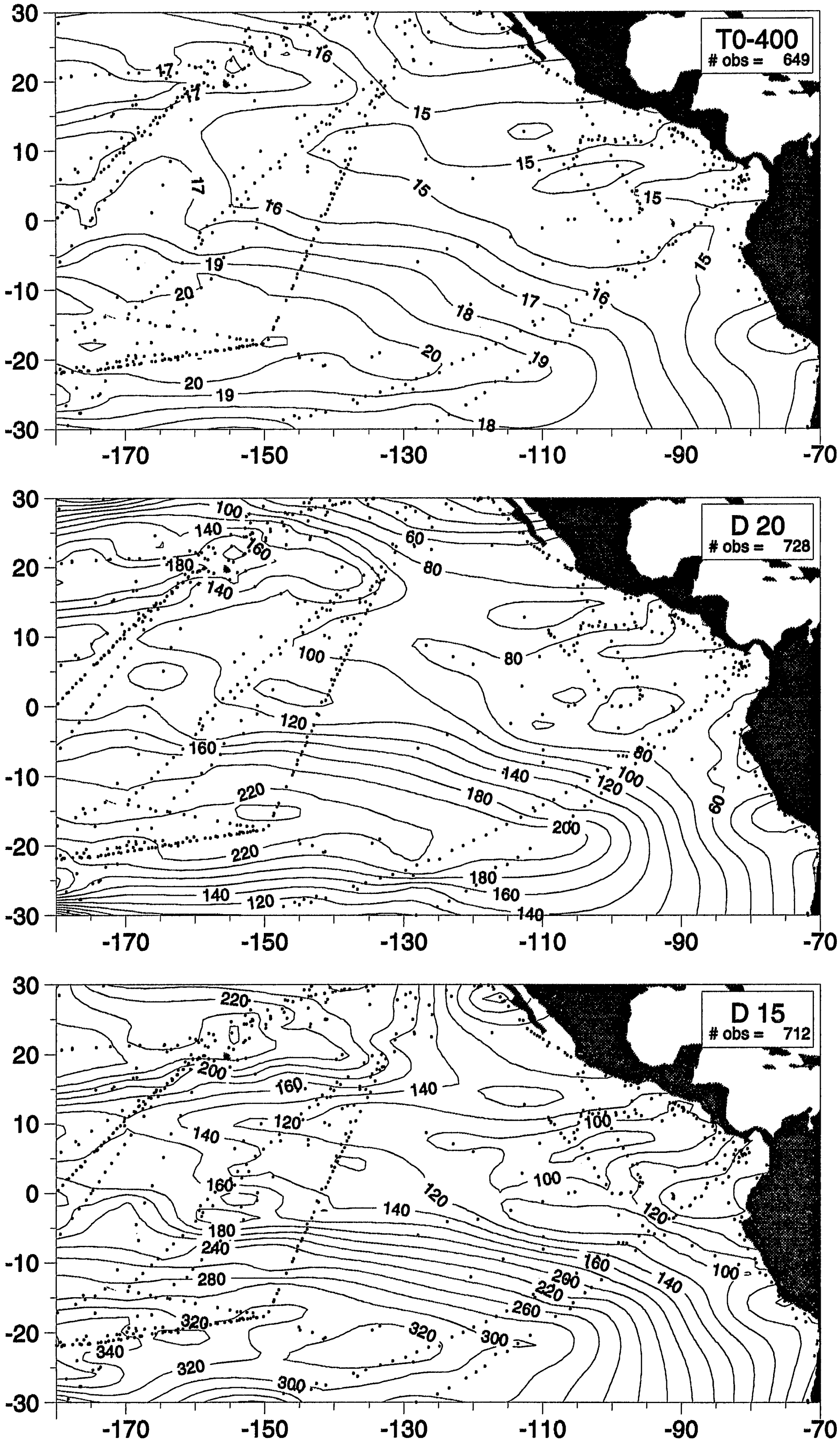

Plate 87 – *continued*. Bimonthly fields for May-June 1992.

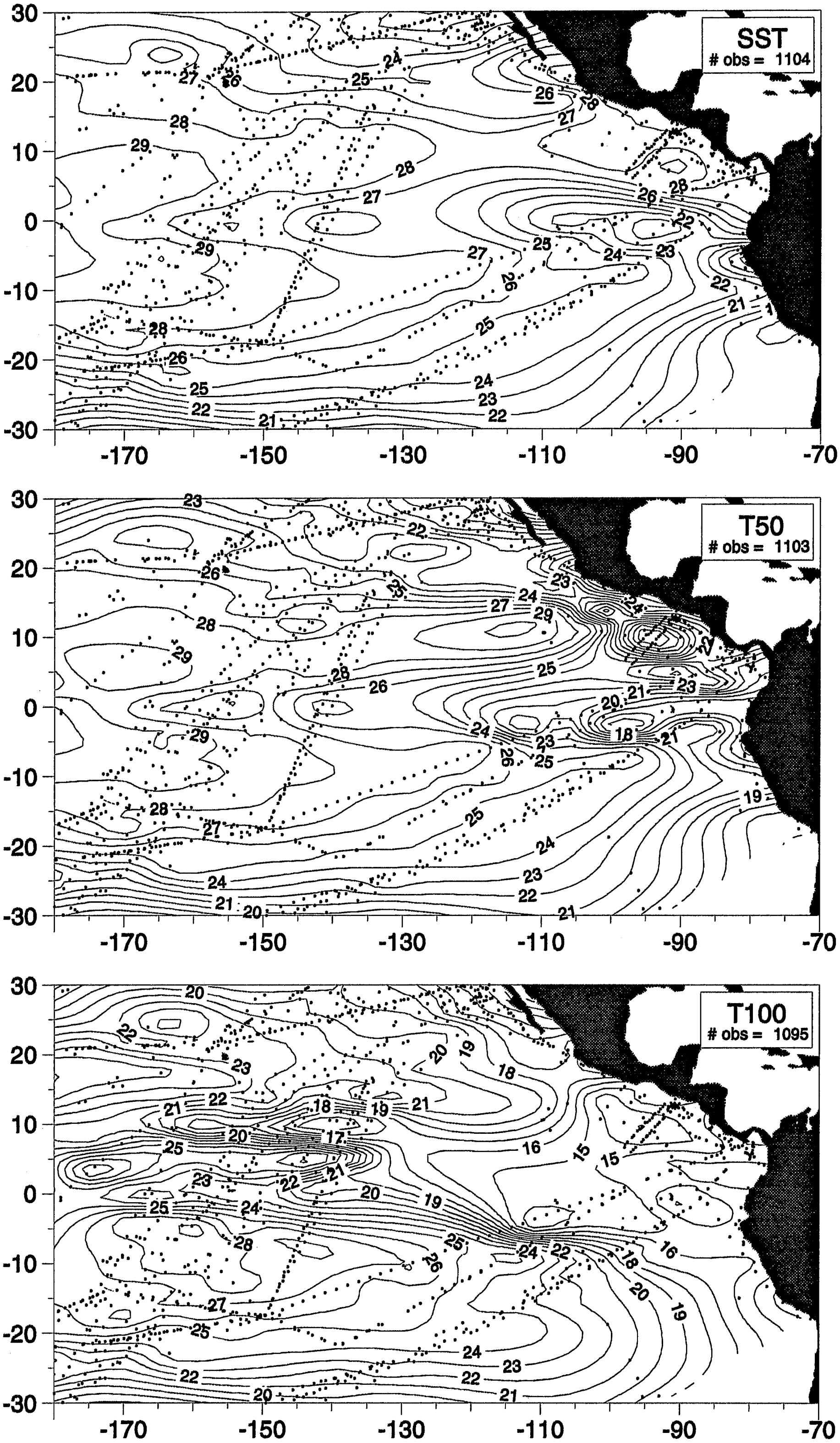

Plate 88. Bimonthly fields for July-August 1992.

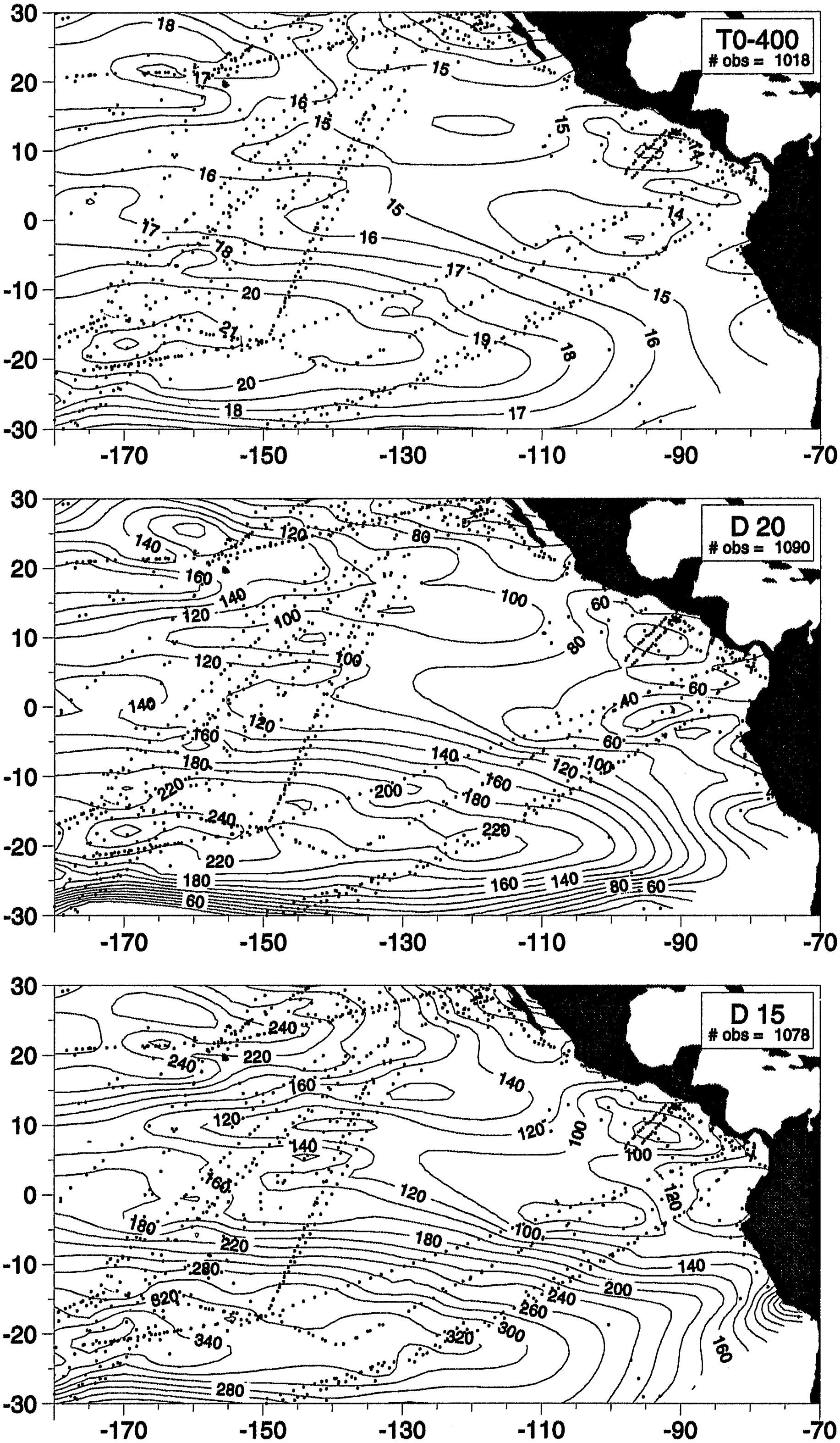

Plate 88 – *continued*. Bimonthly fields for July-August 1992.

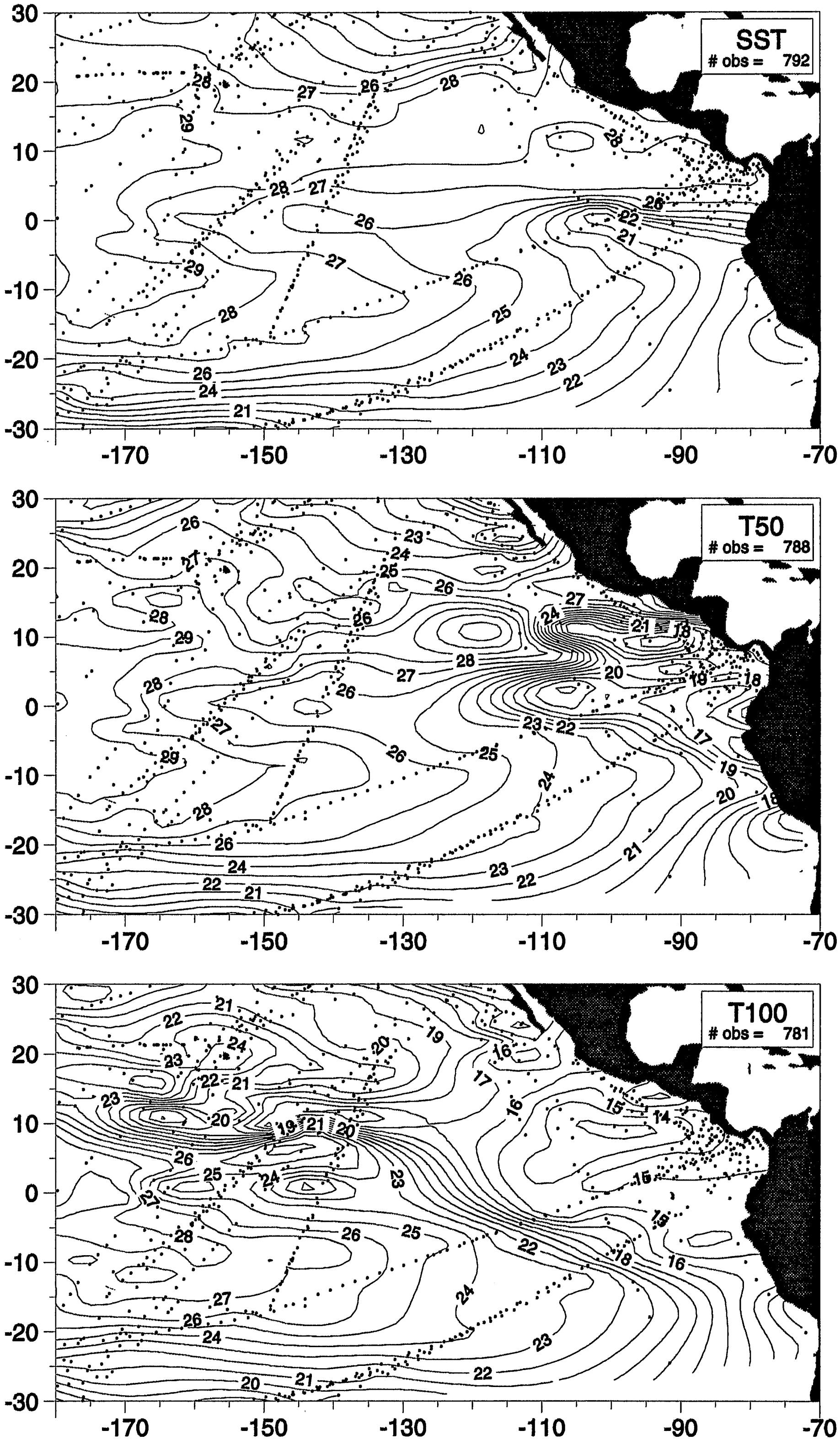

Plate 89. Bimonthly fields for September-October 1992.

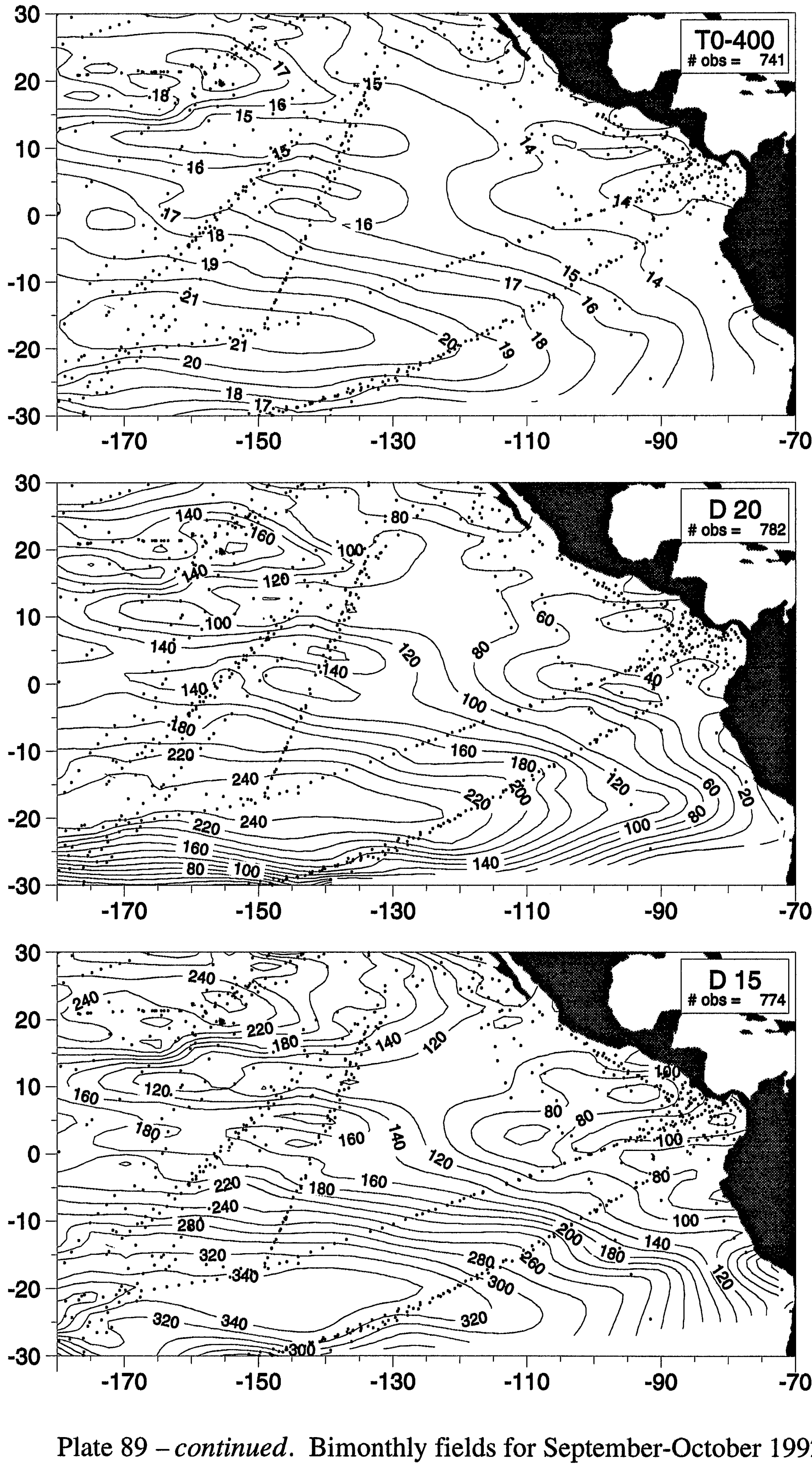

Plate 89 – *continued*. Bimonthly fields for September-October 1992.

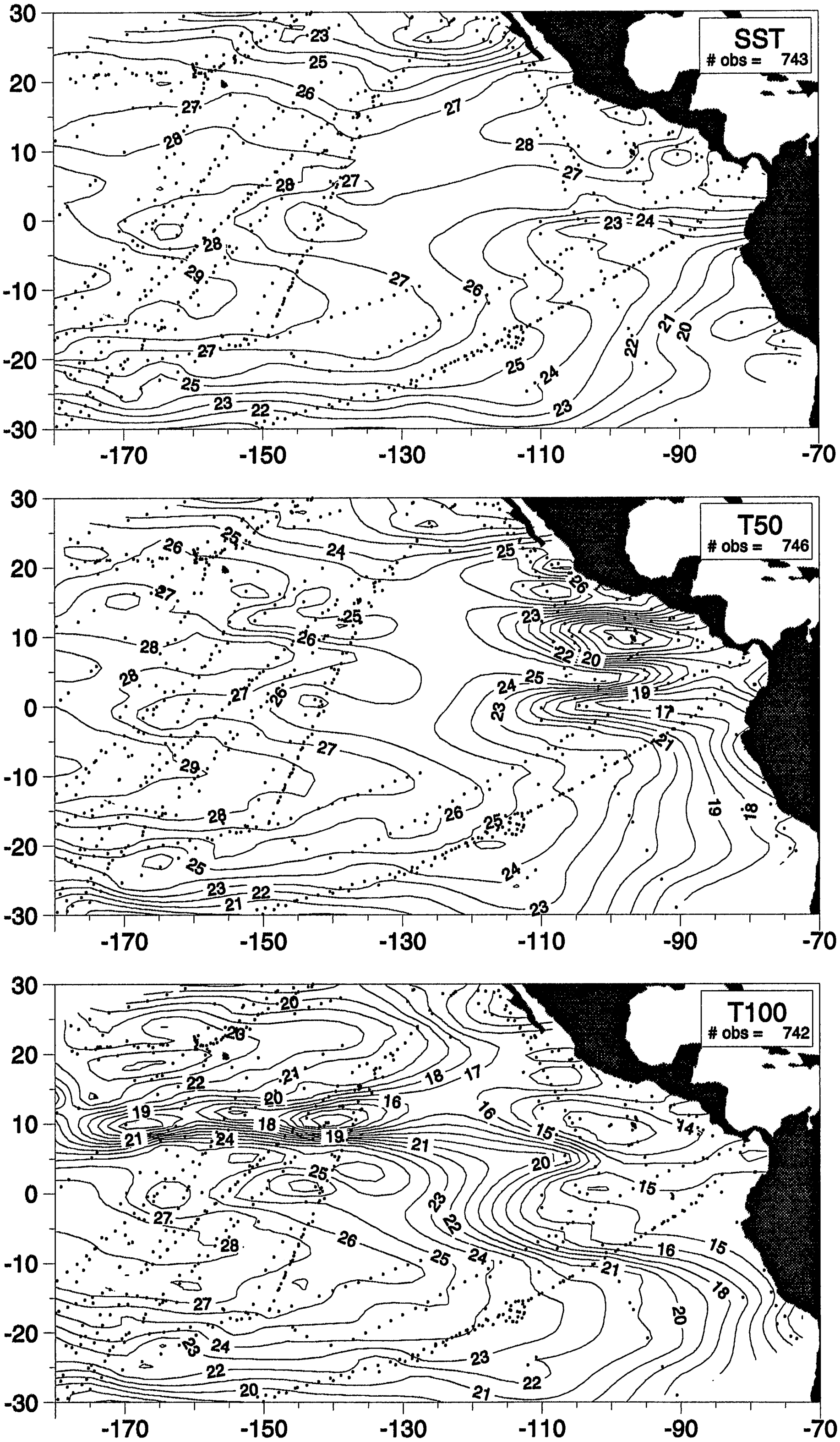

Plate 90. Bimonthly fields for November-December 1992.

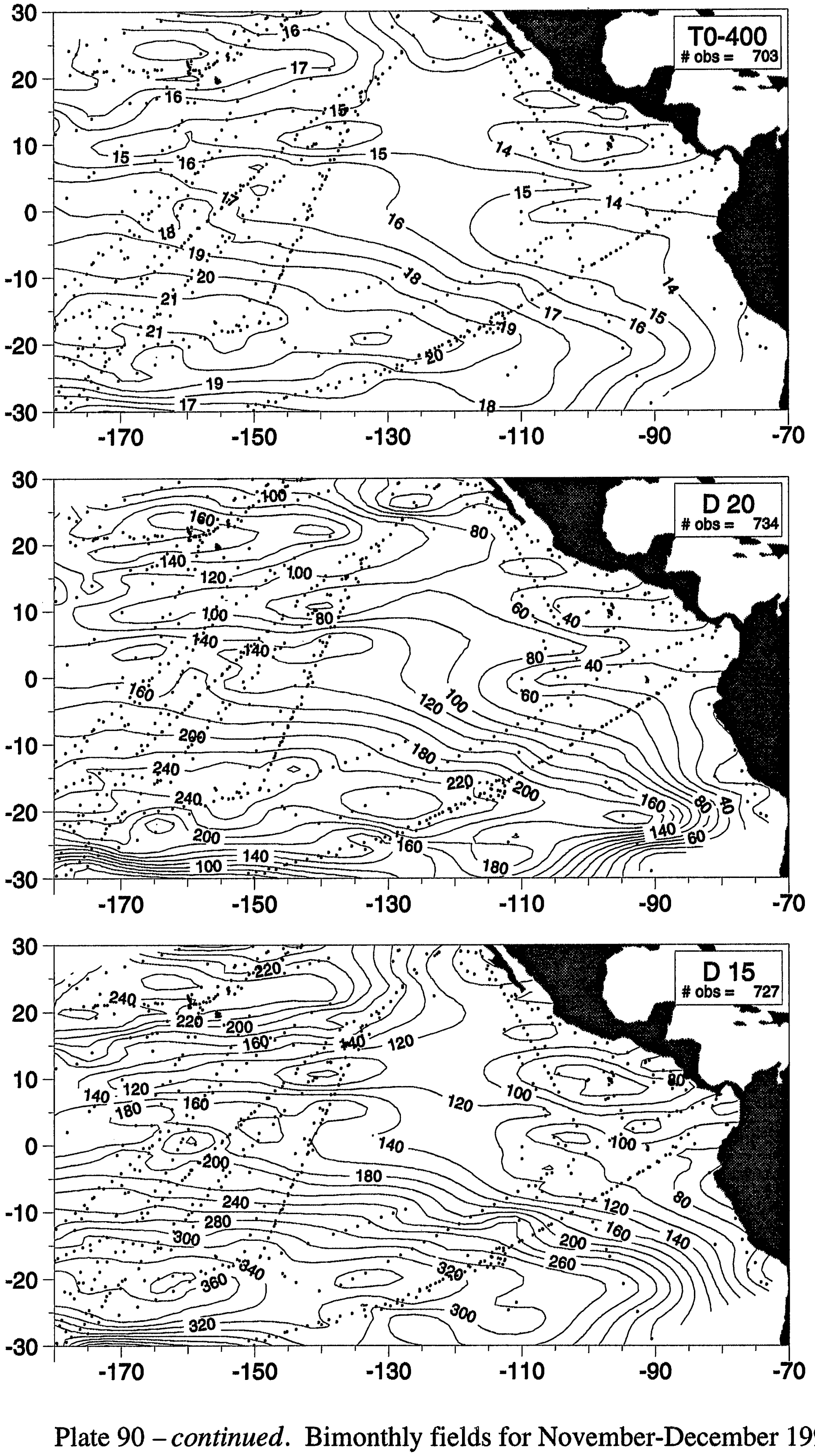

Plate 90 – *continued*. Bimonthly fields for November-December 1992.

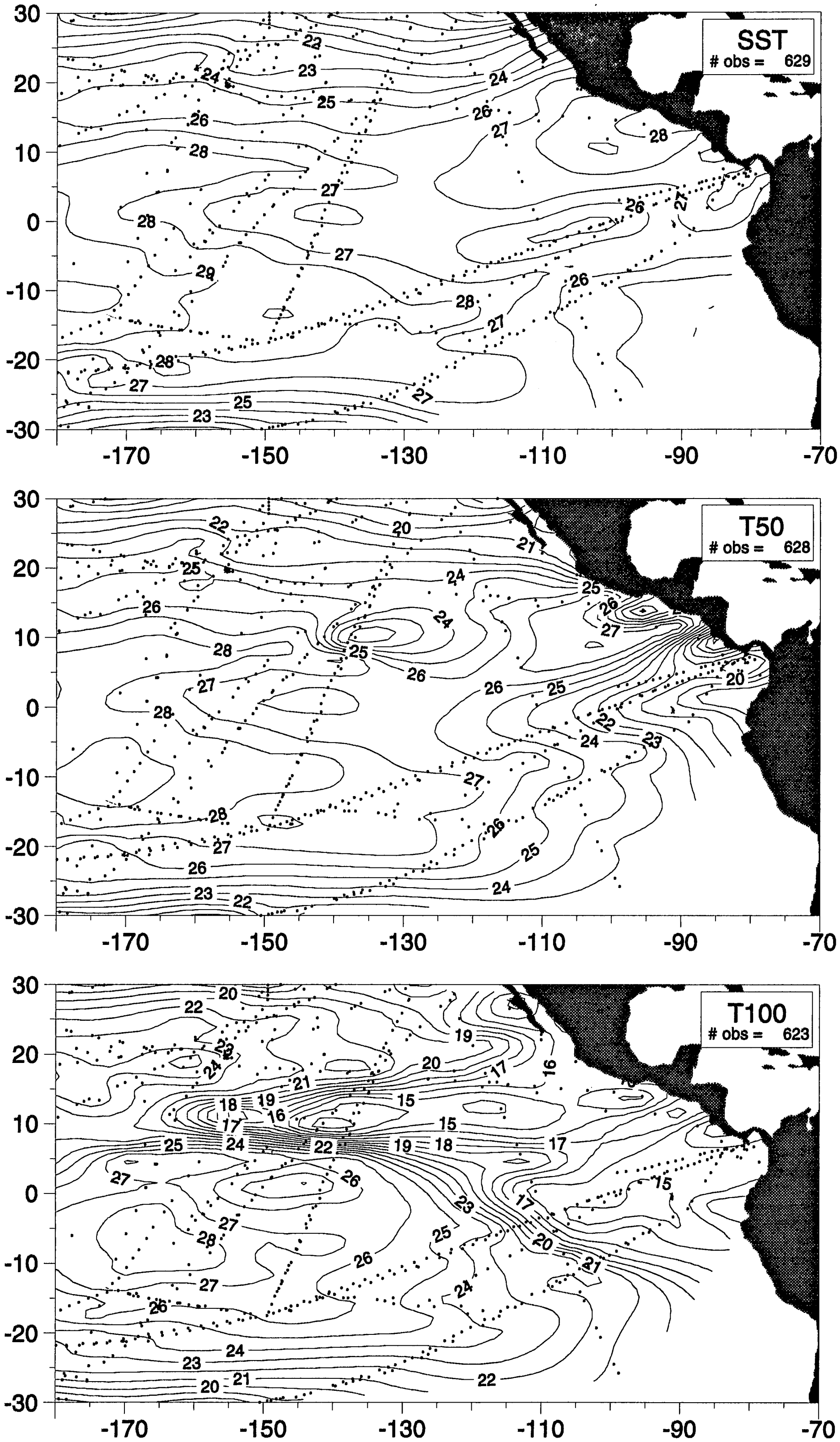

Plate 91. Bimonthly fields for January-February 1993.

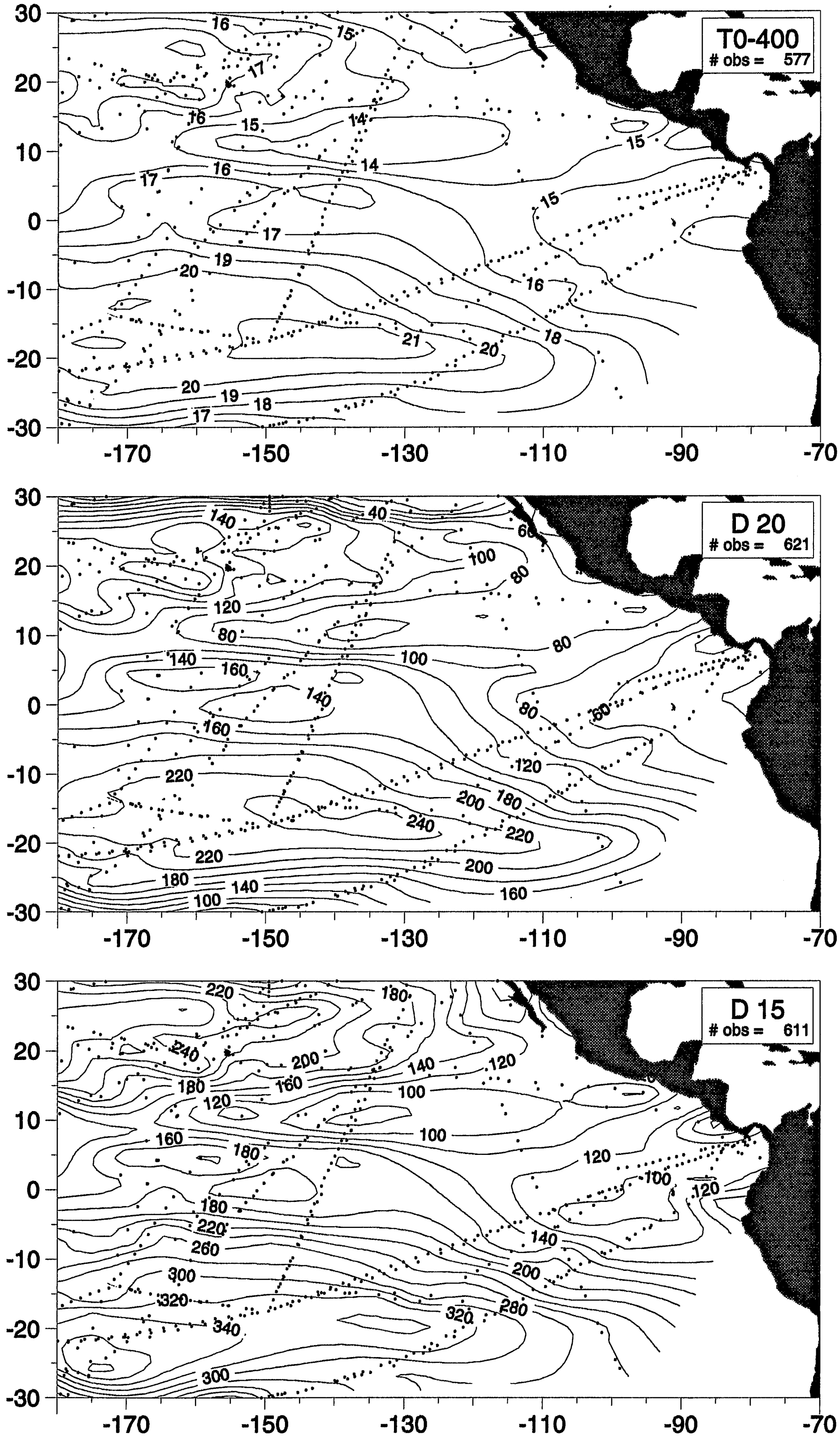

Plate 91 – *continued*. Bimonthly fields for January-February 1993.

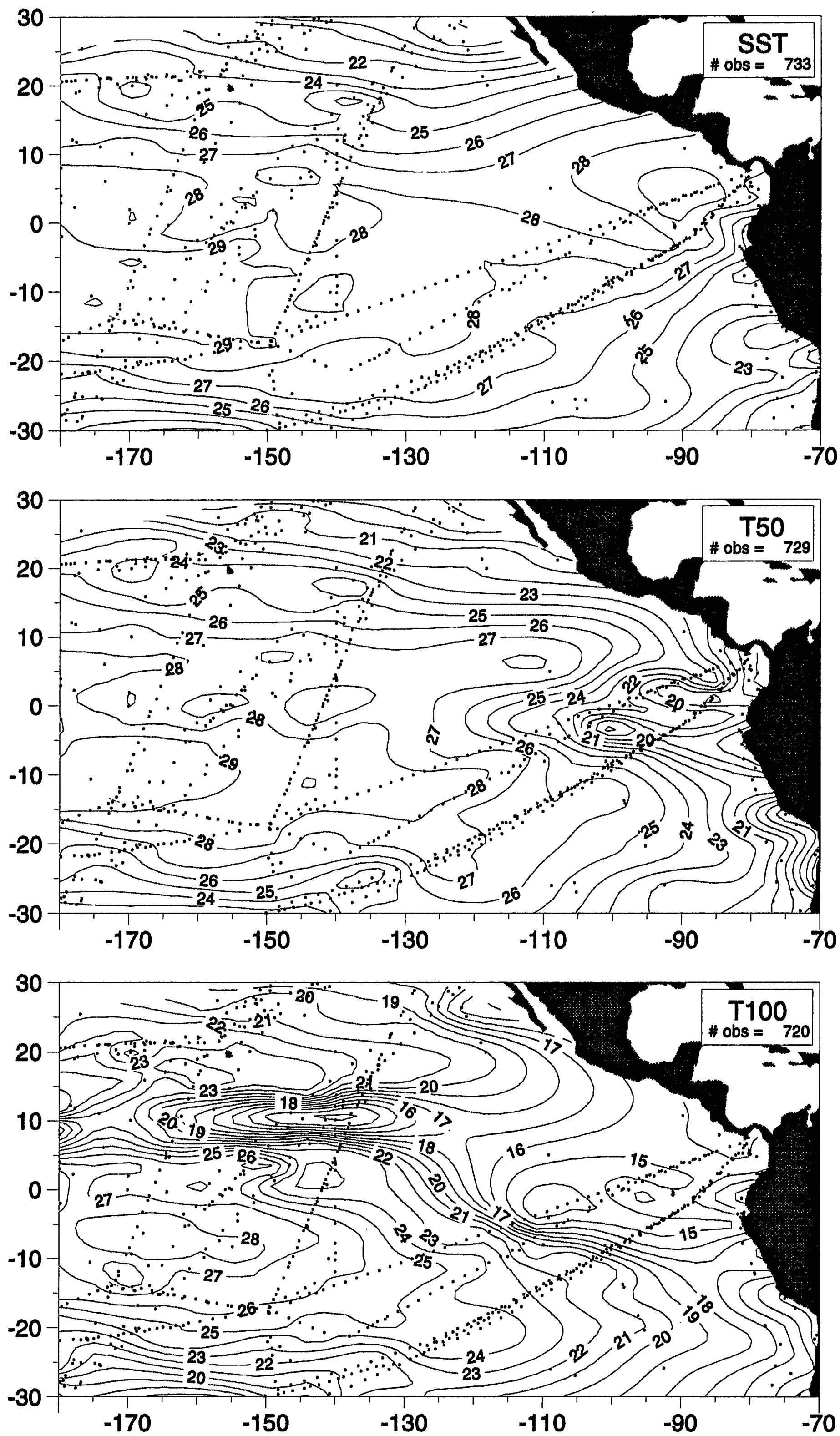

Plate 92. Bimonthly fields for March-April 1993.

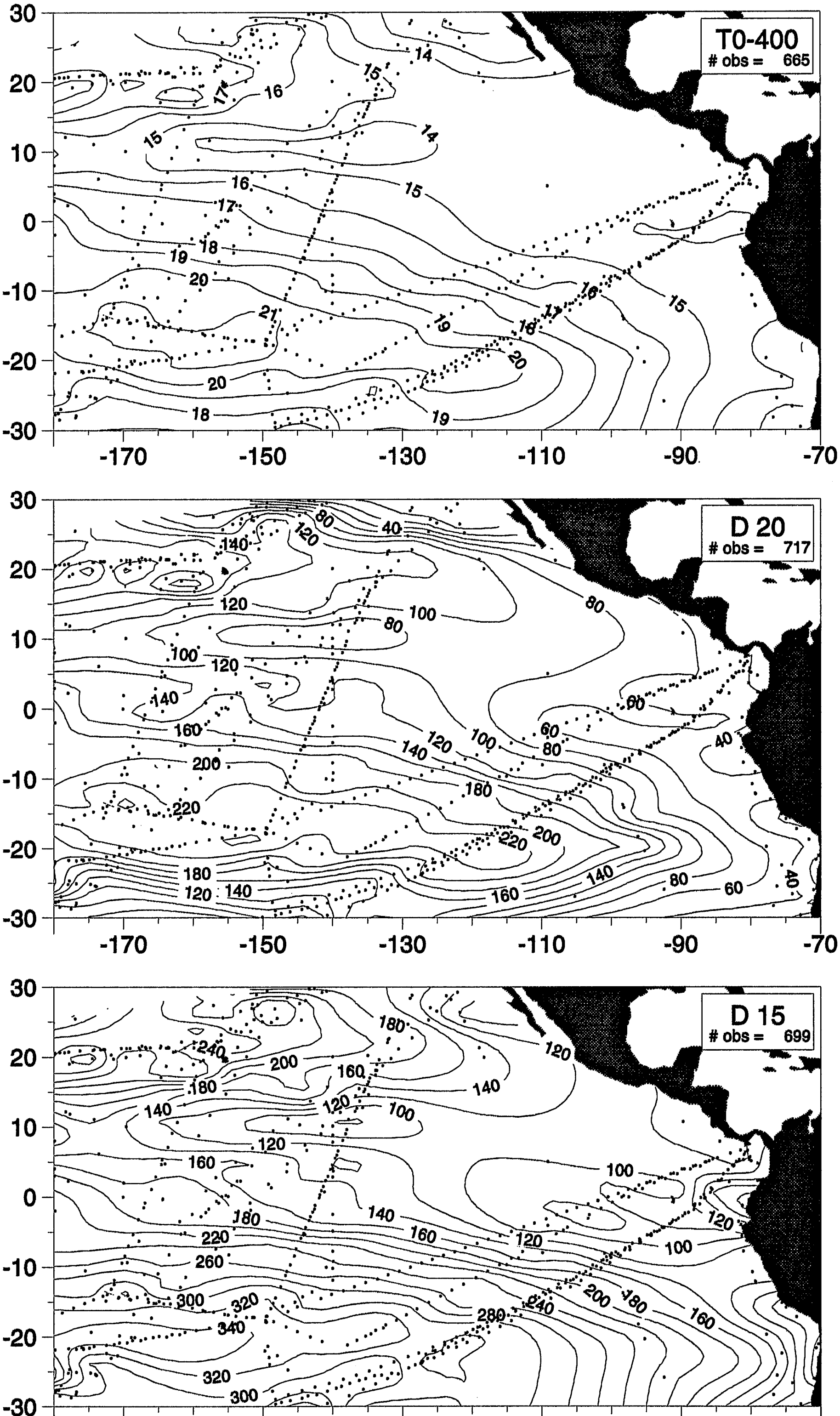

Plate 92 – *continued*. Bimonthly fields for March-April 1993.

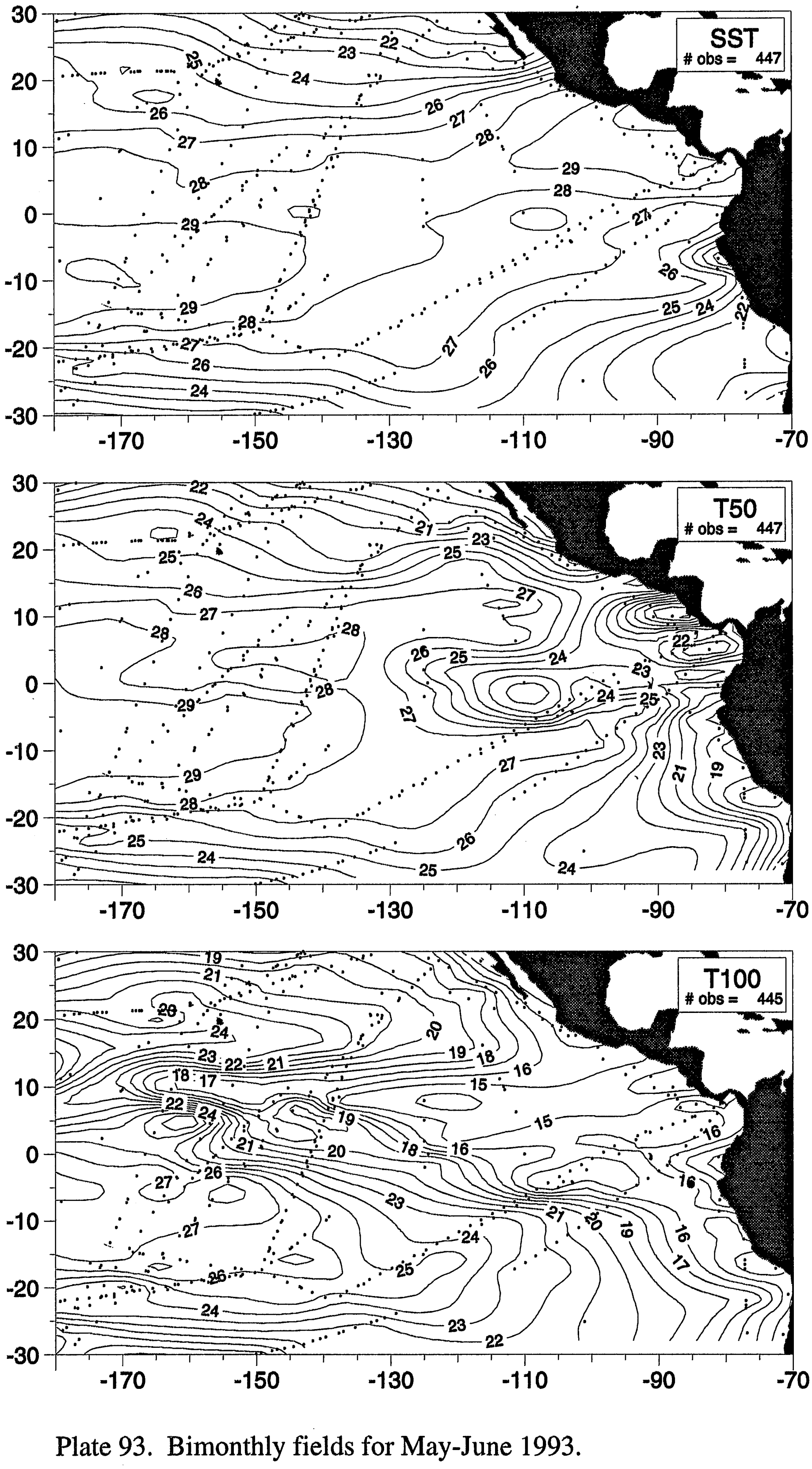

Plate 93. Bimonthly fields for May-June 1993.

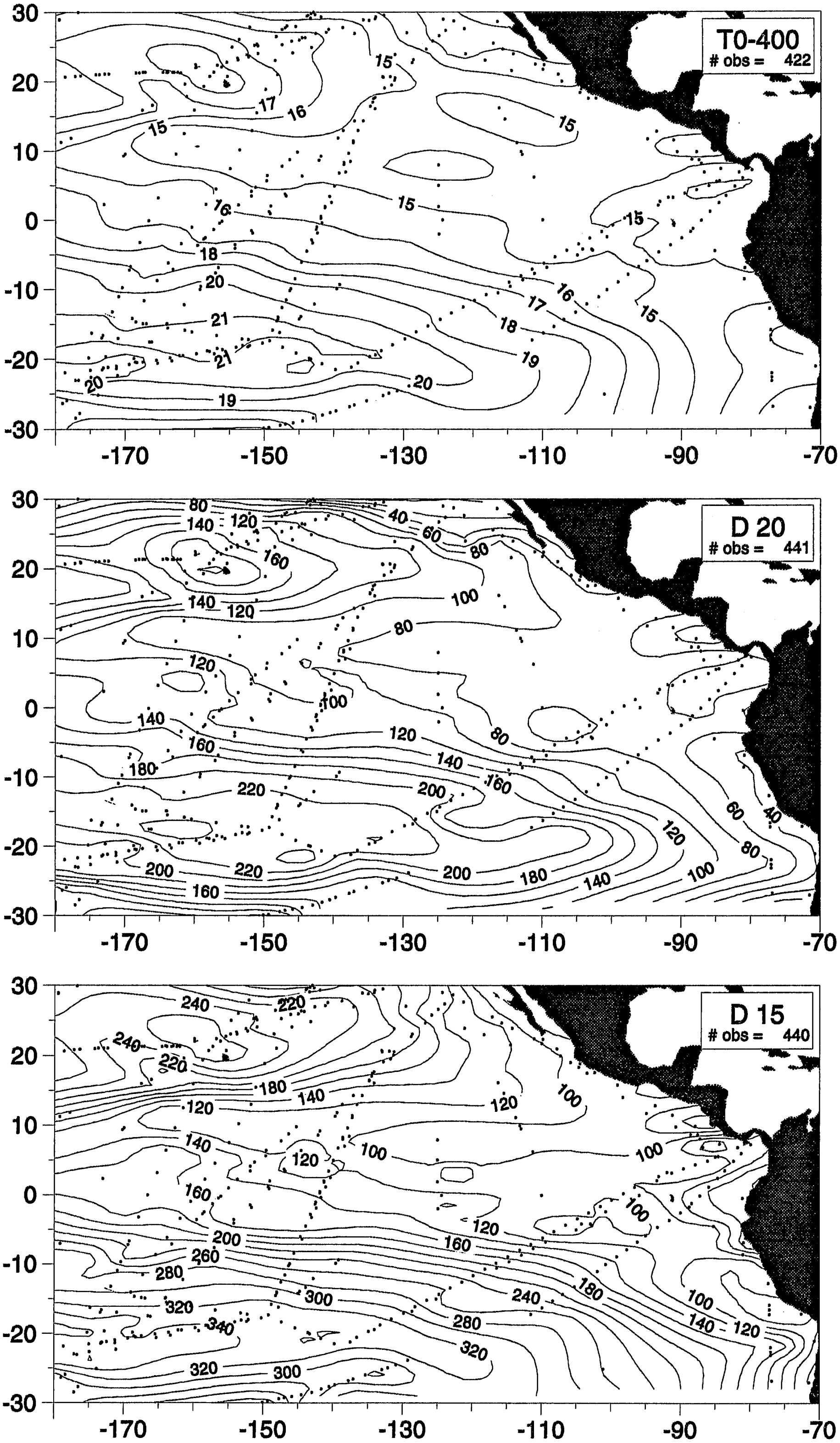

Plate 93 – *continued.* Bimonthly fields for May-June 1993.

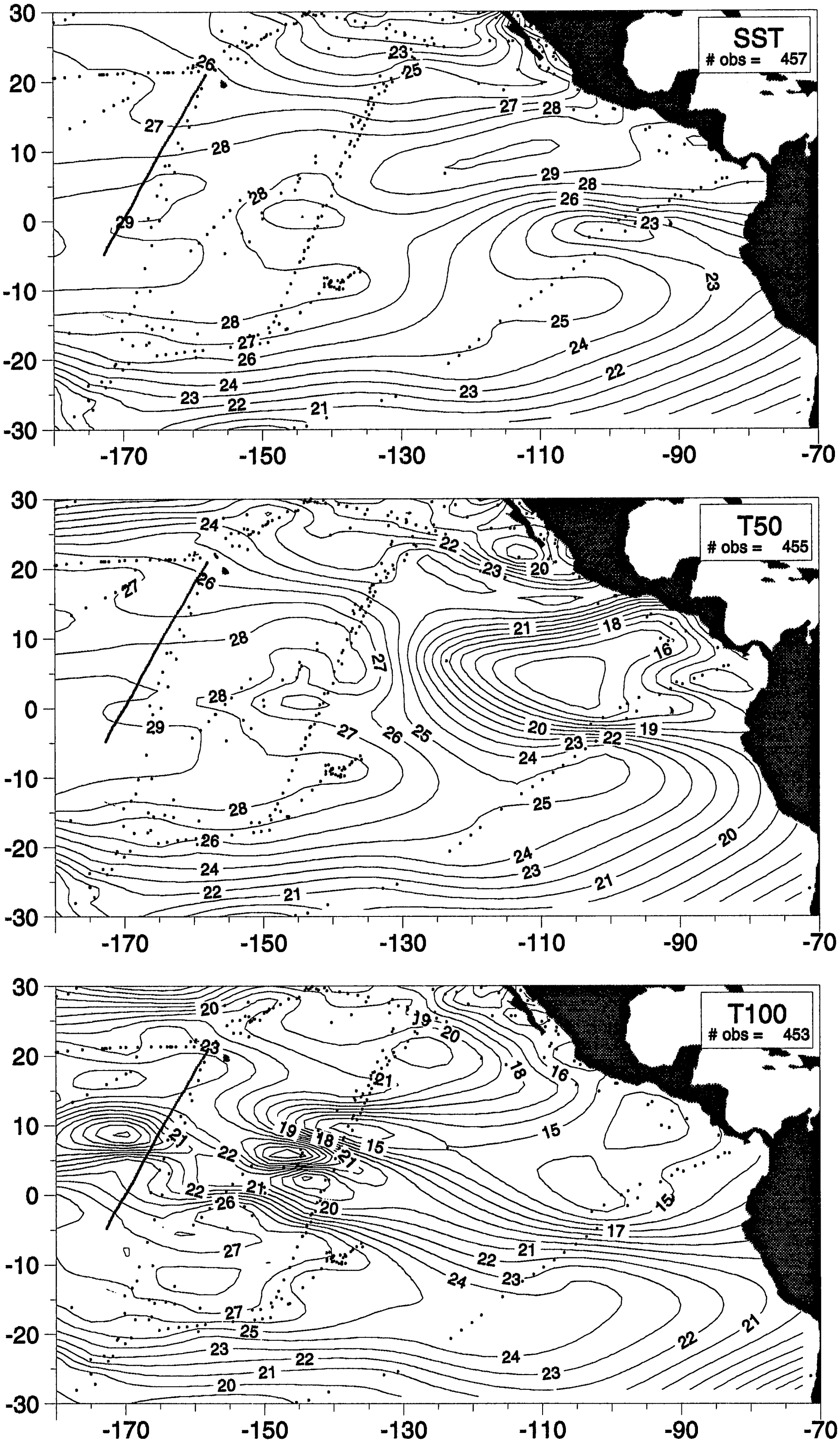

Plate 94. Bimonthly fields for July-August 1993.

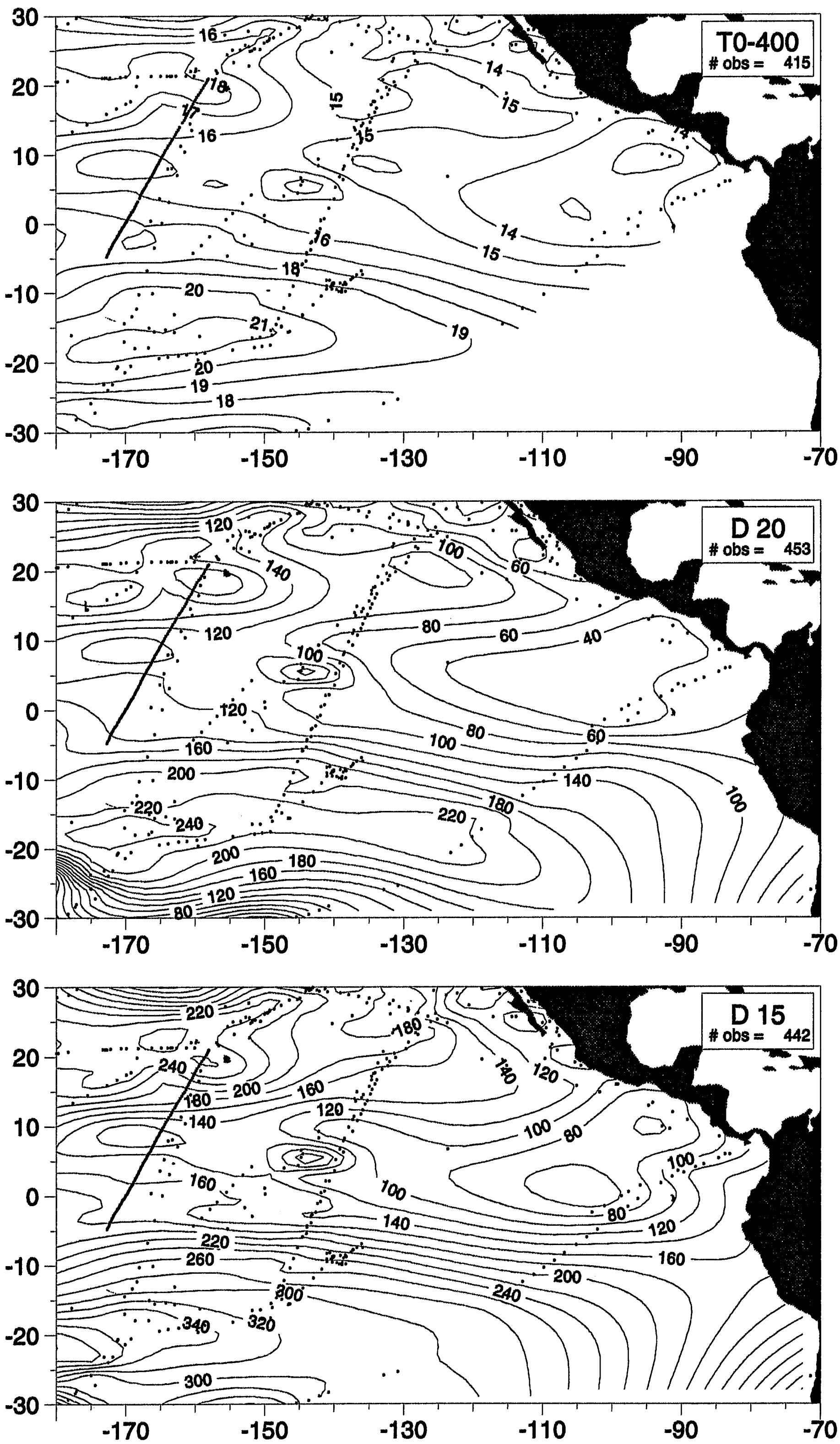

Plate 94 – *continued*. Bimonthly fields for July-August 1993.

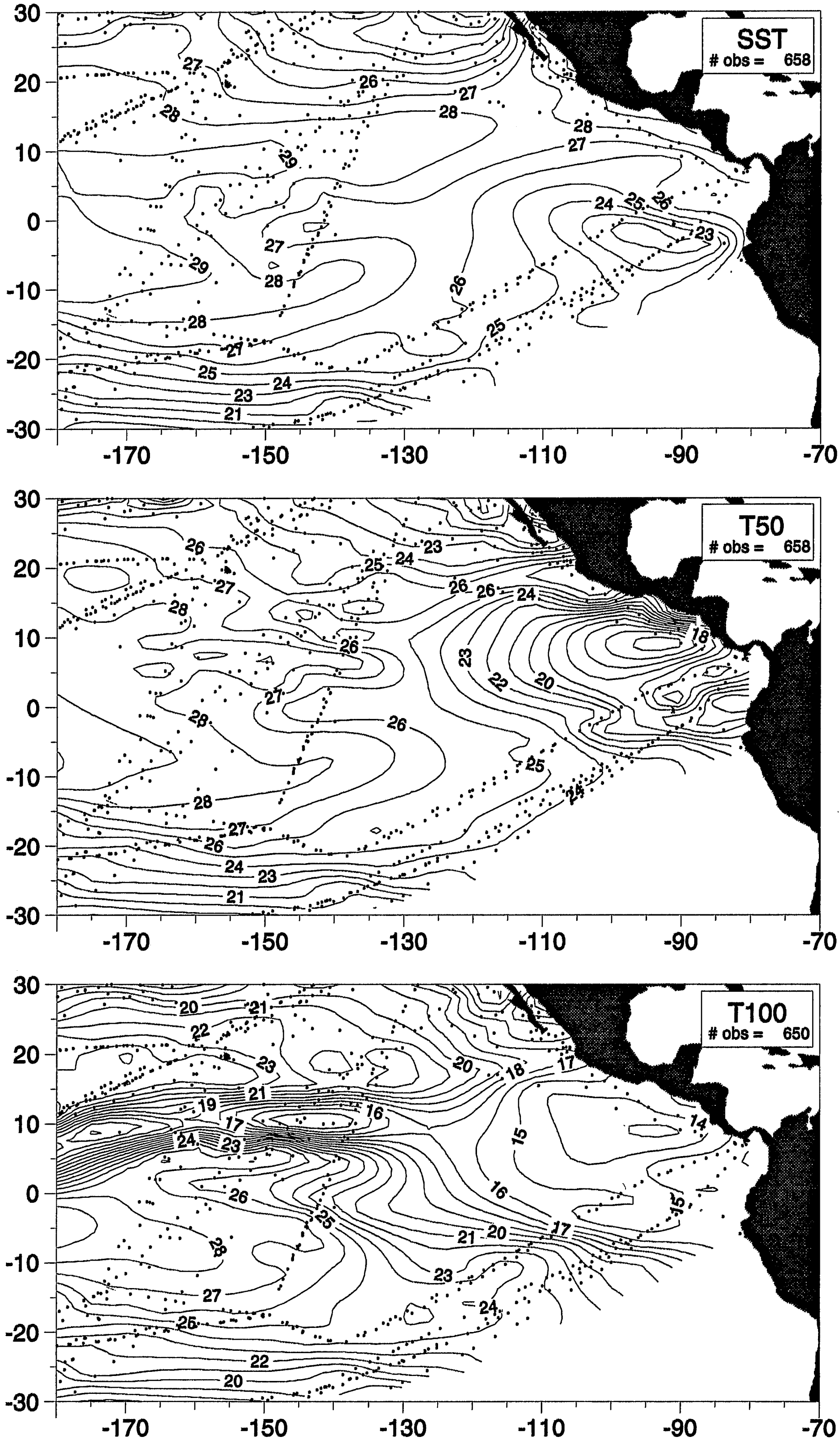

Plate 95. Bimonthly fields for September-October 1993.

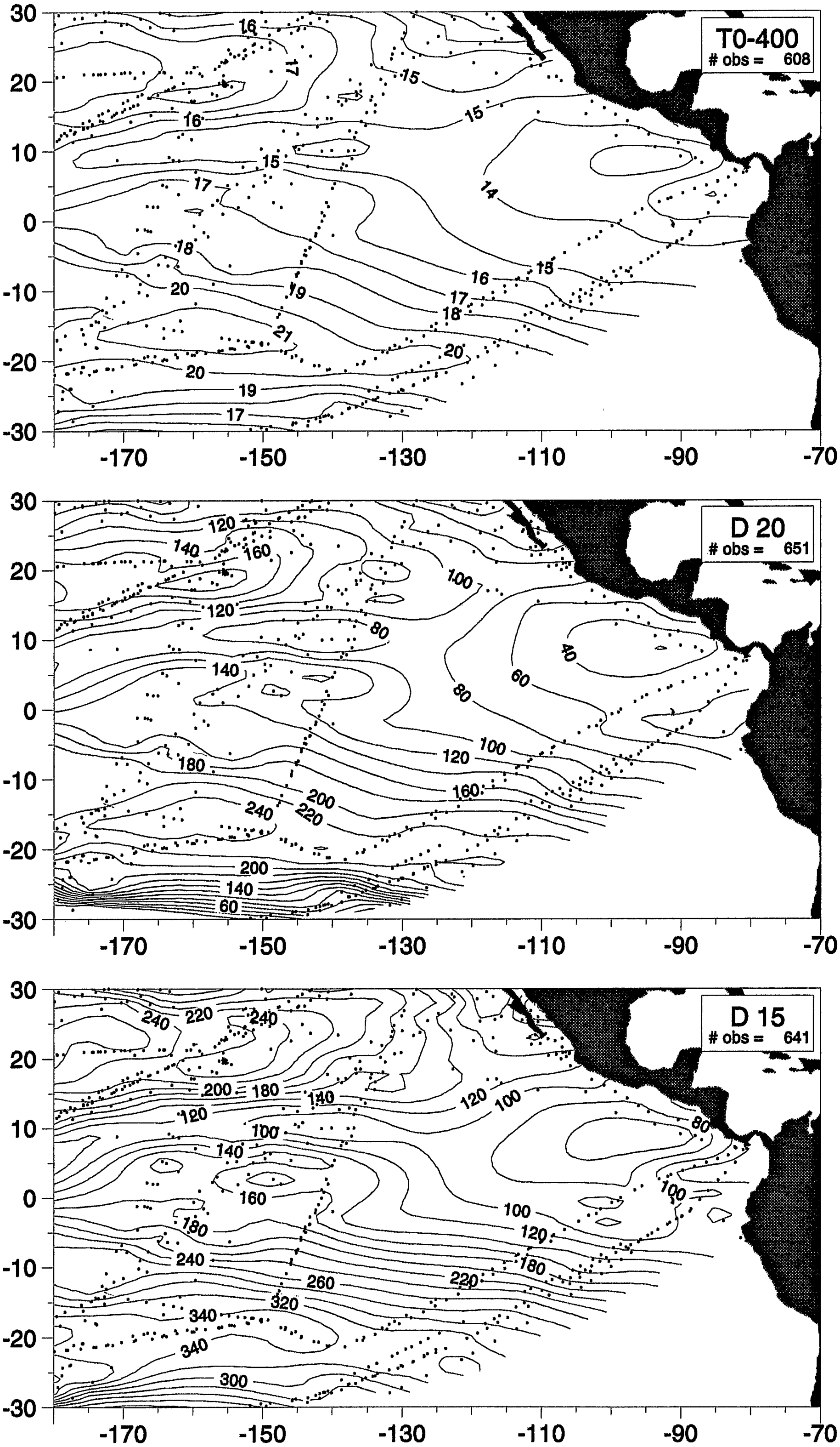

Plate 95 – *continued*. Bimonthly fields for September-October 1993.

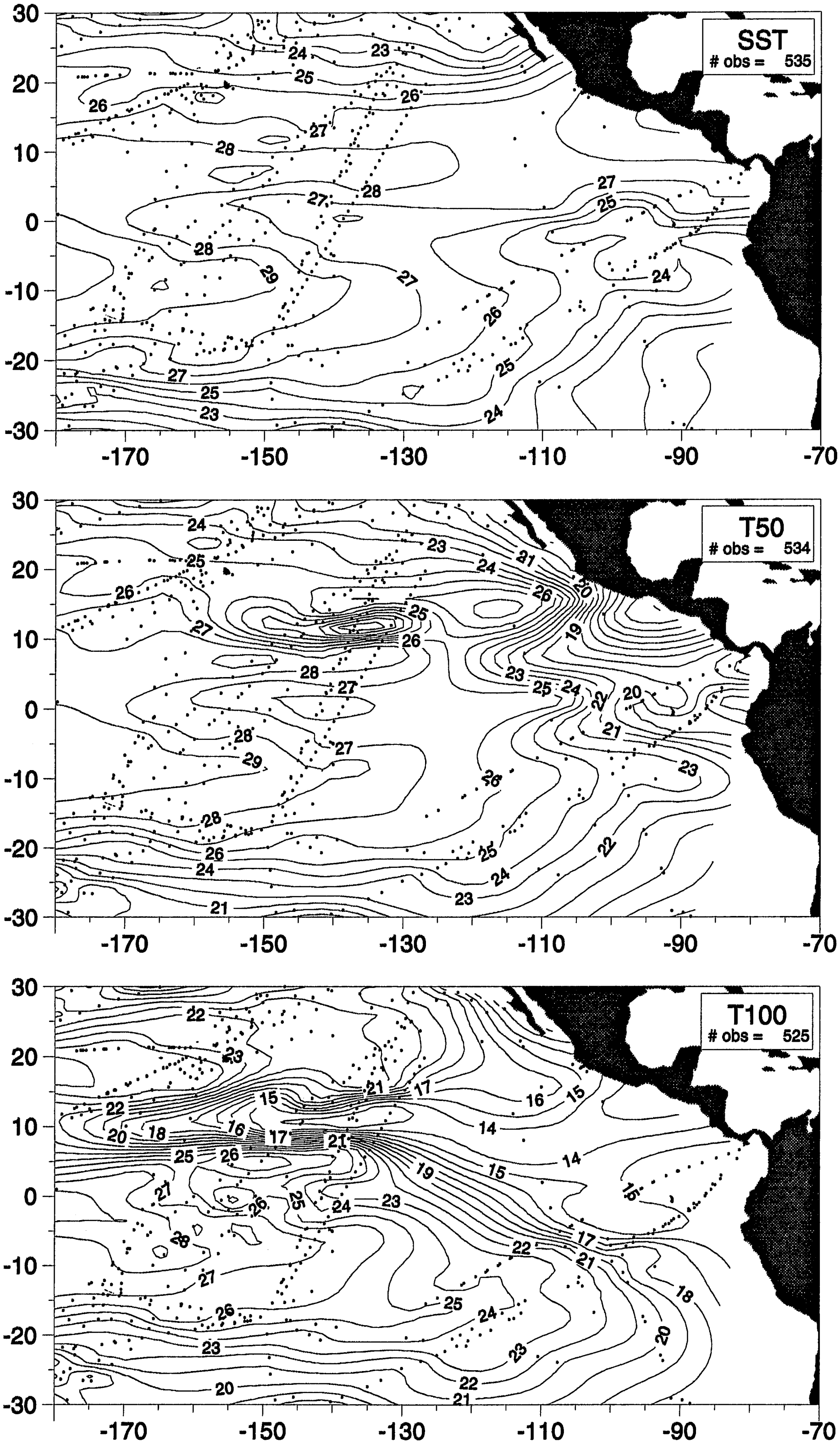

Plate 96. Bimonthly fields for November-December 1993.

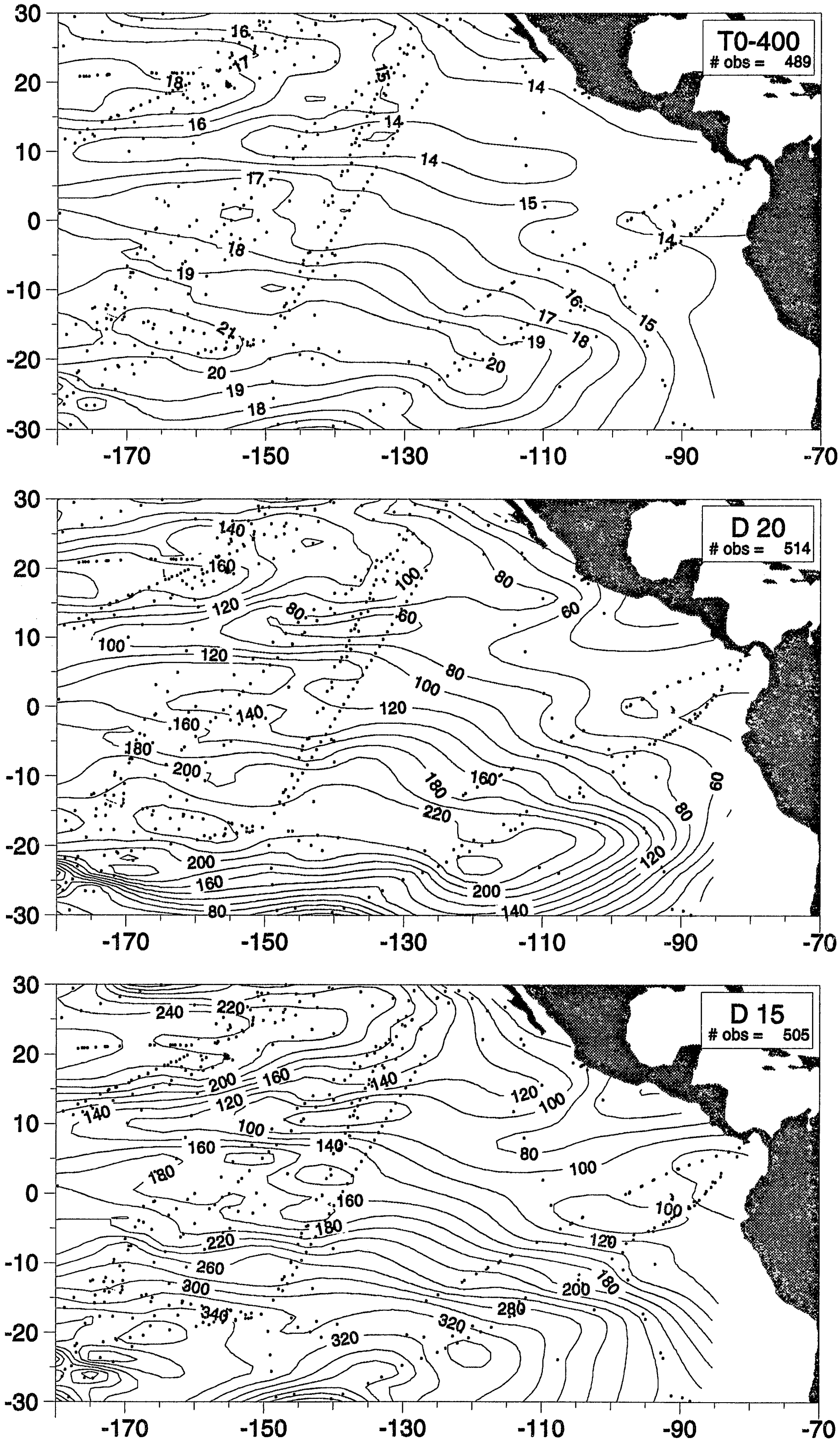

Plate 96 – *continued*. Bimonthly fields for November-December 1993.

*U.S. GOVERNMENT PRINTING OFFICE:1995-673-018/00063